Characterisation of four *Drosophila* proteins involved in regulation of gene expression.

Ditte Skovaa Andersen

Apoptosis and Proliferation Control Laboratory
London Research Institute
Cancer Research UK

A thesis submitted for the degree of Doctor of Philosophy at the University of London

September 2008

ProQuest LLC
789 East Eisenhower Parkway
P.O. Box 1346
Ann Arbor, MI 48106-1346

Declaration by candidate:

I, Ditte Skovaa Andersen, declare that the work presented in this thesis is my own, except where acknowledged. I have acknowledged all quotations and results from the published or unpublished works of others.

Abstract

This thesis concerns the characterisation of four Drosophila proteins that are involved in different steps of gene expression. The first protein, dMCRS2, is a nuclear Forkhead associated (FHA) domain protein. dMCRS2 is an essential protein required for growth during development. *Drosophila* and human MCRS2/MSP58 was previously reported to form a complex with the MOF histone acetyl transferase. My data reveal that in addition to MOF, dMCRS2 can be purified in complex with multiple RNAP II-associated proteins including Cdk11/Pitslre. Moreover, dMCRS2 co-localises with RNAP II complexes on polytene chromosomes *in vivo*. Thus, dMCRS2 might provide a physical link between the chromatin remodelling MOF complex and RNAP II via its ability to associate with Pitslre. Interestingly, the interaction between dMCRS2 and Pitslre seems to be regulated in response to apoptotic stimuli.

The second and third proteins characterised here correspond to the *Drosophila* homologues of Prp38p (dPrp38), a tri-snRNP splicing factor, and Microfibril-Associated Protein 1 (dMFAP1), a previously uncharacterised protein found in some human spliceosomal fractions. I show here that dMFAP1 binds directly to dPrp38 and is required for pre-mRNA processing. dMFAP1, like dPrp38, is essential for growth during development, and my *in vivo* data show that cells with reduced levels of dMFAP1 or dPrp38 proliferate more slowly than control cells and undergo apoptosis. Consistent with this, dsRNA-mediated depletion of dPrp38 or dMFAP1 causes cells to arrest in G2/M, and this is paralleled by a reduction in mRNA levels of the mitotic phosphatase *string/cdc25*. Interestingly dsRNA-mediated depletion of a wide range of core splicing factors elicits a similar phenotype, suggesting that the observed G2/M arrest might be a general consequence of interfering with spliceosome function.

The fourth protein, Pixie, can be isolated from cells in complex with eukaryotic initiation factor (eIF) 3 and small ribosomal proteins and is required for the assembly of translation initiation competent ribosomes. Thus, depletion of Pixie results in the assembly of empty ribosomes lacking mRNAs and reduced levels of translation initiation. Moreover, Pixie associates with the 40S subunit in an ATP-dependent manner. These data are consistent with Pixie playing a catalytic role in the assembly of complexes required for translation initiation.

Acknowledgement

First, I would like to thank my two wonderful supervisors Sally Leevers and Nic Tapon. I am grateful to Sally for teaching me the writing and communication skills that have assisted me in writing this thesis, for many fruitful discussions, for her encouragement and positive attitude to life that has been a great source of inspiration for me, and for being a good friend. I am equally thankful to Nic for allowing me to carry out the last three years of my thesis in his laboratory, for introducing me to the world of *Drosophila*, which made it possible to produce a significant part of the work presented in this thesis, for many inspiring scientific and philosophical discussions, for supporting me scientifically and personally, and for being a good friend. I would also like to thank all previous and current members of Dr. Sally Leevers and Dr. Nic Tapons laboratories, many of which have become valuable friends during my stay at Cancer Research UK. A special thank to Alice, with whom I have shared my moods during the last three years through an endless number of tea breaks. I would also like to thank my second supervisor Julien Lewis for his support and advice and for being one of the most inspiring scientists that I know. Thanks to the people at the Equipment Park for technical support, to the people at the FACS facility for advice and assistance on recording of DNA profiles, to the Protein Identification laboratory for Mass Spectrometry analysis, to the Peptide Synthesis laboratory for generating peptides for antisera production, to the Cell service for large-scale culturing of S2 cells, to Terrence Gilbank, Steve Murray, and Frances Earl of the *Drosophila* facility of Cancer Research UK for maintaining fly stocks, to Terence Herbert and Isabel C. Greenman for advice with polysome profile analysis, and to the Taplin Biological Mass Spectrometry Facility for Mass Spectrometry analysis.

I am also grateful to friends and family for their much appreciated love and support during the last five years. A special thank to Hanne for being a very loyal and caring friend. Finally, I am very thankful to Julien for his generous love and endless support, and for always being there for me.

This work was funded by Cancer Research UK.

Table of contents

List of Figures

List of Abbreviations

aa	Aminoacyl
ABC50	ATP-binding cassette protein 50
AEL	After egg lay
AMP	Adenosine monophosphate
AMPK	AMP kinase
A site	Aminoacyl site
ATP	Adenosine tri-phosphate
BPS	Branch point sequence
BRE	TFIIB recognition element
CAK	Cyclin activating kinase
CBP	Calmodulin binding peptide
Cdk	Cyclin-dependent kinase
CK2	Casein kinase 2
CTD	C-terminal domain
CTDK-1	C-terminal domain kinase 1
CycE	Cyclin E
DIAP1	*Drosophila* inhibitor of apoptosis protein 1
DNA	deoxyribonucleic acid
DPE	Downstream promoter element
DRB	5, 6-Dichloro-1-bD-ribofuranosylbenzimidazole
DSIF	DRB sensitivity-inducing factor
dsRNA	double-stranded RNA
EEC	Early elongation complex
eEF	eukaryotic elongation factor
eIF	eukaryotic initiation factor
ELL	lysine-rich in leukaemia
EM	Electron microscopy
EMS	Ethylmethane sulfonate
ER	endoplasmic reticulum
eRF	eukaryotic release factor
E site	Exit site

EST	Expressed sequence tag
Ex	Expanded
FACT	Facilitates chromatin transcription
FERM	Four point one Ezrin Radixin Merlin
FHA	Forkhead-associated
FLP	Flpase
FRMP	Fragile mental retardation protein
FRT	FLP recombination target
GADD34	Growth arrest and DNA-inducible protein 34
GAP	Guanine GTPase activating protein
Gcd	General control derepressed
GCN2	General amino acid control of gene expression non-derepressable-2
GDP	Guanosine diphosphate
GEF	Guanine nucleotide exchange factor
GFP	Green fluorescent protein
GFT	General transcription factor
GMR	Glass multimer reporter
GSK3	Glycogen synthase kinase 3
GST	Gluthionine S Transferase
GTC	GST-TEV-CBP
GTP	Guanine tri-phosphate
GTPase	Guanine tri-phosphatase
HAT	Histone acetyl transferase
HEXIM	Hexamethylene bisacetamide-inducible protein
H4K16	Histone 4 lysine 16
Hpo	Hippo
HRI	Heme-regulated inhibitor
hs	heat shock
INR	Initiator element
IP	Immunoprecipitation
IR	Ionising radiation
IRS	Insulin receptor substrate
ITC	Initially transcribing complex

LARP7	La-related protein 7
LOF	Loss of function
MAT1	ménage-a-trios-1
Mats	Mob as a tumour suppressor
MCRS2	Microspherule protein 2
MEPCE	Methylphosphate capping enzyme
MFAP1	Microfibril-associated protein
MFC	Multifactor complex
MOF	Males absent on the first
MSL	Male sex lethal
MT	Metallothionein
NBD	Nucleotide binding domain
NSL	Non-sex lethal
PH3	Phospho-Histone 3
Pix	Pixie
Plk1	Polo-like kinase 1
PP1	Protein phosphatase 1
mRNA	messenger RNA
mTOR	mammalian target of rapamycin
Mw	mini-white
NELF	Negative elongation factor
NTc	Nineteen complex
NTD	N-terminal domain
NuRD	Nucleosome remodelling and deacetylase
ORF	Open reading frame
PABP	poly(A) binding protein
PBS	Phosphate buffered solution
PCR	Polymerase chain reaction
PEK	pancreatic eIF2α kinase
PIC	pre-initiation complex
PI3K	Phosphoinositide 3 kinase
PIP2	phosphatidylinositol-4,5-triphosphate
PIP3	phosphatidylinositol-3,4,5-triphosphate
PKD1	3-phosphoinositide-dependent kinase 1

PKR	RNA-dependent protein kinase
Poly(A)	Polyadenylation
PRAS40	proline-rich AKT/PKB substrate 40 kDA
pRb	Retinoblastoma
Pre-mRNA	precursor messenger RNA
Prp	Precursor mRNA processing
PSF	PTB-associated splicing factor
P site	Peptidyl site
P-TEFb	Positive transcription elongation factor
qPCR	quantitative PCR
RFP	RET finger protein
RLI	RNase L inhibitor
RNA	Ribonucleic acid
RNAP II	RNA polymerase II
RNAP II_A	Non-phosphorylated RNAP II
RNAP II_0	Hyper-phosphorylated RNAP II
RRM	RNA recognition motif
Sav	Salvador
Sd	Scalloped
SEM	Scanning electron microscopy
SKIP	Ski oncogene interacting protein
S6K	S6 kinase
Smn1	survivor of motor neuron-1
snRNA	small nuclear RNA
snRNP	small nuclear ribonucleoprotein
SREBP	Serum responsive element binding protein
Stg	String
Sui	Suppressor of initiation codon mutation
TAD	Transcription activation domain
TAF	TBP-associated factor
TBP	TATA-box binding protein
TC	Ternary complex
TEV	Tobacco etch virus
TF	Transcription factor

TOS	TOR signalling
tRNA	transfer RNA
TSC	Tumour sclerosis complex
U2AF65	U2 snRNP auxiliary factor 65 kDa
UAS	Upstream activating sequence
UBF	Upstream binding factor
uORF	Upstream ORF
UTR	Untranslated region
VDRC	Vienna *Drosophila* RNAi Center
W	white
Wt	wildtype
Wts	Warts
XPB	Xeroderma pigmentosum B
XPD	Xeroderma pigmentosum D
Yki	Yorkie

Chapter 1 - Introduction

1.1 Introduction overview

This thesis concerns the characterisation of four *Drosophila* proteins that are implicated in different stages of gene expression. Our data show that two of the proteins, dPrp38 and dMFAP1, function in pre-mRNA processing, one, dMCRS2, might be implicated in transcriptional regulation, and one, Pixie, functions in translation initiation. This introduction is divided into four main sections and aims to provide an overview of three major stages of gene-expression: RNA polymerase II-dependent transcription, pre-mRNA processing, and translation. Section 1 one gives a very short introduction to *Drosophila* as a genetic tool. Section 2 describes various aspects of RNAP II transcription including pre-initiation complex assembly, transcription initiation and elongation, regulation of RNAP II transcription by activators/chromatin remodellers, and the interplay between RNAP II transcription and pre-mRNA processing. Section 2 also includes an update on previous research concerning dMCRS2 and its human homologue MSP58. Section 3 aims to give relatively broad overview of the spliceosome. I have attempted to compile the mechanistic *in vivo* data obtained in yeast with the proteomic data from studies in mammalian cells to highlight similarities and differences between pre-mRNA processing in yeast and metazoans. The fourth and final section of the introduction is dedicated to translation with an emphasis on translation initation. I have included a brief introduction to insulin signalling, which regulates protein synthesis at several stages including translation initiation and elongation. The last part of section 4 provides an overview of previous data on Pixie and its human (RLI) and yeast (Rli1p) homologues.

1.2 *Drosophila* as a model organism

Drosophila melanogaster (commonly known as the fruit fly) has served as a genetic tool to study developmental signalling processes for many years. The small size and the short life cycle (see below) make the fruit fly a convenient model organism. The ease of generating genetic mosaics in flies has been used extensively to induce loss of function (LOF) of genes in a spatially and temporally controlled manner (see below). The high level of conservation between key signalling pathways in flies and humans and the lack of redundancy among key regulatory genes in the fly genome facilitates the analysis of the phenotypic effects of gene LOF. With the completion of the *Drosophila* genome sequencing project in 2000, a foundation for a new era of functional studies has been laid.

1.2.1 The *Drosophila* life cycle

Drosophila has been used extensively as a model organism to study different aspects of development in higher eukaryotes. The relatively short generation time of flies make them a convenient tool for studying genetics. Thus, the life cycle of Drosophila from egg lay to adult is roughly 10 days at 25°C (Figure 1-1). Females lay hundreds of eggs (embryos) a day, which hatch as first instar larvae after approximately 12-15 hours. The emerging first instar larvae enter a growth phase, where they increase in mass by about 400x. During the growth phase larvae moult twice into second- and third-instar larvae at about 24 and 48 hours after eclosion. 4-5 days after egg lay (AEL), third instar larvae pupate and undergo a 4-5 days long metamorphosis, after which the adults emerge. During metamorphosis the majority of the larval tissue breaks down with the exception of the imaginal discs. The imaginal discs are epithelial sheets that give rise to most of the structures of the adult fly including head, legs, wings, thorax and genetalia. They are set aside during embryogenesis, continue to grow during the larval stages, and undergo extensive morphological changes to form the adult structures during pupal stage. The wing and eye imaginal discs are commonly used tissues to study signalling events, growth, and proliferation during development.

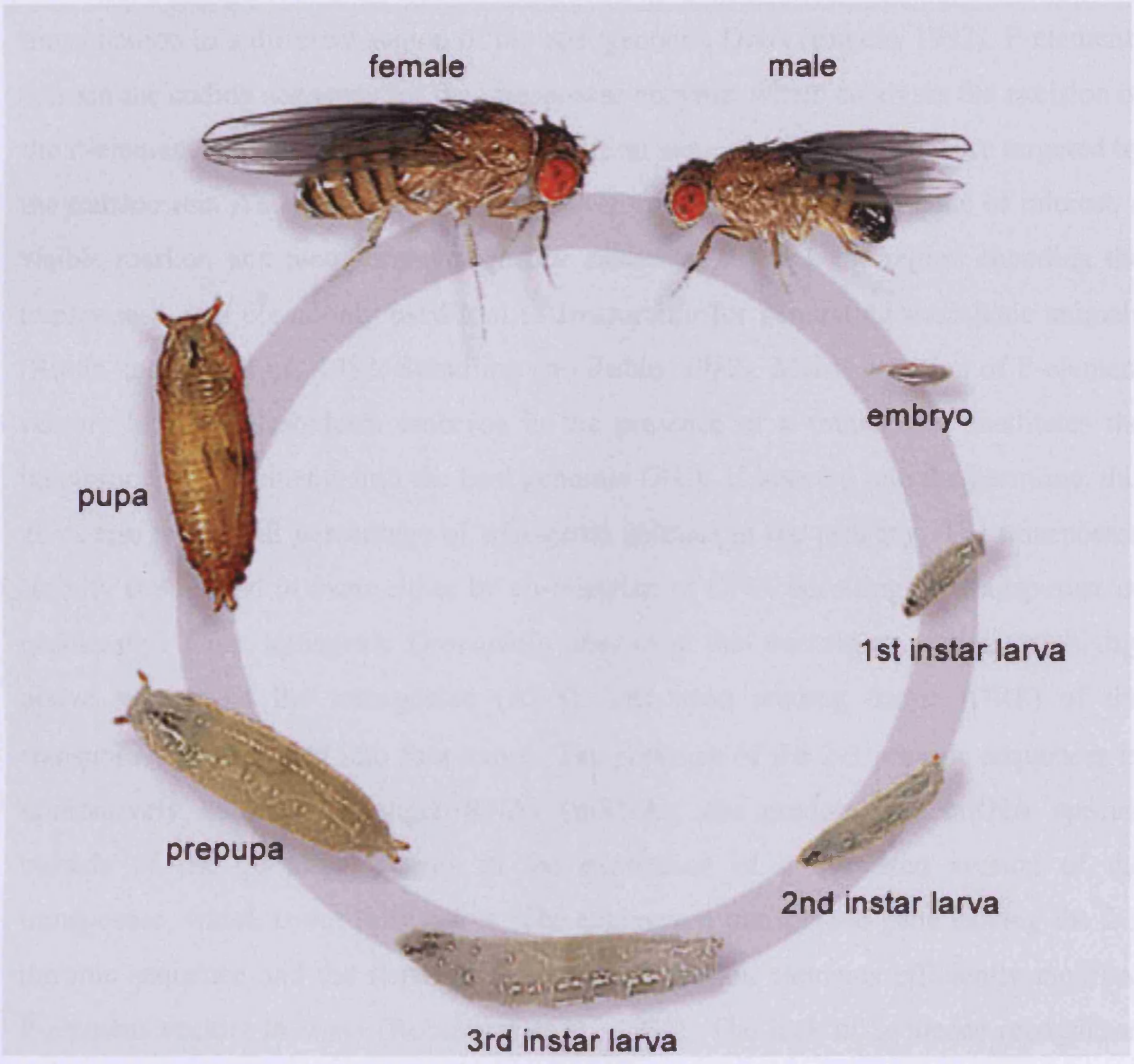

Figure 1-1: The *Drosophila* life cycle. A fertilised female can lay hundreds of eggs (embryos) a day. The embryos develop over 12-15 hours, after which they hatch as first instar larvae. The first instar larvae moult twice into 2nd and 3rd instar larvae 24 and 48 hours after eclosure. Third instar larvae grow and accumulate mass, before they pupate 4-5 days AEL. During the pupal stage, which last about 4-5 days, extensive morphological changes take place. These involve break-down of the majority of the larval tissue and the formation of adult structures. As a result, an adult flies emerge from their pupal case approximately 10 days AEL. Image taken from Flymove: http://flymove.uni-muenster.de.

1.2.2 Genetic tools in *Drosophila*

1.2.2.1 P-elements as a tool for generating transgenic animals

P-elements belong to a family of naturally occurring transposable elements found in *Drosophila*, which have the ability to catalyse their own excision and transposition to a different region of the host genomic DNA (Engels, 1992). P-elements contain the coding sequence for the transposase enzyme, which catalyses the excision of the P-element, and are flanked by the recognition sequence elements that are targeted by the transposase. An engineered P-element vector, which contains the gene of interest, a visible marker, and recognitions sequence elements, but lack the region encoding the transposase, is a commonly used tool in *Drosophila* for generating transgenic animals (Rubin and Spradling, 1982; Spradling and Rubin, 1982). Micro-injection of P-element vectors into pre-blastoderm embryos in the presence of a transposase facilitates the integration of P-elements into the host genomic DNA. If inserted into the germline, this gives rise to a small percentage of transgenic animals in the progeny. The transposase activity is supplied *in trans* either by co-injection of DNA encoding the transposase or genetically. Thus, transgenic *Drosophila* lines exist that contain an engineered highly active version of the transposase (Δ2-3). The open reading frame (ORF) of the transposase is separated into four exons. The presence of the 2-3 intronic sequences in alternatively spliced messenger RNAs (mRNAs, the predominant mRNA species outside of the germline) results in the expression of a truncated version of the transposase, which is not fully active. The engineered transposase gene lacking the 2-3 intronic sequence and the flanking sequence recognition elements efficiently mobilise P-element vectors *in trans* (Robertson et al., 1988). The lack of sequence recognition elements prevents the transposase from "jumping" around in the genome. To avoid continuous remobilisation of the inserted P-element, the transposase is crossed out in the next generation.

1.2.2.2 P-elements as a tool for generating LOF mutants

Injected P-element vectors will integrate randomly into the host genomic DNA including the coding regions of the genome. This provides a method for generating LOF mutations (Salz et al., 1987; Tsubota and Schedl, 1986). Moreover,

mobilisation of P-elements inserted in the vicinity of a gene of interest, by reintroducing the Δ2-3 transposase, can facilitate the generation of LOF mutants. Thus, approximately 2% of mobilised P-elements are imprecisely excised resulting in the deletion of DNA on either or both sides of the insertion point. A large collection of *Drosophila* lines carrying P-element insertion in or near most coding sequences exists, and mobilisation of P-elements has become the most frequent tool for generating LOF mutants in *Drosophila* (Bellen et al., 2004).

1.2.2.3 Generation of mosaic tissue using the FLP-FRT system

Inducing LOF in small areas of tissue (clones) provides a means of bypassing early lethality and studying phenotypes later in development (Perrimon, 1998). The Flip recombinase (FLP)-Flip recombinase target (FRT) system provides a method for generating mosaics of wildtype (wt) and LOF tissue in heterozygous animals. Thus, FRT sequences have been inserted transgenetically near the centromere of each chromosome arm in *Drosophila* (Xu and Rubin, 1993). The expression of FLP *in trans* induces recombination between FRTs at identical sites on homologous chromosomes (Figure 1-2). Usually the mutation of interest is recombined onto a FRT-containing chromosome arm and transgenic flies are crossed to flies harbouring an FRT at an identical position and a visible marker such Green fluorescent protein (GFP) at a more distal position of the chromosome arm (Xu and Rubin, 1993). The FLP transgene is mostly supplied on another chromosome of the FRT-GFP line. Upon expression of FLP, a small number of cells undergo mitotic recombination, giving rise to mosaics of wt (two copies of GFP) and mutant (lack of GFP) tissue surrounded by heterozygous tissue (one copy of GFP) (Figure 1-2). Since, the mutant clones and neighbouring wt twin-spots arise at the same time from a single mitotic recombination event, the wt clones provide an internal control for studying the phenotype of their mutant twins. Moreover, the activity of FLP and therefore mitotic recombination can be temporally and spatially controlled by placing FLP under the control of a heat shock or tissue-specific promoter (Newsome et al., 2000; Xu and Rubin, 1993).

1.2.2.4 The GAL4/UAS system

The GAL4/UAS system is widely used in flies to study over-expression and LOF phenotypes. GAL4 binds to upstream activating sequence (UAS) promoter elements and induces the expression of genes downstream from the promoter region

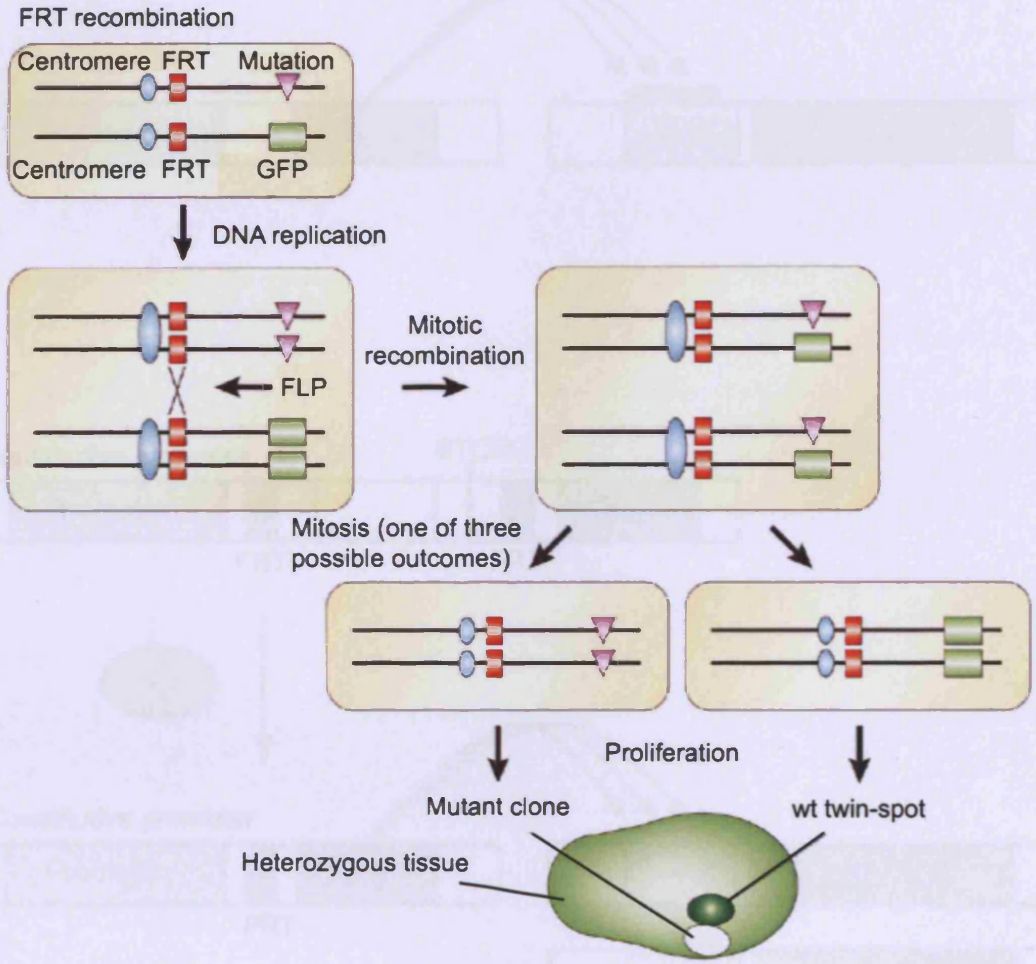

Figure 1-2: FLP-FRT system. FLP induces recombination between FRT sites at identical positions on homologous chromosome arms during mitosis. Usually, transgenic animals carry the mutation of interest on one FRT-containing chromosome and a visible marker like GFP on the other. During S phase each chromosome arm is duplicated, and upon entry into mitosis FLP-dependent mitotic recombination can occur between FRT sites on homologous chromosome arms. Mitotic recombination followed by mitosis gives rise to three outcomes (depending on chromosome segregation). Cells can either have two copies of the mutation (mutant clones, marked by absence of GFP), two copies of GFP (wt twin-spot) or one of each as before mitosis (heterozygous tissue, one copy of GFP). Because mutant clones and their neighbouring wt twin-spots are generated from the same recombination event, the twin-spot functions as an internal control that allows the phenotype of mutant tissue to be assessed. Adapted from (Tabata, 2001).

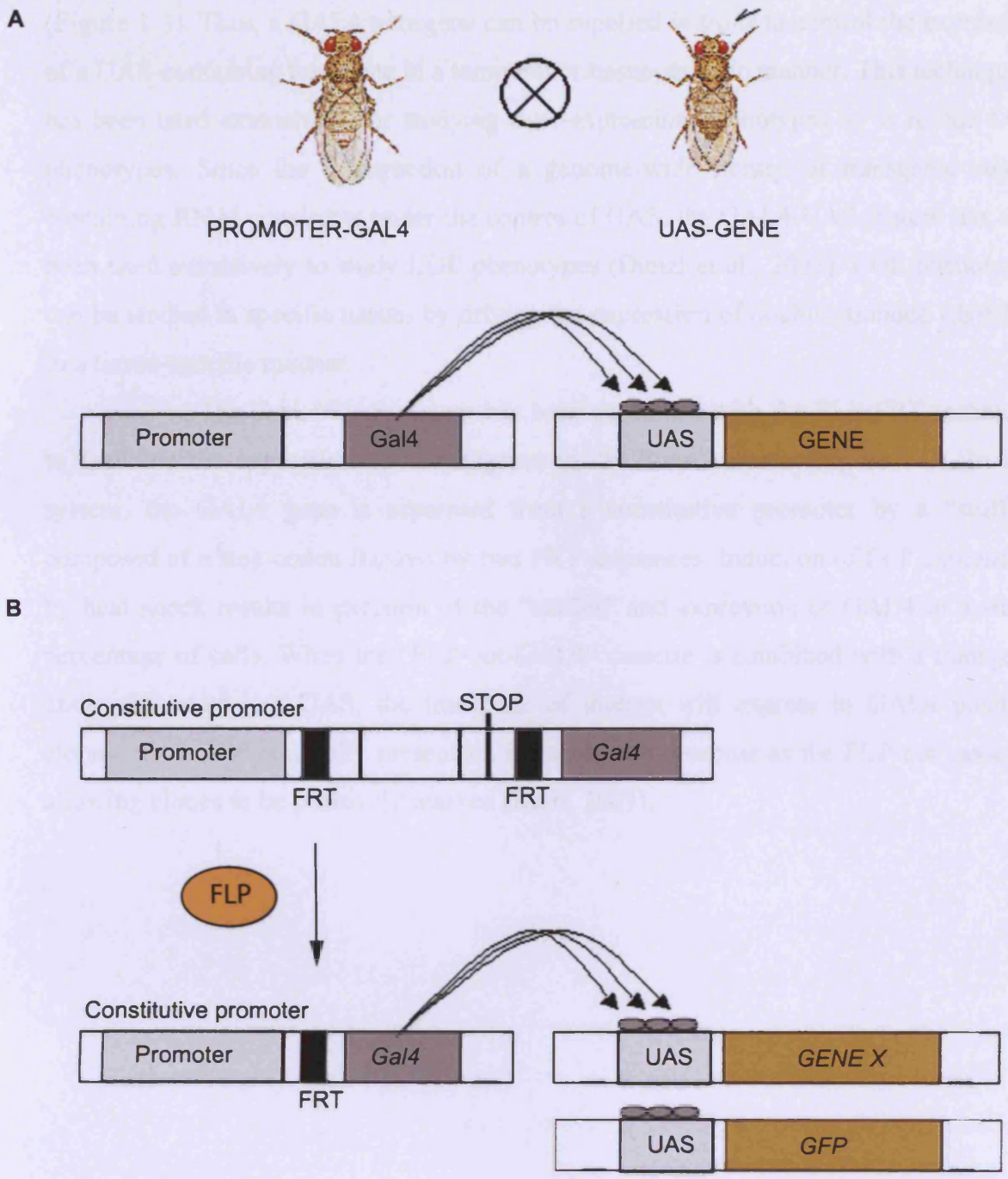

Figure 1-3: The Gal4-UAS system and FLPout technique. Gal4 binds to UAS promoter elements and induces the expression of genes downstream from the promoter region (A). Usually, flies carrying the *gal4* transgene under the control of a tissue-specific promoter are crossed to flies carrying the gene of interest (*gene X*) under the control of the UAS promoter. As a result, *gene X* is expressed in a tissue-specific manner in the progeny. LOF phenotypes can be studied using the Gal4-UAS system if *gene X* is replaced with an RNAi contruct. The GAL4-UAS system has been combined with the FLP-FRT technique to facilitate the temporally controlled expression of a transgenes in "FLP-out" clones (B). Thus, a casette containing a transcriptional stop signal with a FRT site on either side can be inserted between a constitutive promoter and the Gal4-encoding sequence. In the presence of a FLPase, mitotic recombination results in excision of the stuffer and ubiquitous expression of Gal4 in a small number of cells. As a result, gain of function or LOF phenotypes can be studied in clones. Clones can be positively labelled if flies carry an UAS-*GFP* transgene. Moreover, Gal4 expression can be temporarily controlled if the FLPase is placed under the control of a heat shock promoter.

(Figure 1-3). Thus, a GAL4 transgene can be supplied *in trans* to control the expression of a UAS-containing transgene in a temporal or tissue-specific manner. This technique has been used extensively for studying over-expression phenotypes or to rescue LOF phenotypes. Since the construction of a genome-wide library of transgenic stocks containing RNAi constructs under the control of UAS, the GAL4-UAS system has also been used extensively to study LOF phenotypes (Dietzl et al., 2007). LOF phenotypes can be studied in specific tissues by driving the expression of double-stranded (ds)RNA in a tissue-specific manner.

The GAL4/UAS system has been combined with the FLP-FRT technique to facilitate the expression of a transgenes in "FLP-out" clones (Figure 1-3). In this system, the GAL4 gene is separated from a constitutive promoter by a "stuffer" composed of a stop codon flanked by two FRT sequences. Induction of FLP expression by heat shock results in excision of the "stuffer" and expression of GAL4 in a small percentage of cells. When the "FLP-out-GAL4" cassette is combined with a transgene under the control of UAS, the transgene of interest will express in GAL4 positive clones. *UAS-GFP* is usually present on the same chromosome as the FLP-out cassette, allowing clones to be positively marked (Blair, 2003).

1.3 RNA polymerase (RNAP) II Transcription

In eukaryotes there are three RNA polymerases, RNAP I-III, all of which are closely related in structure. Thus, each RNAP complex consists of two large subunits and at least 8 additional subunits, some of which are common to two or all three RNA polymerases. Despite the similar structures, the RNA polymerases have non-overlapping functions. RNAP I is responsible for transcription of rRNA precursors, RNAP II transcribes all protein-encoding genes and some small nuclear RNA genes, and RNAP III is mainly responsible for the transcription of 5S RNA and tRNAs. As previously mentioned, one of the four *Drosophila* protein characterised in my thesis (dMCRS2) is likely to be implicated in regulation of RNAP II transcription. Hence, this section has been dedicated to provide the reader with an overview of the various aspects of RNAP II transcription including pre-initiation complex assembly, transcription initiation and elongation, regulation of RNAP II transcription by activators/chromatin remodellers, and the interplay between RNAP II transcription and pre-mRNA processing.

1.3.1 Assembly of the RNA polymerase II pre-initiation complex

The initiation of mRNA transcription involves the assembly of a transcription pre-initiation complex (PIC) which as a minimum includes RNAP II, the Mediator, and six general transcription factors (GTFs) designated Transcription factor (TF) IIA, -B, -D, -E, -F, and –H at the core promoter DNA region (Lee and Young, 2000; Orphanides et al., 1996; Roeder, 1996). PIC assembly is initiated by binding of the TATA-box binding protein (TBP) subunit of TFIID to the promoter, which is stabilised in the presence of TFIIA and the Mediator (Figure 1-4). Subsequently, TFIIB binds to and stabilises the TFIIA-TFIIB-Mediator-DNA complex, and functions as an adaptor that recruits the pre-formed RNAP II-TFIIF complex to the promoter. TFIIE and TFIIH join at the end to form the complete PIC.

1.3.1.1 TFIID

TFIID consists of TBP and at least 14 TBP-associated factors (TAFs) (reviewed in (Albright and Tjian, 2000)). TATA box recognition by TBP is considered

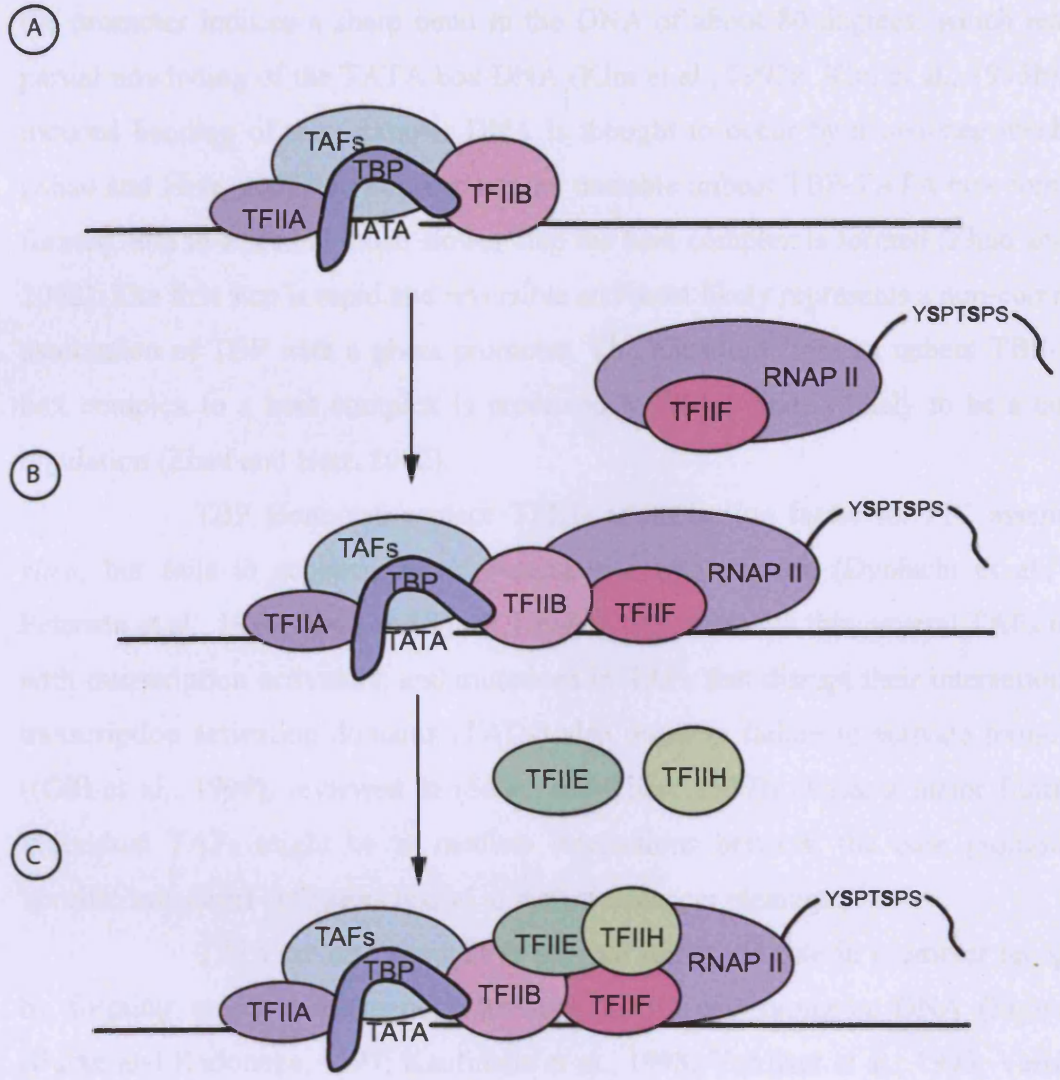

Figure 1-4: RNAP II PIC assembly. The first and rate-limiting step in PIC assembly is binding of TFIID via TBP to the TATA box. The TFIID complex is composed of TBP and at least 14 TBP-associated factors (TAFs), some of which interact with other promoter elements. The association of TBP with the TATA box is greatly stabilised in the presence of the GTFs TFIIA and TFIIB (A). TFIIB binds to TFIID and promoter DNA and functions as an adaptor to recruit the pre-formed TFIIF-RNAP II unit to the promoter-bound TFIID-TFIIA-TFIID complex (B). The Rpb1 subunit of the RNAP II complex contains an extended CTD, which consists of multiple heptapeptide repeats. Finally, TFIIF promotes the recruitment of TFIIE and TFIIH to form the complete RNAP II PIC (C). The kinase and helicase activities of TFIIH are absolutely essential for the subsequent events leading to transcription initiation.

the rate-limiting step in PIC assembly (Ranish et al., 1999). Thus in many cases, activators increase the binding of TBP to promoters in direct proportion to their activity in transcription activation (Kuras and Struhl, 1999; Li et al., 1999). Binding of TBP to the promoter induces a sharp bend in the DNA of about 80 degrees, which results in partial unwinding of the TATA box DNA (Kim et al., 1993a; Kim et al., 1993b). TBP-induced bending of the promoter DNA is thought to occur by a two-step mechanism (Zhao and Herr, 2002). In the first step an unstable unbent TBP-TATA box complex is formed, and in a second much slower step the bent complex is formed (Zhao and Herr, 2002). The first step is rapid and reversible and most likely represents a non-committing association of TBP with a given promoter. The transition from an unbent TBP-TATA box complex to a bent complex is promoted by TFIIB and is likely to be a target of regulation (Zhao and Herr, 2002).

TBP alone can replace TFIID as nucleation factor for PIC assembly *in vitro*, but fails to support activator-dependent transcription (Dynlacht et al., 1991; Peterson et al., 1990; Pugh and Tjian, 1990). Consistent with this, several TAFs interact with transcription activators, and mutations in TAFs that disrupt their interactions with transcription activation domains (TADs) also result in failure to activate transcription ((Gill et al., 1994), reviewed in (Sauer and Tjian, 1997)). Thus, a major function of individual TAFs might be to mediate interactions between the core promoter and specific subsets of activators bound to distant enhancer elements.

TAFs are also thought to play an important role in promoter recognition by forming multiple interactions between TFIID and promoter DNA (Figure 1-5) (Burke and Kadonaga, 1997; Kaufmann et al., 1998; Verrijzer et al., 1995; Verrijzer et al., 1994). This is important because TBP associates weakly with some TATA box-containing promoters and in the case of TATA-less promoters, binding of TBP to the promoter is critically dependent on the presence of factors bound to initiator elements (INRs) and downstream promoter elements (DPEs) (Burke and Kadonaga, 1996; Kaufmann and Smale, 1994; Purnell et al., 1994; Verrijzer et al., 1995). In humans, it has been estimated that more than 78% of promoters lack a TATA-box (Gershenzon and Ioshikhes, 2005). There are several lines of evidence that binding of TAFs to INRs and DPEs stabilises the interaction of TBP with the promoter region. First, human TAF6 and TAF9 exhibit DPE-specific binding activity (Shao et al., 2005). Second, human TAF1 and *Drosophila* dTAF2 bind directly to INRs, and human TAF2 was found to be an essential co-factor for TFIID-dependent transcription from INR-

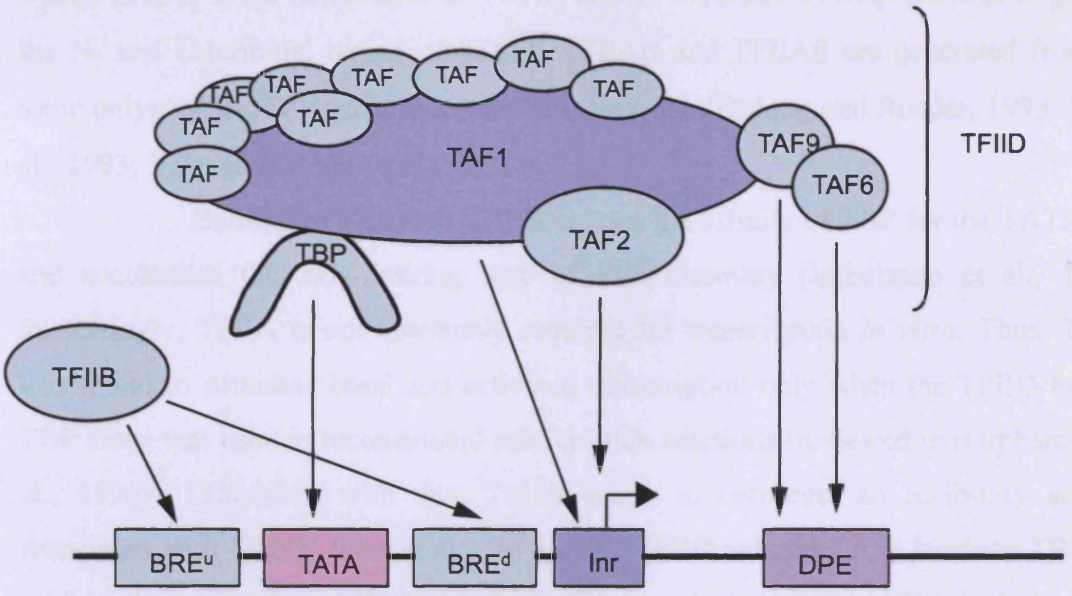

Figure 1-5: TFIIB and TAFs bind to promoter-specific elements. In addition to the TATA box, several other promoter elements have been identified that affect promoter strength. These include Inrs, DPEs, and TFIIB recognition elements (BREs) located upstream or downstream of the TATA box (BRE^u and BRE^d). TAF2, TAF6, and TAF9 are thought to stabilise the binding of TFIID to the promoter by interacting with Inrs and DPEs. This is especially important on TATA-less promoters. The association of TFIID with the promoter is further stabilised in the presence of TFIIB, which interacts with the BRE^u and BRE^d promoter elements. BRE^u and BRE^d seem to behave antagonistically. Thus, the presence of either element stimulates transcription, but BRE^d appears negatively affect transcription in the presence of BRE^u. Adapted from (Thomas and Chiang, 2006).

containing promoters (Kaufmann et al., 1998; Verrijzer et al., 1994). Third, TFIID binds cooperatively to INR and DPE since mutation in either of the two elements or variation in their spacing results in loss or decreased binding of TFIID to the core promoter and reduced levels of basal transcription (Burke and Kadonaga, 1996, 1997; Kutach and Kadonaga, 2000).

1.3.1.2 TFIIA

In yeast, TFIIA is composed of two subunits, TOA1 and TOA2 (Ranish et al., 1992). Human TFIIA consists of three subunits, TFIIAα, TFIIAβ, and TFIIAγ, where TFIIAγ is the homologue of TOA2, and TFIIAα and TFIIAβ are homologous to the N- and C-terminal region of TOA1. TFIIAα and TFIIAβ are generated from the same polypeptide, TFIIAαβ, by proteolytic cleavage (DeJong and Roeder, 1993; Ma et al., 1993; Yokomori et al., 1993).

Binding of TFIIA to TBP increases the affinity of TBP for the TATA-box and accelerates this rate-limiting step of PIC assembly (Imbalzano et al., 1994). Surprisingly, TFIIA is not absolutely required for transcription *in vitro*. Thus, TFIIA was found to stimulate basal and activated transcription only when the TFIID but not TBP alone was used in reconstituted transcription reactions (reviewed in (Orphanides et al., 1996)). Consistent with this, TFIIA seems to derepress an inhibitory activity associated with TFIID (Ozer et al., 1998). The TFIID subunit TAF1 binds to TBP and inhibits the interaction of TBP with the TATA-box (Kokubo et al., 1993; Kokubo et al., 1998; Verrijzer et al., 1995). TFIIA competes with the TAF1 subunit of TFIID for binding to TBP, and binding of TFIIA to TBP is thought to repress the transcriptional inhibitory activity of TAF1 (Ozer et al., 1998). It is not clear how TFIIA competes with TAF1 for binding to TBP, given that TBP and TAF1 are already pre-assembled in the TFIID complex. It is well established that TFIIA is required for activator-mediated conformational changes in TFIID, which stimulates interactions of TFIID with sequences downstream of the transcriptional start site (Lieberman and Berk, 1994; Ozer et al., 1994). Thus, the conformational changes induced upon binding of TFIIA to TBP/TFIID might destabilise the association of TAF1 with TBP leading to transcriptional derepression (Ozer et al., 1998).

TFIIA may not solely derepress TBP inhibition by interfering with TAF1. Thus, TFIIA has been reported to compete with other negative factors for binding to TBP including Mot1 and NC2. Mot1 disrupt pre-formed TBP-TATA complexes in an

ATP-dependent manner, and this is prevented by binding of TFIIA to the TBP-TATA complex (Auble and Hahn, 1993). NC2 binds to TBP after its association with the TATA box and blocks the interaction of this complex with TFIIB *in vitro* (Meisterernst and Roeder, 1991). TFIIA competes with NC2 for binding to TBP, and a recent study suggests that a TAF-dependent INR bound activity shifts the equilibrium in favour of TFIIA (Malecova et al., 2007). Thus, the presence of a functional INR provides resistance to NC2-mediated transcriptional repression (Malecova et al., 2007).

Studies carried out *in vitro* and *in vivo* indicate that TFIIA might be required for transcription of only a subset of TFIID-dependent genes (reviewed in (Thomas and Chiang, 2006)). However unlike TAFs, TFIIA is present at all promoters with an occupancy that strongly correlates with that of TBP (Kuras et al., 2000). Thus, it remains to be determined whether in addition to its function in derepression, TFIIA has a more general function in transcription.

1.3.1.3 TFIIB

TFIIB is composed of a single polypeptide, which interacts with TBP and forms multiple contacts with the core promoter, thereby stabilising the TBP/TFIID-TATA complex (Zhao and Herr, 2002). It binds to specific TFIIB recognition elements located either upstream (BRE^u) (Lagrange et al., 1998) or downstream (BRE^d)(Deng and Roberts, 2005, 2006) of the TATA box, and the presence of either element enhance TFIIB-TBP-TATA complex formation (Figure 1-5) (Deng and Roberts, 2005, 2006; Lagrange et al., 1998). Interestingly, BRE^d can have either positive or negative effects on transcription in a promoter-dependent manner (Deng and Roberts, 2005). Thus, the negative effect of BRE^d appears to correlate with the presence of BRE^u suggesting that the two elements might act antagonistically (Deng and Roberts, 2005).

TFIIB plays a central role in PIC assembly by providing a bridge between promoter bound TBP/TFIID and RNAP II and is absolutely required for the recruitment of the pre-formed TFIIF-RNAP II complex (Buratowski et al., 1989; Reinberg and Roeder, 1987; Sawadogo and Roeder, 1985). Consistent with this, TFIIB forms multiple interactions with TBP, three subunits of RNAP II (RPB1, RPB2, and RPB9), both subunits of TFIIF (RAP30 and RAP74), and the TFIID subunit TAF9 (reviewed in (Deng and Roberts, 2007)). In addition to its crucial function in PIC assembly, TFIIB also interacts with multiple activators and plays a role in activated transcription (reviewed in (Deng and Roberts, 2007)).

Upon transcription initiation, TFIIB dissociates from the PIC and does not continue along with elongating RNAP II (Roberts et al., 1995; Zawel et al., 1995). Mutations in TFIIB have been reported that are compatible with PIC assembly, but prevent transcription initiation, indicating that a step post-assembly is blocked in these mutants (reviewed in (Deng and Roberts, 2007)). It is possible that those mutations affect promoter clearance (discussed later) by interfering with TFIIB dissociation from the RNAP II complex.

1.3.1.4 TFIIF

TFIIF, which is composed of two subunits Rap30 and Rap74, enters the TFIIA-TFIID-TFIIB-TATA complex as a preformed TFIIF-RNAP II unit. The small subunit, Rap30, is sufficient for RNAP II recruitment and PIC assembly (Flores et al., 1991). Consistent with this, Rap30 forms multiple interactions with TFIIB (Ha et al., 1993), RNAP II (McCracken and Greenblatt, 1991), and DNA (Tan et al., 1994b). Importantly, a major function of TFIIF is to prevent RNAP II from binding non-specifically to DNA, and this requires both TFIIF subunits (Killeen and Greenblatt, 1992). Moreover, the large subunit, Rap74, has been implicated in transcription start site selection. Thus, a mutation in the yeast TFIIB gene that causes aberrant start site selection is suppressed by mutations in the gene encoding the yeast Rap74 homologue (Sun and Hampsey, 1995).

In addition to its function in PIC assembly, TFIIF is also required for the subsequent formation of an open complex catalysed by the TFIIH DNA helicase and for synthesis of the first phosphodiester bond of nascent transcripts. The requirement for TFIIF in these processes might be indirect, since TFIIF is needed for the recruitment of TFIIE and TFIIH into the PIC (Maxon et al., 1994). However, the ability of TFIIF to induce wrapping of promoter DNA around RNAP II could directly facilitate formation of an open complex (Robert et al., 1998). Moreover, TFIIF was found to function in promoter escape by increasing the processivity of very early RNAP II elongation intermediates, thus suppressing early abortive transcription, and by cooperating with TFIIH to prevent premature arrest of early RNAP II elongation intermediates (Yan et al., 1999). Finally, TFIIF cooperates with the elongation factor TFIIS to stimulate re-initiation of paused elongation complexes at the 5' end of the gene (Zhang and Burton, 2004).

Following transcription initiation, TFIID remains promoter-bound whereas TFIIB rapidly dissociates from the PIC, followed by TFIIE dissociation prior to formation of the 10th phosphodiester bond, and TFIIH after the transcription complex reaches +30. TFIIB, TFIIE, TFIIE, and TFIIH re-associate with TFIID to form a new PIC nucleation site, whereas TFIIF appears to reversibly associate with the elongating RNAP II complex (Yudkovsky et al., 2000; Zawel et al., 1995). Consistent with this, TFIIF was found to increase the elongation rate of RNAP II *in vitro* (Cheng and Price, 2007; Tan et al., 1994a). Moreover, positive transcription elongation factor b (P-TEFb)-mediated phosphorylation of the negative elongation factor (NELF) results in its dissociation from the RNAP II complex and allows TFIIF to associate with RNAP II to stimulate productive elongation *in vitro* (Cheng and Price, 2007). Intriguingly, TFIIF associates with promoter regions rather than open reading frames of genes *in vivo* (Krogan et al., 2002; Pokholok et al., 2002). Thus it is possible that like TFIIS, TFIIF only associates with coding regions under stress or suboptimal transcription-elongation conditions to facilitate release of RNAP II from a stalled state (Pokholok et al., 2002).

1.3.1.5 TFIIE

TFIIE enters the PIC after the TFIIF-RNAP II unit. Human TFIIE is a $\alpha_2\beta_2$ hetero-tetramer composed of the two highly charged subunits TFIIEα and TFIIEβ (Ohkuma et al., 1990). It interacts with TFIIB, the unphosphosphorylated form of RNAP II (RNAP II_A), both subunits of TFIIF, and TFIIH (reviewed in (Orphanides et al., 1996)). Moreover, it is required for the incorporation of TFIIH into the PIC and for regulation of its kinase and helicase activities (Lu et al., 1992; Ohkuma and Roeder, 1994).

Like TFIIF, TFIIE has been implicated in early events of RNAP II elongation. Thus, TFIIF, TFIIE, and TFIIH are thought to function in a cooperative manner to suppress arrest of early RNAP II elongation intermediates by a mechanism that involves the DNA helicase activity of TFIIH (Dvir et al., 1996; Kugel and Goodrich, 1998; Kumar et al., 1998). Consistent with this, TFIIEα and TFIIEβ both interact with the TFIIH-associated DNA helicase, xeroderma pigmentosum B (XPB) (Maxon et al., 1994). Intriguingly, the interaction of XPB with TFIIEα/β seems to be inhibitory (Drapkin et al., 1994), whereas TFIIEβ alone is capable of stimulating the helicase activity of XPB (Lin and Gralla, 2005). Thus, the positive role of TFIIE in transcription initiation is best explained by structural rearrangements during

transcription initiation that result in TFIIEβ activation through TFIIEα repression. Moreover, TFIIE and TFIIH are both essential for promoter melting and transition from initiation to elongation (Holstege et al., 1996). Consistent with this, TFIIE is capable of binding to single stranded DNA, and TFIIE and TFIIH are dispensable for transcription from pre-melted promoters (Holstege et al., 1996; Kuldell and Buratowski, 1997; Pan and Greenblatt, 1994).

1.3.1.6 TFIIH

TFIIH is the final GTF to join the PIC and is absolutely required for transcription initation. TFIIH is composed of 6 core subunits including p34, p44, p52, p62, and the DNA and DNA-RNA helicases XPB and XPD. In addition, TFIIH contains three more loosely associated subunits, which make up the cyclin activating kinase (CAK) complex. The CAK complex consists of the cyclin-dependent kinase 7 (Cdk7)/Kin28 (humans/yeast), its partner Cyclin H, and the MAT1 (ménage-a-trois-1) protein (Devault et al., 1995; Fesquet et al., 1993; Fisher and Morgan, 1994; Tassan et al., 1995).

TFIIH has several functions in RNAP II transcription including mediating ATP-dependent promoter DNA opening (Holstege et al., 1997), phosphorylation of the RNAP II C-terminal domain (CTD) through its association with CAK (Feaver et al., 1994), and suppression of transcription arrest of early RNAP II elongation complexes (Spangler et al., 2001). The XPB DNA helicase catalyses both the ATP-dependent formation of the open complex prior to transcription (Tirode et al., 1999) and the ATP-dependent suppression of arrest of early elongation intermediates prior to promoter escape (Bradsher et al., 2000; Moreland et al., 1999). In contrast, XPD activity appears to be dispensable for transcription initiation and promoter escape (Bradsher et al., 2000; Tirode et al., 1999). Instead, the ATP-dependent helicase activities of both XPB and XPD are involved in unwinding of DNA during nucleotide excision repair (NER). (Coin et al., 1998; Dubaele et al., 2003).

In the process of promoter clearance and early transcription elongation RNAP II becomes hyper-phosphorylated and pre-existing interactions with transcription initiation-specific factors are disrupted and new interactions with elongation-specific factors are established. The TFIIH-associated CAK activity plays a crucial role in this transition from initiating to elongating RNAP II. Thus, phosphorylation of the CTD of RNAP II by the CAK-associated kinase Cdk7 results in the dissociation of RNAP II

from most of the basal transcription factors (Yudkovsky et al., 2000; Zawel et al., 1995).

1.3.2 The Mediator complex

RNAP II transcription levels depend on the interaction of RNAP II with GFTs that regulate basal transcription from core promoters and a wide range of gene-specific transcription factors that bind to distant regulatory elements. A co-activator complex named the Mediator has been implicated in establishing a link between factors present at those distant regulatory elements and the basal RNAP II complex bound to the core promoter (Bjorklund and Gustafsson, 2005; Kornberg, 2005; Thomas and Chiang, 2006).

1.3.2.1 Purification of the Mediator complex

The Mediator was originally purified from yeast and is composed of approximately 20 subunits that have been divided into head, middle, and tail sub-modules (reviewed in (Boube et al., 2002)). In addition, a sub-module, which contain the Cyclin C-Cdk8 pair, is associated with a subset of yeast Mediator complexes (reviewed in (Carlson, 1997)). Attempts to purify the mammalian Mediator initially led to the purification of a number of complexes with overlapping, but non-identical compositions (reviewed in (Boube et al., 2002)). Subsequently, a more sensitive proteomics method led to the purification of a 30 subunit mammalian Mediator complex, which contained all of the previously purified Mediator-like sub-complexes (Sato et al., 2004). Bioinformatic analyses revealed that all but three yeast Mediator subunits are conserved in the mammalian Mediator complex (reviewed in (Conaway et al., 2005a; Conaway et al., 2005b)).

1.3.2.2 The Mediator is required for basal and activated levels of transcription

The Mediator is required for basal transcription, but also functions to activate transcription by mediating signals from transcription activators bound to distant enhancer elements to the RNAP II promoter (reviewed in (Conaway et al., 2005b)) (Figure 1-6). The requirement for Mediator in basal transcription is most likely explained by the cooperative binding of the Mediator and TBP to the core promoter (Johnson et al., 2002; Wu et al., 2003b). It has been proposed that transcriptional activators function by stabilising the TFIID/TFIIA-Mediator complex at the promoter,

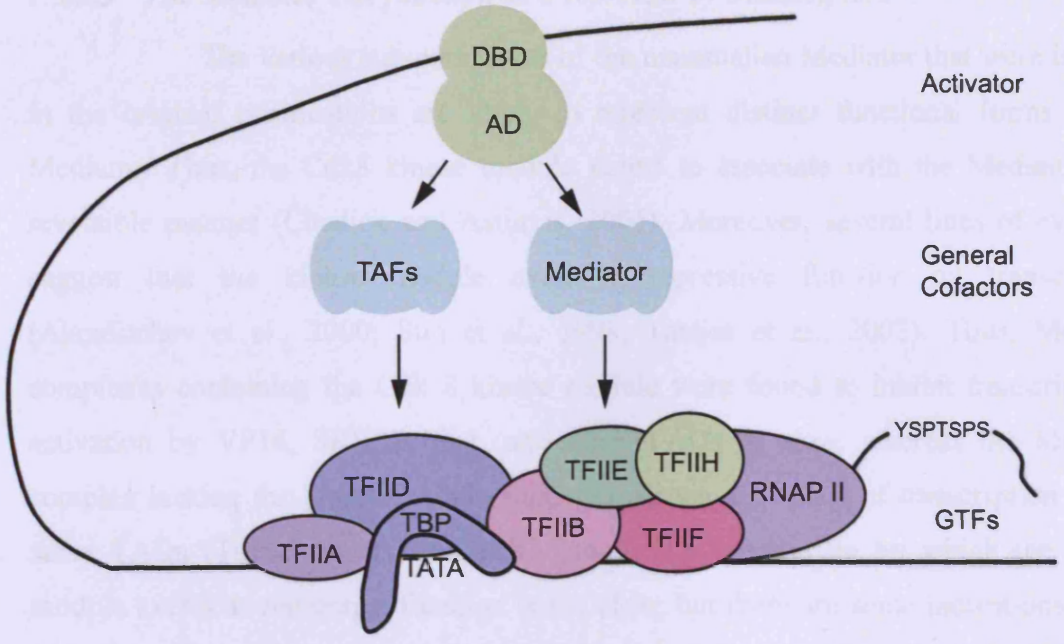

Figure 1-6: The Mediator and TAFs function as general transcriptional co-factors. The Mediator is a multi-subunit complex, which plays a crucial role in basal and activated transcription. Like TAFs, it stimulates basal transcription by stabilising the interaction of TBP with the promoter. Thus, TBP and the Mediator binds to the promoter in a cooperative manner. Moreover, the Mediator and TAFs interact with transcription activators bound to distal promoter elements. This provides a link between the general transcription machinery and gene-specific transcriptional activators, and explains the requirement for TAFs and the Mediator in activated transcription. Adapted from (Thomas and Chiang, 2006).

which in turn stimulate the efficiency and/or rate of transcription initiation complex assembly. Consistent with this, the model activator GAL4-VP16, the Mediator and TFIID/TFIIA assemble onto the promoter in a cooperative manner *in vitro* (Johnson et al., 2002), and the requirement for the activator can be bypassed by pre-assembly of saturating amounts of the Mediator-TFIID/TFIIA complex onto the promoter (Johnson and Carey, 2003). Moreover, under these conditions basal levels of transcription are increased to activated levels (Johnson and Carey, 2003).

1.3.2.3 The Mediator can function as a repressor of transcription

The various sub-complexes of the mammalian Mediator that were isolated in the original purifications are likely to represent distinct functional forms of the Mediator. Thus, the Cdk8 kinase module seems to associate with the Mediator in a reversible manner (Chadick and Asturias, 2005). Moreover, several lines of evidence suggest that the kinase module exerts a repressive function on transcription (Akoulitchev et al., 2000; Sun et al., 1998; Taatjes et al., 2002). Thus, Mediator complexes containing the Cdk 8 kinase module were found to inhibit transcriptional activation by VP16, SREBP, Sp1, and other TADs *in vitro*, whereas the Mediator complex lacking the kinase module supported strong activation of transcription by the same TADs (Taatjes et al., 2002). The molecular mechanism by which the kinase module exerts its repressive function is not clear, but there are some indications. First, the presence of the kinase module might disrupt the interaction between the Mediator and RNAP II. Thus, the Mediator binds to an immobilised Gluthionine S transferase (GST)-tagged CTD fusion protein in absence, but not in the presence, of the kinase module (Naar et al., 2002). Second, the Cdk8-cyclin C complex is capable of phosphorylating the cyclin H subunit of mammalian TFIIH, thereby blocking CAK activity and transcription (Akoulitchev et al., 2000). Third, the kinase module appears to target some transcription activators for phosphorylation and degradation (Fryer et al., 2004). Thus, it has been demonstrated that the Cdk8 kinase is recruited to the promoter of the Notch responsive *HES1* gene shortly after its activation. Subsequently, Cdk8-dependent phosphorylation of the Notch intracellular domain targets it for ubiquitination and degradation and shuts down transcription from the *HES1* promoter (Fryer et al., 2004).

1.3.3 The CTD

RNAP II is composed of 12 subunits. The two largest subunits, Rpb1 and Rbp2, form the catalytic centre of the enzyme, and Rpb3-12 surround these two subunits to provide structural support and regulate RNAP II activity. RNAP II differs from the other two eukaryotic RNA polymerase in that Rpb1 has an extended CTD, which is composed of multiple heptapeptide repeats with the consensus sequence Tyr-Ser-Pro-Thr-Ser-Pro-Ser ($Y_1S_2P_3T_4S_5P_6S_7$) (Dahmus, 1995). Due to its hydrophilic nature, the CTD is thought to adopt an extended flexible structure (Bienkiewicz et al., 2000; Cagas and Corden, 1995) that serves as a platform to coordinate the assembly of multiple complexes associated with RNAP II transcription. These complexes not only include factors that are required for RNAP II transcription but also proteins involved in mRNA capping, pre-mRNA processing, and 3' end cleavage and polyadenylation (Corden and Patturajan, 1997; Goldstrohm et al., 2001; Maniatis and Reed, 2002; Proudfoot et al., 2002). Thus, the CTD is likely to be implicated in multiple steps of mRNA synthesis. Consistent with this, *in vitro* studies of a truncated form of the CTD has been shown to affect not only RNAP II translation initiation and/or early elongation (Meininghaus et al., 2000) but also pre-mRNA processing (Hirose and Manley, 2000).

1.3.3.1 Phosphorylation of the CTD

The RNAP II exists as two complexes with a non- (RNAP II_A) or hyper-phosphorylated (RNAP II_0) CTD subunit. The RNAP II_A complex is thought to engage in promoter binding and early events in the transcription cycle, whereas elongation requires hyper-phosphorylation of RNAP II. Thus, RNAP II_A-specific staining of *Drosophila* polytene chromosomes mostly coincides with inactive genes or polymerases paused at promoter-proximal sites, and RNAP II_0-specific staining with sites of active transcription (O'Brien et al., 1994; Weeks et al., 1993).

The "II_0" designation does not refer to one hyper-phosphorylated RNAP II species, but rather to a heterogeneous group of RNAP IIs with different phosphorylation patterns. CTD phosphorylation occurs predominantly on Ser2 and Ser5 of the repeats, and the phosphorylation pattern changes as RNAP II progresses through the transcription cycle (Figure 1-7) (Dahmus, 1995, 1996). Phosphorylation of Ser5 takes place early on in the transition from pre-initiation to elongation and depends on the activity of the TFIIH-associated kinase Cdk7/Kin28 (Komarnitsky et al., 2000; Schroeder et al., 2000). Subsequently, Ser2s are phosphorylated by the elongation phase

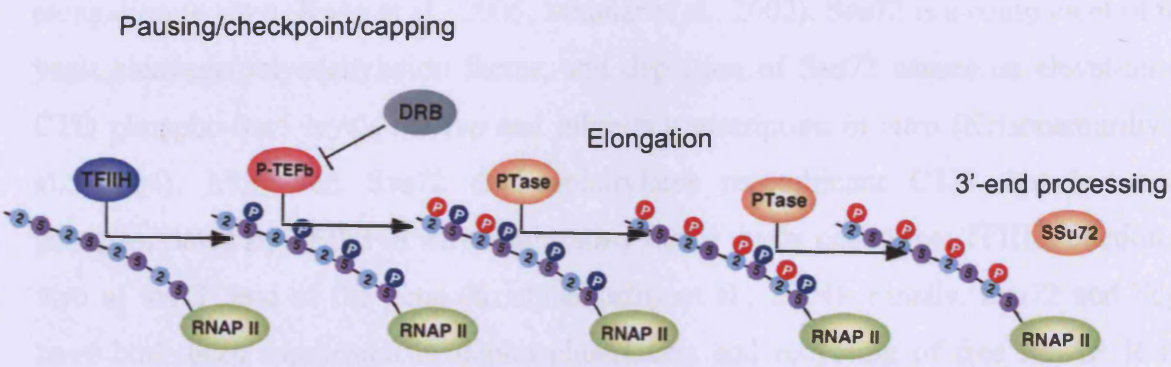

Figure 1-7: The phosphorylation pattern of the CTD changes as RNAP II progresses through the transcription cycle. Transcription initiation requires the activity of the TFIIH-associated Cdk7/Kin28 kinase, which phosphorylates the RNAP II CTD on Ser5s. TFIIH associates with early elongating RNAP II complexes, but dissociates from RNAPII after about 30 nucleotides. The RNAP II enters a pausing phase that is thought to be linked with a capping checkpoint. Proficient elongation requires the action of Cdk9/CTDK-1, which together with its partner cyclin T forms the DRB sensitive positive elongation factor b (P-TEFb). P-TEFb associates with elongating RNAP II and phosphorylates the CTD on Ser2s as RNAP II progresses through the coding region. Towards the 3'end of the coding region, the CTD becomes dephosphorylated on Ser5s by Ser5-specific phosphatases like the yeast Fcp1 and Ssu72 proteins. This change in phosphorylation pattern coincide with the recruitment of 3'-end processing factors that preferentially bind to the Ser2-phosporylated form of the CTD. Adapted from (Sims et al., 2004).

kinase CTDK-1 (Cdk9 in metazoans) to generate elongation proficient RNAP II_0 (Lee and Greenleaf, 1997; Marshall et al., 1996). Towards the 3' end of the gene RNAP II_0 appear to be phosphorylated mainly on Ser2s, indicating that a Ser5-specific phosphatase is involved at some stage (reviewed in (Meinhart et al., 2005)).

A number of CTD phosphatases that dephosphorylate Ser5 have been identified including human and yeast CTD phosphatase 1 (Fcp1) and yeast Ssu72 (Chambers et al., 1995; Kong et al., 2005; Krishnamurthy et al., 2004). Fcp1 associates with TFIIF and stimulates dephosphorylation of RNAP II_0 Ser5 *in vitro* in a reaction that is stimulated by TFIIF and inhibited by TFIIB (reviewed in (Meinhart et al., 2005))(Chambers et al., 1995; Kong et al., 2005)). Moreover, cells lacking Fcp1 accumulates hyper-phosporylated RNAP II specifically in coding regions of genes (Cho et al., 2001; Kobor et al., 1999). Consistent with this, Fcp1 associates with elongating RNAP II *in vivo*, and its phosphatase activity has been shown to stimulate RNAP II elongation *in vitro* (Kong et al., 2005; Mandal et al., 2002). Ssu72 is a component of the yeast cleavage/polyadenylation factor, and depletion of Ssu72 causes an elevation of CTD phospho-Ser5 levels *in vivo* and inhibits transcription *in vitro* (Krishnamurthy et al., 2004). Moreover, Ssu72 dephosphorylates recombinant CTD that has been phosphorylated by TFIIH *in vitro*, suggesting that it might counteract TFIIH function *in vivo* at the 3' end of the gene (Krishnamurthy et al., 2004). Finally, Ssu72 and Fcp1 have both been implicated in dephosphorylation and recycling of free RNAP II for subsequent rounds of transcription (reviewed in (Meinhart et al., 2005; Sims et al., 2004)).

1.3.3.2 Changes in the phosphorylation pattern of the CTD coordinates transcription and RNA processing

It is now widely accepted that transcription and RNA processing are temporally and functionally linked. Towards the 5' end of the gene, phosphorylation of Ser5s results in the recruitment of 5'end processing factors to the CTD including enzymes responsible for capping of the mRNA. Moreover, the activity of the guanylyltransferase, Ceg1, was found to be stimulated by its binding to phosphorylated Ser5s in CTD repeats *in vitro* (Cho et al., 1998; Ho and Shuman, 1999), and genetic interactions between *kin28* and *ceg1* suggest that CTD phosphorylation regulates mRNA capping *in vivo* (Rodriguez et al., 2000). Interestingly, binding of capping enzymes to the CTD was found to stimulate early RNAP II elongation, possibly

providing a checkpoint that ensures that the cap has been added before commitment to productive elongation (reviewed in (Bentley, 2005)). Towards the 3' end of genes, the CTD is predominantly phosphorylated on Ser2s, and not Ser5s. This change in phosphorylation pattern correlates with the binding specificity of a number of processing factors that are recruited to the CTD towards the 3' end of the gene, including cleavage and polyadenylation factors (Ahn et al., 2004; Licatalosi et al., 2002).

In addition to serving as a platform for coupling 5'- and 3'-end processing with transcription, the CTD is likely to recruit factors required for pre-mRNA splicing. Thus, activation of RNAP II-dependent transcription re-localises splicing factors to sites of transcription, but this does not occur if RNAP II has a truncated CTD (Misteli and Spector, 1999). Moreover, various splicing related factors, including Precursor mRNA processing protein (Prp)40p (Morris and Greenleaf, 2000), U2 small nuclear ribonucleoprotein (snRNP) auxiliary factor 65 kDa (U2AF65) (Listerman et al., 2006), SAF-B (Nayler et al., 1998), PTB-associated splicing factor (PSF), UsnRNPs, and SR proteins (Yuryev et al., 1996) have been identified in large RNAP II complexes and/or bind directly to the CTD. In the case of U2AF65 and Prp40p, they were found to bind specifically to phosphorylated CTDs, suggesting that they are recruited to elongating RNAP II complexes (Listerman et al., 2006; Morris and Greenleaf, 2000). The association of splicing factors with the CTD is likely to be functionally relevant, since truncation of the CTD causes a defect in splicing (Misteli and Spector, 1999) and affects splice site selection (de la Mata and Kornblihtt, 2006). Thus, truncation of the CTD abolishes SRp20-mediated exclusion of a fibronectin cassette exon, indicating that the CTD can regulate alternative splicing *in vivo* (de la Mata and Kornblihtt, 2006). The CTD therefore plays a central role in coordinating transcription and multiple RNA processing events.

1.3.4 Early Elongation

1.3.4.1 Promoter escape

Once the PIC has assembled onto the promoter, promoter escape and proximal pausing (discussed below) represent the main rate-limiting steps in gene expression. The promoter escape step is initiated by promoter opening, which involves unwinding of 11-15 base pairs (the transcription bubble) by the TFIIH-associated XPB

DNA helicase (Tirode et al., 1999; Wang et al., 1992). The RNAP II complex is now referred to as the initially transcribing complex (ITC). Abortive initiation is relatively frequent during synthesis of the first one to four nucleotides, after which the ITC forms a meta-stable complex (Holstege et al., 1997; Kugel and Goodrich, 2000). This is often referred to as "escape commitment". During the post commitment phase the ITC can still undergo upstream transcript slippage (Holstege et al., 1997; Pal and Luse, 2003). Promoter escape is completed during the transition from the 8th to the 9th nucleotide and coincides with a number of events. These include a reduction in upstream slippage, end of abortive transcript release, and collapse of the transcription bubble (reviewed in (Saunders et al., 2006)). Moreover, TFIIH activity is no longer required at this stage (Hieb et al., 2006). The RNAP II complex is now referred to as an early elongation complex (EEC). Promoter escape is followed by a transition to a pause region where transcript slippage is frequent until +23 nucleotides, and backtracking occurs until +30 nucleotides (Pal and Luse, 2003). TFIIF cooperates with TFIIS to suppress pausing during this phase (Zhang and Burton, 2004).

1.3.4.2 Promoter proximal pausing

Promoter proximal pausing or stalling at the 5' end of the gene is a rate-limiting step in the expression of many genes and is likely to represent a checkpoint before commitment to productive elongation. A number of proteins have been implicated in regulation of this step. 5, 6-Dichloro-1-bD-ribofuranosylbenzimidazole (DRB) sensitivity-inducing factor (DSIF) and NELP have both been found to inhibit elongation at this stage (Price, 2000). DSIF is composed of Spt4 and Spt5 and NELP of four subunits A, B, C/D, and E. Interestingly Spt5 interacts with the capping enzyme, and stimulates capping activity *in vitro* (Wen and Shatkin, 1999). Thus, it is possible that promoter proximal pausing both facilitates capping and provides a checkpoint to ensure that capping has taken place before commitment to productive elongation. Release from pausing requires the positive elongation factor P-TEFb, which is inhibited by DRB (Figure 1-8) (Price, 2000). P-TEFb consists of Cdk9/CTDK1 complexed with its partner cyclin T and phosphorylates DSIF, NELF, and the CTD on Ser2s (Fujinaga et al., 2004; Price, 2000; Yamada et al., 2006). As a result NELF dissociates from the RNAP II complex and productive elongation can take place (Fujinaga et al., 2004). DSIF stays associated with the elongating RNAP II and appears to stimulate elongation at this stage (Hartzog et al., 1998). Consistent with its crucial function in RNAP II

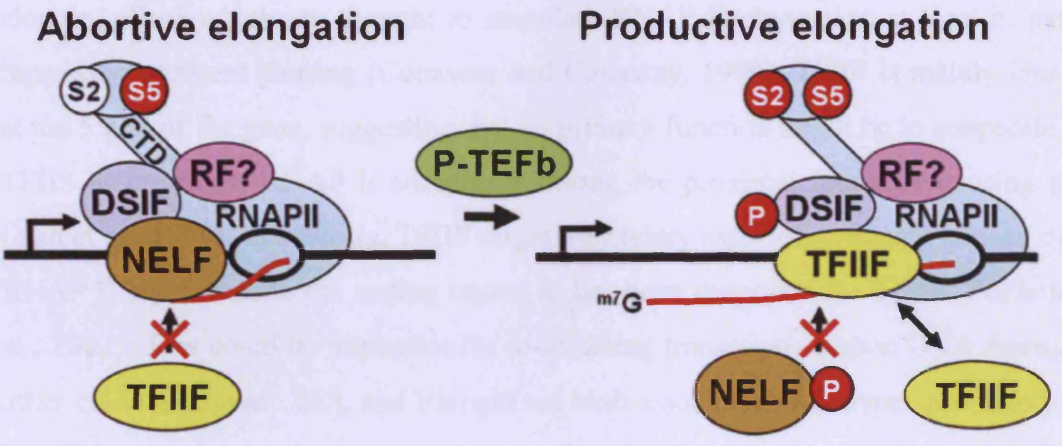

Figure 1-8: P-TEFb activity is required for productive elongation. Escape from promoter proximal pausing is a rate-limiting step in the expression of many genes. The conversion of paused RNAP II complexes into productive elongating complexes requires the action of P-TEFb, which phosphorylates the CTD on Ser2s. P-TEFb also phoshorylates and derepresses the inhibitory effect of the two negative elongation factors DSIF and NELF. Phosphorylation of NELF results in its displacement from the RNAP II complex and allows TFIIF to bind and stimulate RNAP II elongation rates. DSIF stays associated with elongating RNAP IIs and appears to stimulate elongation at this stage. Taken from (Cheng and Price, 2007).

elongation, P-TEFb localises to active genes *in vivo* (Lis et al., 2000), and its depletion results in a global decrease in density of RNAP II on genes (Ni et al., 2004; Shim et al., 2002).

1.3.5 Productive elongation

Once the RNAP II complex has cleared the promoter region, successful transcript elongation is dependent on a number of factors. These include elongation factors, which stimulate the processivity of the RNAP II complex, and chromatin remodellers, which "loosen up" the chromatin structure to facilitate RNAP II read through.

1.3.5.1 Elongation factors

A number of proteins have been identified that stimulate the rate of RNAP II elongation. These include TFIIF, eleven-nineteen lysine-rich in leukaemia (ELL), and elongin, all of which are thought to stimulate RNAP II elongation at least in part by repressing transient pausing (Conaway and Conaway, 1999). TFIIF is mainly localised at the 5'end of the gene, suggesting that its primary function might be to cooperate with TFIIS to re-initiate RNAP II complexes during the proximal promoter pausing phase (Yan et al., 1999). In addition, TFIIF might transiently associate with and release stalled RNAP II complexes in the coding region as has been described for TFIIS (Pokholok et al., 2002). This could be important for re-initiating transcription upon DNA damage or other cellular stresses. ELL and Elongin are both associated with hyper-phosphorylated RNAP II on polytene chromosomes, suggesting that they remain associated with RNAP II throughout the elongation phase (Gerber et al., 2001; Gerber et al., 2005). Paf1C, another complex that associates with elongating RNAP II, forms a scaffold for recruitment of Histone modifiers and chromatin remodellers (discussed below, and reviewed in (Saunders et al., 2006)).

1.3.5.2 Histone modification factors

The tight wrapping of DNA around histones (nucleosomes) represents a barrier to the elongating RNAP II complex. Thus, active transcription requires remodelling and partial disassembly of nucleosomes to allow the RNAP II complex to read through. Modifications that result in remodelling of nucleosomes include

acetylation, methylation, ubiquitylation and phosphorylation of histones (Figure 1-9) (reviewed in (Saunders et al., 2006)).

Histone acetylation is mostly associated with actively transcribing regions. The Elongin multi-factor complex contains a histone acetyl transferase (HAT) activity, and depletion of Elongin results in reduced levels of transcription *in vivo*. This suggests that Elongin might in part facilitate RNAP II elongation via its ability to modify the chromatin structure (Close et al., 2006).

Histone H3-K4 tri-methylation predominantly takes place at the 5' end of actively transcribed genes and is catalysed by a number of Set1 family members including MLL1, MLL2, and Set1 (Pokholok et al., 2005). Consistent with this, some Set1 family members preferentially bind to the Ser5-phosphorylated form of CTD, which dominates at the 5' end of genes (Ng et al., 2003). In contrast, Set2 family members, which methylate histone H3 on K36 (reviewed in (Dillon et al., 2005)), bind the Ser2P-Ser5P form of RNAP II and associate with the entire transcribed region (Krogan et al., 2003b).

Mono-ubiquitylation of H2BK120 is catalysed by the H2B ubiquitylating complex and stimulates transcription *in vitro* (Pavri et al., 2006). The H2B ubiquitylating complex is present both at promoter regions and coding regions (Kao et al., 2004; Zhu et al., 2005), and H2BK120 ubiquitylation is required for correct methylation of H3-K4 and H3-K79 (Briggs et al., 2002; Sun and Allis, 2002). The elongation factor Paf1C is required for the association of the H2B ubiquitylating complex with hyper-phosphorylated RNAP II and for the recruitment of Set1 and Set2 (Krogan et al., 2003a; Krogan et al., 2003b; Ng et al., 2003; Wood et al., 2003).

1.3.5.3 Chromatin remodellers

Chromatin remodellers are implicated in repositioning, disassembly and re-assembly of nucleosomes. There are four families of ATP-dependent chromatin remodellers: ISWI, SNF2, CHD, and INO80/SWR (Lusser and Kadonaga, 2003). These are thought to modify chromatin structure by repositioning nucleosomes in *trans* to another DNA molecule or in *cis* by displacing them upstream or downstream from their original position. The ISWI, SNF2, and CHD family members, ISWI, SWI/SNF, and CHD1, all associate with coding regions, but none of them are thought to function exclusively in elongation (reviewed in (Saunders et al., 2006)). Notably, depletion of

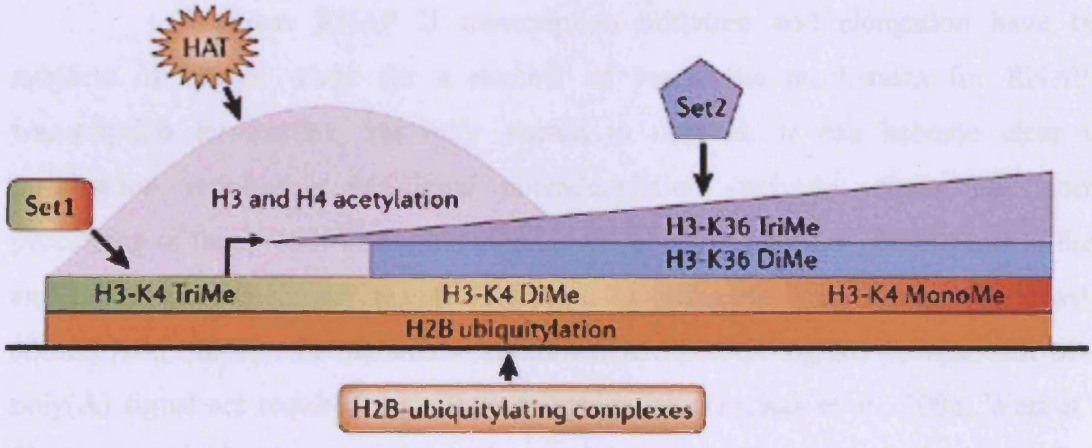

Figure 1-9: Typical distribution pattern of histone modifications on active genes. The nucleosomes represents a barrier to the elongating RNAP II complex, and extensive remodelling of the chromatin structure is required to allow RNAP II to read through. This is faciliated by acetylation, methylation, and ubiquitylation of histones, which results in partial diassembly of the nucleosomes. H3 and H4 acetylation by histone acetyl transferases is frequent towards the 5'-end of actively transcribing regions. Histone methylation is carried out by members of the Set1 and Set2 families. Wheras Set1-mediated tri-methylation of H3K4 predominantly takes place at the 5'-end, Set2-mediated di- and tri-methylation of H3-K36 is more frequent towards to 3'-end of transcribed regions. Ubiquitylation of H2B occurs within the entire transcribed region. Taken from (Saunders et al., 2006).

ISWI, or SWI/SNF2 only affects a small number of genes in yeast (Lusser and Kadonaga, 2003; Tran et al., 2000).

The FACT (for FAcilitates Chromatin Transcription) complex and Spt6 are major players in the disassembly and re-assembly of nucleosomes. The FACT complex, which consists of SSRP1 and Spt16, facilitates displacement of H2A-H2B dimers and stimulate RNAP II elongation through chromatin *in vitro* ((Belotserkovskaya et al., 2003) and reviewed in (Sims et al., 2004)). Spt6 interacts with H3 and H4 and seems function in nucleosome re-assembly (Bortvin and Winston, 1996; Kaplan et al., 2003). Thus, mutations in Spt6 result in increased sensitivity of chromatin to micrococcal nuclease digestion, indicating an open chromatin structure (Kaplan et al., 2003). Consistent with their predicted functions, the FACT complex and Spt6 both localise at coding regions of actively transcribed genes (Andrulis et al., 2000; Saunders et al., 2003). Moreover, their co-localisation with elongating RNAP II depends on the presence of Paf1C (Adelman et al., 2006). In the case of Spt6, the interaction appears to be co-dependent (Adelman et al., 2006; Kaplan et al., 2005).

1.3.6 Transcription termination

Whereas RNAP II transcription initiation and elongation have been subjects of intense study for a number of years, the mechanism for RNAP II transcription termination has only started to unravel. It has become clear that termination requires a functional polyadenylation (poly(A)) signal and correct processing of the 3' end. Thus, mutations in the poly(A) signal or components of the 3' end processing machinery results in failure to terminate transcription (reviewed in (Buratowski, 2005)). In mammals, additional termination signals downstream of the poly(A) signal are required for efficient termination (Gromak et al., 2006; West et al., 2006). A model has been put forward to explain transcription termination in mammals, which is referred to as the "torpedo model" (Figure 1-10) (reviewed in (Buratowski, 2005)). According to the "torpedo model", recognition of the poly(A) signal renders the RNAP II complex prone to termination. Subsequently, cleavage at the poly(A) site or further downstream generates a new 5' end, which acts like an entry point for exonucleases and/or helicase to degrade nascent RNA associated with the elongating RNAP II complex. This eventually results in dissociation of the RNAP II complex from nascent RNA and template DNA (Buratowski, 2005). The torpedo model has gained substantial support from a recent study by West and co-workers (West et al., 2008).

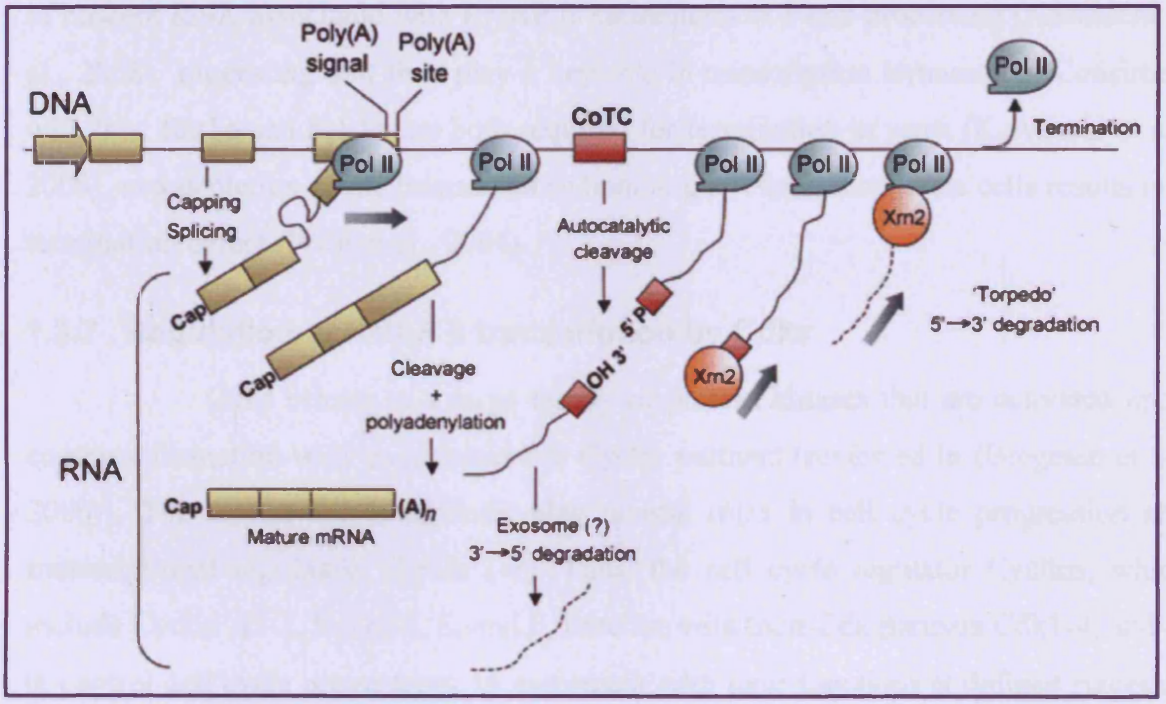

Figure 1-10: The "Torpedo Model". A model (referred to as the "torpedo model") has been put forward to explain transcription termination in mammals. Termination is initiated by recognition of the poly(A) signal, which renders the RNAP II complex termination competent. Cleavage at the poly(A) site by 3' poly(A)/cleavage factors or at terminator sequences downstream of the poly(A) site by a co-transcriptional cleavage event (CoTC) generates a new uncapped 5'-end. This acts as an entry point for "torpedoes" like the Xm2 5'-›3' exonuclease, which degrades nascent RNA associated with the elongating RNAP II complex. Dissociation of the ternary RNAP II-RNA-DNA complex is thought to occur when Xm2 "catches up " with the elongating RNAP II. Taken from (Kornblihtt, 2004).

First, they were able to show that poly(A) signal recognition occurs rapidly and is crucial to render the RNAP II complex termination competent. Second, 5'-3' exonucleolytic degradation of cleaved nascent RNA precedes dissociation of the RNAP II complex from the DNA template. Third, in the presence of terminator sequences downstream of the poly(A) signal, cleavage occurs at those sites and poly(A) site cleavage and pre-mRNA dissociation takes place after template release. In the absence of terminator sequences, poly(A) signal cleavage takes place in the ternary RNAP II-template-pre-mRNA complex, and pre-mRNA release precedes degradation of nascent RNA and dissociation of RNAP II from the template (West et al., 2008). Recently, yeast Rat1p exonuclease and Sen1p DEAD-box helicase were found to promote degradation of nascent RNA associated with RNAP II subsequent to 3'end processing (Kawauchi et al., 2008), suggesting that they play a key role in transcription termination. Consistent with this, Rat1p and Sen1p are both required for termination in yeast (Kawauchi et al., 2008), and depletion of the human Rat1p homologue, Xrn2, from Hela cells results in a termination defect (West et al., 2004).

1.3.7 Regulation of RNAP II transcription by Cdks

Cdks belong to a large family of protein kinases that are activated upon complex formation with their respective Cyclin partners (reviewed in (Bregman et al., 2000)). The Cyclin-Cdk complexes play pivotal roles in cell cycle progression and transcriptional regulation (Table 1-1). Thus, the cell cycle regulator Cyclins, which include Cyclin A1-2, B, D1-3, E, and F, function with their Cdk partners Cdk1-4, and -6 to control cell cycle progression. In agreement with their functions at defined stages of the cell cycle, these Cyclins are synthesised and degraded in a cyclical fashion every cell division. The transcription regulator Cdks 7, 8, 9, and 11 function together with Cyclins C, H, K, L1-2 and T1-2 and generally regulate RNAP II transcription. The levels of cyclins that are complexed with Cdks involved in transcriptional regulation remain constant during the cell cycle (reviewed in (Bregman et al., 2000)).

1.3.7.1 Cdk7

As previously mentioned, Cdk7/Kin28 (humans/yeast) forms a trimeric CAK complex with its partner cyclin H and the MAT1 protein (Devault et al., 1995; Fesquet et al., 1993; Fisher and Morgan, 1994; Tassan et al., 1995). CAK regulates transcription through phosphorylation of the RNAP II CTD and a number of general

Symbol	Identity to Cdk1 (%)	Cyclin-binding domain	Main activating cyclin (other cyclins)	Function
CDK1	100	PSTAIRE	A1 ,A2, B1, B2 (E, B3)	Cell cycle (G2-M)
CDK2	65	PSTAIRE	A1, A2, E1, E2 (D1, D2, B1, B3)	Cell cycle (G1-S)
CDK3	63	PSTAIRE	E1, E2, A1, A2, C	Cell cycle (G0-G1-S)
CDK4	42	PISTVRE	D1, D2, D3	Cell cycle (G1-S)
CDK5	56	PSSALRE	P35, p39 (D-, E-, and G-type cyclins	Senescence, postmitotic neurons
CDK6	43	PLSTIRE	D1, D2, D3	Cell cycle (G1-S)
CDK7	38	NRTALRE	H	RNAP II Transcription (initiation), DNA repair
CDK8	28	SMSACRE	C (K?)	RNAP II Transcription
CDK9	34	PITALRE	T1, T2, K	RNAP II Transcription (elongation)
CDK10	37	PISSLRE	Unknown	RNAP II Transcription, cell cycle (G2-M)
CDK11	26	SMSACRE	L1, L2 (D)	RNAP II Transcription, Splicing, cell cycle (M)

Table 1-1: Summary of Cdk-cyclin complexes and their functions. Cdks 1-4 and 6 function with their respective cyclin partners to control cell cycle progression. The activity of Cdks 1-4 and 6 is controlled by the levels of their cyclin partners, which fluctuate during the cell cycle. Cdks 7-11 function with a different set of cyclins to regulate RNAP II transcription. Contrary to what their names imply, the levels of cyclins that form complexes with Cdks 7-11 remain constant during the cell cycle. Adapted from (Malumbres and Barbacid, 2005).

and regulatory transcription factors. These include TBP, TFIIEα, TFIIFα, p53, retinoblastoma protein (pRb), and retinoic receptor alpha (RARα) (Reviewed in (Oelgeschlager, 2002)). CAK can exist as a free complex or as part of TFIIH, and the association of CAK with TFIIH increases its substrate specificity for the RNAP II CTD (Yankulov and Bentley, 1997). Finally, CAK phosphorylates and presumably activates all cell cycle regulatory Cyclin/Cdk complexes (Harper and Elledge, 1998; Larochelle et al., 1998).

1.3.7.2 Cdk8

In contrast to Cdk7, Cyclin C-Cdk8 mediates transcriptional repression *in vitro* in both yeast and mammals (Pavri et al., 2005; Spahr et al., 2003; Sun et al., 1998; Taatjes et al., 2002). Cyclin C-Cdk8 forms a Cdk8 sub-complex with Med12/Srb8 and Med13/Srb9 (humans/yeast) (Bjorklund and Gustafsson, 2005; Borggrefe et al., 2002; Samuelsen et al., 2003), which negatively regulate transcription through its reversible association with the Mediator (Chadick and Asturias, 2005). In yeast, transcriptional repression of the Cyclin C-Cdk8-responsive genes is thought to occur by Cdk8-mediated phosphorylation of a set of transcription factors including Ste12, Gcn4, and Msn2 (Chi et al., 2001; Nelson et al., 2003). Moreover, the human Cyclin C/Cdk8 complex is capable of repressing Cdk7 activity by phosphorylation of Cyclin H (Akoulitchev et al., 2000). Loss of any of the four subunits of the Cdk8 sub-module has little effect on viability in budding yeast (Holstege et al., 1998; van de Peppel et al., 2005). In contrast, knock-out of Cdk8 in mice results in early embryonic lethality, indicating that Cdk8 function is required early in development (Westerling et al., 2007).

1.3.7.3 Cdk9

Cdk9 and its partner Cyclin T make up the positive elongation factor P-TEFb. P-TEFb kinase activity is absolutely crucial for the conversion of promoter proximal paused RNAP IIs into productive elongating complexes ((Marshall et al., 1996) and reviewed in (Price, 2008)). In mammals, P-TEFb activity is negatively controlled by its reversible interaction with Methylphosphate capping enzyme (MEPCE), La-related protein 7 (LARP7), and the 7SK snRNP, which contains Hexamethylene bisacetamide-inducible protein (HEXIM)1 and HEXIM2 ((Jeronimo et al., 2007) and reviewed in (Peterlin and Price, 2006)). By analogy to studies of HIV transcriptional control, it has been suggested that P-TEFb release from 7SK snRNP and

its recruitment to paused RNAP II complexes might be regulated by cellular factors bound to enhancer elements ((Sedore et al., 2007) and reviewed in (Peterlin and Price, 2006)). Cellular factors that have been implicated in recruiting P-TEFb to promoter regions include NF-κB, CIITA, and Brd4 (reviewed in (Peterlin and Price, 2006)).

1.3.7.4 Cdk11

The Cdk11 protein kinases belong to a larger family of p34cdc2-related kinases and have been suggested to function as tumour supressors (Eipers et al., 1991). The two related genes, *cdc2L1* and *cdc2L2*, encode at least 20 different Cdk11 isoforms. The larger Cdk11^{p110} isoforms form complexes with at least four different cyclin L isoforms including cyclins L1α/β and L2α/β (Loyer et al., 2008). Cdk11^{p110} is thought to have dual functions in RNAP II transcription and pre-mRNA splicing and might provide a link between the two processes. Consistent with this, Cyclin L/Cdk11^{p110} complexes localise to nuclear speckles, which are storage and assembly sites for splicing factors, and to the nucleoplasm (Hu et al., 2003; Yang et al., 2004). In agreement with a function in splicing, Cdk11^{p110} and Cyclins L1α/β and L2α/β associate with multiple splicing factors including the SR proteins SF2/ASF, SC35, 9G8, SRp75, SRp55, SRp40, SRp30a/b, and SRp20 and are required for normal splicing (Hu et al., 2003; Loyer et al., 2008; Yang et al., 2004). Over-expression of the Cyclin isoforms alone or in combination with Cdk11^{p110} differentially affects alternative splicing, indicating that Cdk11^{p110} can function as a regulator of alternative splicing (Loyer et al., 2008). Consistent with this, the alternative splicing factor 9G8 is a target of Cdk11^{p110} phosphorylation, and depletion of Cdk11^{p110} decreases 9G8 phosphorylation and inhibits splicing (Hu et al., 2003).

There are several indications pointing to a role of Cdk11^{p110} in transcription. Thus, Cdk11^{p110} and its partner Cyclin L2 both bind to hyper-phosphorylated RNAP II (Trembley et al., 2002; Yang et al., 2004), and antibody-mediated repression of Cdk11^{p110} activity results in suppression of RNAP II transcription (Trembley et al., 2002). Moreover, Cdk11^{p110} interacts with several proteins implicated in RNAP II elongation including ELL2, both subunits of TFIIF, TFIIS, and the FACT complex (Trembley et al., 2002). In contrast, Cdk11^{p110} does not co-purify with ELL, elongin A, or elongin B proteins, suggesting that Cdk11^{p110} associates with a specific subset of RNAP II complexes (Trembley et al., 2002).

Cdk11^{p58} is a shorter isoform of Cdk11^{p110}, and both are translated from a single transcript (Cornelis et al., 2000). Cdk11^{p110} is generated by classical cap-dependent translation, and Cdk11^{p58} is produced by translation initiation from an internal ribosome entry site (IRES) (Cornelis et al., 2000). Whereas Cdk11^{p110} is present at constant levels throughout the cell cycle, Cdk11^{p58} is expressed specifically during the G2/M transition (Cornelis et al., 2000). Consistent with this, Cdk11^{p58} is a centrosome-associated kinase that promotes centrosome maturation and bipolar spindle formation (Petretti et al., 2006). Thus, depletion of Cdk11^{p58} results in diminished centrosomal levels of the protein kinases Polo-like kinase 1 (Plk1) and Aurora A that are known to function in microtubule nucleation and spindle stabilisation (Petretti et al., 2006). Consistent with this, Cdk11$^{p110/p58}$-deficient mice exhibit mitotic arrest and fail to develop beyond the blastocyst stage (Li et al., 2004).

The Cdk11^{p46} isoform contains the catalytic kinase domain and is generated from the Cdk11^{p110} and Cdk11^{p58} isoforms by proteolytic cleavage in response to apoptosis (Ariza et al., 1999; Tang et al., 1998). Thus, Fas-induced apoptosis or staurosporine treatment results in caspase-dependent cleavage of the longer Cdk11 isoforms to generate Cdk11^{p46} and is accompanied by Cdk11^{p46}-mediated phosphorylation of histone H1 and apoptosis (Ariza et al., 1999; Lahti et al., 1995). Moreover, ectopic expression of Cdk11^{p46} is sufficient to induce apoptosis (Bunnell et al., 1990; Lahti et al., 1995). Cdk11^{p46} interacts directly with eukaryotic translation initiation factor (eIF) 3f, and this interaction is strengthened upon apoptotic stimuli (Shi et al., 2003). Moreover, Cdk11^{p46} phosphorylates eIF3f on Ser46 and inhibits translation *in vitro* (Shi et al., 2003). Thus, Cdk11^{p46}-mediated phopsphorylation of eIF3f could inhibit translation *in vivo* in response to apoptosis (Shi et al., 2003). Consistent with this, eIF3f is phosphorylated on Ser46 in apoptotic cells (Shi et al., 2003).

1.3.8 Casein Kinase 2 (CK2)

CK2 is a key regulator of multiple cellular processes and is thought to be an important mediator of cell survival. Thus, increased CK2 activity is associated with cellular stress responses, and loss of CK2 activity is associated with cell death (reviewed in (Ahmed et al., 2002)). Recent studies suggest that CK2 might function in the regulation of transcription. First, CK2 can be purified in complex with RNAP II, TFIIF and Cdk11 and is capable of phosphorylating these proteins (Egyhazi et al., 1999; Payne et al., 1989; Trembley et al., 2003). The importance of these phosphorylation

events have not yet been addressed, but CK2-mediated phosphorylation of the CTD could potentially affect RNAP II elongation rates or the recruitment of specific cellular factors to the RNAP II complex (Trembley et al., 2003). Second, CK2 co-localise with TFIIF and elongating RNAP II complexes on *Drosophila* polytene chromosomes *in vivo* (Egyhazi et al., 1999). Third, CK2 phosphorylates and regulates the activity of the general splicing factor RNSP1, which is also associated with RNAP II complexes (Trembley et al., 2005). Thus, CK2 activity might be implicated in coordinating transcription and pre-mRNA processing

1.3.9 Males absent on the first (MOF)

The MOF proteins are of particular interest to my work, since *Drosophila* and human MOF were previously isolated in complex with my proteins of interest Microspherule protein 2 (dMCRS2)/Microspherule protein 58 (MSP58) (*Drosophila*/humans) (Mendjan et al., 2006). The MOF histone acetyl transferase belongs to the MYST family (from founding members MOZ, Ybf2/Sas3, Sas2, and Tip60) (reviewed in (Yang, 2004)). In *Drosophila*, MOF is part of the male-specific lethal (MSL) complex, which is required for dosage compensation. Thus, the MSL complex binds to multiple sites along the male X chromosome and mediates a two-fold up-regulation of gene expression (Akhtar and Becker, 2000; Hilfiker et al., 1997; Smith et al., 2000). In addition to the MSL complex, MOF is part of another complex, which consists of dMCRS2 (my protein of interest), NSL1-3 (for non-specific lethal 1-3), WDS, and MBD-R2 (Mendjan et al., 2006). This complex is conserved in humans, and it has been speculated that it might have a more general function in transcription and/or chromatin remodelling (Mendjan et al., 2006). Consistent with this idea, MOF, but not MSL proteins, binds to the promoter region of genes on all four *Drosophila* chromosomes, and regulates transcription of both X-linked and autosomal genes (Kind et al., 2008).

Human MOF (hMOF) is thought to function in multiple processes including chromosome remodelling, transcriptional regulation, and DNA damage response. Thus, depletion of hMOF results in G2/M arrest, chromosomal aberrations, reduced transcription of a subset of genes, and impaired DNA repair (reviewed in (Rea et al., 2007)). hMOF specifically acetylates Histone 4 on lysine 16 (H4K16), and depletion of human MOF results in severely reduced levels or complete loss of H4K16Ac, suggesting that it is the main factor responsible for acetylation of H4K16

(Akhtar and Becker, 2000; Hilfiker et al., 1997; Smith et al., 2005; Smith et al., 2000; Taipale et al., 2005). Similarly, MOF-deficient mouse embryos fail to acetylate H4K16, but have normal acetylation on other N-terminal histone lysine residuces (Thomas et al., 2008). As a result, *Mof*$^{-/-}$ embryonic cells exhibit abnormal chromatin structure, and MOF-deficient embryos do not develop beyond the blastocyst stage (Thomas et al., 2008). Histone acetylation is often associated with regions of active transcription. Thus, hMOF has been proposed to cooperate with the methyl transferase MLL1, which binds to H4K16Ac and methylates H3K4, to stimulate transcription *in vitro* and *in vivo* (Dou et al., 2005).

Histone acetylation is also thought to play a role in DNA repair. Thus, generation of double-strand breaks induces H4 acetylation, including at K16, at the area surrounding the break (Tamburini and Tyler, 2005). Once DNA has been repaired, Histone deacetylases are recruited to the site of repair and Histone deacetylation takes place (Tamburini and Tyler, 2005; Utley et al., 2005). It has been proposed that acetylation and deacetylation might function to promote opening and closing of the chromatin structure to facilitate DNA repair or as a signal to attract the DNA repair machinery (Tamburini and Tyler, 2005). In accordance with this, hMOF is thought to function in DNA repair. First, hMOF-depleted cells exhibit a delay in the kinetics of the DNA repair process (Taipale et al., 2005), and expression of dominant-negative MOF results in inefficient repair of double-strand breaks (Gupta et al., 2005). Second, hMOF is activated in response to ionising radiation (IR)-induced DNA damage, and this is paralleled by an increase in H4K16Ac levels (Gupta et al., 2005). Third, yeast 2-hybrid data have shown that hMOF interacts with the ataxia-telangiectasia-mutated (ATM) protein, which is a key player in DNA damage response (Gupta et al., 2005). Moreover, inactivation of hMOF results in a decrease in ATM activity, and it has been proposed that hMOF might directly or indirectly regulate ATM in response to DNA damage (Gupta et al., 2005). Given that hMOF-mediated H4K16 acetylation occurs independent of ATM, it is possible that H4K16 acetylation rather than hMOF triggers ATM activation.

Interestingly, hMOF seems to have several independent functions in DNA damage response. Thus, hMOF was found to acetylate p53 on lysine 120 in response to DNA damage (Sykes et al., 2006). As a result, p53K120Ac accumulates specifically on promoters of pro-apoptotic genes rather than other target genes (Sykes et al., 2006).

This suggests that hMOF-mediated acetylation of p53 makes cells prone to apoptosis rather than DNA repair.

1.3.10 MSP58 – the human homologue of *Drosophila* dMCRS2

MSP58 (also known as p78/MCRS1), the human homologue of *Drosophila* dMCRS2, is a nuclear protein with a conserved forkhead-associated (FHA) domain at its C-terminus (Ren et al., 1998). FHA domains are found almost exclusively in nuclear proteins that function in transcription regulation, DNA repair, or cell cycle progression (Durocher et al., 1999; Hofmann and Bucher, 1995; Li et al., 2000). Consistent with this, there is some evidence that MSP58 is implicated in transcription regulation and possibly cell cycle progression (Hirohashi et al., 2006a; Shimono et al., 2005).

Yeast 2-hybrid screens have identified several MSP58 binding partners including Mi-2β, RET finger protein (RFP), and upstream binding factor (UBF) (Lin and Shih, 2002). Mi-2β is a component of a nucleosome remodelling and deacetylase (NuRD) complex (Tong et al., 1998; Wade et al., 1998; Zhang et al., 1998), RFP is a transcriptional regulator (Shimono et al., 2000; Shimono et al., 2003), and UBF is an essential component of the RNAP I initiation complex. Whereas the NuRD complex has mainly been associated with transcriptional repression, Mi-2β seems to function outside the NuRD complex as a transcriptional activator (Hirose et al., 2002; Shimono et al., 2003; Williams et al., 2004). MSP58 was found to co-localise with Mi-2β, RFP, and UBF in the nucleolus (Shimono et al., 2005), a sub-nuclear compartment in eukaryotic cells responsible for rRNA synthesis and ribosome biogenesis. Consistent with their localisation, MSP58, Mi-2β, and RFP were found to bind to rDNA and up-regulate transcriptional activity from rDNA promoters (Shimono et al., 2005). Notably, the *Drosophila* homologue of MSP58, dMCRS2, is part of a MOF containing complex that has been proposed to function in chromatin remodelling and regulation of RNAP II transcription (Mendjan et al., 2006). Thus, a function of MSP58/dMCRS2 in chromosome remodelling and transcriptional regulation might be conserved between flies and humans.

MSP58 was also identified as a binding partner for the two centrosome-associated proteins Su48 and Ndel (Hirohashi et al., 2006a; Hirohashi et al., 2006b). Whereas the majority of MSP58 is found in the nucleus, a fraction of MSP58 was found to co-localise with Su48 and Ndel at centrosomes (Hirohashi et al., 2006a). Moreover,

the association of MSP58 with Ndel seems to be regulated by phosphorylation. Thus, mutation of six putative phosphorylation sites in Ndel enhances its binding to MSP58 (Hirohashi et al., 2006a). Depletion of MSP58 results in mitotic delay and apoptosis, suggesting that MSP58 might function in cell cycle progression (Hirohashi et al., 2006a). Consistent with this, MSP58 expression levels fluctuate in a cell cycle dependent manner with a peak of expression in early S phase (Ren et al., 1998; Song et al., 2004).

1.4 pre-mRNA processing

As previously mentioned, this thesis concerns the characterisation of four *Drosophila* proteins, two of which (dPrp38 and dMFAP1) are required for pre-mRNA processing. In the following section, I have attempted to provide the reader with an overview of the different stages of the spliceosome cycle including spliceosome assembly, spliceosome activation, and the two catalytic reactions resulting in the excision of an intron from a pre-mRNA. I have compiled the mechanistic *in vivo* data obtained in yeast with the proteomic data from studies in mammalian cells to highlight similarities and differences between pre-mRNA processing in yeast and metazoans.

1.4.1 The spliceosome cycle

Splicing of pre-mRNA is a catalytic reaction that involves two successive trans-esterification steps. This process is carried out by a highly conserved ribonucleoprotein complex, named the spliceosome. The spliceosome consists of five small nuclear RNAs (snRNAs) (U1, U2, U4, U5, and U6) and more than 200 proteins, making it one of the largest and most complex studied cellular machine (Jurica and Moore, 2003). Spliceosome assembly has traditionally been described as a sequential process that is initiated by the recruitment of the U1 snRNP to the 5'-splice donor site to form a "commitment complex" (E complex in mammals) (Figure 1-11) (Rosbash and Seraphin, 1991; Ruby and Abelson, 1988). Subsequently, recruitment of the U2 snRNP to the branch site by U2AF65 generates the "pre-spliceosome" (A complex in mammals) (Merendino et al., 1999; Singh et al., 2000; Wu et al., 1999; Zorio and Blumenthal, 1999). A preformed U4-U5-U6 tri-snRNP unit then binds to the U1-U2-pre-mRNA complex to form a "complete spliceosome" (B complex in mammals). In order to activate the spliceosome, several conformational rearrangements must take place (reviewed in (Brow, 2002)). These include unwinding of base-pairings between U1 and the 5'-splice site and between U6 and U4 and are accompanied by the formation of new base pair interaction between U6 and the 5'-splice site and U6 and U2. As a result, U1 and U4 snRNPs are released from the pre-spliceosome and an active spliceosome (B* complex in mammals) is formed (Madhani and Guthrie, 1994; Staley and Guthrie, 1998). The activated spliceosome promotes splicing of the pre-mRNA by two subsequent catalytic reactions. In the first catalytic reaction, a nucleophilic attack by the 2' oxygen of the intronic branch point adenosine on the phosphorous atom that

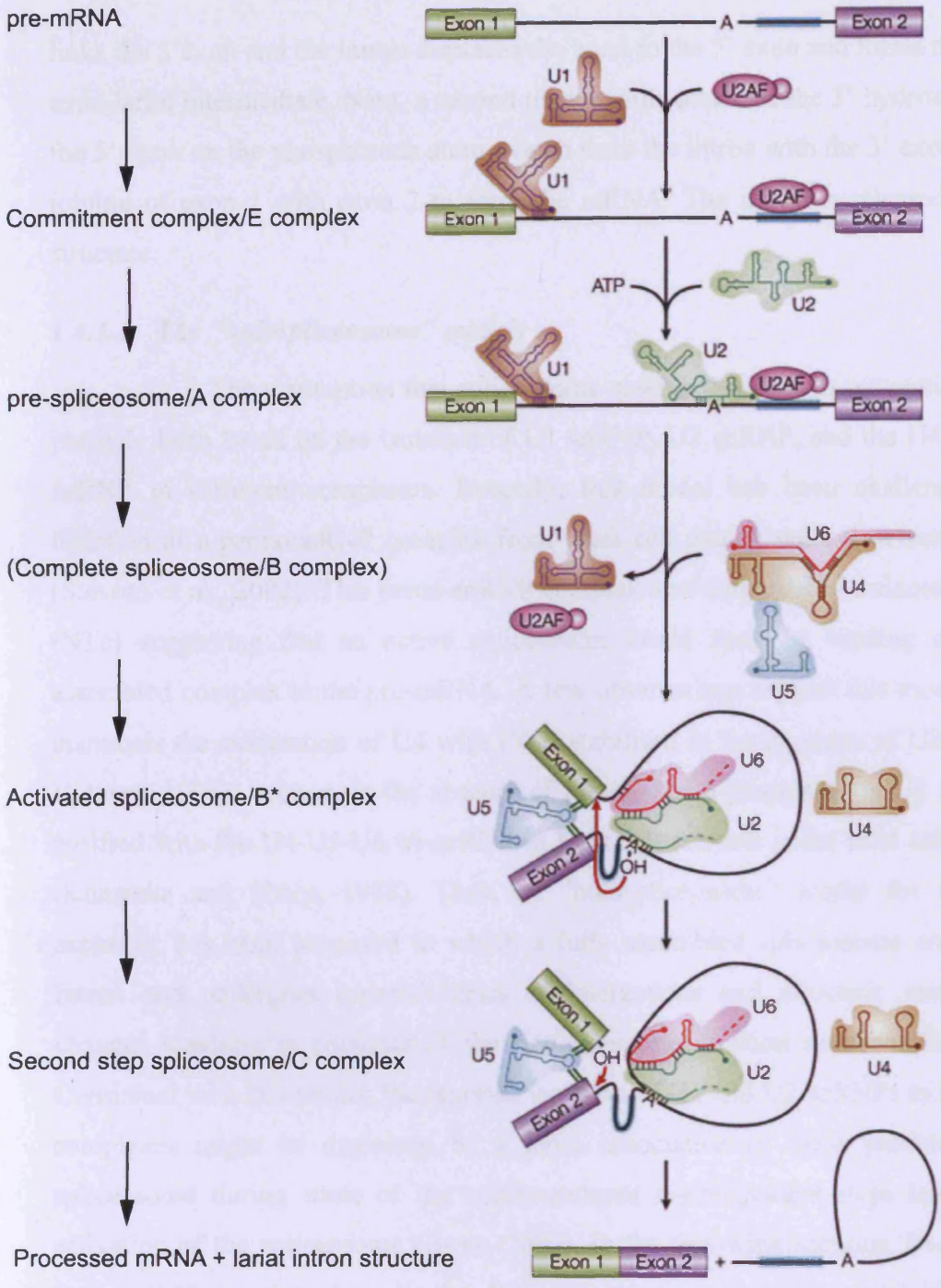

Figure 1-11: Spliceosome assembly and catalysis. Spliceosome assembly is initiated by binding of the U1 snRNP to the 5'-splice site and U2AF65 to the branch site region to generate the commitment complex/E complex. Binding of U2AF65 to the branch site region promotes recruitment of the U2 snRNP to the branch point and formation of the pre-spliceosome/A complex. Following recruitment of the tri-snRNP to generate the complete spliceosome/B complex, several conformational changes take place, which result in dissociation of the U1 and U4 snRNPs and activation of the spliceosome (referred to as the B* complex in mammals). The activated spliceosome catalyses the the first transesterification reaction, which involves a nucleophile attack by the 2' oxygen of the branch point adenosine on the phosphorous atom, which links the intron and exon 1. Additional structural rearrangements take place after the first catalytic reaction to generate a complex that is competent to carry out the second catalytic reaction. In mammals, this complex is referred to as the C complex. The second catalytic reaction involves a nucleophile attack of the hydroxyl group of the 3' nucleotide of exon 1 on the phosphorous atom that links the intron with exon 2. As a result, the 3'-end of exon 1 is spliced to the 5'-end of exon 2, and the intron is released as a lariat structure. Adapted from (Schroeder et al., 2004).

links the 5'exon and the intron displaces the bond to the 5' exon and forms the intron/3' exon lariat intermediate. Next, a second nucleophilic attack of the 3' hydroxyl group of the 5' exon on the phosphorous atom, which links the intron with the 3' exon, results in joining of exon 1 with exon 2 to form the mRNA. The intron is released as a lariat structure.

1.4.1.1 The "holospliceosome" models

The assumption that spliceosome assembly occurs in sequential steps has partially been based on the isolation of U1 snRNP, U2 snRNP, and the U4-U5-U6 tri-snRNP in different complexes. Recently, this model has been challenged by the isolation of a penta-snRNP complex from yeast cell extract under low salt conditions (Stevens et al., 2002). This penta-snRNP complex also contained the nineteen complex (NTc) suggesting that an active spliceosome could form by binding of this pre-assembled complex to the pre-mRNA. A few observations support this model. First, in mammals the association of U4 with U6 is stabilised in the presence of U2 (Brow and Vidaver, 1995). Second, in the absence of pre-mRNA a proportion of U2 snRNPs co-purified with the U4-U5-U6 tri-snRNP in Hela cell extracts under mild salt conditions (Konarska and Sharp, 1988). Thus, an "holospliceosome" model for spliceosome assembly has been proposed in which a fully assembled spliceosome encounters an intron and undergoes ordered series of interactions and allosteric conformational changes resulting in catalysis of the first trans-esterification reaction (Brow, 2002). Consistent with this model, the reported isolation of U1 and U2 snRNPs as independent complexes might be explained by a loose association of these particles with the spliceosome during some of the conformational rearrangement steps leading to the activation of the spliceosome (Brow, 2002). In the following sections, I will refer the "sequential" model to describe the different steps in spliceosome assembly, but each step can equally well be interpreted as conformational changes in the "holospliceosome" model.

1.4.2 DExD/H-box RNA helicases

The unwinding of RNA-RNA duplexes during the spliceosome cycle requires energy and is facilitated by RNA helicases. RNA helicases predominantly belong to three highly conserved families of DEAD-box, DEAH-box, and ski2-like

proteins commonly referred to as DExD/H-box RNA helicases (reviewed in (Bleichert and Baserga, 2007).

1.4.2.1 Conserved domains in DExD/H RNA helicases

DExD/H-box RNA helicases have been classified based on eight conserved motifs that reside within two domains. Consistent with the general idea that RNA helicases promote unwinding of RNA helixes by hydrolysis of NTPs, most of these motifs have been implicated in NTP binding and hydrolysis and/or specifying binding of the helicase to its RNA substrate (Figure 1-12). Domain 1 contains motifs I (Walker A), Ia, Ib, II (Walker B), III and Q (in DEAD-box proteins) (Tanner et al., 2003), and domain 2 contains motifs IV, V, and VI. Walker A and B motifs are found in many NTP binding proteins and are required for ATP/NTP binding and hydrolysis, respectively (Caruthers and McKay, 2002; Cordin et al., 2006; Rocak and Linder, 2004). In DEAD-box helicases, the conserved DEAD consensus amino acid motif that gives name to the family resides within the Walker B motif. Motifs 1a, 1b, IV, and V are involved in substrate RNA binding (Cordin et al., 2006), and motif III is thought to couple NTP hydrolysis with helicase activity (Silverman et al., 2003). There is some evidence that motif VI functions in both ATP hydrolysis and binding of substrate RNA suggesting that it might provide another link between NTP hydrolysis and helicase activity (Pause et al., 1993). Finally, the Q motif is thought to sense ATP binding and promote hydrolysis in DEAD-box proteins (Cordin et al., 2006).

1.4.2.2 DExD/H RNA helicases are required at multiple steps of the spliceosome cycle

In yeast, three DEAD-box (Sub2p, Prp28p, and Prp5p), four DEAH-box (Prp2p, Prp16p, Prp22p, Prp43p), and one ski2-like (Brr2p) proteins have been implicated in the dynamic rearrangements that occurs during the processing of a pre-mRNA (de la Cruz et al., 1999; Silverman et al., 2003; Staley and Guthrie, 1998). Individual RNA helicases has been shown to function in different steps of the spliceosome cycle (Figure 1-13). Sub2p (UAP56 in humans) and Prp5p facilitate binding of U2 snRNP to the branch point (Kistler and Guthrie, 2001; O'Day et al., 1996). The DEAD-box protein, Prp28p, and the ski2-like protein, Brr2p, both function in the activation step of the spliceosome (Staley and Guthrie, 1998). Prp28p is thought to be important for the unwinding of base-pairings between U1 and the 5'-splice site

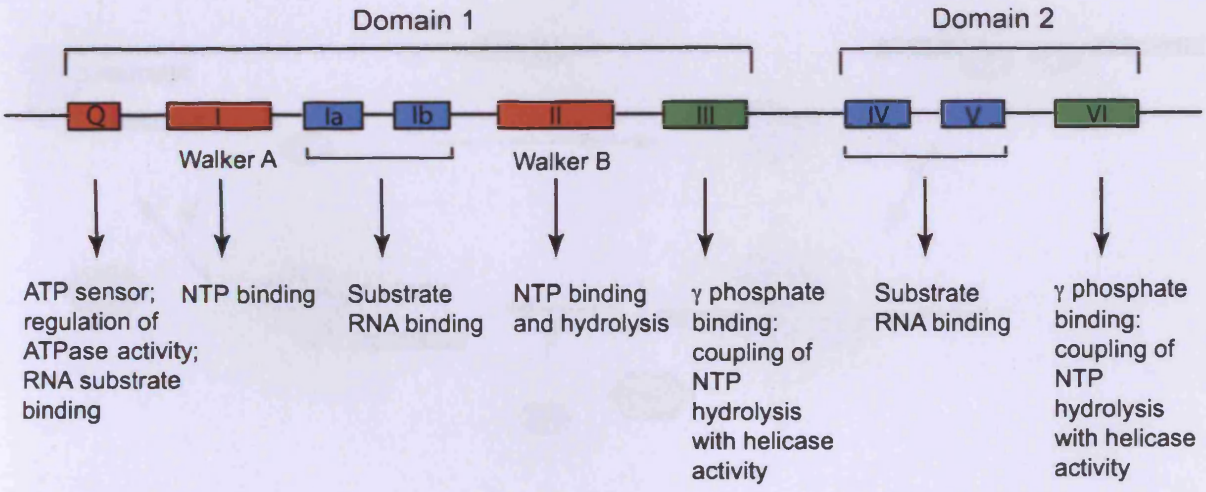

Figure 1-12: Domain structure of DExD/H Box RNA helicases. DexD/H Box RNA helicases contain eight highly conserved motifs, which reside in two domains. Each of the motifs has been assigned different functions including substrate binding, NTP-binding and hydrolysis, and/or helicase activity. DEAD-box RNA helicases contain an additional Q motif in the N-terminal of domain 1, which is thought to sense ATP binding and promote hydrolysis. Adapted from (Bleichert and Baserga, 2007).

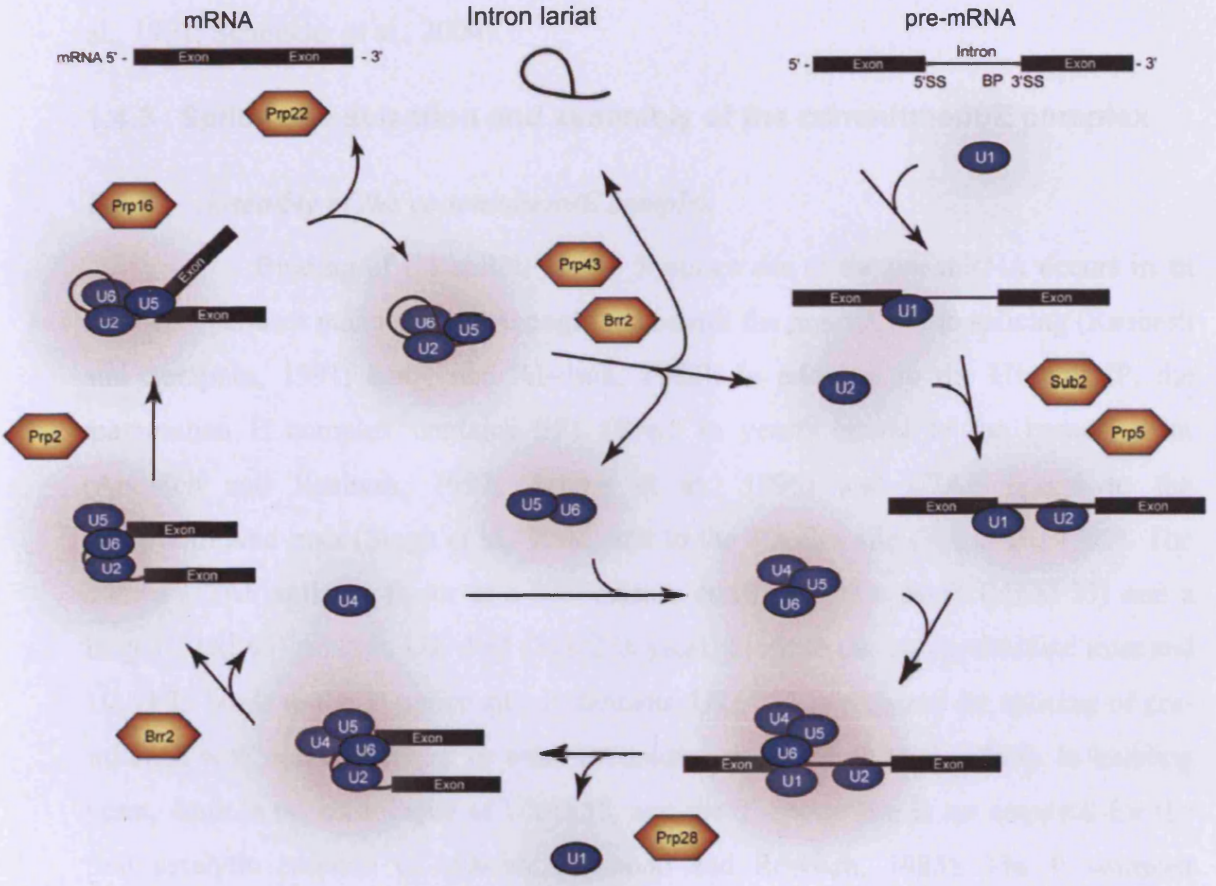

Figure 1-13: DExD/H Box RNA helicases function a different stages of the spliceosome cycle. The yeast DeXD/H box RNA helicases Sub2p and Prp5p facilitate the recruitment of the U2 snRNP to the branch point region. Prp28p and Brr2p function during the activation step and are required for the release of U1 and U4 snRNPs, respectively. Prp2p is implicated in the structural rearrangements that take place prior to the first catalytic reaction. Prp16 functions before and during the second catalytic reaction. Prp22, Prp43, and Brr2p are required for spliceosome disassembly and release of the spliced mRNA. Adapted from (Bleichert and Baserga, 2007).

(Chen et al., 2001b) and Brr2p is implicated in unwinding the U4/U6 duplex, which is essential for the release of U4 snRNP (Raghunathan and Guthrie, 1998). Prp2 is implicated in structural rearrangements rendering the spliceosome active for the first catalytic reaction, and Prp16 function before or during the second transesterification reaction. Finally, Brr2p, Prp43 and Prp22p are required for disassembly of the spliceosome and release of the spliced mRNA (Arenas and Abelson, 1997; Company et al., 1991; Schneider et al., 2004).

1.4.3 Splice site selection and assembly of the commitment/E complex

1.4.3.1 Assembly of the commitment/E complex

Binding of U1 snRNP to the 5'-splice site of the pre-mRNA occurs in an ATP-independent manner and is thought to commit the pre-mRNA to splicing (Rosbash and Seraphin, 1991; Ruby and Abelson, 1988). In addition to the U1 snRNP, the mammalian E complex contains SF1 (Bbp1 in yeast) bound to the branch point (Abovich and Rosbash, 1997; Arning et al., 1996) and U2AF bound to the polypyrimidine tract (Singh et al., 2000) and to the 3'splice site (Wu et al., 1999). The human U2AF splicing factor is a heterodimer consisting of a small (U2AF35) and a large (U2AF65) subunit. U2AF65 (Mud2 in yeast) binds to the polypyrimidine tract and U2AF35 binds to the 3'-splice site. In humans, U2AF35 is required for splicing of pre-mRNAs with non-consensual or weak pyrimidine tracts (Guth et al., 1999). In budding yeast, there is no homologue of U2AF35, and the 3′-splice site is not required for the first catalytic reaction of splicing (Rymond and Rosbash, 1985). The E complex contains an additional set of factors that are required for its stabilisation. These belong to the family of SR proteins (see below) and are thought to stabilise the complex by generating an extensive network of interactions between the 5'-splice site and the branch point and 3'-splice site (Abovich and Rosbash, 1997; Boukis et al., 2004; Shen et al., 2004). Thus, the two SR proteins, SF2/ASF and SC35, have both been implicated in E complex assembly. SF2/ASF has been shown to increase U1 snRNP binding to the 5'-splice site (Eperon et al., 1993; Kohtz et al., 1994), and SC35, which bridges U1 snRNP and U2AF35, cross-links with the 3'-splice site (Staknis and Reed, 1994; Wu and Maniatis, 1993).

The yeast commitment complex has a less complex structure consisting of U1 snRNP bound to the 5'-splice site, Bbp1 bound to the branch point, and Mud2p

bound to the pyrimidine tract. In addition, the formation of a stable commitment complex requires cross-intron bridging of complexes at the 5'-splice site and the branch point sequence (BPS), which is accomplished by protein-protein interactions between U1 snRNP and Bbp1 (Abovich and Rosbash, 1997).

1.4.3.2 Yeast and metazoan U1 snRNPs vary in size and composition

Interestingly, the yeast U1 snRNP is significantly larger than the vertebrate U1 snRNP. In addition to U1-70K, U1-A, U1C and Sm proteins B/B', D1, D2, D3, E, and F, which are found in both the yeast and vertebrate U1 snRNPs, the yeast U1 snRNP complex contains at least 8 proteins that are not stably associated with vertebrate U1 snRNPs. These include Snu71p, Snu65p, Snu56p, Prp39p, Prp40p, Prp42p, Nam8, and Luc7p (Fortes et al., 1999; Gottschalk et al., 1998). The reason for this difference in U1 snRNP composition might reflect different mechanisms for splice site selection in yeast and metazoans. In metazoans, the recruitment of the U1 snRNP "core activity" to the pre-mRNA is thought to be regulated by the combinatorial association of a commonly used set of splicing factors with the 5'-splice site. Thus, the strength of a given splice site is determined by the combined affinity of the factors at a given site for the U1 snRNP core complex (discussed in "SR proteins" section below). The ability of the U1 snRNP complex to differentiate between different strengths of splice sites is crucial in higher eukaryotes, where regulated and alternative splicing is of major importance. Thus, a recent study estimates that at least 74% of multi-exon transcripts are alternatively spliced in humans (Johnson et al., 2003). In contrast, these processes are almost non-existent in yeast.

1.4.3.3 SR proteins

The splice site sequences in higher eukaryotes display a much higher variability than those in yeast. To compensate for this loss in sequence information, a family of SR proteins have evolved in higher eukaryotes that recognise and bind to weak consensus sequences within the pre-mRNA. The binding of SR proteins to splice site sequences generally leads to an increased affinity of the spliceosome for those sites (Figure 1-14). SR proteins are characterised by a C-terminal domain rich in arginine/serine di-peptides (RS domain), which mediates protein-protein (Wu and Maniatis, 1993) and protein-RNA interactions (Shen and Green, 2004; Shen et al., 2004). In addition, SR proteins contain one or more N-terminal RNA recognition

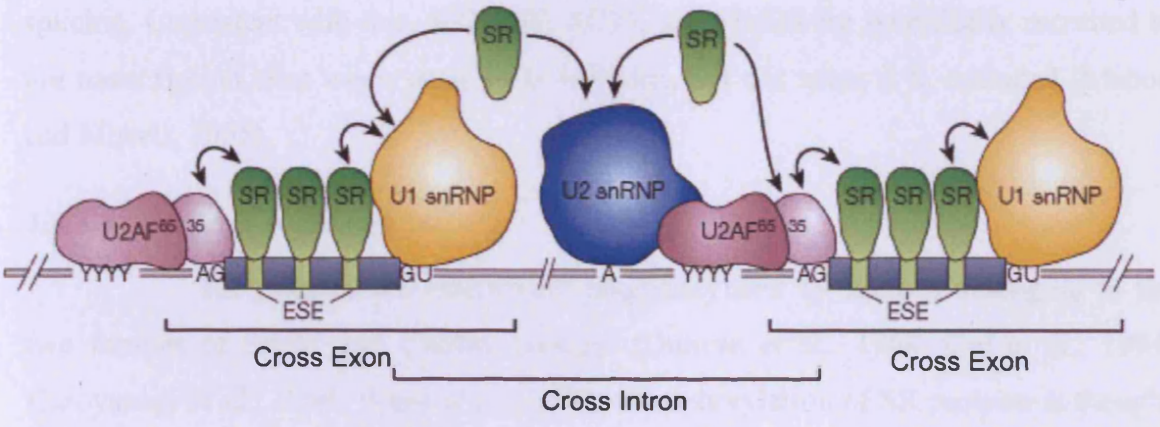

Figure 1-14: SR proteins affect the strength of a given splice site. SR proteins binds to exonic splicing enhancers (ESE) within exons and promote the recruitment of the U1 snRNP to the 3'-splice site and U2AF65 and UAF35 (in mammals) to the branch site region and the 5'-splice site, respectively. Binding of U2AF65 to the branch site region facilitates the recruitment of the U2 snRNP. SR proteins mediate cross-intron interactions by interacting with the pre-mRNA and splicing factors bound to the 5'- and 3'-splice sites. Binding of SR proteins to ESEs also play a key role in cross-exon recognition by bridging interactions between the U1 snRNP bound at the upstream 5'-splice site and the U2 snRNP bound at the branch point. Cross-exon recognition can affect the strength of the upstream 5'-splice site and is a major determinant in alternative splicing. Taken from (Maniatis and Tasic, 2002).

domains (RRMs) that are likely to increase their binding affinities for RNA. Several studies suggest that SR proteins bind to the pre-mRNA through their RMMs and RS domains and attract the spliceosome through RS domain-mediated protein-protein interactions (Crispino et al., 1994; Staknis and Reed, 1994; Wu and Maniatis, 1993; Zuo and Maniatis, 1996).

Consistent with the general idea that SR proteins are positive regulators of splicing, SF2/ASF and SC35 were shown to activate splicing *in vitro* (Expert-Bezancon et al., 2004). Moreover, they both behave antagonisticly to the inhibitory splicing factor, hnRNPA1, by competing for binding to the same sequence element (Expert-Bezancon et al., 2004). The antagonistic behaviours of SF2/ASF and hnRNPA1 on splicing can be explained by their opposite effects on recruitment of U1 snRNP to the 5'-splice site (Eperon et al., 2000). SF2/ASF promotes and hnRNPA1 inhibits binding of U1 snRNP to the 5'-splice site (Eperon et al., 2000). In addition to a function in constitutive splicing, SR proteins are thought to play a major role in regulation of alternative splicing. Consistent with this, SF2/ASF, SC35, and SRp20 are specifically recruited to *tau* transcription sites when exon 10 is included, but not when it is excluded (Mabon and Misteli, 2005).

1.4.3.4 SR protein kinases

SR proteins are extensively phosphorylated by kinases belonging to the two familes of SRPK and Clk/Sty proteins (Duncan et al., 1998; Gui et al., 1994; Kuroyanagi et al., 1998; Wang et al., 1998). Phosphorylation of SR proteins is thought to affect their substrate specificity and ability to regulate alternative splicing (Duncan et al., 1997; Prasad et al., 1999; Xiao and Manley, 1997). Thus, hypo- and hyper-phosphorylation of SR proteins by the Clk/Sty kinase was found to affect both their constitutive and alternative splicing activities (Prasad et al., 1999). Phosphorylation of SR proteins also affects their intracellular localisation (Caceres et al., 1997; Lai et al., 2003; Lin et al., 2005; Misteli and Spector, 1996). Thus, SRPK1-mediated phosporylation of ASF/SF2 causes its redistribution from the cytoplasm to nuclear storage sites (speckles) (Ma et al., 2008; Ngo et al., 2005). Once inside the nucleus, SR proteins are further modified by Clk/Sty kinases, and this is thought to cause their re-localisation from speckles to splicing sites (Colwill et al., 1996) (Ngo et al., 2005). Thus, SR protein kinases regulate both the localisation and the activity of SR proteins

and could potentially function as signal transmitters to modulate spliceosome activity according to cellular clues.

1.4.3.5 Heterogenous nuclear ribonuclear proteins

In contrast to SR proteins, some heterogenous nuclear ribonucleoproteins (hnRNPs) have been found to function as repressors of splicing. Thus, hnRNPA1 functions as a general sequence-independent regulator of alternative splicing by antagonising the function of SR proteins like SF2/ASF (Eperon et al., 2000). The balance between binding of SR proteins and hnRNPs to a pre-mRNA can determine the strength of a given splice site provides a mechanism for regulating constitutive and alternative splicing in metazoans (reviewed in (Matlin et al., 2005)).

1.4.4 Stepwise assembly of the pre-catalytic spliceosome

1.4.4.1 Formation of the pre-spliceosome/A complex

In contrast to the formation of the commitment/E complex, which occurs in an ATP-dependent manner, addition of the U2 snRNP to the pre-mRNA requires energy. Consistent with this, two DEAD-box RNA helicases, Sub2p and Prp5p, have both been implicated in binding of U2 snRNP to the branch point (Kistler and Guthrie, 2001; O'Day et al., 1996). Yeast genetics suggest that Sub2p is required for removal of Mud2p from the branch point to allow binding of the U2 snRNP. Thus, deletion of the MUD2 gene can bypass the requirement for the essential Sub2p RNA helicase (Kistler and Guthrie, 2001). Likewise, pre-spliceosome assembly requires Prp5p-dependent ATP hydrolysis (Xu et al., 2004), but occurs in an ATP independent manner in the absence of Cus2p, suggesting that Prp5p is required for the removal of Cus2p (Perriman and Ares, 2000; Perriman et al., 2003). Prp5p is, however, not dispensable in the absence of Cus2p, indicating that Prp5p activity is required in a later step (Perriman and Ares, 2000). Interestingly, a recent study suggests Prp5p-dependent ATP-hydrolysis links with a fidelity event related to base pairing between the branch region and U2 RNA (Xu and Query, 2007). Xu and co-worker were able to show that reduced Prp5p ATPase activity *in vitro* correlated with improved splicing of substrates with suboptimal branch region *in vivo*, whereas complementary mutations in U2 that increased U2-branch region pairing abrogated this effect (Xu and Query, 2007). Thus, the ATP requirement for the recruitment of the U2 snRNP and the formation of the pre-

spliceosome/A complex might provide kinetics that are compatible with a proofreading/check point event.

1.4.4.2 Formation of the complete spliceosome/B complex

Although U2/U4/U5/U6 and penta-snRNP complexes can be isolated under certain conditions, recent studies support the idea that the A complex is a functional intermediate, which can be converted into the B complex by addition of the tri-snRNP. Thus, the A complex assembles *in vivo* in the absence of U4 and U6 RNAs, and proceeds to form a functional spliceosome when added to extracts depleted of U2 snRNPs (Behzadnia et al., 2006; Tardiff and Rosbash, 2006).

Protein-protein interactions between the U4/U5/U6 tri-snRNP and the U1 and U2 snRNP-associated proteins are thought to stabilise the complete/B complex and to link 3'- and 5'-splice site recognition with the recruitment of the tri-snRNP. Consistent with this, SPF30 was found to bridge an interaction between the E complex protein U2AF35 and the U4/U5/U6 tri-snRNP protein hPrp3 (Little and Jurica, 2008). Thus, SPF30 might provide a link between 3'-splice site recognition and B complex formation in metazoans (Little and Jurica, 2008). In yeast, the U5 snRNP proteins Prp8p and Brr2p interact with several components of the U1 snRNP including U1-70K, Prp39, and Prp40 (Abovich and Rosbash, 1997; Fromont-Racine et al., 1997; van Nues and Beggs, 2001b). These interactions could provide a link between 5'-splice site recognition and the formation of the pre-spliceosome. Importantly, sustained association of the tri-snRNP with the pre-mRNA requires unwinding of base pairings between the 5'-splice site and the U1 snRNP and formation of new base pairs between the 5'splice site and U5 and U6 snRNPs (Lund and Kjems, 2002).

1.4.5 Activation of the spliceosome

The complete/B complex, which consists of all five snRNPs bound to the pre-mRNA, is catalytically inactive. Several conformational rearrangements must take place in order to generate a mature spliceosome. These include unwinding of the base pairings between the U1 snRNP and the 5' splice site and between U4 snRNP and U6 snRNP as well as formation of new base pairs between U5 and U6 snRNPs and the 5'splice site and between U6 and U2 snRNPs. As a result U1 and U4 snRNPs are released and the catalytic core of the spliceosome is formed (Figure 1-15). The essential DExD/H-box RNA helicases, Prp28 and Brr2p are both implicated in the

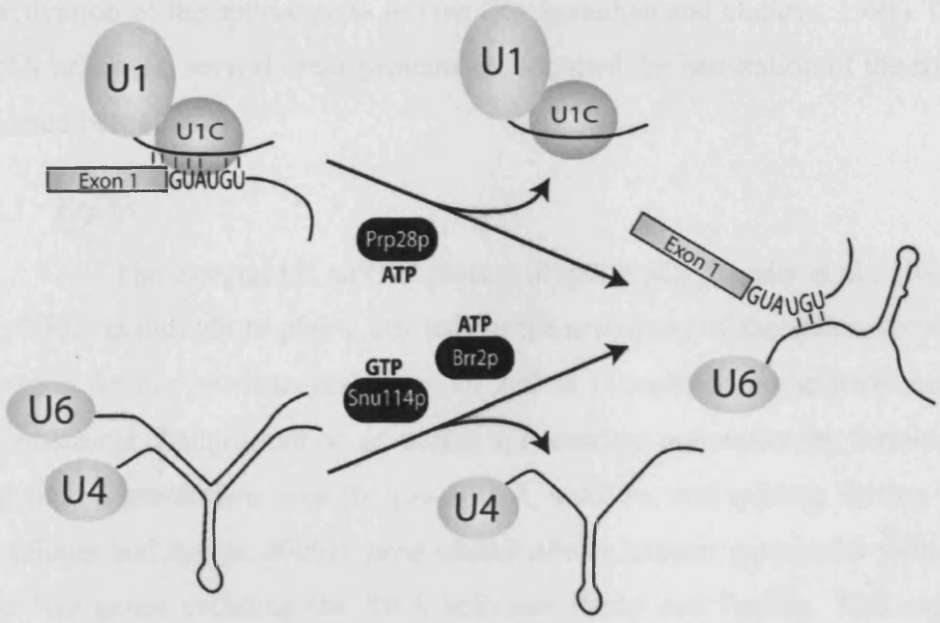

Figure 1-15: Activation of the spliceosome involves unwinding of pre-existing RNA duplexes and the formation of new base pairs. The yeast DexD/H-box RNA helicases Prp28p and Brr2p are both implicated in the activation step of spliceosome. Prp28p is thought to facilitate unwinding of basepairings between the U1 snRNA and the 5'-splice site, which results in the release of the U1 snRNP from the complete spliceosome. Brr2p promotes unwinding of the U4-U6 duplex and is required for release of the U4 snRNP and spliceosome activation. The small G protein, Snu114p, has also been implicated in maturation of the spliceosome and is thought to function upstream of Brr2p to regulate its activity. Unwinding of base pairings between U4 and U6 allows U6 to form new base pairs with the 5'-splice site once the U1 snRNP has been released.

rearrangements that occurs during activation of the spliceosome. Prp28p is thought to be important for the unwinding of base-pairings between U1 and the 5'-splice site (Chen et al., 2001b; Staley and Guthrie, 1999). Thus, genetics has shown that the requirement for Prp28p function in spliceosome activation can be bypassed by mutations that destabilise the interaction between U1 snRNP and the 5'-splice site (Chen et al., 2001b). Brr2p is likely to be responsible for unwinding the U4/U6 duplex (Raghunathan and Guthrie, 1998). First, U5-200kD, the human homologue of Brr2p, has been shown to unwind protein-free U4/U6 in vitro (Laggerbauer et al., 1998). Second, Brr2p is required for unwinding of the U4/U6 duplex, release of U4 snRNP, and activation of the spliceosome *in vivo* (Raghunathan and Guthrie, 1998). In addition to RNA helicases, several other proteins are required for maturation of the spliceosome (discussed below).

1.4.5.1 Prp8p

The integral U5 snRNP protein dPrp8/Prp8p (Lossky et al., 1987; Stevens et al., 2001) is thought to play a key role in the activation of the spliceosome. Prp8p is the largest known nuclear yeast protein and is thought to orchestrate many of the conformational changes that occur during spliceosome maturation by forming multiple and dynamic interactions with the pre-mRNA, snRNPs, and splicing factors. (reviewed in (Grainger and Beggs, 2005)). *prp8* mutant alleles interact genetically with mutations in the two genes encoding the RNA helicases Brr2p and Prp28p. This suggests that Prp8p might regulate the activity of both DExD/H proteins. Consistent with a role of Prp8p in modulating Brr2p activity, genetics has demonstrated that Prp8p regulates unwinding of the U4/U6 duplex (Kuhn and Brow, 2000). Thus, 44 different *prp8* single site mutant alleles were found to suppress a cold sensitive mutation in yeast U4 snRNP (U4-cs1) (Kuhn and Brow, 2000). The U4-cs1 mutation results in hyper stabilisation of the U4/U6 duplex and the accumulation of pre-catalytic spliceosomes containing stable U4/U6 dimers (Kuhn et al., 1999; Murray and Jarrell, 1999; Staley and Guthrie, 1998, 1999). The observed defect in pre-mRNA splicing in the U4-cs1 mutant is due to masking of a site in U6 that is required for its base pairing with the 5'-splice site (Li and Brow, 1996). These and other data lead Kuhn and Brow to propose a model in which Prp8p facilitate unwinding of the U4/U6 duplex only when U6 can correctly recognise the 5'-splice site (Kuhn and Brow, 2000). Thus, Prp8p might function as a control switch that negatively regulates the activity of Brr2p and possibly Prp28p until a signal

indicates that all factors are in place to support splicing (Reviewed in (Grainger and Beggs, 2005). In addition to Brr2p, the GTPase Snu114p (Bartels et al., 2002; Small et al., 2006) and the tri-snRNP proteins Prp38p and Spp381 (Lybarger et al., 1999; Xie et al., 1998) are all required for U4 snRNP release and spliceosome activation. Thus, these proteins are possible candidates for signalling upstream of Prp8p and/or Brr2p to promote Brr2p RNA helicase activity.

1.4.5.2 Snu114p

A recent study suggests that Snu114p acts as a classic regulatory G protein to regulate both spliceosome activation and disassembly (Small et al., 2006). Thus, unwinding of the U4/U6 helix and disassembly of the postsplicing U2/U6-U5-intron is repressed by Snu114p bound to GDP and derepressed by Snu114p bound to GTP or a non-hydrolysable GTP analogue (Small et al., 2006). Like Snu114p, Brr2p is also required for spliceosome activation and disassembly, and both are associated with the spliceosome throughout the splicing cycle (Lebaron et al., 2005; Ohi et al., 2002; Stevens et al., 2002). Moreover, Snu114p and Brr2p both bind directly to Prp8p (Achsel et al., 1998; van Nues and Beggs, 2001a), and *prp8* mutant alleles interact genetically with mutations in *snu144* (Brenner and Guthrie, 2005) and *brr2* (Kuhn et al., 2002; van Nues and Beggs, 2001a). This lead Small and co-workers to propose that changes in the guanine nucleotide state of Snu11p regulates Brr2p activity required for unwinding of the U4/U6 duplex either directly or upstream of Prp8p (Small et al., 2006). The signal that induces the switching of Snu114p from a GDP to a GTP bound state and vice versa remains to be identified.

1.4.5.3 Prp38p and Spp381

Prp38p was the first splicing factor reported to function in the activation of the spliceosome (Xie et al., 1998). Prp38p is a small acidic protein associated with the U4/U6-U5 tri-snRNP. Like Brr2p, Prp8p, and Snu114p, Prp38p activity is dispensable for the initial assembly of the spliceosome, but is required for the release of U4 snRNP and activation of the spliceosome (Xie et al., 1998). The molecular function of Prp38 in spliceosome activation is not clear, but it has been speculated that Prp38p might recruit (or activate) an RNA unwinding activity necessary for the release of U4 snRNA and the integration of U6 snRNA into the active site of the spliceosome (Xie et al., 1998). As discussed above, Brr2p is likely to represent the RNA unwinding activity

required for the release of U4 snRNP. The observation that Brr2p is stably associated with the spliceosome throughout the splicing cycle suggests that Prp38p is more likely to activate than recruit Brr2p (Ohi et al., 2002; Stevens et al., 2002).

The essential protein, Spp381, was identified in a dosage suppressor screen for proteins that function together with Prp38p (Lybarger et al., 1999). Like Prp38p, Spp381 is a small acidic protein associated with the U4/U6-U5 tri-snRNP. Spp381 interact directly with Prp38p and is required for splicing *in vivo* (Lybarger et al., 1999). Oddly, Spp381 does not appear to be required for splicing *in vitro*, and thus the splicing step at which Spp381 is required has not been determined (Lybarger et al., 1999).

1.4.5.4 Nineteen-complex (NTc)

A pre-assembled Prp19p-associated protein complex, named the NTc in yeast (Tarn et al., 1994) and the Prp19-CDC5 complex in humans (Ajuh et al., 2000; Makarova et al., 2004) plays an important role in the activation step of the spliceosome (Chan et al., 2003; Makarova et al., 2004). The budding yeast NTc consists of at least eleven tightly associated components most of which are evolutionary conserved. These include Ntc90/Syf1p, Ntc85/Cef1p (Cdc5 in *S. Pombe*), Ntc77/Clf1p, Ntc50/Prp46p, Ntc40/Cwc2p and Prp19p encoded by essential genes, and Ntc31p/Syf2p, Ntc30p/Isy1p, Ntc25p/Snt309p, and Ntc20p, which are not essential for growth (Chen et al., 2001a; Chen et al., 2002; Chen et al., 1998; Tsai et al., 1999). Prp19p, due to its ability to form tetramers (Ohi et al., 2005), is thought to function as a main organiser of the NTc. Consistent with this, mutations in Prp19p results in degradation of Cef1p and NTc instability (Ohi and Gould, 2002). The human Cdc5-Prp19 complex consists of at least 8 components and possibly as many as 30 (Ajuh et al., 2000; Makarova et al., 2004). Of these, Cdc5 and Prp19 are the only proteins that share homology with components of the NTc (Makarova et al., 2004).

The NTc enters the spliceosome around the time of the release of U1 and U4 snRNPs (Tarn et al., 1993). This led to the hypothesis that NTc might activate the spliceosome by promoting the release of U4 and/or U1 snRNPs (Tarn et al., 1993). However, recent studies have demonstrated that the NTc complex associates with the spliceosome only after dissociation of U1 and U4 snRNPs, and therefore is not required for the release of U4 snRNP (Bessonov et al., 2008; Chan et al., 2003). Instead the NTc appear to function by stabilising the interactions of U5 and U6 snRNPs with the pre-

mRNA after the release of U1 and U4 snRNPs (Chan and Cheng, 2005; Chan et al., 2003). This stabilisation is achieved in part by specifying the interaction between U6 and the 5'-splice site and between U5 and the pre-mRNA (Chan and Cheng, 2005; Chan et al., 2003). In humans, the Cdc5-Prp19 complex joins the B-complex after addition of the tri-snRNP and prior to the first catalytic reaction (Makarova et al., 2004). Moreover, the Cdc5-Prp19 complex is required for the first catalytic reaction to take place (Makarova et al., 2004). Thus, despite the striking difference in composition of the NTc and the Cdc5-Prp19 complex, their function in spliceosome activation may be conserved between yeast and humans (Makarova et al., 2004).

Recently, an additional NTc component, Yju2, was discovered, which associates with the NTc in a dynamic manner (Liu et al., 2007). Thus, whereas NTc remains associated with the spliceosome throughout both catalytic reactions, Yju2 dissociates from the NTc after the first catalytic step (Liu et al., 2007). Consistent with this, Yju2 was found to be required for pre-mRNA splicing *in vivo* and *in vitro*, and to promote the first catalytic reaction in concert with a heat resistant unknown factor (HP) (Liu et al., 2007).

In addition to a function in spliceosome activation, the NTc has also been implicated in U4/U6 biogenesis and spliceosome recycling (Chen et al., 2006a). Thus, cells depleted of NTc components accumulate free U4 snRNPs concomitant with reduced U4/U6 snRNP levels and exhibit impaired splicing and growth (Chen et al., 2006a). The accumulation of U4 is a consequence of insufficient amounts of U6, since over-expression of U6 in NTc-depleted cells prevents accumulation of U4 and partially rescues the growth defect (Chen et al., 2006a).

Interestingly, Prp19p contains a U-box at its N-terminus with structural similarity to RING finger domains (Ohi et al., 2003). Like many RING finger proteins, both human and budding yeast Prp19 exhibit E3 ubiquitin ligase activity *in vitro* (Ohi et al, 2003). The importance of this activity for their function in splicing remains to be determined, but it is possible that the Prp19 proteins regulate the activity of certain splicing factors via ubiquitylation. Thus, because Snu114p is ubiquitylated (Peng et al., 2003), it has been proposed that Prp19p might regulate the guanine bound state of Snu11p by reversible ubiquitylation (Small et al., 2006).

1.4.6 Excision of an intron by a two step catalytic reaction

1.4.6.1 The first catalytic reaction

The DExD/H-box RNA helicase Prp2p is required subsequent to U4/U6 unwinding, but prior to the first catalytic reaction (Kim and Lin, 1996). ATP hydrolysis by Prp2p is thought to induce structural rearrangements of the spliceosome required for the first catalytic reaction to take place (Kim and Lin, 1996). The essential gene encoding Spp2 interacts genetically with the *Prp2-1* mutation and is thought to be required for Prp2p function, possibly by mediating Prp2p binding to the spliceosome. Upon ATP hydrolysis, both proteins appear to leave the spliceosome, and no further rearrangements are required prior to the first attack of the branch point on the 5'-splice site. The first catalytic reaction involves a nucleophile attack by the 2' oxygen of the intronic branch point adenosine on the phosphorous atom that links the 5'exon and the intron. This results in the displacement of the phosphodiester bond between the intron and the 5' exon and the formation of an intron/3' exon lariat intermediate.

1.4.6.2 The second catalytic reaction

For the second catalytic reaction to occur, a 3'-splice site must be selected, and the phosphorous atom, which links the intron with the 3' exon, must be positioned for attack by the 3' hydroxyl group of the 5' exon. Consistent with this idea, most second step factors have been implicated in 3'-splice site selection and/or restructuring of the spliceosome. The essential DExD/H-box RNA helicase Prp16p binds to the spliceosome after lariat intermediate formation (Schwer and Guthrie, 1991), and its ATPase activity promotes the structural rearrangements that take place prior to the second catalytic reaction (Schwer and Guthrie, 1992). The association of Prp16p with the spliceosome is transient, and its release upon ATP hydrolysis is required for the second catalytic reaction to occur (Schwer and Guthrie, 1991). Interestingly, the rate of Prp16p-dependent ATP hydrolysis and release of Prp16p from the spliceosome has implications for spliceosome fidelity (Villa and Guthrie, 2005). Thus, in *prp16* mutants with reduced ATPase activity, the release of Prp16p is inhibited and as a result splicing of pre-mRNAs with mutated branch points occurs with increased frequency (Burgess and Guthrie, 1993). Splicing fidelity is restored in *prp16* mutants upon deletion of the gene encoding the NTc factor Isy1p (Villa and Guthrie, 2005). Consistent with this, deletion of Isy1p is found to promote the release of mutant Prp16p, thereby allowing

activation of the second step of splicing with normal kinetics (Villa and Guthrie, 2005). Moreover, in an *ISY1* single mutant strain, fidelity of the 3'-splice site is reduced (Villa and Guthrie, 2005). Thus, Prp16p and Isy1p are likely to be part of a surveillance mechanism that ensures proper selection of the 3'-splice site before initiation of the second catalytic step.

The non-essential yeast protein Prp17p is thought to join the spliceosome together with Prp16p in an ATP-dependent manner (Jones et al., 1995). Consistent with it being non-essential, Prp17p is only required for maximum efficiency of second catalytic step *in vitro* (Jones et al., 1995). The presence of Prp17p at the 3'-splice suggests that it might affect splice site recognition (Umen and Guthrie, 1995a). Unlike Prp16p, it remains associated with the 3'-splice site upon ATP hydrolysis (Umen and Guthrie, 1995a).

Subsequent to Prp16p release, the catalytic reaction itself occurs in an ATP-independent manner. This step involves the essential factors Slu7p and Prp8p, and the non-essential factor Prp18p (Grainger and Beggs, 2005; Umen and Guthrie, 1995c). Based on a number of studies, Prp8p is thought to be required for stabilisation of U5/exon interactions (Aronova et al., 2007; Teigelkamp et al., 1995). Thus, cross-linking studies have shown that Prp8p binds to U5 and to bases at the ends of both exons (Teigelkamp et al., 1995). A function of Prp8p in stabilising interactions between the 5'-splice site and U5 is further supported by the finding that the *prp8-R1753* mutant allele, which is thought to weaken spliceosome/exon interactions, is suppressed by mutations in U5 that are thought to strengthen the interaction of U5 with the exons (Aronova et al., 2007).

Prp18p is also thought to stabilise the interaction between U5 and the exons. Thus, gain of function mutations in *prp18* was found to suppress the *prp8-R1753* mutation (Aronova et al., 2007). This is consistent with previous studies carried out with another *prp18* mutant allele (Bacikova and Horowitz, 2005; Crotti et al., 2007), suggesting that Prp18p function together with Prp8p to stabilise U5/exon interactions.

Consistent with its function after Prp16p release, Slu7p crosslinks most strongly with the 3'-splice site after ATP hydrolysis and just before the second catalytic step (Umen and Guthrie, 1995b). *In vitro* studies suggest that Slu7p is required for proper positioning of the 3' hydroxyl of exon 1 for its attack on the 3'-splice site phosphodiester bond (Chua and Reed, 1999). Consistent with this, Slu7p affects 3'-splice site selection *in vitro* in yeast (Frank and Guthrie, 1992) and humans (Chua and

Reed, 1999). Moreover, gain-of-function mutations in *prp18* were found to suppress *slu7* mutants, suggesting an additional role for Slu7p in U5/exon stabilisation (Aronova et al., 2007).

Prp8p, Prp16p, Prp17p, Prp18p, and Slu7p are all evolutionary conserved, and previous studies suggest that the human proteins Prp16, Prp17, Prp18, and Slu7 function before or during the second catalytic reaction (Horowitz and Krainer, 1997; Umen and Guthrie, 1995a; Zhou and Reed, 1998). Thus, the mechanism underlying the second catalytic reaction is likely to be conserved between yeast and higher eukaryotes.

1.4.7 Disassembly of the spliceosome

Release of the spliced mRNA and disassembly of the spliceosome requires energy and involves the three DExD/H-box helicases Brr2p, Prp22p and Prp43p. Prp22p binds to the spliceosome at the stage of exon ligation (James et al., 2002b) and is required for release of the spliced mRNA (Schwer and Gross, 1998; Wagner et al., 1998). Moreover, Prp22p was shown to provide an ATP-dependent proofreading activity that discriminates against splicing of pre-mRNAs containing intronic mutations (Mayas et al., 2006). Mayas and co-workers were able to show that the proofreading of intronic intermediates is disabled in *prp22* mutants that are impaired in ATPase or RNA unwindase activity (Mayas et al., 2006). Thus, Prp22p is another example of a DExD/H-box helicase that confers fidelity to the spliceosome at the expense of ATP-hydrolysis. Prp43p replaces Prp22p (James et al., 2002b) and promotes release of the excised intron and disassembly of the spliceosome (Arenas and Abelson, 1997; Martin et al., 2002; Tsai et al., 2005; Tsai et al., 2007).

In addition to Prp43, Snu114p and Brr2p are both required for disassembly of the postsplicing U2/U6-U5-intron complex. Thus, intron release and spliceosome disassembly are blocked by mutations in *prp43* (Small et al., 2006; Tsai et al., 2005), *brr2* (Small et al., 2006), and *snu114* (Small et al., 2006). As previously mentioned, spliceosome assembly is repressed by Snu114p bound to GDP and derepressed by Snu114p bound to GTP or a non-hydrolysable GTP analogue (Small et al., 2006). This led Small *et al* to propose a model where spliceosome dynamics are regulated by the guanine nucleotide-bound state of Snu114p (Figure 1-16). According to this model, upon release of U4 snRNP and completion of spliceosome activation, a signal induces GTP hydrolysis switching Snu114p to its GDP bound inactive state during the chemical steps of splicing. Once splicing is complete another signal triggers the exchange of GDP

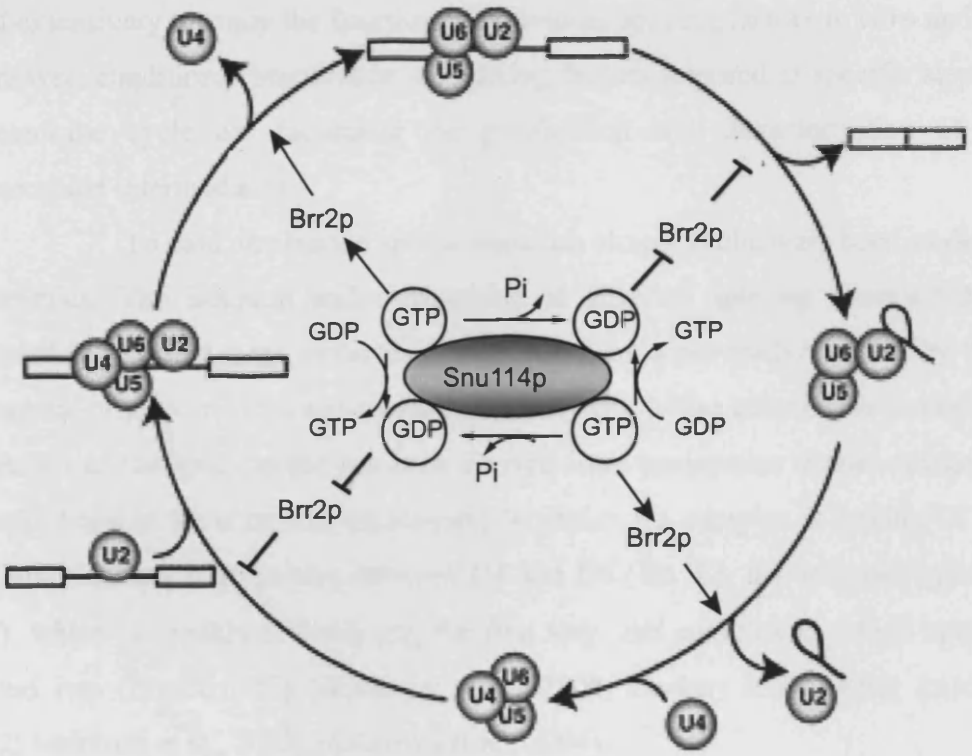

Figure 1-16: Activation of the spliceosome by Snu114p. A model has been put forward, which proposes that the guanine nucleotide state of Snu114p might regulate Brr2p activity to control spliceosome activation and disassembly. According to this model, Snu114p switches between its GDP-bound inactive and GTP-bound active form during the spliceosome cycle. The GTP-bound form of Snu114p activates Brr2p, which in turn executes the RNA helicase activities required for spliceosome activation or disassembly. In between spliceosome activation and disassembly, Snu114p-mediated GTP hydrolysis results in Brr2p inactivation. The signal that triggers GTP hydrolysis remains to be identified. Taken from (Small et al., 2006).

for GTP to activate Snu114p and promote intron release and spliceosome disassembly. Snu114p might then revert to its GDP bound inactive form until the next round of spliceosome activation (Small et al., 2006). Thus Snu114p could function as a regulatory switch to modulate the function of Brr2p, which in turn executes the RNA helicase activities required for spliceosome activation and disassembly.

1.4.8 The mammalian spliceosome

In yeast, biochemistry combined with the ease of genetics has contributed hugely to our understanding of the dynamic structure of the spliceosome. As discussed above, temperature-sensitive mutations in genes encoding splicing factors have been used extensively to study the function of individual splicing factors *in vitro* and *in vivo*. Moreover, conditional inactivation of splicing factors required at specific steps of the spliceosome cycle has facilitated the purification and characterisation of various spliceosome intermediates.

To date, the human spliceosome has almost exclusively been studied using proteomics. The isolation and comparison of different splicing intermediates have revealed that by and large, removal of an intron from a pre-mRNA occurs by the same sequential process in yeast and humans. The majority of the information concerning the dynamics of the spliceosome has been derived from proteomics studies comparing the compositions of the complete spliceosome (complex B), complex B lacking U1 snRNP, but still retaining base pairing between U4 and U6 (BΔ1C), the activated spliceosome (B*), which is capable of catalysing the first step, and complex C, which catalyse the second step (Figure 1-17) (Bessonov et al., 2008; Deckert et al., 2006; Jurica et al., 2002; Makarov et al., 2002; Makarova et al., 2004).

Mass spectrometry analysis of complexes B and C has revealed that the composition of the spliceosome changes substantially upon activation (Bessonov et al., 2008). As expected, U1 and U4 snRNP proteins are lost in complex C, whereas factors required for the second catalytic step are enriched. Upon activation of the spliceosome, the Cdc5-Prp19 complex appears to become more stably associated with the spliceosome. This is consistent with the reported association of the similar yeast NTc with the spliceosome during the activation step. Finally, proteins comprising the heterodimeric SF3a and SF3b complex are largely underrepresented in the C versus B complex. SF3a and SF3b complexes contact the pre-mRNA at and/or upstream of the BPS and stabilise the U2-BPS interaction (Gozani et al., 1996). Whereas this

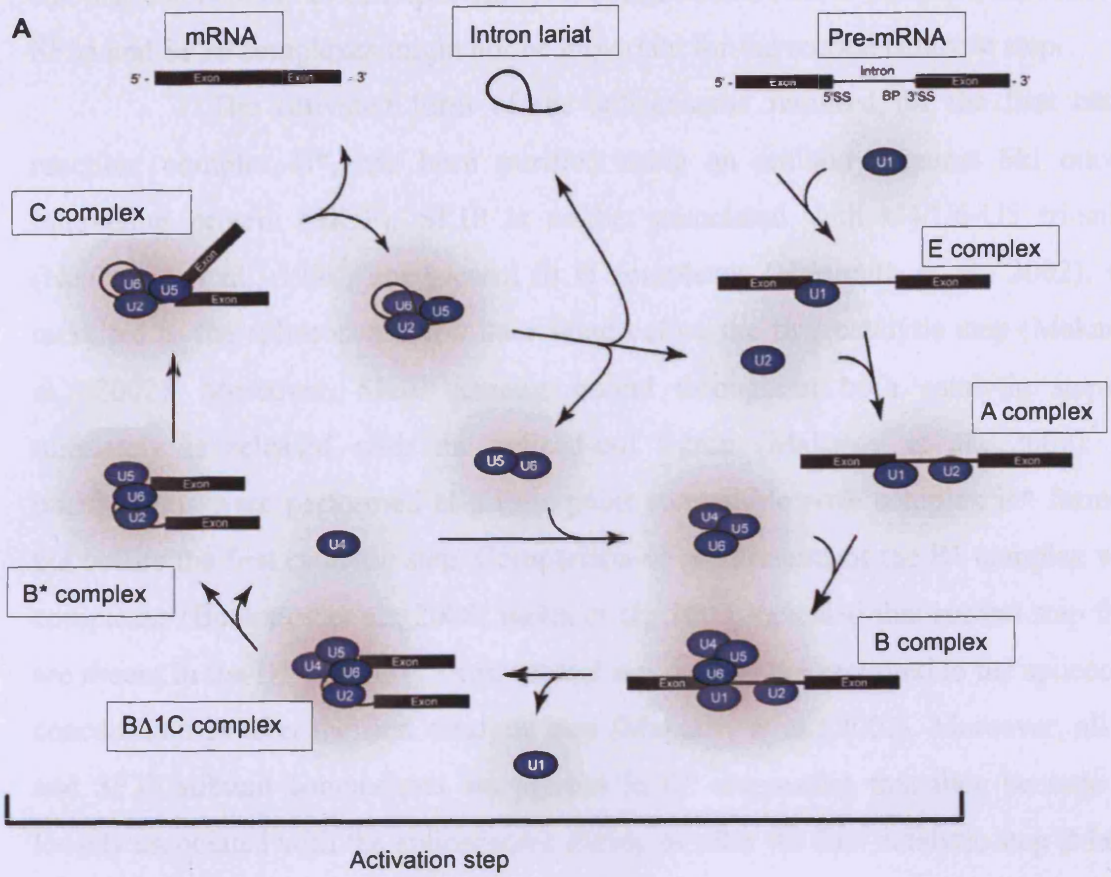

B

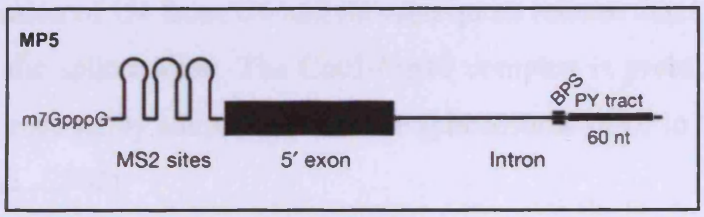

Figure 1-17: Purification of mammalian spliceosome intermediates. (A) The dynamics of the mammalian spliceosome has mainly been studied by comparing the composition of different splicing intermediates. Various methods have been employed to obtain highly homogenous purifications of trapped splicing intermediates. Purification of the A complex was accomplished by depletion of ATP, since assembly of the A complex, but not the B complex occurs in an ATP-independent manner. The BΔ1C complex was purified using an antibody directed against an U4/U6-specific 61K protein. The B* complex was isolated using an antibody against SKIP, which is not associated with the tri-snRNP or the B complex, but joins the spliceosome prior to the first catalytic reaction. B and later C complexes were assembled onto PM5 pre-mRNAs containing the BPS and the pyrimidine tract, but lacking the 3'-splice site and 3'-exon (B). The coliphage coat protein MS2 was used to purify complexes assembled onto the MP5 pre-mRNA at early (B complex) and late (C complex) time points. The C complexes assembled onto PM5 represent authentic intermediates, since they are able to catalyse the second transesterification reaction when offered a 3'-splice site-containing RNA *in trans*. Figures adapted from (Bleichert and Baserga, 2007) (A) and (Bessonov et al., 2008) (B).

stabilisation is likely to be important for the formation of the B complex, the function of SF3a and SF3b complexes might not be important for the second catalytic step.

The activated form of the spliceosome required for the first catalytic reaction, complex B*, has been purified using an antibody against Ski oncogene interacting protein (SKIP). SKIP is neither associated with U4/U6-U5 tri-snRNPs (Neubauer et al., 1998) nor present in B complexes (Hartmuth et al., 2002), but is recruited to the spliceosome at a later stage before the first catalytic step (Makarov et al., 2002). Moreover, SKIP remains bound throughout both catalytic steps and ultimately is released with the spliced-out intron (Makarov et al., 2002). SKIP purifications were performed at a time point compatible with complex B* formation, but before the first catalytic step. Comparison of constituents of the B* complex with C complexes (Bessonov et al., 2008; Jurica et al., 2002) revealed that second step factors are absent in the B* complex. Thus, second step factors are recruited to the spliceosome concomitant or after the first catalytic step (Makarov et al., 2002). Moreover, all SF3a and SF3b subunit components are present in B* suggesting that they become more loosely associated with the spliceosome during or after the first catalytic step (Makarov et al., 2002). As expected, no U1 snRNP-specific proteins were present in the B* complex. Moreover, all U4 and U4/U6 snRNP-specific proteins and two tri-snRNP proteins were absent in the B* complex (Makarov et al., 2002). This is likely to be due to the dissociation of U4 from U6 and its subsequent release that takes place during the activation of the spliceosome. The Cdc5-Prp19 complex is present in the B* complex and thus becomes stably associated with the spliceosome prior to the first catalytic step (Makarov et al., 2002).

In yeast, many conformational changes and structural rearrangements take place after the addition of the tri-snRNP and before the first catalytic step. To further investigate the dynamics during this process, Lührmann and co-workers used an antibody that recognises the U4/U6-specific 61K protein to isolate a spliceosomal intermediate that contains an intact U4/U6-U5 snRNP, but lack the U1 snRNP (BΔ1C) (Makarova et al., 2004). Cross-linking studies showed that U4 and U6 are still base paired in the BΔ1C complex, indicating that this complex represents an intermediate step between the formation of the B and the B* complex. Consistent with this, the tri-snRNP is largely intact in the BΔ1C complex, whereas all U4/U6 specific proteins are lost in the B* complex. Mass spectrometry analysis of the BΔ1C complex revealed the

absence of the Cdc5-Prp19 complex. Thus, the Cdc5-Prp19 complex joins the spliceosome after the addition of the tri-snRNP, but before the first catalytic step (Makarov et al., 2002; Makarova et al., 2004). Consistent with this, Cdc5-Prp19 complex function is required for the first catalytic step (Makarova et al., 2004).

The above studies suggest that the majority of the information derived from functional studies of the spliceosome in yeast is relevant to spliceosome function in humans. Like in yeast, U1 and U4 snRNPs are lost during spliceosome activation, the Cdc5-Prp19 complex joins the spliceosome after the addition of the tri-snRNP and prior to the first catalytic step, and a set of highly conserved second step factors are recruited to the spliceosome prior to the second catalytic step (Bessonov et al., 2008; Deckert et al., 2006; Jurica et al., 2002; Makarov et al., 2002; Makarova et al., 2004).

Significant progress in purification of splicing intermediates combined with proteomics has contributed a great deal to our understanding of the dynamics of the spliceosome. However, very little is known about its three-dimensional structure. This is mostly due to the highly complex and dynamic nature of the spliceosome and the difficulty of obtaining homogenous preparations of splicing intermediates. In spite of this, the recent years of research have seen advances in obtaining low-resolution images of different spliceosome intermediates using cryo-electron microscopy. Moreover, high-resolution studies have been carried out on a smaller scale (Deckert et al., 2006; Jurica et al., 2004; Sander et al., 2006; Schellenberg et al., 2006; Stark and Luhrmann, 2006). Thus, the future holds a promise that major advances will be made in understanding this highly complex cellular machine in the next few years.

1.4.9 Links between cell cycle and splicing

1.4.9.1 Yeast studies

The first clues that pointed to a link between splicing and cell cycle progression came from studies in yeast. A number of genes that were originally isolated in genetic screens for cell cycle regulators were later shown to function in splicing (Hwang and Murray, 1997; Johnston and Thomas, 1982; Lundgren et al., 1996; Nasmyth and Nurse, 1981; Potashkin et al., 1998; Shea et al., 1994; Takahashi et al., 1994; Vaisman et al., 1995; Vijayraghavan et al., 1989). These include *prp3*, *prp17*, *prp8*, *cef1*, *prp22* (*S. cerevisiae*) (Boger-Nadjar et al., 1998; Hartwell et al., 1973; Hwang and Murray, 1997; Johnston and Thomas, 1982; Ohi et al., 1998; Shea et al.,

1994; Vaisman et al., 1995) and *prp2*, *cdc28/prp8*, and *cdc5* (*S. pombe*) (Lundgren et al., 1996; Nurse et al., 1976; Ohi et al., 1998; Takahashi et al., 1994). Whereas mutations in some of these genes cause cells to arrest heterogeneously throughout the cell cycle, *cef1-13*, *prp17Δ*, and *prp22-1* mutants arrest homogenously in G2/M (Burns et al., 2002). The source of the variability in timing and cell cycle arrest phenotypes among splicing factor mutants is unclear. It is possible that the observed range of cell cycle arrest phenotypes reflects differences in the severity of splicing defects in those mutants. Moreover, a model has been put forward to explain the variability of the timing of cell cycle arrest, which suggests that splicing factors are differentially required for efficient splicing of single transcripts or a subset of transcripts (Burns et al., 2002). Consistent with this idea, removal of a single intron from the α-tubulin-encoding gene *TUB1* alleviates both the G2/M arrest and cell division defect observed in the *cef1-13* mutant, but only partially rescues the cell division defect observed in the *prp17Δ* and *prp22-1* mutants (Burns et al., 2002; Chawla et al., 2003). Instead, the G2/M arrest and growth defect in the *prp17Δ* mutant can be rescued by removal of an intron from the *ANC1* gene (Dahan and Kupiec, 2004). The molecular basis for this specificity remains unclear.

1.4.9.2 Mammalian studies

A number of studies carried out in vertebrate cells suggest that splicing and cell cycle progression are also connected in higher eukaryotes. For instance, the human homologue of Cef1p/Cdc5 (*S. cerevisiae/S. pombe*) was found to regulate G2 progression and mitotic entry. Thus, over-expression of hCdc5 shortens G2, whereas expression of a dominant negative mutant of hCdc5 slows down G2 progression and delays entry into mitosis (Bernstein and Coughlin, 1998). ASF/SF2 is another splicing factor that is required for cell cycle progression. Conditional knockout of ASF/SF2 in chicken B-cells results in G2/M arrest and programmed cell death (Li et al., 2005a). A third example is U2AF35, which is required for splicing of pre-mRNAs with non-consensual or weak pyrimidine tracts (Guth et al., 1999). Depletion of human U2AF35 results in reduced cell viability and mitotic arrest (Pacheco et al., 2006). The mitotic arrest might be a consequence of the strong effect that U2AF35 depletion has on Cdc25 mRNA levels, since Cdc25 is required for progression through mitosis (Pacheco et al., 2006).

So far, studies of vertebrate splicing factors and their requirement for cell cycle progression are few and mostly concern splicing factors that are only required for processing of a subset of mRNAs. It still remains to be addressed whether inactivation of different core components of the metazoan spliceosome would give rise to the same variability in cell cycle phenotypes observed in yeast. In this context it is worth mentioning that a recent genome wide RNA interference screen in Hela cells for genes required for cell division identified a few, but far from all core components of the splicing machinery (Kittler et al., 2004).

1.4.10 Splicing defects as a primary cause of disease in higher eukaryotes

Mutations in *cis*-acting elements can result in the disruption of splicing codes required for recruitment of the splicing machinery, the generation of cryptic splice sites, and the alteration of secondary structures within the pre-mRNA. Several studies suggest that mutations in *cis*-acting splicing elements are the primary cause of many human diseases. Thus, a recent study estimates that 60% of mutations that cause diseases do so by disrupting splicing (Lopez-Bigas et al., 2005).

Whereas mutations in *cis*-acting splicing elements are likely to affect just one transcript, mutations in splicing factors or proteins required for spliceosome function can potentially affect splicing of several transcripts. Consistent with key role of splicing factors in regulating gene expression, mutations in *trans*-acting factors have been reported for several diseases. Two examples are spinal muscular atrophy (SMA) and retinitis pigmentosa, the most common form of blindness (Mordes et al., 2006; Winkler et al., 2005). SMA is caused by loss of the *survivor of motor neuron-1* (*smn1*) gene product, which has been implicated in maturation of snRNPs (Winkler et al., 2005). Whereas a defect in maturation of snRNPs has not been proven to be the primary cause of SMA, spliceosome function is likely to be altered in this disease. Retinitis pigmentosa has in several cases been linked with mutations in three core components of the spliceosome, Prpf31, Prpf8, and hPrp3, suggesting that altered splicing patterns in some cases is the primary source of this disease (Chakarova et al., 2002; McKie et al., 2001; Vithana et al., 2001).

There is clear evidence that mutations in *cis*-acting elements of oncogenes, tumor suppressors and other cancer-relevant genes or in trans-acting factors that regulate their splicing are a frequent source of cancer initiation and progression (reviewed in (Srebrow and Kornblihtt, 2006)). Proteins belonging to the SR protein

family constitute a group of trans-acting factors that are frequently mutated in various types of cancer (Ghigna et al., 2005; Karni et al., 2007; Sjoblom et al., 2006). As previously discussed, SR proteins function in splice site selection and have been implicated in regulated and alternative splicing. Thus, mutations in SR proteins are likely to affect the expression of only a subset of genes and could potentially target oncogenes or tumor suppressor genes specifically.

Genome-wide microarray assays to assess the splicing differences associated with normal variation or disease might prove useful for detecting alternative splicing signatures related with specific diseases and therefore may provide a future tool for diagnosing many diseases.

1.4.11 The spliceosome – an evolutionary conserved splicing machine

Group II self-splicing introns catalyse auto-excision from pre-mRNAs by a strikingly similar chemical reaction to that catalysed by the spliceosome. This has led to the general belief that RNAs form the catalytic core of the spliceosome, and that RNAs are largely responsible for the excision of intronic sequences. In addition to five RNAs, the spliceosome comprises more than 200 splicing factors, making it one of the most complex cellular machineries. The vast number of splicing factors is thought to assist the conformational changes of the RNAs required for the catalytic reactions to take place.

So what are the advantages of having a macromolecular complex over group II self-splicing introns, given that both are capable of excising an intron from a pre-mRNA? First, the requirement for *trans*-acting factors means that splicing can be regulated by modulating the levels of individual splicing factors and/or their activities. This is particularly striking in metazoans where alternative splicing of multi-exon pre-mRNAs occurs frequently and in a highly regulated manner. Second, the presence of multiple weak consensus splicing sites within the same pre-mRNA puts a high demand on the spliceosome for splice site recognition. Consistent with this, additional splicing factors, including SR proteins, are required to ensure substrate specificity. The combinatorial binding of SR proteins and other factors to weak consensus sequences in the pre-mRNA is thought to determine the strength of a given splice site. Third, the substrate specificity of SR protein depends on their phosphorylation status, which in turn is regulated by SR protein kinases. Thus, reversible phosphorylation events regulates the recruitment of the spliceosome to a particular splice site and allows the

temporal expressing of a subset of genes in response cellular signalling. Fourth, it has recently become clear that the spliceosome contains an intrinsic quality surveillance system. Thus, ATP-hydrolysis by DExD/H RNA helicases is thought to provide kinetics that are compatible with substrate proofreading at multiple steps of the spliceosome cycle. Prp5p dependent ATPase activity ensures that the U2 snRNP is base paired only with optimal branch point sequences. ATP hydrolysis by Prp16p provides kinetics that are compatible with a proofreading event prior to the second catalytic reaction. Prp22p provides an ATP-dependent activity that discriminates against excision of mutated introns. Thus, the spliceosome has evolved to become a high-fidelity splicing machinery with a substrate specificity that can be fine-tuned according to the metabolic state of the cell. Future research will reveal more structural details of this highly dynamic and complex cellular machine.

1.5 Translation initiation

The fourth *Drosophila* protein characterised in my thesis, Pixie/RLI/Rlip (*Drosophila*/humans/yeast), is required for normal levels of translation initiation in flies (shown here) and yeast (Dong et al., 2004; Kispal et al., 2005; Yarunin et al., 2005). Thus, in the fourth and final section of the introduction, I have attempted to provide the reader with an overview of translation with an emphasis on translation initation. This section also includes a brief introduction to insulin signalling, which regulates protein synthesis at several stages including translation initiation and elongation.

1.5.1 Assembly of a functional 80S ribosome

Translation initiation is a multi-step process involving the sequential assembly of various large pre-initiation complexes (PICs) (Figure 1-18). First, eukaryotic initiation factor (eIF) 1, eIF1A, eIF3, eIF5 and the ternary complex (TC), which consists of eIF2 bound to GTP and the initiator $tRNA_i^{Met}$, are recruited to the small 40S ribosomal subunit to form the 43S PIC. Then, the 40S subunit binds to the capped 5'end of the mRNA in a reaction requiring eIF4E, eIF4G, eIF4A, and eIF4B. This complex scans the mRNA and positions itself on the correct initiation AUG codon, thereby forming the 48S PIC. Finally, the eIFs are displaced by the large 60S ribosomal subunit in an eIF5B-dependent reaction to generate functional 80S ribosomes (Chen, 2000; Hinnebusch, 2000).

1.5.1.1 eIF3

The eIF3 complex is composed of at least 13 different subunits in mammals (eIF3a-m) and flies (eIF3-S1-13) ((Lasko, 2000) and reviewed in (Hinnebusch, 2006)). Only six of the 13 subunits are conserved in budding yeast. Thus, budding yeast eIF3 is composed of Tif32p/eIF3-S10/eIF3a, Nip1p/eIF3-S8/eIF3b, Prt1p/eIF3-S9/eIF3c, Tif35p/eIF3S-4/eIF3g, Tif34p/eIF3-S2/eIF3i, and one loosely associated component, Hcr1p/Adam/eIF3j (yeast/flies/humans) (reviewed in (Hinnebusch, 2006)). Of these, Hcr1p is the only non-essential protein, suggesting that Hcr1p has a regulatory rather than a core function (Valasek et al., 1999). The other five yeast components are thought to make up the core eIF3 complex, and protein-protein interaction studies of yeast and mammalian eIF3 suggest that the architecture of the

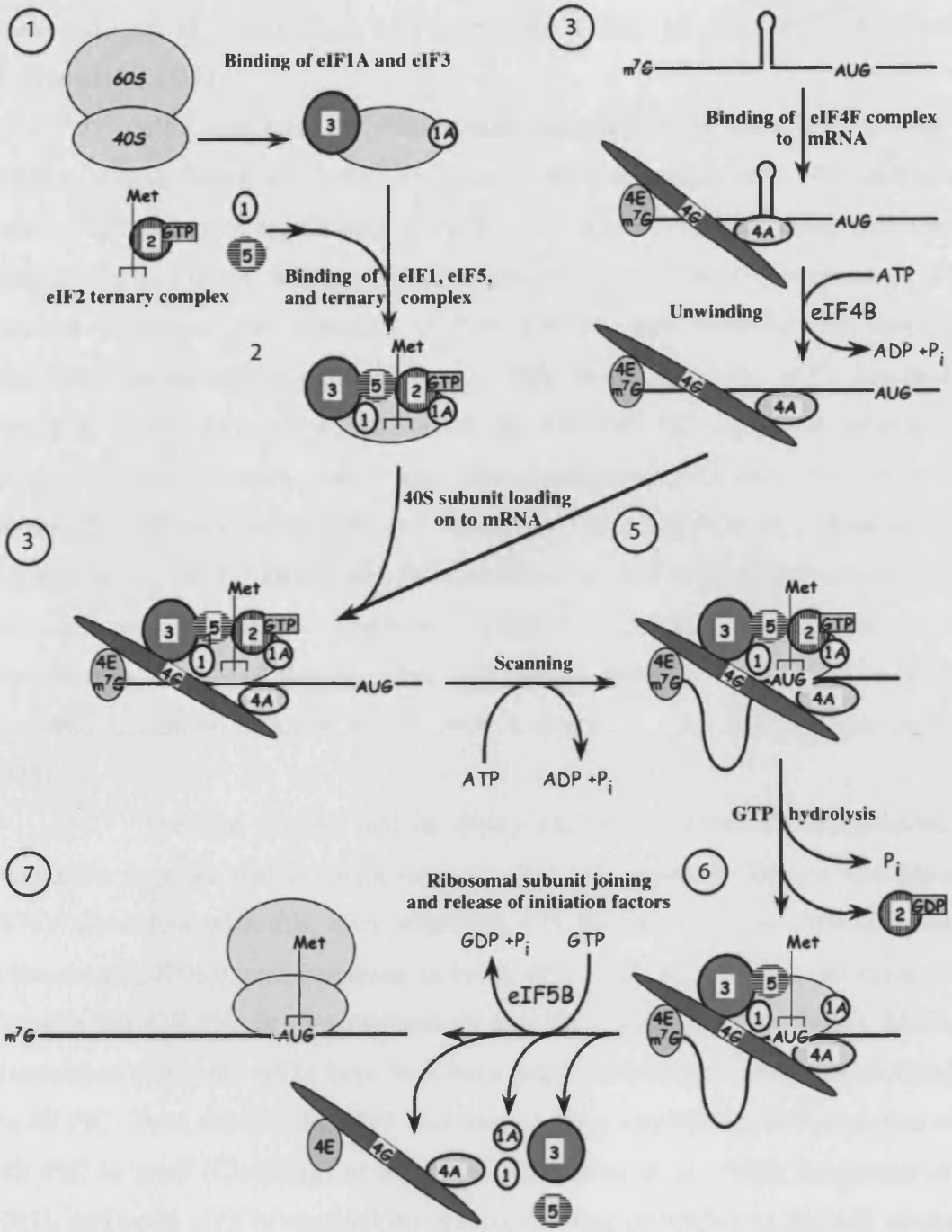

Figure 1-18: Translation initiation. eIF3 binds to free 40S subunits and prevents the spontanous assembly of 40S and 60S subunits into empty 80S ribosomes lacking mRNA (1). 40S-bound eIF3 promotes the recruitment of the TC and eIFs 1, 1A, and 5 to the 40S subunit to generate the 43S PIC (2). Next, the mRNA is recruited to the 43S PIC (3). This is facilitated by an interaction between eIF3 and the 5'-cap-binding complex, eIF4F, which is composed of eIF4E, eIF4G, and eIF4A. eIF4E binds to the 5'-cap structure of the mRNA, eIF4G bridges an interaction between eIF4F and eIF3, and the eIF4A RNA helicase activity is thought to remove secondary structures in the mRNA that hinder 43S PIC recruitment (4). Once assembled onto the mRNA, eIF1 and eIF5 stimulates downstream scanning for a start site and positioning of the 43S PIC onto an AUG start codon to generate the 48S PIC (5). Base pairing between the Met-tRNA$_i^{Met}$ and the AUG start codon stimulates eIF5-dependent hydrolysis of eIF2-bound GTP and the subsequent release of eIF2-GDP (6). Finally, the eIF5B GTPase promotes joining of the 40S and 60S subunits and release of the rest of the eIFs (7). Taken from (Jackson, 2005).

conserved part of mammalian eIF3 is similar to that of yeast eIF3 (reviewed in (Hinnebusch, 2006)).

eIF3 can bind the 40S subunit independent of other eIFs (Benne and Hershey, 1976). Based on a cryo-EM model of the mammalian eIF3-40S complex, the bulk of eIF3 subunits are thought to bind to the solvent surface rather than the 60S subunit interface of the 40S subunit (Siridechadilok et al., 2005). Nevertheless, eIF3 is required to prevent the assembly of free 40S and 60S subunits into empty 80S ribosomes lacking mRNA (Thomas et al., 1980; Thompson et al., 1977; Trachsel and Staehelin, 1979). This is important since the 40S and 60S ribosomal subunits have strong affinities for each other, and their spontaneous assembly into empty 80S ribosomes represents an obstacle to translation initiation (Falvey and Staehelin, 1970; Henshaw et al., 1973). Importantly, the association of eIF3 with the 40S subunit alone is not sufficient to prevent premature 40S-60S subunit assembly, but requires simultaneous binding of the TC, eIF3, eIF1, eIF1A and RNA nucleotides to the small ribosomal subunit (Chaudhuri et al., 1999; Kolupaeva et al., 2005; Majumdar et al., 2003).

The size of eIF3 and its ability bind the 40S subunit independently of other eIFs suggests that it might nucleate 43S PIC assembly (Benne and Hershey, 1976). Consistent with this, eIF3 stimulates 43S PIC assembly *in vitro* (reviewed in (Hinnebusch, 2006)), and mutations in yeast eIF3 result in reduced association of the TC with the 43S PIC *in vivo* (Valasek et al., 2002; Valasek et al., 2004). Moreover, mammalian and yeast eIF3s have both been implicated in the subsequent assembly of the 48 PIC. Thus, mammalian eIF3 stimulates mRNA recruitment and formation of the 48S PIC *in vitro* (Chaudhuri et al., 1999; Kolupaeva et al., 2005; Majumdar et al., 2003), and yeast eIF3 is required for optimal binding of mRNA to the 40S ribosomal subunit *in vivo* (Danaie et al., 1995; Phan et al., 1998). The exact mechanism by which eIF3 stimulates 48S PIC assembly is not clear, but there are a few indications. The eIF3 complex forms multiple contacts with eIF4 and is likely to bridge an interaction between the eIF4-mRNA complex and the 40S subunit. Thus, mammalian eIF3 interacts with eIF4B, eIF4G and the cap-binding subunit eIF4E *in vitro* ((Holz et al., 2005; Methot et al., 1996) and reviewed in (Hinnebusch, 2006)). Interestingly, the eIF3-eIF4G interaction is stimulated by the mTOR pathway (Harris et al., 2006), suggesting that bridging between eIF3 and eIF4G might regulate the rate of 48S PIC assembly on mTOR-responsive mRNAs (Harris et al., 2006).

In addition to a role in 43S and 48S PIC assembly, eIF3 has also been implicated in mRNA scanning and start site recognition. Thus, mutations in eIF3, which disrupt its interaction with eIF1 or eIF5, impair scanning and facilitate initiation at UUG codons *in vivo* (Valasek et al., 2004). This might be an indirect effect, since eIF3 is required for optimal recruitment of eIF1 and eIF5, both of which have defined functions in mRNA scanning. eIF5 promotes hydrolysis of eIF2-associated GTP, an event which is tightly linked with AUG start site selection (Das et al., 2001), and eIF1 promotes scanning and ensures that phosphate is released from eIF2-GDP-P_i only when the AUG start codon has been located in the peptidyl (P) site (Algire et al., 2005; Pestova and Kolupaeva, 2002). However, it has been shown that eIF3 and the eIF4F-m^7GTP complex can restrain eIF5-dependent GTP hydrolysis in the absence of an AUG start codon in the P site (Majumdar and Maitra, 2005). Thus, eIF3 might not only function as a scaffold for eIF1 and eIF5, but could directly regulate their activities.

With the exception of eIF3j, relatively little is known about the individual subunits of mammalian eIF3. Like its yeast homologue Hcr1p, eIF3j is loosely associated with the eIF3 complex (Fraser et al., 2004; Phan et al., 1998; Unbehaun et al., 2004; Valasek et al., 2001). Moreover, eIF3j binds to the 40S subunit independently of other eIF3 components and promotes the recruitment of the eIF3 complex to the 40S subunit *in vitro* and *in vivo* (Fraser et al., 2007; Fraser et al., 2004; Nielsen et al., 2006; Unbehaun et al., 2004). A recent study provided further insight into the function of eIF3j in PIC assembly (Fraser et al., 2007). The eIF3j binding site on the 40S subunit was mapped to the aminoacyl (A) site and the mRNA entry channel, placing eIF3 right in the decoding center of the small ribosomal subunit. Moreover, binding of eIF3j to the mRNA entry channel was found to reduce the affinity of the 40S subunit for mRNA. High affinity for mRNA was only restored upon recruitment of the TC and positioning of Met-$tRNA_i^{Met}$ in the P site, suggesting that eIF3 might control the order of TC and mRNA recruitment (Fraser et al., 2007). Interestingly, the association of eIF3j with the 40S subunit seems to be regulated in a mTOR-dependent manner, suggesting that eIF3j might stimulate the rate of eIF3-40S complex formation in accordance with the metabolic state of the cell (Miyamoto et al., 2005). Consistent with a regulatory function of eIF3j, yeast eIF3j (Hcr1p) is not essential for survival, though its depletion does result in a slow growth phenotype (Valasek et al., 1999).

1.5.1.2 eIF2

Recruitment of the TC to the 40S subunit is a key step in 43S PIC assembly. In yeast, eIF1 and eIF1A seem to play critical roles in promoting stable association of the TC with the 40S subunit *in vitro* (Algire et al., 2002; Maag et al., 2005). Yeast eIF3 only minimally affects binding of the TC to the 40S subunit *in vitro*, but is required for efficient recruitment of the TC to the 40S subunit *in vivo* (Algire et al., 2002; Maag et al., 2005). The requirements for mammalian eIFs 1, 1A, and 3 for stable association of the TC with the 40S subunit *in vitro* are controversial. Originally, eIF3 was found to promote recruitment of the TC to the 40S subunit in a reaction stimulated by eIFs 1 and 1A. More recently using an identical *in vitro* system, eIFs 1, 1A, and 3 appeared to be only minimally required for stable association of the TC with the 40S subunit (reviewed in (Kapp and Lorsch, 2004)). Either way, eIFs 1, 1A, and 3 might promote recruitment of the TC to the 40S subunit *in vivo*, like their yeast counterparts.

Translation initiation requires the assembly of 80S ribosomes onto mRNAs with a Met-tRNA$_i^{Met}$ positioned in the P site and base-paired to the AUG start codon. Once positioned on the AUG start codon, hydrolysis of eIF2-bound GFP takes place in a reaction that requires the activity of the GTPase activating protein eIF5. This ultimately leads to dissociation of the eIF2-GDP complex from the 40S subunit before the 60S subunit joins to form the 80S ribosome (Hinnebusch, 2000). Importantly, the eIF2-GDP complex must be converted back to the eIF2-GTP form to render it available for another round of translation initiation. This is facilitated by the GDP dissociation factor eIF2B, which promote dissociation of GDP from eIF2-GDP and conversion of eIF2 into its GTP-bound form (Williams et al., 2001). The incorporation of eIF2-GTP into the TC is further promoted by the ATP-binding cassette protein 50 (ABC50) (Tyzack et al., 2000).

eIF2 is composed of the three subunits α, β, and γ, where the γ subunit binds to GTP and the Met-tRNA$_i^{Met}$. The exchange of GDP for GTP, which is a key regulatory step in translation initiation, is regulated by phosphorylation of eIF2 (reviewed in (Proud, 2005)). Thus, phosphorylation of the α and/or β subunits of eIF2 blocks its interaction with eIF2B and inhibits translation initiation (Rowlands et al., 1988). In mammals, four different protein kinases have been identified that phosphorylate and inactivate eIF2 in response to cellular stress or low nutrient

conditions (Figure 1-19). These are the PEK (pancreatic eIF2α kinase), HRI (heme-regulated inhibitor), PKR (RNA-dependent protein kinase), and GCN2 (general amino acid control of gene expression non-derepressible-2) protein kinases (reviewed in (Dever, 2002; Proud, 2005)).

Finally, eIF2 activity might be regulated in accordance with its cellular localisation. In a recent study, yeast eIF2 and eIF2B were found to localise to discrete regions of the cytoplasm (Campbell et al., 2005). eIF2B seems to be a permanent component of these cytoplasmic foci, whereas eIF2 shuttles in and out of them. Mutations in eIF2B that reduce its Gunanin exchange factor (GEF) activity also inhibit shuttling of eIF2 into the cytoplasmic foci, suggesting that eIF2 activation take place within those discrete regions (Campbell et al., 2005).

1.5.1.3 Regulation of eIF2 activity in response to various types of stress

As previously mentioned, eIF2-GDP must be converted back to eIF2-GTP at the end of each round of translation to render it active for a new round of 43S PIC assembly. This is a key regulatory step and is regulated by phosphorylation of eIF2 on its regulatory subunits. The PEK, PKR, HIR, and GCN2 protein kinases all negatively regulate eIF2 activity in response to various types of stress (Figure 1-19). PEK-mediated phosphorylation of eIF2 occurs in response to endoplasmic reticulum (ER) stress and blocks translation of new ER destined proteins. This allows the organelle to recover and deal with its existing load (Bertolotti et al., 2000; Harding et al., 2000b; Kaufman, 1999). PKR plays a major role in the stress response to viral infection. Thus, its expression is induced by interferons, and binding of double-stranded (ds)RNA to the N-terminal domain of PKR results in its activation and phosphorylation of eIF2, preventing translation of viral RNAs (Nanduri et al., 2000). HRI is activated in response to heme deprivation, oxidative stress and heat shock (Chen, 2000; Lu et al., 2001). GCN2 is activated in response to limited nutrient conditions. Thus, amino acid starvation leads to accumulation of uncharged tRNAs, which bind to and activate GCN2 (reviewed in (Proud, 2005)). GCN2 activation results in eIF2 phosphorylation and a reduction in global levels of translation. Importantly, GCN2 activity also induces the expression of a small subset of genes encoding proteins involved in amino acid biosynthesis to compensate for the decrease in cellular amino acid uptake (reviewed in (Proud, 2005)). The implication of GCN2 in this type of stress response is clearly demonstrated by the phenotype of the *gcn2* knock-out mice (Zhang et al., 2002). Thus,

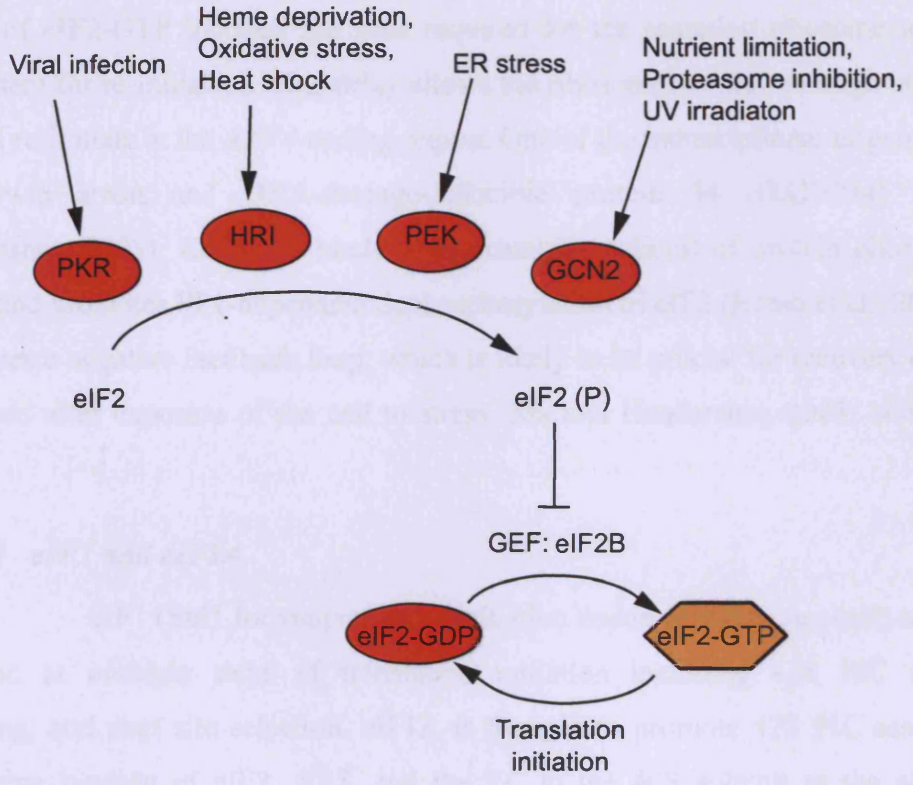

Figure 1-19: Regulation of eIF2 activity in response stress. The PKR, HRI, PEK, and GCN2 kinases phosporylate eIF2 in response to different types of stress. Phosphorylation of eIF2 prevents its interaction with eIF2B and keeps eIF2 in its GDP-bound inactive form. As a result, translation initiation is blocked .

GCN2-deficient mice are significantly less tolerant to amino acid deficiency (Zhang et al., 2002).

The mammalian transcriptional activator ATF4 belongs to another sub-group of proteins that are synthesised in response to several types of cellular stress that affect eIF2-GFP levels (Harding et al., 2000a; Jiang et al., 2004; Vattem and Wek, 2004). This is facilitated by two upstream open reading frames (uORFs) in the ATF4 mRNA (Vattem and Wek, 2004). uORF1, which encodes three amino acids, is a positively acting element that facilitate scanning and re-initiation at downstream coding regions (Vattem and Wek, 2004). uORF2 is 59 residues long and functions as an inhibitory element that blocks ATF4 expression (Vattem and Wek, 2004). Reduced levels of eIF2-GTP increase the time required for the scanning ribosome to become competent for re-initiation. This delay allows the ribosomes to scan through uORF2 and instead re-initiate at the *ATF4*-coding region. One of the transcriptional targets of AFT4 is growth arrest and DNA-damage-inducible protein 34 (GADD34) (Ma and Hendershot, 2003). GADD34 binds to the catalytic subunit of protein phosphatase 1 (PP1) and promotes PP1-dependent dephosphorylation of eIF2 (Brush et al., 2003). This generates a negative feedback loop, which is likely to be crucial for recovery of protein synthesis after exposure of the cell to stress (Ma and Hendershot, 2003; Novoa et al., 2003).

1.5.1.4 eIF1 and eIF1A

eIF1 (Sui1 for suppressor of initiation codon mutation in yeast) and eIF1A function at multiple steps of translation initiation including 43S PIC assembly, scanning, and start site selection. eIF1A is thought to promote 43S PIC assembly by stabilising binding of eIF3, eIF5, and the TC to the 40S subunit in the absence of mRNA (Battiste et al., 2000; Chaudhuri et al., 1999; Fekete et al., 2005). Thus, a mutations in the central OB-fold of eIF1A or a C-terminal truncation of eIF1A (eIF1AΔC) results in reduced levels of 40S-bound eIF3, eIF5, and TC and inhibits translation *in vivo* (Fekete et al., 2005).

Mutations in the C-terminal domain of eIF1A results in the assembly of aberrant 48S PIC *in vitro* and utilisation of non-AUG start sites *in vivo* (Fekete et al., 2005). This indicates that eIF1A is required not only for its function in 43S PIC assembly, but also later for start site recognition. Consistent with this, eIF1A and eIF1 have both been implicated in downstream scanning for an initiation site (Battiste et al.,

2000). Thus, an aberrant 43S PIC consisting of eIFs 2, 3, 4B, and the cap-binding complex eIF4F, but lacking eIF1 and eIF1A, is capable of assembling at promoter proximal positions, but fails to scan downstream to the initiation codon (Pestova et al., 1998). Addition of eIFs 1 and 1A together, but not individually, permits downstream scanning and 48S PIC assembly at the correct initiation codon (Pestova et al., 1998).

eIF1 prevents 48S PIC assembly at near-cognate triplets or at AUGs in poor initiation context (i.e. where the surrounding sequence deviates too far from an optimal Kozak sequence) *in vitro* (Pestova and Kolupaeva, 2002). Thus, eIF1 is thought to increase fidelity of start site selection by linking eIF2-GTP hydrolysis with base-pairing between the Met-tRNA$_i^{Met}$ and the AUG start codon (Unbehaun et al., 2004). Consistent with this, eIF5 stimulates eIF2 GTP hydrolysis at similar rates in the 43S and 48S PICs in the absence of eIF1 (Unbehaun et al., 2004). Moreover, eIF5-dependent GTP hydrolysis is much slower in 43S PICs containing eIF1 than 43S and 48S PICs without eIF1. Positioning of the Met-tRNA$_i^{Met}$ in the P site and base pairing of the Met-tRNA$_i^{Met}$ with the AUG start codon relieves the inhibitory effect of eIF1 on eIF5 and permits GTP hydrolysis (Unbehaun et al., 2004). In agreement with data obtained *in vitro*, mutations in yeast eIF1 (*Sui*$^-$) that reduce its interaction with the 40S subunit *in vitro* and *in vivo* and/or accelerate eIF1 dissociation and P_i release from PICs *in vitro* also increases initiation from non-AUG start codons *in vivo* (Cheung et al., 2007). Moreover, a hyper-accuracy mutation in eIF1, which suppresses the *Sui*$^-$ mutant, decreases the eIF1 off-rate (Cheung et al., 2007). Thus, one function of eIF1 seems to be to prevent premature GTP hydrolysis and ensure that the 48S PIC has been positioned on the AUG start codon, before events leading to the assembly of the 80S ribosome are initiated (Cheung et al., 2007; Unbehaun et al., 2004).

1.5.1.5 eIF5

In yeast, a pre-assembled multifactor complex (MFC) exists that consists of the TC and eIFs 1, 3, and 5 (Asano et al., 2000). Binding of the pre-assembled MFC to the 40S subunit is likely to represent an alternative route to 43S PIC formation (Asano et al., 2000). eIF5 interacts with eIF1 and the N-terminal domains (NTDs) of eIF3c and eIF2β and is thought to play a key role in the assembly of the MFC (Asano et al., 2000; Singh et al., 2005; Yamamoto et al., 2005). Moreover, genetic studies suggest that TC-eIF5 complex formation is rate-limiting for MFC assembly (Singh et al., 2005). Consistent with this, the affinity of eIF5 for eIF3c is greatly enhanced by pre-incubation

of eIF5 with the NTD of eIF2β (Singh et al., 2004). The interaction of eIF5 with eIF2 does not seem to depend on the guanine state of eIF2, and a recent study suggests that about 40% of cellular eIF2 is bound to eIF5 (Algire et al., 2005; Singh et al., 2007). As previously mentioned, eIF2B activity is required to revert eIF2 into its GTP-bound state and for TC formation (reviewed in (Webb and Proud, 1997)). eIF5 appears to compete with the catalytic subunit of eIF2B, eIF2Bε, for binding to eIF2 (Singh et al., 2006). Thus, over-expression of eIF5 prevents binding of eIF2B to eIF2, TC formation, and MFC assembly *in vitro* (Singh et al., 2006). Moreover, over-expression of wt eIF5, but not eIF5 mutated in the eIF2 interaction domain, results in a Gcd$^-$ (general control derepressed) phenotype indicative of impaired recruitment of the TC to the 40S subunit *in vivo* (Singh et al., 2006). Over-expression of the eIF2Bε subunit also gives a Gcd$^-$ phenotype, suggesting that excess binding of eIF2Bε to eIF2 might prevent its association with eIF5. Consistent with this, the eIF2Bε over-expression phenotype is exacerbated by mutations in the eIF2-binding interface of eIF5 (Singh et al., 2006). Thus, the eIF2-eIF2B to eIF2-eIF5 ratio needs to be kept in check to allow cycling of eIF2 between its GTP and GDP-bound states and efficient translation initiation.

eIF2 has no intrinsic GTPase activity, and the GTPase activating protein (GAP) eIF5 is required for hydrolysis of eIF2-bound GTP prior to joining of the 60S subunit (Das and Maitra, 2001). Importantly, eIF5 only stimulate GTP hydrolysis when the TC is bound to the 40S subunit, and yeast genetics suggest that GTP hydrolysis is tightly linked with AUG recognition (Das and Maitra, 2001; Huang et al., 1997; Raychaudhuri et al., 1985). Thus, mutations in eIF5, which increases its GAP activity or in eIF2 that increases its intrinsic GTPase activity, result in initiation at non-AUG codons (Huang et al., 1997). Moreover, a mutation in eIF2 that results in a higher rate of dissociation of charged Met-tRNA$_i^{Met}$ from the TC in the absence of GTP hydrolysis elicits a similar phenotype (Huang et al., 1997).

1.5.1.6 eIF5B

eIF5-induced hydrolysis of eIF2-bound GTP results in dissociation of eIF2-GDP, but not eIF1, eIF1A and eIF3 from the 40S subunit (Unbehaun et al., 2004). This occurs at a later step concomitant with joining of the 60S subunit and requires the GTPase eIF5B (Algire et al., 2002; Pestova et al., 2000; Shin et al., 2002). Thus, eIF5B promotes dissociation of eIF1, eIF1A and eIF3 from the 40S subunit only in the presence of the 60S subunit (Unbehaun et al., 2004). Whereas dissociation of eIF1 and

eIF3 seems to occur concomitant with or after 40S/60S subunit joining, eIF5B GTP-hydrolysis is required for the release of eIF1A and eIF5B (Fringer et al., 2007). Thus, a point mutation in eIF5B that disrupts its GTPase activity (eIF5B-T439) permits subunit joining *in vitro*, but eIF1A and eIF5B are retained on the 80S ribosomes (Fringer et al., 2007). A similar outcome is observed with wildtype eIF5B in the presence of a non-hydrolysable GTP analogue (Fringer et al., 2007). Consistent with a function of eIF5B in dissociation of eIF1A from the 80S ribosome *in vivo*, the slow growth phenotype of eIF5B mutant cells is greatly enhanced by over-expression of eIF1A (Choi et al., 2000).

Strains lacking eIF5B exhibit an extreme slow-growth phenotype and are severely affected under starved conditions (Choi et al., 1998). Nevertheless, yeast eIF5B is a non-essential protein, indicating that an eIF5B-independent pathway for ribosome assembly exists in yeast (Choi et al., 1998). In agreement with this, strains harbouring the dominant-negative eIF5B-T439 GTPase mutant exhibit a growth phenotype that is significantly more severe than cells lacking eIFB (Fringer et al., 2007). Moreover, the severe slow-growth defect of eIF5B-T439 mutant strains is suppressed by mutations in eIF1A that disrupt eIF1A-mediated recruitment of eIF5B to the 40S subunit (Fringer et al., 2007). This indicates that in the eIF5B-dependent pathway, dissociation of eIF5B from the 80S ribosome is crucial for translation initiation (Fringer et al., 2007).

1.5.1.7 eIF4

eIF4, which is a multifactor complex composed of eIFs 4A, 4B, 4E, and 4G, is dispensable for 43S PIC assembly, but required for recruitment of mRNA and the formation of the 48S PIC (Figure 1-20). The presumed first step in 48S PIC assembly is binding of eIF4E to the m^7GpppX (where X is any nucleotide) cap structure at the 5'-end. The importance of the eIF4E-5'-cap interaction is well established. Thus, translation levels are increased by 3-30 fold in reactions containing capped versus uncapped mRNA in both yeast and mammals (Iizuka et al., 1994; Preiss and Hentze, 1998; Tarun and Sachs, 1995). Moreover, in the absence of eIF4E, translation of capped mRNAs proceeds at similar rates to that of uncapped mRNAs *in vitro* (Tarun and Sachs, 1995). eIF4E binds to the large eIF4G subunit and together with eIF4A they form a sub-complex, eIF4F, that plays a key role in translation initiation by binding to the 5'-cap structure and bridging interactions between the mRNA and the 40S subunit. Consistent

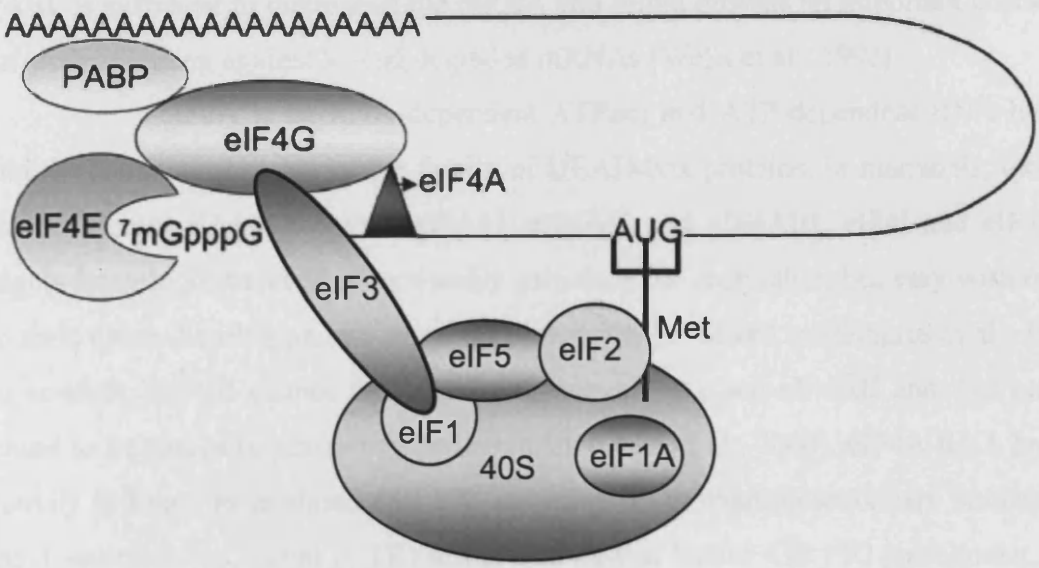

Figure 1-20: The 48S PIC. 48S PIC assembly is thought to be initiated by binding of eIF4E to the 5'-cap structure of the mRNA. eIF4E also binds to eIF4G and together with eIF4A they form the eIF4F sub-complex. eIF4G is a large polypeptide and functions as a scaffold for 48S PIC assembly. Thus, eIF4G promotes 48S PIC formation by bridging an interaction between the mRNA (via eIF4E and eIF4A) and the 43S PIC (via eIF3). Moreover, eIF4G links the 5'-cap structure (via eIF4E) with the poly(A) tail (via PABP), which results in circulisation of the mRNA. This further stimulates 48S PIC assembly and might provide a checkpoint for discriminating against 3'-end degraded mRNAs. The eIF4A RNA helicase is thought to facilitate 48S PIC assembly by removing secondary structures in the 5'-end of the mRNA that hinder recruitment of the 43S PIC. Adapted from (Lopez-Lastra et al., 2005).

with this, eIF4F complex assembly is the rate-limiting step in translation initiation and largely depends on the availability of eIF4E (reviewed in (Kapp and Lorsch, 2004)).

eIF4G functions as a scaffold that coordinates multiple interactions between the cap structure (via its RNA binding domain and eIF4E), the 40S subunit (via eIF3), and the polyadenylated (poly(A)) tail (via poly A binding protein (PABP)) (reviewed in (Kapp and Lorsch, 2004)). The 3'-end poly(A) tail positively regulates translation *in vitro* and *in vivo* (Gallie, 1991; Michel et al., 2000; Preiss and Hentze, 1998; Tarun and Sachs, 1995) in a PABP-dependent manner (Tarun and Sachs, 1995). This can be explained by the ability of the poly(A) tail to interact with and stimulate the cap-binding and ATPase activities of eIF4F (via PABP) (reviewed in (Kapp and Lorsch, 2004)). Moreover, binding of eIF4G to the 5'-cap via eIF4E and to the poly(A) tail via PABP is sufficient to circularise the mRNA and might provide an important checkpoint for discriminating against 3'-end degraded mRNAs (Wells et al., 1998).

eIF4A is an RNA-dependent ATPase and ATP-dependent RNA helicase and the founding member of the family of DEAD-box proteins. In mammals, there are three different eIF4A isoforms: eIF4AI, eIF4AII, and eIF4AIII. eIF4I and eIF4II are highly homologous and can functionally substitute for each other, but vary with respect to their tissue distribution and temporal expression (reviewed in (Gingras et al., 1999)). In contrast, eIF4III cannot functionally replace eIF4AI and eIF4AII and was recently found to be part of the exon-junction complex (Chan et al., 2004). eIF4A RNA helicase activity is likely to facilitate 48S PIC assembly by unwinding secondary structures in the 5'-untranslated region (UTR) of the mRNA that hinder 43S PIC recruitment. First, its ATPase activity facilitates unwinding of RNA duplexes *in vitro* (Lawson et al., 1989; Pause and Sonenberg, 1992; Ray et al., 1985; Rozen et al., 1990), and eIF4A is required for translation initiation *in vivo* (Blum et al., 1992). Second, a dominant negative eIF4A mutant lacking ATPase and RNA helicase activities inhibits the translation of structured mRNAs significantly more than that of unstructured mRNAs *in vitro* (Svitkin et al., 2001). Third, eIF4A is not required for translation of small mRNAs lacking secondary structures in their 5' UTR, nor does it stimulate their translation (Algire et al., 2002; Benne and Hershey, 1978; Lorsch and Herschlag, 1999).

The enzymatic activity of eIF4A is stimulated by its incorporation into eIF4F (Rogers et al., 2001; Rozen et al., 1990), and its helicase activity by eIF4B and eIF4H (in mammals) (Richter-Cook et al., 1998; Rogers et al., 2001; Rogers et al., 1999). eIF4B and eIF4H have no intrinsic catalytic activities and seem to play

redundant roles with respect to stimulation of eIF4A activity (Richter-Cook et al., 1998). The ability of eIF4B to stimulate eIF4A function is thought to be mediated at least in part by its stimulatory effect on eIF4A affinity for RNA and ATP (Abramson et al., 1988; Bi et al., 2000).

Two models have been proposed to explain how eIFs, 4A, 4B, and 4H might function to unwind RNA duplexes. According to the first model, eIF4B and eIF4H bind to and stabilise the structure of single stranded RNA generated by the unwinding activity of the eIF4F-bound eIF4A RNA helicase. In the second model, eIF4F is proposed to function as a nucleation centre for the transient polymerisation of eIF4A along the mRNA resulting in the disruption of secondary structures (reviewed in (Kapp and Lorsch, 2004)). Consistent with this model, eIF4A is approximately 50 times as abundant as the other components of eIF4F, and an excess of eIF4A to RNA substrate of around 500:1 is required for efficient activation of translation *in vitro* (Duncan et al., 1987; von der Haar and McCarthy, 2002). The functions of eIF4B and eIF4H do not differ between the two models. Consistent with the idea that eIF4B and eIF4H seed the mRNA subsequent to the action of eIF4A, both proteins bind to the mRNA in an eIF4A- and ATP-dependent manner ((Lindqvist et al., 2008; Sonenberg, 1981) and reviewed in (Cristofari and Darlix, 2002)), and a recent crosslinking study showed that eIF4B and eIF4H contact multiple positions downstream of the cap structure (Lindqvist et al., 2008).

1.5.2 Translation elongation/termination

1.5.2.1 Elongation

Translation elongation starts with a peptidyl-tRNA bound to the ribosomal P site and the recruitment of a ternary complex composed of an aminoacyl(aa)-tRNA, eukaryotic elongation factor 1A (eEF1A), and GTP to the acceptor (A) site (Figure 1-21). Both cognate and non-cognate aa-tRNAs can bind to the A site, but only the correct codon-anticodon recognition results in activation of eEF1A and peptide bond formation. Base pairings between the codon and anticodon in the A site leads to several conformational changes, which ultimately activates the eEF1A GTPase. eEF1A-mediated GTP hydrolysis results in dissociation of eEF1A-GDP from the ribosome and the release of aa-tRNA into the A site in a form that is competent to generate a peptide bond. The ribosomal peptidyl transferase center then catalyses the formation of a new

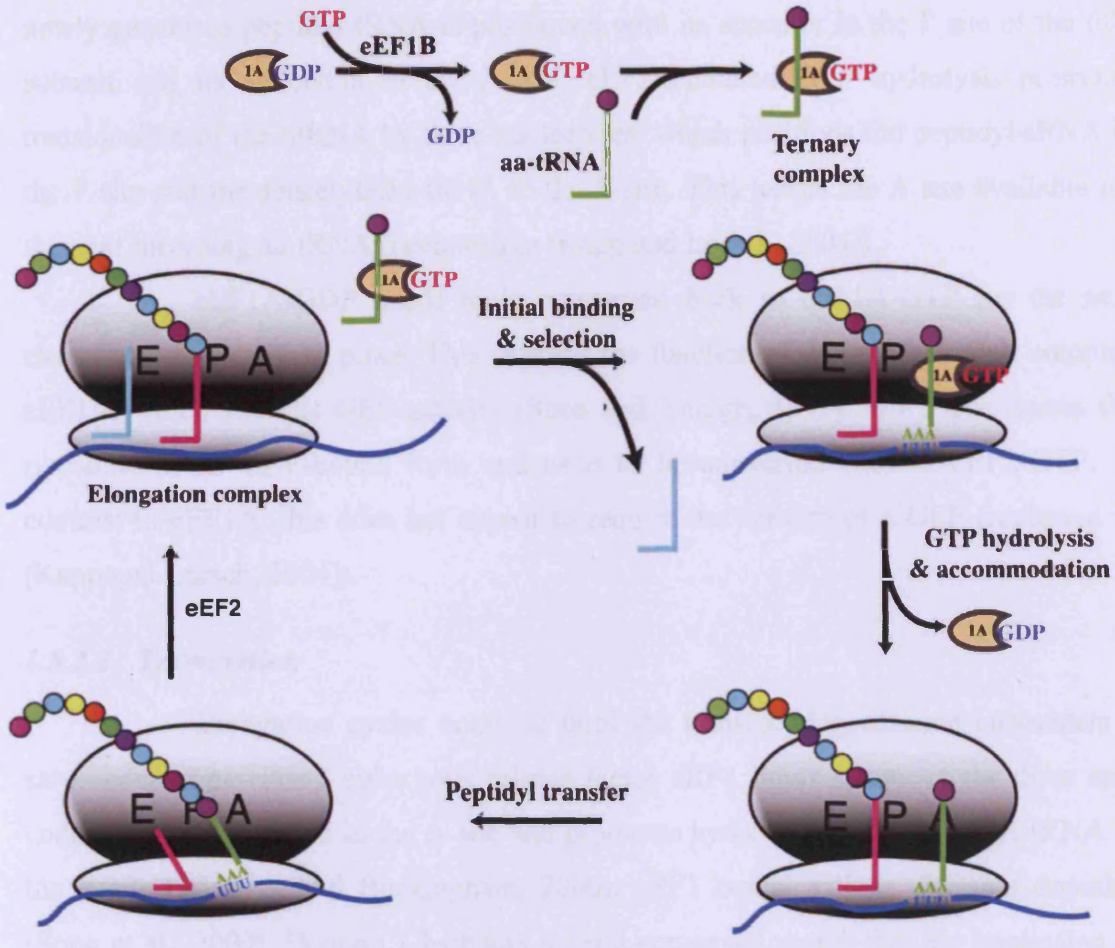

Figure 1-21: Translation elongation. The translation elongation cycle starts with a peptidyl-tRNA positioned in the ribosomal P site and a vacant A site. An aa-tRNA is recruited to the A site as part of a ternary complex with eEF1A and GTP. Base pairing of the incoming aa-tRNA with the A site codon induces several conformational changes, which leads to activation of the eEF1A GTPase. GTP hydrolysis results in the relase of eEF1A-GDP from the ribosome and positioning of the aa-tRNA in the catalytic center of the ribosome ("accommodation"). Next, the peptidyl transferase center catalyses the formation of a new peptide bond between the incoming amino acid and the 3'-end amino acid of the nascent peptide bound to its tRNA in the P site. This results in deacetylation of the tRNA in the P site, which is now positioned with its acceptor in the E site of the 60S subunit and its anticodon in the P site of the 40S subunit. The newly formed peptidyl-tRNA is positioned with its acceptor in the P site of the 60S subunit and its anticodon in the A site of the 40S subunit. eEF2-mediated GTP hydrolysis promotes mRNA translocation by three nucleotides and positions the peptidyl-tRNA in the P site and the deacetylated tRNA in the E site. This leaves the A site empty and the ribosome ready for another elongation cycle. Taken from (Kapp and Lorsch, 2004).

peptide bond between the incoming amino acid in the A site and the last amino acid of the nascent peptidyl chain bound to its tRNA in the P site. This results in deacetylation of the peptidyl-tRNA and positioning of the deacetylated tRNA with its acceptor in the exit (E) site of the 60S subunit and its anticodon in the P site of the 40S subunit. The newly generated peptidyl tRNA is positioned with its acceptor in the P site of the 60S subunit and its anticodon in the A site. eEF2-mediated GTP hydrolysis promotes translocation of the mRNA by three nucleotides, which positions the peptidyl-tRNA in the P site and the deacetylated tRNA in the E site. This leaves the A site available for the next incoming aa-tRNA (reviewed in (Kapp and Lorsch, 2004)).

eEF1A-GDP needs to be converted back to eEF1A-GTP for the next elongation cycle to take place. This requires the function of the multi-subunit complex eEF1B, which exhibits GEF activity (Sheu and Traugh, 1997). eEF2 also leaves the ribosome in its GDP-bound form and need to be converted back to eEF2-GTP. In contrast to eEF1A, this does not appear to require the activity of a GEF (reviewed in (Kapp and Lorsch, 2004)).

1.5.2.2 Termination

Elongation cycles continue until the translocating ribsome encounters a stop codon. The class I eukaryotic release factor eRF1 binds to any of the three stop codons when positioned in the A site and promotes hydrolysis of the peptidyl-tRNA in the P site (Kisselev and Buckingham, 2000). eRF1 contains three different domains (Song et al., 2000). Domain 1 harbours several conserved motifs that are implicated in stop codon recognition (Frolova et al., 2002; Ito et al., 2002; Kolosov et al., 2005). Domain 2 contains a highly conserved GGQ motif, which is required for hydrolysis of peptidyl-tRNA (Frolova et al., 1999; Song et al., 2000). Domain 3 interacts with the class II eukaryotic release factor 3 (eRF3) (Frolova et al., 2000; Merkulova et al., 1999).

Two mammalian (eRF3a and eRF3b) and one yeast (Sup35/eRF3p) class II release factors have been identified, all of which are required for termination *in vivo* ((Chauvin et al., 2005) and reviewed in (Kisselev and Buckingham, 2000)). eRF3 contains three domains: N, M, and C. The N and M domains are dispensable for viability and translation termination in yeast, whereas the C domain, which contains the GTPase fold and the binding site for eRF1, is essential for survival (Ter-Avanesyan et al., 1993). eRF1 and GTP binds to eRF3 with strong cooperativity, and the GTP form of eRF3 is thought to predominantly exist in a long lived ternary complex with eRF1

(Hauryliuk et al., 2006; Pisareva et al., 2006). eRF3 GTPase activity strictly requires the presence of both eRF1 and the ribosome (Frolova et al., 1996), and yeast genetics suggest that eRF3's GTPase activity might couple termination codon recognition by eRF1 with efficient peptide release (Salas-Marco and Bedwell, 2004). Thus, mutations in eRF3 that reduce its GTPase activity also reduce the efficiency of termination at some, but not all stop codons (Salas-Marco and Bedwell, 2004). Importantly, the reduced efficiency of termination at specific stop codons is not simply a consequence of insufficient levels of eRF3 since lowering levels of eRF1 and/or eRF3 reduce termination efficiency at all stop codons. Instead, the rate of eRF3-dependent GTP hydrolysis seems to affect stop codon recognition by eRF1 (Salas-Marco and Bedwell, 2004).

Recently, Alkalaeva and co-workers used a reconstituted system to study translation termination *in vitro* (Alkalaeva et al., 2006). They were able to show that binding of eRF1 and eRF3-GTP to pre-termination complexes induces a structural rearrangement, which manifests itself as a two-nucleotide shift of the toe print attributed to the termination complex. This structural rearrangement is followed by eRF3-mediated GTP hydrolysis and eRF1-dependent peptide release (Alkalaeva et al., 2006). eRF3-mediated GTP hydrolysis is likely to correctly position the GGQ motif of eRF1 for it to induce the peptidyl-tRNA hydrolysis (Alkalaeva et al., 2006). Thus, eRF3 functions prior to peptidyl-tRNA hydrolysis and is likely to link stop codon recognition with peptidyl-tRNA hydrolysis and peptide release (Alkalaeva et al., 2006; Salas-Marco and Bedwell, 2004).

1.5.3 Control of TOR activity

The nutrient-sensitive mammalian target of rapamycin (mTOR) kinase plays a crucial role in regulation of translation in response to insulin and/or amino acid deprivation (Figure 1-22). Signalling upstream of TOR in response to insulin stimulation has been studied extensively in mammalian cells and in flies using genetics (reviewed in (Averous and Proud, 2006)). In contrast, the mechanism by which mTOR is activated in response to nutrient deprivation remained poorly characterised until recently (see below).

mTOR exists in two different complexes that are referred to as mTORC1 and mTORC2 (reviewed in (Sarbassov et al., 2005a)). The mTORC1 complex is composed of mTOR, Raptor, mLST8, and the newly identified component proline-rich

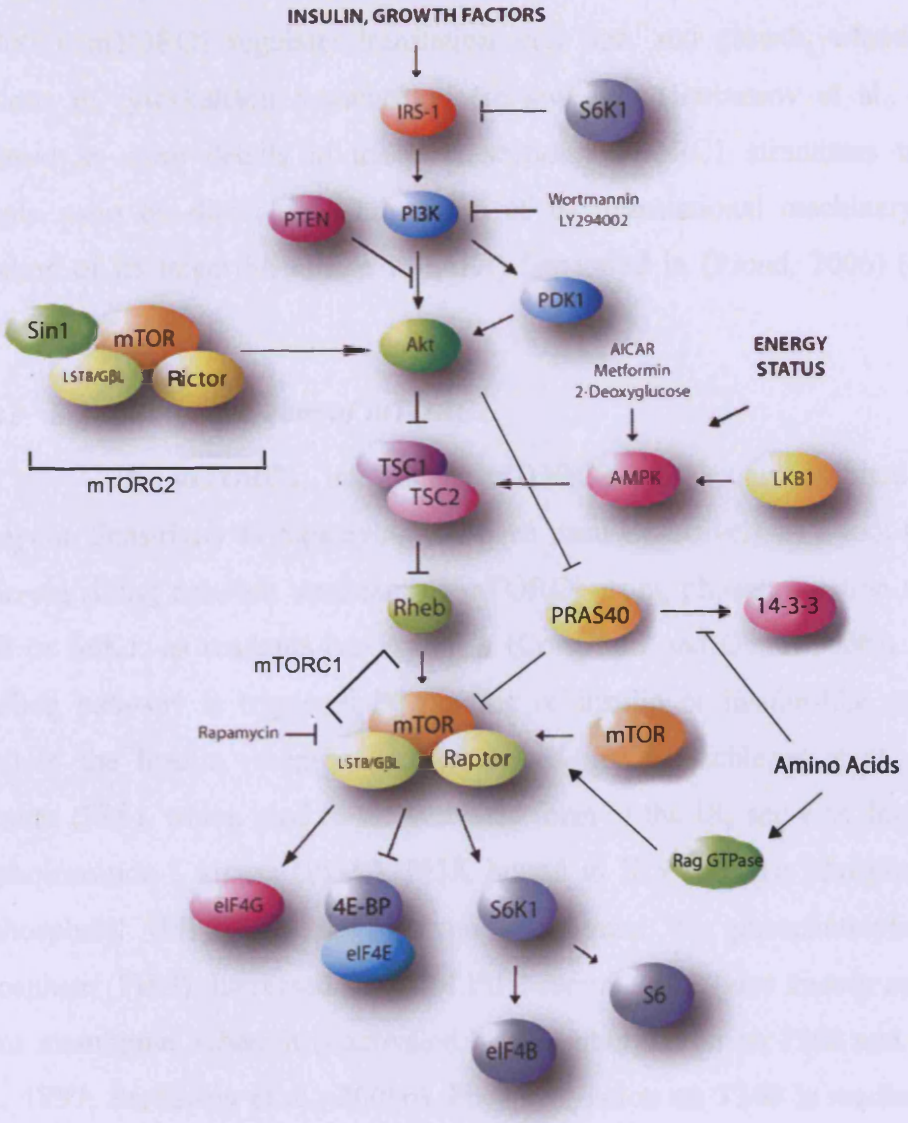

Figure 1-22: The insulin signalling pathway. The insulin signalling pathway stimulates translation and growth in response to insulin and growth factors. PIP3 is generated by PI3K in response to binding of insulin and growth factors to receptor tyrosine kinases. Increased levels of PIP3 recruits AKT to the membrane, where it is phosphorylated and activated by PDK1 and mTOR bound to Rictor in the mTORC2 complex. PI3K activity is counteracted by the lipid phosphatase PTEN, which converts PIP3 back to PIP2. AKT phosphorylates and inhibits TSC2 activity and thereby allows Rheb to activate mTOR bound to Raptor in the mTORC1 complex. AKT also stimulates mTORC1 activity via its effect on PRAS40, which associates with and inhibits mTOR activity in the absense of insulin signalling. In addition to growth factor signalling, mTORC1 activity is also regulated by amino acid levels through the Rag GTPases. mTORC1 signalling directly or indirectly (via S6K1) results in phosphorylation of the translational machinery and increased translation levels. Adapted from (Mamane et al., 2006).

AKT/PKB substrate 40 kDa (PRAS40) (Vander Haar et al., 2007), and the mTORC2 complex is composed of mTOR, Rictor, mLST8, and Sin1 (Frias et al., 2006; Jacinto et al., 2006). mTORC1 regulates translation, cell size, and growth, whereas mTORC2 functions in cytoskeleton organisation (reviewed in (Sarbassov et al., 2005a)). As discussed in more details in the next section, mTORC1 stimulates translation in multiple ways by direct phosphorylation of the translational machinery or through activation of its target S6 kinase 1 (S6K1) (reviewed in (Proud, 2006) (Averous and Proud, 2006)).

1.5.3.1 Signalling upstream of mTORC1

The mTORC1, but not the mTORC2 complex, is inhibited by the drug rapamycin. Sensitivity to rapamycin has been used extensively as a tool to dissect the insulin-signalling network upstream of mTORC1 using phosphorylation of its targets, eIF4B or S6K1, as readouts (reviewed in (Corradetti and Guan, 2006)). The insulin-signalling pathway is triggered by binding of insulin or insulin-like growth factors (IGFs) to the insulin receptor (IR) (reviewed in (Wullschleger et al., 2006b)). IR substrates (IRS), which bind to the activated form of the IR, serve as docking sites for phosphoinositide-3 kinase (PI3K). PI3K bound to IRS converts phosphatidylinositol-4,5-phosphate (PIP2) in the plasma membrane to phosphatidylinositol-3,4,5-triphosphate (PIP3). Increased levels of PIP3 recruit AKT (also known as PKB) to the plasma membrane, where it is activated by phosphorylation on T308 and S473 (Alessi et al., 1997; Sarbassov et al., 2005b). Phosphorylation on T308 is mediated by the 3-phosphoinositide-dependent kinase 1 (PDK1) (Alessi et al., 1997), and phosphorylation on S473 by the mTORC2 complex (Sarbassov et al., 2005b). Activation of AKT stimulates mTOR signalling via its inhibitory effect on TSC2 (Inoki et al., 2002; Potter et al., 2002). Thus, in the absense of AKT signalling, TSC2 in complex with its partner TSC1 inhibits mTOR-signalling via its effect on Rheb (Garami et al., 2003; Inoki et al., 2003a; Tee et al., 2003). Rheb is a small GTPase (Saucedo et al., 2003; Stocker et al., 2003), which in its GTP-bound form binds to and activates mTOR *in vitro* and *in vivo* (Long et al., 2005a; Long et al., 2005b; Urano et al., 2005). TSC2 functions as a GAP for Rheb to convert it into its GDP-bound form, which in turn inhibits mTORC1 signalling (Garami et al., 2003; Inoki et al., 2003a; Tee et al., 2003). Hence, AKT-mediated inhibition of TSC2 relieves the inhibitory effect of TSC2 on Rheb activity and stimulates mTORC1 signalling. AKT kinase also stimulates mTORC1-signalling

independent of its effect on TSC2. Thus, phosphorylation of PRAS40 by AKT results in its dissociation from the mTORC1 complex and relieves the inhibitory effect of PRAS40 on mTOR activity (Vander Haar et al., 2007).

As previously mentioned, the mechanism whereby amino acid levels regulate mTORC1 activity remained elusive for many years. However, recently it was shown that the Ras-related GTP-binding Rag proteins regulate mTORC1-signalling in response to amino acid levels by affecting the localisation of mTOR (Sancak et al., 2008). Thus, only when amino acids are not limited, mTOR co-localises with its activator Rheb (Sancak et al., 2008). Consistent with this, insulin signalling cannot activate mTOR-signalling when amino acids are in limited supply (reviewed in (Wullschleger et al., 2006).

In addition to insulin and amino acids levels, the mTORC1 activity is also regulated by cellular energy levels via the AMP-activated kinase (AMPK) (reviewed in (Wullschleger et al., 2006). AMPK senses the energy status of the cell and is activated in response to low energy levels (high AMP/ATP ratio). Activated AMPK phosphorylates and stimulates the GAP activity of TSC2, which in turn decreases mTORC1 activity (Inoki et al., 2003b). The tumour suppressor LKB1 has been identified as an upstream kinase for AMPK and functions in conjunction with AMP to regulate AMPK activity (reviewed in (Wullschleger et al., 2006).

1.5.3.2 Signalling downstream of mTORC1

There are two S6Ks in mammals (S6K1 and S6K2) and one in *Drosophila* (S6K) (Avruch et al., 2001). In mammals, Raptor mediates the binding of the mTORC1 complex to S6K1, which is phosphorylated and activated in response to insulin signalling. S6K1 is directly phosphorylated by mTOR on Thr389, and this potentiates PDK1-mediated phosphorylation on Thr229 (Alessi et al., 1998; Pullen et al., 1998). Phosphorylation on Thr229 in the activation loop of S6K1 results in S6K1 activation (Avruch et al., 2001). Activated S6K1 phosphorylates eIF4B (Raught et al., 2004) and thereby increases the affinity of eIF4B for the translational machinery and stimulates translation initiation (Holz et al., 2005). S6K1 also phosphorylates the small ribosomal protein S6 on multiple sites, though the physiological relevance of this is not clear (reviewed in (Ruvinsky and Meyuhas, 2006)). Thus, mutating multiple S6 phosphorylation sites to alanines in knock-in mice results in decreased cells size, but increased rates of protein synthesis (Ruvinsky et al., 2005). Chronic S6K activation

results in reduced expression and inhibition of IRS1 (Harrington et al., 2004; Haruta et al., 2000; Shah et al., 2004). Since IRS1 functions as a positive transmitter of signalling between the insulin receptor and the phosphatidylinositol-3-kinase, this generates a negative feedback loop on the insulin pathway.

1.5.4 Regulation of translation by the insulin pathway

Protein synthesis and ribosome biogenesis are among the most energetically demanding cellular processes and must be kept in check and coordinated with cellular energy and nutrient levels. The insulin pathway represents a major node for the integration of multiple signals representing the metabolic state of the cell and regulates protein synthesis according to energy levels. The global effect on translation induced by insulin signalling can be divided into a rapid response, which depends on the pre-existing translational machinery, and a long-term effect, which involves the synthesis of additional ribosomal building blocks. The focus here will be on the rapid response of the translational machinery to insulin signalling (reviewed in (Proud, 2006)).

1.5.4.1 Multiple modes of regulation of translation initiation

Insulin signalling exerts its stimulatory effect on protein synthesis at different stages of translation including formation of the TC, recruitment of mRNA to the 43S PIC, and translation elongation (Figure 1-23 and (reviewed in (Proud, 2006)). As previously mentioned, eIF2 leaves the ribosome in its GDP-bound form and needs to be converted back to its GTP-bound form to engage in the formation of the TC. This is a critical step in translation initiation and requires the GEF activity of eIF2B. The eIF2Bβ subunit contains multiple phosphorylation sites, and its activity is negatively regulated by glycogen synthase kinase 3 (GSK3)-mediated phosphorylation (Welsh et al., 1998; Welsh and Proud, 1992). Thus, phosphorylation of a single residue near the catalytic domain of eIF2B impairs its GEF activity (Welsh et al., 1998). GSK3 itself is phosphorylated and inactivated by AKT/PKB in response insulin signalling and growth factors. As a result, insulin signalling relieves the inhibitory effect of GSK3 on eIF2B GEF activity and stimulates TC formation (reviewed in (Cohen and Frame, 2001)).

Assembly of eIF4E, eIF4G, and eIF4A into eIF4F is a rate-limiting step in translation initiation and largely depends on the availability of the cap-binding protein

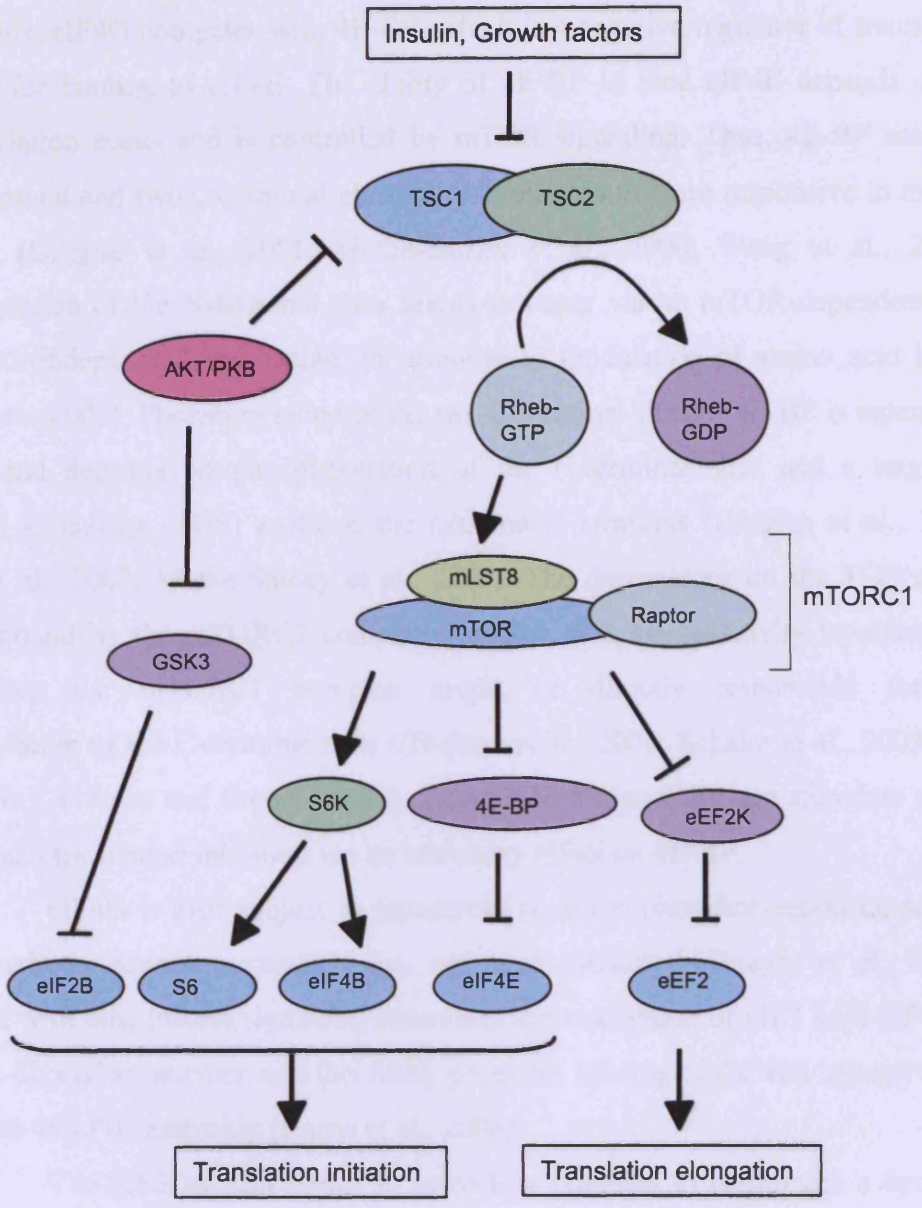

Figure 1-23: Regulation of translation by the insulin pathway. Insulin signalling regulates translation at multiple stages including TC formation, 48S PIC assembly, and translation elongation. TC formation is controlled by eIF2B activity, which is required for the conversion of eIF2-GDP into eIF2-GTP at the end of each translation cycle. eIF2B activity is inhibited by the GSK3 kinase, which itself is negatively regulated by AKT/PKB. Thus, insulin signalling derepresses the inhibitory effect of GSK3 on eIF2B and facilitates TC formation. mTORC1 signalling stimulates translation initiation directely or indirectly via activation of its substrate S6K1. Thus, mTOR-dependent phosphorylation of 4E-BP relieves the inhibitory effect of 4E-BP on translation initiation. 4E-BP inhibits 48S PIC assembly by competing with eIF4G for binding to the 5'-cap-binding protein eIF4E. mTOR-dependent phosphorylation of 4E-BP results in its dissociation from eIF4E and hence promotes 48S PIC assembly and translation initiation. S6K1 phosphorylates the 40S subunit ribosomal protein S6 and eIF4B. Phosphorylation of eIF4B promotes its recruitment to the translational machinery and stimulates translation initiation. mTORC1 signalling also affects translation elongation rates. In the absense of mTORC1 signalling, the elongation factor eEF2 is phosphorylated and inhibited by eEF2K. In response to insulin signalling, mTOR phosphorylates and inhibits eEF2K activity, and as a result activates eEF2 and stimulates translation elongation rates.

eIF4E. Thus, eIF4G competes with 4E-BP, which is a negative regulator of translation initiation, for binding to eIF4E. The ability of 4E-BP to bind eIF4E depends on its phosphorylation status and is controlled by mTOR signalling. Thus, 4E-BP contains two N-terminal and two C-terminal phosphorylation sites that are responsive to mTOR signalling (Gingras et al., 2001; Mothe-Satney et al., 2000; Wang et al., 2005). Phosphorylation of the N-terminal sites seems to occur via an mTOR-dependent, but raptor/rictor-independent mechanism in response to modulation of amino acid levels (Wang et al., 2005). Phosphorylation of the two C-terminal sites of 4E-BP is rapamycin sensitive and depends on phosphorylation of the N-terminal sites and a target of rapamycin signalling (TOS) motif at the extreme C terminus (Gingras et al., 2001; Herbert et al., 2002; Mothe-Satney et al., 2000). The dependence on the TOS motif, which is bound by the mTORC1 component raptor, and the sensitivity to rapamycin suggest that the mTORC1 complex might be directly responsible for the phosphorylation of the C-terminal sites ((Nojima et al., 2003; Schalm et al., 2003) and reviewed in (Averous and Proud, 2006)). Thus, mTOR signalling can stimulate eIF4F assembly and translation initiation via its inhibitory effect on 4E-BP.

eIF4G is also subject to rapamycin sensitive phosphorylation on several sites, though the kinase responsible has not been identified (Raught et al., 2000). Consistent with this, insulin signalling stimulates the association of eIF3 with eIF4G in an mTOR-dependent manner, and this likely promotes binding of the 40S subunit to the mRNA and 48S PIC assembly (Harris et al., 2006).

The eIF3 subunit seems to provide a platform to coordinate a dynamic sequence of events in response to insulin signalling. Thus, in its inactive form, S6K1 is recruited to the translational machinery by the eIF3 complex (Holz et al., 2005). Insulin signalling results in the recruitment of the mTORC1 complex to eIF3, leading to activation and release of S6K1 (Holz et al., 2005). Following activation and dissociation from the translational machinery, S6K1 phosphorylates and activates eIF4B. eIF4B phosphorylation promotes its recruitment to the translational machinery via its association with eIF3 (Holz et al., 2005). Thus, insulin signalling appears to stimulate 48S PIC assembly by promoting eIF4F assembly via its effect on 4E-BP, by mRNA recruitment to the 40S subunit via its effect on eIF4G binding to eIF3 (as part of the 43S PIC) , and by recruitment of eIF4B to the translation machinery.

1.5.4.2 Regulation of translation elongation

In mammals, insulin signalling not only regulates translation initiation, but also stimulates elongation rates (reviewed in (Averous and Proud, 2006)). Phosphorylation of eEF2 by the eEF2 kinase prevents its binding to ribosomes and inhibits translation elongation (Carlberg et al., 1990). Phosphorylated eEF2 exhibit decreased affinity for GTP, but not GDP, suggesting that phosphorylation inactivates eEF2 by shifting the balance in favour of the GDP-bound form (Dumont-Miscopein et al., 1994). The eEF2 kinase is itself regulated by insulin signalling (reviewed in (Proud, 2006)). Thus, mTOR signalling inhibits eEF2 kinase activity via three phosphorylation sites in eEF2 kinase (Browne and Proud, 2004; Knebel et al., 2001; Wang et al., 2001). S6K1 seems to be responsible for phosphorylation of at least one of these sites (Wang et al., 2001). Phosphorylation and inactivation of eEF2 kinase relieves its inhibitory effect on eEF2. Consistent with this, translation elongation rates are accelerated in response to mTOR signalling (Redpath et al., 1996)(reviewed in (Proud, 2006)).

1.5.5 Pixie – the *Drosophila* homologue of RNAse L inhibitor (RLI)

Pixie, one of the four *Drosophila* proteins characterised in this thesis, was originally identified in a genetic interaction screen carried out in Leevers laboratory to identify molecules that regulate growth and interact with PI3K signalling (Coelho et al., 2005b). Mutations in *pixie* have an unusual effect on fly growth that is similar to the effect of mutations in some genes encoding ribosomal proteins. For example, weak *pixie* mutant combinations and some heterozygous ribosomal protein mutants (termed *Minute* mutations) have slender bristles and show developmental delays, yet their final adult body size can be near normal (Coelho et al., 2005a; Lambertsson, 1998)(Marygold et al., 2007). In addition, *pixie* and ribosomal protein mutant wing imaginal discs show complex defects in growth and cell survival that vary spatially and temporally (Coelho et al., 2005a). Thus during the fast growing phase (early to mid third instar larvae), *pixie* and ribosomal protein function is required more in the fast growing region of the disc (the pouch), and in the slow growing phase (late third instar larvae), their function is required more in the slow growing region (the hinge) (Coelho et al., 2005a). So far, all but one of the known *Minute* loci were found to correspond to genes encoding ribosomal proteins, suggesting that the Minute phenotype arises from suboptimal protein synthesis (Marygold et al., 2007). Thus, the impact that mutating *pixie* has on

growth might arise via an effect on translation. Consistent with this, dsRNAi-mediated depletion of Pixie reduces global translation (Coelho et al., 2005a).

Pixie is an exceptionally conserved protein found in all eukaryota and archaea sequenced so far (Gabaldon and Huynen, 2004). For example, Pixie and yeast Rli1p share 66% amino acid identity, and yeast Rli1p and human RLI have 67% amino acid identity. Pixie belongs to the ABCE subfamily of ABC proteins, which contain two nucleotide-binding domains (NBDs) and two N-terminal iron sulfur (FeS) clusters. In contrast to most ABC domain proteins, members of this subfamily do not contain the membrane-spanning domains that would enable them to function as transporters (Kerr, 2004). The structure of *Pyrococcus furiosus* RLI lacking the FeS domain was recently solved and revealed some similarity to the structure of known ABC enzymes (Karcher et al., 2005). Binding of ATP to the interface of the two opposing NBDs in *P. furiosus* RLI is thought to induce a power stroke. Thus, RLI might function as an ATP-driven mechano-chemical enzyme to promote structural modulations of its substrates (Karcher et al., 2005). Consistent with this, mutations in the ATP binding regions of yeast Rli1p and Pixie are not viable (Coelho et al., 2005a; Dong et al., 2004; Karcher et al., 2005).

The human Pixie ortholog RLI, also known as ABCE1, was first characterised via its ability to inhibit the antiviral activity of RNAse L (Bisbal et al., 1995; Martinand et al., 1999; Martinand et al., 1998). However, RNAse L is only found in mammals, so this function of RLI does not account for its conservation in non-mammalian species (Gabaldon and Huynen, 2004). More recently, three independent studies have provided evidence that Pixie (shown here and (Andersen and Leevers, 2007)) and the yeast ortholog of Pixie, Rli1p, associate with translation initiation factors and the 40S ribosomal subunit and play a role in translation initiation (Dong et al., 2004; Kispal et al., 2005; Yarunin et al., 2005). Additional data suggest that the vertebrate and Caenorhabditis elegans RLI orthologs also play roles in translation (Chen et al., 2006c; Le Roy et al., 2005; Zhao et al., 2004). These fundamental functions are likely to explain the high degree of conservation of the RLI/Pixie protein family and are consistent with the *pixie* mutant phenotypes observed in *Drosophila* (Coelho et al., 2005a).

In addition to its role in translation initiation, Rli1p has also been shown to play a role in processing of the small and large ribosomal subunits (Dong et al., 2004; Kispal et al., 2005; Yarunin et al., 2005). Thus, depletion of Rli1p results in impaired processing and nuclear export of the 40S and 60S subunits (Kispal et al., 2005; Yarunin

et al., 2005). Moreover, Rli1p interacts physically and genetically with the eIF3 component, Hcr1p, which has also been implicated in ribosome biogenesis (Kispal et al., 2005; Yarunin et al., 2005).

1.5.6 Project Aims

The overall aim of my projects was to identify novel proteins that regulate growth during fly development. In Dr. Tapon's laboratory, we used the rough-eye phenotype caused by excess Hpo signalling in a candidate-based genetic interaction screen for novel components of the Hpo pathway. In Dr. Leevers' laboratory, we used the small-wing phenotype caused by reduced insulin signalling in the wing to screen for growth regulators that interact with insulin signalling. These two approaches led to the identification of the four *Drosophila* proteins characterised in this thesis. The data presented here show that all four proteins are indeed required for growth and proliferation during development. A more detailed functional study reveals that they are required at different stages of gene expression. One protein, dMCRS2, is likely to play a role in RNAP II transcription, two proteins, dPrp38 and dMFAP1 are required for normal levels of pre-mRNA processing, and the fourth protein, Pixie, is required for normal levels of translation initiation. The results chapters have been organised in the same order as those three steps of gene expression: RNAP II transcription (dMCRS2), pre-mRNA processing (dPrp38 and dMFAP1), and translation initiation (Pixie).

Chapter 2 - Materials and methods

2.1 Molecular biology and Biochemistry

2.1.1 Antibodies

Polyclonal rabbit antisera were raised against a N-terminal peptide of Adam (2T, aa 1-16), eIF3-S10 (5T, aa 1-19), and RpS25 (NT2 or NT1, aa 1-20) and a C-terminal peptide of eIF3-S2 (CT1, aa 312-326), eIF3-S8 (CT2, aa 892-910), and eIF3-S9 (CT1, aa 671-685) (Cancer Research UK). All peptides were coupled via cysteines in their N- or C-terminal aminoheaxanoic acid spacers (EAHX-Cys) to maleimide-activated keyhole limpet haemocyanin (KLH, Pierce) as directed. The anti-Pitslre (953), anti-eIF2-α (2396), anti-Rps13 (I2), anti-dPrp38p_N and anti-dPrp38p_C rabbit antibodies and the anti-dMFAP1 and anti-dMCRS2 guinea pig antibodies were generated and affinity-purified by Eurogentec SA (Seraing, Belgium) against peptides corresponding to amino acids 119-133 of dMCRS2, 884-898 of Pitslre, 4-14 and 314-328 of eIF2-α, 128-142 of Rps13, 1-15 and 315-330 of dPrp38, and 43-57 of dMFAP1 (Eurogentec).

2.1.2 Cell culture

Drosophila S2 cells were grown in Schneider medium (Invitrogen) and $S2R^+$ cells in Shields and Sang M3 Insect Medium (M3) (Sigma) supplemented with 10% heat-inactivated Fetal Bovine Serum (Sigma), 50 U/ml penicillin, and 50 μg/ml streptomycin (Invitrogen, "Complete Medium") at 25°C. S2 cells were transfected with pDA9-1, pDA9-2, and pDA10-1 (see plasmids below) using a calcium phosphate transfection kit (Invitrogen). For all other plasmids, S2 and $S2R^+$ cells were transfected using an effectene transfection kit (Qiagen). S2 cells stably expressing GTC-Pixie, GTC-PixieΔABC, GTC-PixieE501Q, GTC-dMCRS2 or the GTC tag alone were selected in complete Schneider medium containing 300 μg/ml hygromycin. For insulin treatment S2 cells were treated with 1 μM bovine insulin in complete medium.

2.1.3 dsRNA

dsRNAs were synthesised with a Megascript T7 kit (Ambion). DNA templates for dsRNA synthesis were PCR amplified from fly genomic DNA or plasmids

using primers that contained 5′T7 RNA polymerase-binding sites followed by sense or anti-sense sequences (Table 2-4). The primers were designed using the E-RNAi web site at the DKFZ, Heidelberg http://www.dkfz-heidelberg.de/signaling/ernai.html. For *GFP*, GFP_RNAi_S and GFP_RNAi_A, for *dmrs2*, dMCRS2_RNAi_S and dMCRS2_RNAi_A, for *pitslre*, Pitslre_RNAi_S and Pitslre_RNAi_A, for *CG6049/cus2*, CG6049/cus2_RNAi_S and CG6049/cus2_RNAi_A, for *CG6905/cefl CG6905/cefl*, CG6905/cefl_RNAi_S and CG6905/cefl_RNAi_A, for *CG8877/prp8*, CG8877/prp8_RNAi_S and CG8877/prp8_RNAi_A, for *CG32604/prp16*, CG32604/prp16_RNAi_S and CG32604/prp16_RNAi_A, for *CG6015/prp17*, CG6015/prp17_RNAi_S and CG6015/prp17_RNAi_A, for *CG6011/prp18*, CG6011/prp18_RNAi_S and CG6011/prp18_RNAi_A, for *CG5519/prp19*, CG5519/prp19_RNAi_S and CG5519/prp19_RNAi_A, for *CG8241/prp22*, CG8241/prp22_RNAi_S and CG8241/prp22_RNAi_A, for *CG30342/dprp38*, CG30342/dprp38_RNAi_S and CG30342/dprp38_RNAi_A, for *CG1017/dmfap1*, CG1017/dmfap1_RNAi_S and CG1017/dmfap1_RNAi_A, for *pixie*, Pixie_RNAi_S and Pixie_RNAi_A, for *adam*, Adam_RNAi_S and Adam_RNAi_A, for *eIF3-S2*, eIF3-S2_RNAi_S and eIF3-S2_RNAi_A, for *eIF3-S8*, eIF3-S8_RNAi_S and eIF3-S8_RNAi_A, for *eIF3-S9*, eIF3-S9_RNAi_S and eIF3-S9_RNAi_A, for *eIF3-S10*, eIF3-S10_RNAi_S and eIF3-S10_RNAi_A, for *rps25*, Rps25_RNAi_S and Rps25_RNAi_A, for *rps13*, Rps13_RNAi_S and Rps13_RNAi_A.

2.1.4 Luciferase assay

$S2R^+$ cells were seeded in a 96-well plate at a density of $2x10^5$ cells/mL in 60μL serum-free medium (M3) containing 800 ng dsRNA targeting the relevant genes (Figure 3-3D). One hour later, 140μL complete M3 medium with transfection mix prepared according to the Qiagen effectene protocol was added to each well. The transfection mix contained the following amounts of plasmids:

UAS-Luc: 20 ng

Yki-Gal4: 10 ng

pIZ-Renilla: 10 ng

and:

pAC-Hpo-Myc, pAC-Wts-Myc, pAC-Sav-Myc: 10 ng each

or

empty pAC-Myc: 30 ng (control)

The plate was spun at 1000 rpm for one minute and incubated at 25°C for 72 hours. On day four, the medium was removed by aspiration, and for the subsequent steps the Dual-Luciferase® Reporter 1000 Assay System kit (Promega) was used. First, 20μL Passive Lysis Buffer was added to each well. Plates were spun at 1000 rpm for one minute, and cells were lysed at room temperature with shaking for 20 minutes. Second, 100μL LAR II reagent was added. Third, the luciferase signal was read on Perkin Elmer Envision. Finally, 100μL of Stop&Glo reagent was added, and the Renilla signal was measured on the same reader. The Renilla signal functions as a read-out for transfection efficiency. To compare the Yki-luciferase activity between different samples (wells) the luciferase signal was normalised to the Renilla signal. For each condition, eight replicates were made.

2.1.5 DNA profiles

S2 cells were seeded in 35 mm wells at a density of 7×10^5 cells/ml in a total of 3 ml complete medium/well and treated with dsRNA (20 μg/well) targeting *eGFP* or genes encoding the relevant gene products for the indicated number of days (Figures 3-6A, 4-3A, and 4-10). Subsequently, cells were harvested, collected by centrifugation, washed two times in PBS (137 mM NaCl, 2.7 mM KCl, 4.3 mM Na_2HPO4, 1.47 mM KH_2PO_4, pH=8), fixed in cold 70% ethanol and stored at 4°C. Subsequent steps were performed at room temperature. Fixed cells were washed twice in PBS, treated with 50 μl 100 μg/ml RNase A (Sigma-Aldrich) for 15 min and 250μl 40μg/ml propidium iodide for a further 30 min, and then analysed by flow cytometry.

2.1.6 BrdU-pulse chase

S2 cells were seeded in 35 mm wells at a density of 7×10^5 cells/ml in a total of 3 ml complete medium/well and treated with dsRNA (20 μg/well) targeting *eGFP*, *dprp38*, or *dmcrs2* for 4 (*dprp38*, Figure 4-4) or 6 (*dmcrs2*, Figure 3-7) days. After 3 (*dprp38*) or 5 (*dmcrs2*) days, cells were re-seeded in 35 mm wells at a density of $2x10^6$ cells/mL. After 12 hours, 15μM BrdU (Sigma Aldrich) was added to the medium for 15 minutes, then cells were washed three times with PBS, and BrdU-free medium was added. Cells were harvested at the indicated time points, collected by centrifugation, washed two times in PBS, fixed in cold 70% ethanol, and stored at 4°C. Subsequent steps were performed at room temperature. Fixed cells were washed twice

in PBS and once in PBS-BT (PBS + 0.1% BSA + 0.2% Tween-20). 2 µl monoclonal mouse anti-BrdU (Becton Dickinson) were added directly to the cell pellets, incubated for 20 minutes in the dark, then cells were washed twice in PBS-BT and incubated in 50µl of FITC-conjugated rabbit anti-mouse F(ab')2fragments (DAKO) diluted 1:10 in PBS-BT for 20 minutes. Cells were washed twice in PBSA, treated with 50 µl 100 µg/ml RNaseA (Sigma-Aldrich) for 15 min and 250µl 40µg/ml propidium iodide for a further 30 min and then analysed by flow cytometry.

2.1.7 Cloning

The plasmids to express recombinant Pixie or PixieΔABC tagged at the N-terminus with glutathione-S-transferase (GST) followed by a tobacco etch virus (TEV) protease cleavage site and a Calmodulin binding peptide (CBP, 'GTC') was generated in three steps. First, the entire Pixie ORF or Pixie lacking the second ABC domain (PixieΔABC), with EcoRV, HindIII and EcoRI sites inserted before the start codon and with a Kpn I site inserted after the stop codon was PCR-amplified using the Pixie_sense and Pixie_anti (Pixie) or PixieΔABC_anti (PixieΔABC) primers. The PCR fragments were inserted into pGEM-T (Promega) giving rise to the pDA3-1 and pDA3-3 plasmids, and the insert DNA sequences were verified. Second, a cassette encoding the GTC-tag (Zachariou et al., 2003) was subcloned from pCN-GTCtag (gift from Pascal Meier) into pDA3-1 and pDA3-3 using the HindIII and EcoRI restriction sites, thereby generating pDA8-1 and pDA8-2, respectively. Third, N-terminally GTC-tagged Pixie and PixieΔABC were inserted in front of the inducible MT promoter of the pMK33 vector using the unique EcoRV and SpeI restriction sites to generate pDA9-1 and pDA9-2, respectively. GTC-PixieE501Q (pDA9-3) was generated by introducing a point mutation in the second ABC domain of Pixie (G1483C) by three consecutive PCRs. First PixieE501Q_S1 and PixieE501Q_A1 (PCR1) or PixieE501Q_S2 and PixieE501Q_A2 (PCR2) primers were used to produce two overlapping PCR fragments containing the desired point mutation. The final PCR fragment was amplified using the PCR1 and PCR2 fragments as template and the PixieE501Q_S1 and PixieE501Q_A2 primers, which covers a unique BstEII restriction site 5' of the point mutation, and inserts a SpeI site 3' of the stop codon, respectively. This PCR fragment was inserted into pCR®2.1-TOPO® (Invitrogen) generating pDA3-5, and the DNA sequence was verified. Finally, the Pixie fragment containing the point mutation was subcloned into

pDA9-1 using the unique BstEII and SpeI restriction sites to generate pDA9-3. A control plasmid expressing the GTC-tag alone was generated by PCR amplification from pCN-GTCtag using primers that added a EcoRV site in front of the ATG and and a SpeI site after the stop codon, respectively. This fragment was subcloned into pMK33 to generate pDA10-1. To generate GTC-dMCRS2, the entire dMCRS2 ORF, with an EcoRI site inserted before the start codon and with a NotI site inserted after the stop codon was PCR-amplified using the GTC_dMCRS2_S and GTC_dMCRS2_A primers. This PCR fragment was subcloned into pDA8-1 using the unique EcoRI and NotI sites. Next, N-terminally GTC-tagged dMCRS2 was inserted in front of the inducible MT promoter of the pMK33 vector using the unique EcoRV and SpeI restriction sites to generate GTC-dMCRS2.

To generate His-dPrp38, the entire open reading frame of dPrp38 was PCR amplified with a KpnI site inserted before the start codon and a HindIII site inserted after the stop codon using dPrp38/pENTR-TOPO (see below) as a template and the dPrp38_GST_S and dPrp38_GST_A primers. Next, this PCR fragment was inserted into the pRSET A vector using the unique KpnI and HindIII sites. To generate GST-dMFAP1, the entire open reading frame of dMFAP1 was PCR amplified with an EcoRI site inserted before the start codon and a Sal I site inserted after the stop codon using dMFAP1/pENTR-TOPO (see below) as a template and the dMFAP1_GST_S and dMFAP1_GST_A primers. Next, this PCR fragment was inserted into the pGEX 4T-1 vector using the unique EcoRI and Sal I sites.

The construct used to generate the *dmfap1 D2-1* RNAi line was cloned by inserting two 400 bp inverted repeats of *dmfap1* into the pMF3 vector using the unique EcoRI and XbaI restriction sites. The 400 bp repeats were amplified from genomic DNA using a forward primer containing a Bgl II site at the 5' end (dMFAP1ForwBglII) and reverse primers containing an EcoRI (dMFAP1RevEco) or a XbaI (dMFAP1RevXba) site at the 3' end. The two PCR products were digested with Bgl II and EcoRI or Bgl II and XbaI and cloned into the same pMF3 vector digested with EcoRI and XbaI.

dMCRS2-Flag, dMCRS2ΔFHA-Flag, HA-Pitslre, HA-PitslreK587R, MOF-HA, dMFAP1-Myc, HA-dMFAP1ΔN, HA-dMFAP1ΔC, HA-dPrp38^{P} and dPrp38Δ were cloned using the Gateway system (Invitrogen). dMCRS2 was PCR amplified from an EST (1794) using the dMCRS2_S and dMCRS2_A primers, Pitslre

was PCR amplified from an EST (39519) using the Pitslre_S and Pitslre_A primers, dMFAP1 was PCR amplified from an EST (7619) using the dMFAP1_S and dMFAP1_A primers, dPrp38 was PCR amplified from an EST (13395) using the dPrp38_S and dPrp38_A primers, and MOF was PCR amplified from an EST (8841) using the MOF_S and MOF_A primers. PCR products were run on 1% agarose gels (TAE + 1% agarose (Invitrogen) + 1 µl of Ethidium Bromide (Roche)), and bands of the correct size were cut out, purified using the QIAquick gel extraction kit (Qiagen), and ligated into the pENTR-TOPO vector (Invitrogen) according to manufacturers instructions. dMCRS2ΔFHA was PCR amplified from dMCRS2/pENTR using the dMCRS2ΔFHA_S and dMCRS2ΔFHA_A primers, dMFAP1ΔN and dMFAP1ΔC were PCR amplified from dMFAP1/pENTR using dMFAP1ΔN_S and dMFAP1ΔN_A or dMFAP1ΔC_S and dMFAP1ΔC_A primers, respectively, HA-dPrp38^{P} and dPrp38Δ were PCR amplified from dPrp38/pENTR using dPrp38^{P}_S and dPrp38^{P}_A or dPrp38Δ_S and dPrp38Δ_A primers, respectively. PitslreK587R was generated by three consecutive PCRs. First Pitslre_S and PitslreK587R_A (PCR1) or PitslreK587R_S and and Pitslre_A (PCR2) primers were used to produce two overlapping PCR fragments containing the desired point mutation. Second, the final PCR fragment was amplified using PCR1 and PCR2 fragments as template and the Pitslre_S and Pitslre_A primers. All of the above PCR products were purified and cloned into pENTR-TOPO (Invitrogen). dMCRS2, dMCRS2ΔFHA, Pitslre, PitslreK587R, dMFAP1, dMFAP1ΔN, dMFAP1ΔC, HA-dPrp38^{P}, dPrp38Δ, and MOF were then transferred from pENTR-topo to Gateway expression vectors by the LR reaction. These included pActin 3xHA, pActin 6xMyc, and pActin 3xFlag for expression of tagged proteins in S2 cells and pUASP for generation of *UAS-dprp38*, *UAS-dmfap1*, and *UAS-dmcrs2* transgenic lines. Midi-preps were made of all plasmids using the High-Speed Plasmid Midi Kit (Qiagen). The resulting plasmid DNs was quantified using the Nanodrop (Nanodrop) and stored at -20°C. All Gateway vectors were obtained from the Gateway Drosophila Vector Collection (Murphy lab, Carnegie Institution).

2.1.8 DNA Sequencing

DNA was sequenced by the Sequencing Service at Cancer Research UK using a 3730 DNA Analyzer (Applied Biosystems). Extension products were amplified

and purified using the DyeEx Spin kit (Qiagen). Purified extension products were handed to the Sequencing Service for sequencing.

2.1.9 Polymerase chain reaction (PCR)

PCR products were amplified using the Taq PCR Master-mix kit (Qiagen) and a PTC-200 peltier thermal cycler (MJ Research). For cloning the PWO Master-mix (Roche), which contains a high-fidelity polymerase, was used. A typical PCR reaction of 50µl was set up as follows:

25µl Master-mix
1µl 5'-primer (20µM)
1µl 3'-primer (20µM)
1µl Template DNA (10-50ng)
22µl distilled H_2O

A typical PCR reaction was run on the following PCR program:

1) 95°C for 10 mins
2) 95°C for 40 seconds
3) 56°C for 30 seconds
4) 72°C for minute per kb of product
5) go to step (2) – 24 cycles
6) 72°C for 10 minutes

PCR products were run on 1% Agarose gels, and gels were photographed using an IMAGO compact imaging system.

2.1.10 Quantitative RT-PCR

S2 were treated with dsRNA (20 µg/well) targeting genes encoding the indicated gene products for three days. Total RNA was isolated from the cells using the RNeasy kit (Qiagen) and treated with RQ1 DNase (Promega). Total RNA (1.5 µg) was used for first-strand cDNA synthesis with AMV Reverse Transcriptase and oligo-p(dT)15 primer (mRNA) or oligo-p(dN)6 (total RNA) (Roche). To measure pre-mRNA levels, quantitative PCRs (qPCRs) were performed on reverse-transcribed total RNA

using one intron- and one exon-specific primer. To measure mRNA levels, qPCRs were carried out on reverse transcribed total mRNA using exon-specific primers. For *stg* mRNA, Stg_mRNA_S and Stg_mRNA_A, for *γ-tubulin(23C)* pre-mRNA, γ-tubulin_pre_mRNA_S and γ-tubulin_pre_mRNA_A, for *γ-tubulin(23C)* mRNA, γ-tubulin_mRNA_S and γ-tubulin_mRNA_A, for *eIF3-S10* pre-mRNA, eIF3S10_pre_mRNA_S and eIF3S10_pre_mRNA_A, for *eIF3-S10* mRNA, eIF3S10_mRNA_S and eIF3S10_mRNA_A, for *dmcrs2* pre-mRNA, dMCRS2_pre_mRNA_S and dMCRS2_pre_mRNA_A, for *dmcrs2* mRNA, dMCRS2_mRNA_S and dMCRS2_mRNA_A, for *hpo* pre-mRNA, Hippo_pre_mRNA_S and Hippo_pre_mRNA_A, for *hpo* mRNA, Hippo_mRNA_S and Hippo_mRNA_A, and for *his3,* Histone3_transcript_S and Histone3_transcript_A primers were used. Real-time qPCR was performed with Platinum® SYBR® Green qPCR SuperMix-UDG (Invitrogen). PCR was carried out in 96-well plates using the Chromo 4 Real-time qPCR Detection System (MJ Research). All reactions were performed in four replicates. The relative amount of specific mRNAs and pre-mRNAs under each condition was calculated after normalization to the intronless *histone 3* (*his3*) transcript.

2.1.11 Tandem Affinity Purification

Two-step purifications were performed from $1x10^{10}$ S2 cells expressing recombinant GTC-Pixie, GTC-dMCRS2 or the GTC-tag alone. Cells were lysed in 50ml Buffer A (50 mM Hepes-KOH, pH 8, 100 mM KCl, 10 mM MgCl2, 0.1% Triton X-100, 2 mM DTT, 10% glycerol, 10 mM NaF, 0.25 mM NaVO4, 1 mM PMSF, 0.1 mg/ml aprotinin, 10 μg/ml leupeptin), and cell extracts were cleared of nuclear and membranous material by centrifugation at 10,000 rpm for 15 min. In the first purification step, the cleared cell extracts were incubated with glutathionine sepharose beads (Amersham) for 2 hours at 4°C. Post incubation, beads were washed three times in 12 ml Buffer A and 3 times in Cleavage Buffer (CB; 10 mM TrisHCl pH 8, 150 mM NaCl, 0.1% Triton X-100, 0.5 mM EDTA, 1 mM DTT). Beads were resuspended in 300 μl CB containing 50U of TEV protease (Invitrogen) and incubated at 16°C for two hours. After the first round of cleavage, the supernatant was recovered and a second round of cleavage was performed at 4°C overnight. In the second purification step, the supernatants from the two cleavage reactions were pooled and mixed with three

volumes of Calmodulin (CaM) Binding Buffer (CaMBB; 10 mM TrisHCl pH 8, 150 mM NaCl, 0.1% Triton X-100, 1 mM $Mg(CH_3COO)_2$, 1 mM Imidazole, 2 mM $CaCl_2$, 10 mM β-mercaptoethanol), before incubation with CaM beads (SepharoseTM4B, Amersham) at 4°C for 4 hours. Subsequently, the beads were washed 6 times in 10 ml CaMBB and Pixie and Pixie-associated or dMCRS2 and dMCRS2-associated proteins were eluted in CaM elution Buffer (10 mM TrisHCl pH 8, 150 mM NaCl, 0.1% Triton X-100, 1 mM $Mg(CH3COO)_2$, 1 mM Imidazole, 2 mM EGTA, 10 mM β-mercaptoethanol) at 4°C. Finally, the eluates from the CaM beads were concentrated by centrifugation in Microcon YM-10 concentrators (Millipore) and resolved by SDS-PAGE on 4-12% gradient gels (Invitrogen). Individual protein bands were visualized by Brilliant Blue G-colloidal concentrate (Sigma) staining, cut out and identified by MALDI-TOF mass spectrometry

2.1.12 Immunoprecipitation

Immunoprecipitations were performed from $1x10^9$ (large-scale, Figures 4-5 and 4-7) or $1x10^7$ S2 cells. Cells were lysed in 10 ml (large-scale, Figures 4-5 and 4-7) or 200 µl buffer B (50 mM Tris-HCl, pH 8, 150 mM NaCl, 0.5% NP50, 1 mM EGTA, 0.5 M NaF, phosphatase inhibitor cocktail 2 (Sigma), Complete protease inhibitor cocktail (Roche)), and cell extracts were cleared of membranous material by centrifugation at 10,000 rpm for 15 min. Extracts were incubated with protein A-sepharose 4B beads (Amersham) for one hour to reduce unspecific binding of proteins to the beads in the subsequent purifications. Next, the pre-cleared extracts were incubated with 800 µl (large-scale, Figures 4-5 and 4-7) or 80 µl of protein A-sepharose beads and 10 µl (large-scale, Figures 4-5 and 4-7) or 1 µl of the relevant antibody for two hours. A rabbit anti-GFP antibody was used in the control purifications. Subsequently, beads were washed 3 times in buffer B, boiled in sample buffer (Invitrogen), and resolved by SDS-PAGE on 8-16% gradient gels (Biorad, Figure 4-7) or 4-12% Nupage Bis-Tris gels (Invitrogen). Individual protein bands were visualized by Brilliant Blue G-colloidal concentrate (Sigma) staining, cut out and identified by MALDI-TOF mass spectrometry at the Taplin Biological Mass Spectrometry Facility (large-scale, Figures 4-5 and 4-7).

2.1.13 GST pull-down

For the GST pull-downs, 1μg bacterial-produced GST or GST-dMFAP1 protein was incubated with 50ng bacterial-produced His-dPrp38 protein and 80μl pre-washed Gluthionine-Sepharose beads (Pharmacia) in 250μl buffer B at 4°C (Figure 4-6A). For the Histidine (His) pull-downs, 500ng of bacterial-produced His-dPrp38 or His-Peptide (control) was incubated with 800ng of cleaved GST-dMFAP1 and 80μl pre-washed Ni-NTA agarose beads (Qiagen) in 250μl buffer B at 4°C (Figure 4-6B). After two hours, Gluthionine sepharose and Ni-NTA agarose beads were spun down at 200 rcf for two minutes, the supernatant was removed, and beads were washed three times for two minutes in buffer B at 4°C. After the final wash, beads were spun down and 18μl of sample buffer (Invitrogen) and 3μl of reducing buffer (Invitrogen) was added. Samples were incubated at 70°C for 10 minutes, and the supernatants resolved by SDS-PAGE on 4-16% Nupage Bis-Tris gels (Invitrogen).

2.1.14 Western blotting

Proteins were separated by SDS-PAGE using 12% gels or 4-12% gradient gels (Invitrogen) and transferred electrophoretically to polyvinylidene difluoride membranes (PDVF, Millipore or Amersham). For detection by the Odyssey Infrared Imaging System (LI-COR Biosciences), membranes were blocked for one hour in Blocking Buffer A (LI-COR Biosciences) supplemented with 0.1% Tween 20, and incubated overnight at 4°C in the same buffer containing primary antibodies at the indicated concentrations (Table 2-2). Membranes were washed three times in TBS-T (10 mM Tris-HCl pH 8, 150 mM NaCl, 0.1% Tween-20) or PBS-T (PBS + 0.1% Tween-20), then probed with secondary antibodies labelled with Alexa Fluor 680 (Molecular Probes) or IRDyeTM 800 (Rockland Immunochemicals) diluted 1/6000 in a buffer containing 1/3 volume TBS-T or PBS-T, 2/3 volume Blocking Buffer A for one hour at room temperature. After washing in TBS-T or PBS-T, bands were detected using the Odyssey Infrared Imaging System (LI-COR Biosciences). For detection by chemiluminescence, membranes were blocked for one hour in Blocking Buffer B (PBS + 5% milk) and incubated overnight at 4°C in the same buffer containing primary antibodies at the indicated concentrations (Table 2-2). Membranes were washed three times in PBS-T, blocked for one hour in Blocking Buffer B, then probed with Horseradish Peroxidase conjugated secondary antibodies diluted 1/5000 in blocking

buffer B for one hour at room temperature. After three washes in PBS-T, chemiluminescence was observed using the ECL-plus Western blotting detection system (Amersham Biosciences).

2.1.15 Velocity Sedimentation

To generate the data shown in Figures 4-12B and 5-6 to 5-13, $5x10^8$ S2 cells were treated with 100μg/ml cycloheximide (Sigma) for 10 min and lysed in 0.6 ml 50mM Hepes-KOH pH 7.2, 100mM KCl, 10mM MgCl2, 0.1% Triton X-100, 1 mg/ml Heparin, 2 mM DTT, 100μg/ml cycloheximide, RNAguardTM (Amersham). Cell debris was removed via centrifugation for 10 min at 13,000 rpm, and extracts were resolved on 7.5-30% sucrose density gradients by centrifugation for 4.5 h at 39,000 rpm at 4°C using the SW41Ti rotor (Beckman). 600μl fractions were collected while recording the A_{254} profile using a single path UV monitor (Pharmacia).

To generate the data shown in Figure 4-12C, $5x10^8$ S2 cells were lysed in 0.6 ml lysis Buffer (25mM Hepes-KOH pH 7.6, 0.1 mM EDTA, 60mM KCl, 1% Triton X-100, 1mM DTT, 1mM PMSF, 0.5 M NaF, phosphatase inhibitor cocktail 2 (Sigma), Complete protease inhibitor cocktail (Roche)). Cell debris was removed via centrifugation for 10 min at 13,000 rpm, and extracts were resolved on 7.5-35% glycerol density gradients by centrifugation for 7 h at 37,000 rpm at 4°C using the SW41Ti rotor (Beckman). 600μl fractions were collected and stored at -20°C.

2.1.16 Polysome Profiles

To generate the data shown in Figure 5-5, S2 cells were seeded in 35 mm wells at a density of $7x10^5$ cells/ml in a total of 3 ml complete medium/well and treated with dsRNA (25 μg/well) targeting *eGFP* (control), *pixie*, or *eIF3-S10*, for 7-8 (Pixie) or 5 (eIF3-S10) days, and the effectiveness of the dsRNAi-mediated depletion was assessed by immunoblotting. To stimulate growth, cells were starved for an hour in PBS containing 2mg/ml glucose (Sigma) and subsequently stimulated in complete media containing 1μM insulin (Sigma) for three hours. Cells were then treated with 100μg/ml cycloheximide (Sigma) for 10 min and extracts were prepared from 3×10^7 cells as described above. The cleared extracts were resolved on 7.5-60% sucrose density gradients by centrifugation at 39,000 rpm for 2 hours at 4 °C using a SW41Ti rotor (Beckman). The A_{254} profiles were recorded as described above.

2.2 Genetics and Immunohistochemistry

2.2.1 Immunohistochemistry

Mosaic tissues were obtained using the hs-Flp/FRT system (Xu and Rubin, 1993). Salivary glands and wing and eye imaginal discs were dissected from L3 larvae (120 hr AEL) in 1× PBS. S2 cells were seeded at a density of $5x10^6$/mL on chamber slides (Nunc, Figure 4-11A-D). Tissues and S2 cells (Figure 4-11A-D) were fixed in 4% formaldehyde in PBS for 20 min at room temperature, washed four times in PBS containing 0.1% Triton X-100 (PBS-T), blocked for 2 hrs in PBS-T containing 10% goat serum (PBS-TG), and incubated with primary antibodies diluted in PBS-TG overnight at 4°C. The dilutions of the primary antibodies are indicated in Table 2-2. The next day, tissues and cells were washed, blocked in PBS-TG, and incubated with secondary antibodies for two hours at room temperature. The dilutions of the secondary antibodies are indicated in Table 2-3. Hoechst (Sigma) was added to the secondary antibody mixture during the last 30 minutes of the incubation to stain DNA. After washes, cells and tissues were mounted in Vectashield. Fluorescence images were acquired using a Zeiss LSM510 Confocal Laser Scanning Microscope (25× and 40x objectives) and processed using Adobe photoshop CS2.

2.2.2 Staining of Polysome Chromosome spreads

Salivary glands were dissected from third instar larvae in 1× PBS, and fixed for 10 minutes in a droplet of fix (3.7% paraformaldehyde and 50% acetic acid) on a siliconised coverslip. Next, the coverslip was picked up with a poly-L-lysine-treated slide, and the salivary gland cells broken up by tapping the coverslip with an eraser and applying a firm pressure with the thumb. After examination of the polytene chromosome preparations under the light microscope to check that the chromosome arms are well spread, the slides frozen in liquid nitrogen and the coverslips were removed using a razor blade. Next, slides were washed in 1xPBS, the polytene chromosome preparations were permeabilised in PBS containing 1% Triton X-100 for 10 minutes, blocked for 2 hrs in 5% milk in PBS ,and incubated with anti-RNAP II and anti-dMCRS2 antibodies diluted 1/100 in 5% milk in PBS overnight at 4°C. The next day, slides were washed, blocked in 5% milk in PBS, and incubated with secondary antibodies for two hours at room temperature. The dilutions of the secondary antibodies are indicated in Table 2-3. After washes, polytene chromosome spreads were mounted

in Vectashield. Fluorescence images were acquired using a Zeiss LSM510 Confocal Laser Scanning Microscope (40x objective) and processed using Adobe photoshop CS2.

2.2.3 Scanning electronic microscopy (SEM)

Adult female flies of the relevant genotypes were collected and transferred to fresh vials for 6 hours. They were then submerged in 10% ethanol for 30 minutes followed by consecutive incubations in ethanol solutions of increasing concentrations (30%, 50%, 70%, 90%, and 100%). Samples were prepared and imaged by Anne Weston of the Cancer Research UK electron microscopy (EM) facility using a Jeol JSM 6700F Scanning electron microscope.

2.2.4 Mutagenesis by imprecise P-element excision

The *G19491* P-element (Genexel Inc.) is inserted 798 bp into the open reading frame of *dprp38* (*dprp38*^{G19491}). The *dprp38*^{E1} mutant was generated by imprecise excision of the G19491 P-element. Below is shown the cross scheme used to obtain the *dprp38*^{E1} mutant:

P_0 ♂♂ *w ; G19291(mv) / CyO* **X** *w ; Sp/CyO ; Δ2-3, Sb / TM6B* ♀♀

F_1 ♂♂ *w ; G19291(mv) / CyO ; Δ2-3, Sb / +* **X** *w ; Sp / CyO* ♀♀

F_2 Single ♂ *w ; G19291* / CyO* **X** *w ; Sp / CyO* ♀♀

In the first cross, the P-element line (*G19491*) was crossed to the transposase source (*Δ2-3*). Hybrid males (mosaic orange and white eyes) were selected from the F_1 and crossed *en masse* to second chromosome balancer virgins (*Sp / CyO*). In the F_2 generation, white-eyed excision males (*G19291**) were selected and crossed individually to (*Sp / CyO*) virgins. Males were lifted from this cross after four days and screened for deletions by PCRs using genomic DNA as a template and the dPrp38-5.03 and dPrp38-3.3 primers. The genomic DNA from individual adult flies was prepared using the DNeasy kit (Qiagen) by following manufacturers directions. Once mutant chromosomes had been identified, the relevant crosses to *Sp / CyO* were kept and progeny were mated *inter se* to obtain balanced mutant stocks.

2.2.5 Generation of recombinant chromosomes

For generation of all recombinant chromosomes, similar crossing schemes were used. Shown below as an example is the crossing scheme used to recombine the *dmcrs2*^{rG166} mutation onto the *FRT80B, Ubi-GFP* chromosome:

P$_0$ ♂♂ *w ; dmcrs2*^{rG166} */ TM3, Sb* **X** *w ; FRT80B Ubi-GFP / TM6B* ♀♀

F$_1$ ♂♂ *w ; TM3, Sb / TM6B* **X** *w ; dmcrs2*^{rG166} */ FRT80B Ubi-GFP* ♀♀

F$_2$ ♂ *w ; FRT80B Ubi-GFP (?) , dmcrs2*^{rG166}*(?)/ TM6B* **X** *w ; TM3, Sb / TM6B* ♀♀

In the first cross, *dmcrs2*^{rG166} */ TM3, Sb* flies were crossed to *FRT80B , Ubi-GFP / TM6B* flies. Virgin females were selected in F$_1$ that have both *dmcrs2*^{rG166} and *FRT80B , Ubi-GFP* by the absence of the dominantly marked balancer chromosomes, *TM3, Sb* and *TM6B*. These females were crossed *en masse* to *TM3, Sb / TM6B* males, and the meiotic recombination event occured in the female germline. The F$_2$ generation were crossed to third chromosome balancer virgins, then lifted after four days, and screened for the presence of both *dmcrs2*^{rG166} and *FRT80B , Ubi-GFP* by PCRs of genomic DNA. Crosses from recombinant males were kept and the progeny mated *inter se* to obtain recombinant stocks.

2.2.6 Density controlled wing measurements

Crosses to obtain the relevant genotypes were initiated. Once females were laying eggs (1-2 days), the flies were transferred to a container, which was inverted over an agar and apple juice substrate. Eggs were collected for 4 hours before the flies were removed. The embryos were kept at 25°C until eclosion. When the flies eclosed from the density-controlled crosses, males of the relevant genotype were collected and put into 100% ethanol. Wings were removed with micro-dissection tweezers, dried on a piece of tissue, and mounted on slides in Euparal (Sigma). A coverslip was placed over the wings, and the slides were dried overnight on a 65°C hotplate. Wings were digitally photographed using a LeicaDC200 camera on a MFIII dissection microscope. Wing areas were then measured using the Polygonal Lasso tool on Adobe Photoshop. Generally, the areas of 20 male wings were measured for each genotype.

2.2.7 Transgenic Flies

The *dmfap1 D2-1* RNAi, *UAS-dprp38*, *UAS-dmfap1*, and *UAS-dmcrs2* transgenic lines were generated by the Fly facility at Cancer Research UK. The pMT-dMFAP1_RNAi, pUAS-dPrp38, pUAS-dMFAP1, and pUAS-dMCRS2 constructs were introduced into the germline by injections in the presence of transposase as previously described (Brand and Perrimon, 1993; Rubin and Spradling, 1982). The *dMFAP1* (15610) and *dPrp38* (21136) RNAi lines were obtained from the Vienna *Drosophila* RNAi Center (VDRC).

Table 2-1: Genotypes shown in figures

Figure Number	Genotype
3-2B	*GMRsav,wts/+*
3-2C	*GMRsav,wts/dmcrs2^{rG166}*
3-3B-C'	*hs-FLP; FRT80B, dmcrs2^{rG166}/FRT80B, Ubi-GFP*
3-4B-D	*hs-FLP; FRT80B, Ubi-GFP, dmcrs2^{rG166}/FRT80B, M(3)67c4*
3-4E-G	*hs-FLP; FRT80B, Ubi-GFP, dmcrs2^{c07041}/FRT80B, M(3)67c4*
3-4H-J	*hs-FLP; FRT80B, Ubi-GFP, dmcrs2^{c00114}/FRT80B, M(3)67c4*
3-10D-I	*w^{iso}; engrailed-Gal4, UAS-GFP/UAS-dmcrs2*
4-1C-D	*w^{iso}; engrailed-Gal4, UAS-GFP/UAS-dPrp38RNAi*
4-2C-D	*w^{iso}; hs-FLP; FRT42D, dprp38^{G19491}/FRT42D, Ubi-GFP*
4-2E-F,H	*w^{iso}; hs-FLP; FRT42D,Ubi-GFP,dprp38^{E1}/FRT42D, M(2)53^{1}*
4-9A-C	*w^{iso}; hs-FLP; Act >cd2 > Gal4, UAS-GFP*
4-9D-F	*w^{iso}; hs-FLP; UAS-RNAi-dmfap1/Act >cd2 >Gal4, UAS-GFP*
4-9G-I	*w^{iso}; hs-FLP; UAS-RNAi-dprp38/Act >cd2 >Gal4, UAS-GFP*
4-9J	*w^{iso}; engrailed-Gal4, UAS-GFP/+; UAS-dPrp38/MKRS*
4-9J	*w^{iso}; engrailed-Gal4, UAS-GFP/+; UAS-dMFAP1/+*

Table 2-2: Primary antibodies used

Primary Antibody	Species	Concentration	Source
Pixie	Rabbit	1:5000	Cancer Research UK
Adam	Rabbit	1:1000	Cancer Research UK
eIF3-S2	Rabbit	1:1000	Cancer Research UK
eIF3-S8	Rabbit	1:1000	Cancer Research UK
eIF3-S9	Rabbit	1:1000	Cancer Research UK
eIF3-S10	Rabbit	1:1000	Cancer Research UK
eIF2-α	Rabbit	1:000	Eurogentec, Belgium
eIF4A	Rabbit	1:1000	Gift from Chris Proud
Rps13	Rabbit	1:1000	Eurogentec, Belgium
Rps25	Rabbit	1:1000	Cancer Research UK
RpLP		1:500	ImmunoVision
dMFAP1	Guinae Pig	1:1000	Eurogentec, Belgium
dPrp38	Rabbit	1:1000/1:500 (WB/IF)	Eurogentec, Belgium
dMCRS2	Guinae Pig	1:1000/1:500 (WB/IF)	Eurogentec, Belgium
Cleaved Caspase 3	Rabbit	1:500	Cell signalling
phospho-Histone H3	Rabbit	1:1000	Upstate
β-tubulin	Mouse	1:2000	Developmental Studies Hybridoma Bank
α-tubulin	Mouse	1:1000	Sigma
BrdU	Mouse	1:1	Becton Dickinson
DIAP1	Mouse	1:500	Bruce Hay
CycE	Rat	1:500	Helen McNeill
Pitslre	Rabbit	1:1000	Eurogentec, Belgium
RNAP II serum	Goat	1:2000	Arno L. Greenleaf
RNAP II (7G5)	Mouse	1:100	Lazslo Tora
Myc	Mouse	1:000	Santa Cruz
HA (3F10)	Rat	1:000	Roche
FLAG	Rabbit	1:1000	Sigma
GST	Rabbit	1:1000	Sigma

Table 2-3: Secondary antibodies used

Secondary antibody	Species	Concentration	Source
Anti-GpRRX	Guinae Pig	1:500	Jackson
Anti-RbRRX	Rabbit	1:500	Jackson
Anti-MouseRRX	Mouse	1:500	Jackson
Anti-RatRRX	Rat	1:500	Jackson
Anti-GpAlexa633	Guinae Pig	1:500	Molecular Probes
Anti-RbFITC	Rabbit	1:500	Jackson
IRdye800-labelled	Rabbit	1:6000	Rockland
IRdye700DX-labelled	Rabbit	1:6000	Rockland
IRdye700DX-labelled	Mouse	1:6000	Rockland
Anti-mouseHRP	Mouse	1:5000	Amersham
Anti-RabbitHRP	Rabbit	1:5000	Amersham
Anti-RatHRP	Rat	1:5000	Amersham
Anti-GpHRP	Guinae Pig	1:5000	Sigma
Anti-goatHRP	Goat	1:5000	Sigma
Anti-mouseFITC	Mouse	1:10	DAKO

Table 2-4: Primers used

Primer Name	Primer sequence
dMCRS2_S	CACCATGGAGGCATCAAGAATAACCG
dMCRS2_A	GTTGAGGGGATTCGATGTCTTG
dMFAP1_S	CACCATGAGTGCAGCCACCGCCGC
dMFAP1_A	CTCCATCTTTTTTCGCTTCG
dMCRS2_RNAi_S	CCGGGGACACCTAGCACTGTTG
dMCRS2_RNAi_A	GGTGCCAAGCAGATCCTCCTC
GTC_dMCRS2_S	GAATTCGAGGCATCAAGAATAACCG
GTC_dMCRS2_A	ACTAGTGCGGCCGCTAGTTGAGGGGATTCGATGTC
Pitslre_S	CACCATGGTCAATTCGTCTGGCAGC
Pitslre_A	TCAGAACTTCAGACTGAATCC
dMCRS2ΔFHA_S	CACCATGGAGGCATCAAGAATAACCG
dMCRS2ΔFHA_A	CGGCCACACAAGCAGGCCAG
PitslreK587R_S	GAGATTGTGGCTCTTAGGCGTCTGAAAATGGAG
Pitslre K587R_A	CTCCATTTTCAGACGCCTAAGAGCCACAATCTC
Pitslre_RNAi_S	CGCTGAATTTCACATTTCCA
Pitslre_RNAi_A	GACGAATTGACCATTTTCGG
MOF_S	CACCATGTCTGAAGCGGAGCTGGAAC
MOF_A	GCCGGAATTTCCCGGAGCTCTG
dPrp38-5.03	CTTTGCTCTCACTGCGGAGCT
dPrp38-3.3	AGCGAGCAAGTAGGAACGGAACGGAACGGC
GFP_RNAi_S	GGTGGTGCCCATCCTGGT
GFP_RNAi_A	TCGCGCTTCTCGTTGGGG
dPrp38_RNAi_S	AGCGTGTCTGCGACATTATACTGCCCC
dPrp38_RNAi_A	AGCCTCGCGAGTCCCGTTCCC
dMFAP1_GST_S	CCGGAATTCATGAGTGCAGCCACCGCCGCCG
dMFAP1_GST_A	CCGGTCGACTTACTCCATCTTTTTTCGCTTCG
dPrp38_His_S	CGTGGTACCATATGGCCAACCGCACGGTGAAGG
dPrp38_His_A	AACAAGCTTTTAGTAGCGTCGTCGGTCACGC
dMFAP1_ΔN_S	CACCATGGACAACGAACCCCGCCTGAAG
dMFAP1_ΔN_A	TTACTCCATCTTTTTTCGCTTCG
dMFAP1_ΔC_S	CACCATGAGTGCAGCCACCGCCGCCG
dMFAP1_ΔC_A	CTCCTCGCTTTCGGTCTCCTC
$dPrp38^{P}$_S	CACCATGGCCAACCGCACGGTGAAGG
$dPrp38^{P}$_S	TCCTCGTTGTGGGTGTCCCG
dPrp38Δ_S	CACCATGGCCAACCGCACGGTGAAGG
dPrp38Δ_A	GATTTCGTTGTTTTCCTCGAG

γ-tubulin_mRNA_S	GGCGGACGACGACCACTAC
γ-tubulin_mRNA_A	GGATAGCGGTCCGCCAGGCGC
γ-tubulin_pre_mRNA_S	GCGCCAAACCTACTATTAACTC
γ-tubulin_pre_mRNA_A	CTACATCACTGATCTCGTCCTG
dMCRS2_mRNA_S	GCAGCTGCGAGCACACTAATC
dMCRS2_mRNA_A	CTGGATAATTCTGGGAGGTGG
dMCRS2_pre_mRNA_S	GGAGGCATCAAGAATAACCG
dMCRS2_pre_mRNA_A	GTTTCGATGCAAAAGGAGCTG
Hippo_mRNA_S	CGGTGAATACCAACAGAGCTC
Hippo_mRNA_A	CGCCACGGCCATCTCCCGC
Hippo_pre_mRNA_S	GGAAAACGGAATGCAACAAC
Hippo_pre_mRNA_A	CAATAACAAATGGCCAGCCCTTTC
eIF3-S10_mRNA_S	GGCCCGCTATACGCAACGTC
eIF3-S10_mRNA_A	CGGCCATTTTCAGGTAGCCG
eIF3-S10_pre_mRNA_S	GCGGTGTCTGAAGAGAAAC
eIF3-S10_pre_mRNA_A	CCGCGGATTACATTTTCCAG
Histone3_transcript_S	GTGAAGTAGTGAACGTGAAC
Histone3_transcript_A	CCGCCGAGCTCTGGAATCGC
dMFAP1ForwBglII	GAGAGATCTCGACGAGGTGGAATACGAGG
dMFAP1RevEco	GGAATTCCGAACTTGGTGGTGTCCTGG
dMFAP1RevXba	GTCTAGACGAACTTGGTGGTGTCCTGG
CG6049/cus2_RNAi_S	CTCCTCCTTTCTCTTGGCCT
CG6049/cus2_RNAi_A	CAAAACGGACGAAACTCCAT
CG6905/cef1_RNAi_S	TCTCTAGCTCTCGCTTTCGG
CG6905/cef1_RNAi_A	AGCAGGTAGTCAAGCTGGGA
CG8877/prp8_RNAi_S	TTGCTCCTTGGTCTGCTTTT
CG8877/prp8_RNAi_A	CATTCACACCTCTGTGTGGG
CG32604/prp16_RNAi_S	CTCCTCCTTTCTCTTGGCCT
CG32604/prp16_RNAi_A	GCCGGAATCGATAACGTAGA
CG6015/prp17_RNAi_S	CATTGATGTGGGCCTTCTCT
CG6015/prp17_RNAi_A	CACGCACCATCCCTAGTTTT
CG6011/prp18_RNAi_S	GATGTCTCGCAGACTGTCCA
CG6011/prp18_RNAi_A	CTGAACGCCAAGAACACAGA
CG5519/prp19_RNAi_S	AGCCAGATAGGTTCCGCTTT
CG5519/prp19_RNAi_A	ACAAACACTGGGCATTCTCC
CG8241/prp22_RNAi_S	GCAGTCGGCTTTGTCTAAGG
CG8241/prp22_RNAi_A	ATGGTGTAGCCAACCTCCTG
dMFAP1_RNAi_S	AGGGAGCACAGGGAGCGATTCAGCGG
dMFAP1_RNAi_A	AGCATTCGCTTGAGTTCACGCAGCTTC

Stg_mRNA_S	GCAGTTCTCCTTCTCAACGG
Stg_mRNA_A	GGAGGAGCTGTCGTTCTACG
Rps13_RNAi_S	CGTGACTCGCACGGAG
Rps13_RNAi_A	GCAGTGCTCGACTCGTAT
Rps25_RNAi_S1	ATTCAAGTGCAAGTTGTTAATAC
Rps25_RNAi_A1	TGTGTAGATGACCTGGAATGATG
Rps25_RNAi_S2	TTGCAACATTCCAGCCGCCTAAGAA
Rps25_RNAi_A2	CTTGGTGGCACGTGTGTA
eIF3-S2_RNAi_S	GACATGCAGTTGAGCAAGGA
eIF3-S2_RNAi_A	CATGGCACACCATTTACTCG
eIF3-S8_RNAi_S	GCGCATCACTGTCTAGTGGA
eIF3-S8_RNAi_A	TGCTGATCGAGGTGTAGACG
eIF3-S9_RNAi_S	TGATGGAGATCCCCAAGAAG
eIF3-S9_RNAi_A	TTAACGCCCTTGTTCACCTC
eIF3-S10_RNAi_S	TGTTCTGGAGCTGGATGACC
eIF3-S10_RNAi_A	GTAGTTGGCCATGGTTTTGG
Pixie_RNAi_S	GGAGAAGCACACAACGCATCG
Pixie_RNAi_A	TGATCGAATGGTCAAGGCAGC
Adam_RNAi_S1	CGACGATTGGGAATCCGCA
Adam_RNAi_A1	CCTTCCAGCTGAGCGTTGC
Adam_RNAi_S2	CGTGCGGAGGTCTTGACG
Adam_RNAi_A2	CATGAAGTCGTCATAGTCTTCG
eIF2alpha_RNAi_S	TTCGAAAAGTCCAAATTGCC
eIF2alpha_RNAi_A	CAGGCGGTCTTCTGGTAGAG
Pixie_sense	CGATATCGGAAGCTTGAGAATTCGCCACCATGGGTACCTCGC
Pixie_anti	CGCGGCCGCCTAGTTGCAGGCTTCGTCCTCC
PixieΔABC _sense	CGATATCGGAAGCTTGAGAATTCGCCACCATGGGTACCTCGC
PixieΔABC _anti	CGCGGCCGCCTAGATTAGCATGCGAATGAACGT
PixieE501Q_S2	GAACCCTCTGCCTACTTGGATTCACAGCAGCGTCTGGTGGCCG CCAAGGTTATCAAACGTTACATTCTGCACGCCAAGAAAACTGG
PixieE501Q_A1	TGATAACCTTGGCGGCCACCAGACGCTGCTCTGAATCCAAGTA GGCAGAGGGTTGGTCGATGAGGTAGACATCCGCTGGC
PixieE501Q_S1	CCGGTAACCTCCAACCCGATGG
PixieE501Q_A2	ACTAGTGCGGCCGCTTAGTTGCAGGCTTCGTCCTCCA

Chapter 3 – Results and discussion part I

3.1 A putative role of dMCRS2 in RNAP II transcription

3.1.1 Background to the project

Over the past five years, much of the research in Dr. Tapon's laboratory has been aimed at obtaining a better understanding of the Hippo (Hpo) signalling. The Hpo signalling pathway plays a key role in restricting organ size by controlling both cell cycle exit and apoptosis (Harvey and Tapon, 2007). In brief, the Hpo pathway comprises the two kinases Hpo (Harvey et al., 2003; Jia et al., 2003; Pantalacci et al., 2003; Udan et al., 2003; Wu et al., 2003a) and Warts (Wts) (Justice et al., 1995; Xu et al., 1995), the adaptors Salvador (Sav) (Kango-Singh et al., 2002; Tapon et al., 2002) and Mob1 as a tumour suppressor (Mats) (Lai et al., 2005), the transcriptional co-activator Yorkie (Yki) (Huang et al., 2005), and the transcription factor Scalloped (Sd) (Goulev et al., 2008; Wu et al., 2008; Zhang et al., 2008) (Figure 3-1). Activation of the Hpo kinase results in phosphorylation of Wts, which in turn phosphorylates and inactivates the co-activator Yki. This switches off transcription of Yki target genes including the cell cycle regulator *cyclin E (cycE)* and and the anti-apoptotic gene *diap1 (Drosophila inhibitor of apoptosis protein 1)* (Huang et al., 2005). Thus, activation of the Hpo pathway restricts tissue growth by repressing the cell cycle and promoting apoptosis. The Hpo signalling pathway is activated by unknown signals, but the protocadherin, Fat (Bennett and Harvey, 2006; Cho et al., 2006; Cho and Irvine, 2004; Silva et al., 2006; Willecke et al., 2006), and the FERM (Four point one Ezrin Radixin Merlin) domain proteins, Expanded and Merlin (Hamaratoglu et al., 2006), appear to be involved. Expanded and Merlin are themselves transcriptional targets of Yki, leading to an inhibitory feedback loop on the Hpo network.

In 2003, Paul Langton initiated a candidate-based screen in the laboratory to identify novel components of the Hpo pathway. At this time, Hpo, Sav, and Wts were the only known members of the pathway. He used the rough-eye phenotype caused by over-expression of Sav and Wts using the eye-specific *GMR (Glass Multimer Reporter)* promoter as a sensitised background to screen for novel components of the Hpo pathway. Candidates were selected based on a protein-protein interaction map of the *Drosophila* proteome generated from yeast 2-hybrid data (Curagen Inc.), and included

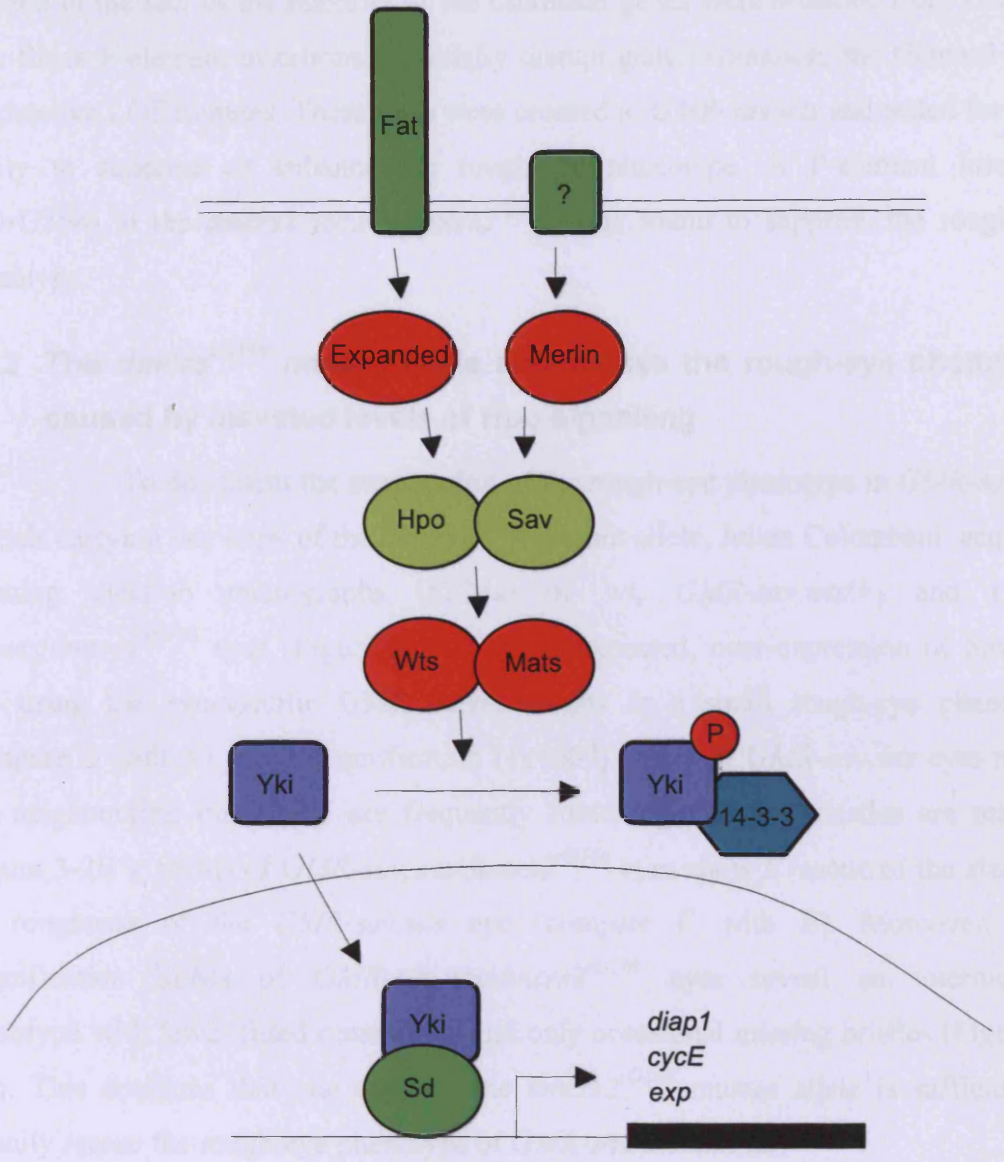

Figure 3-1: The Hippo signalling pathway. Fat, Expanded, and Merlin function upstream of Hippo (Hpo) to regulate its kinase activity. Hpo bound to Salvador (Sav) phophorylates and activates Warts (Wts) kinase, which in turn phosphorylates Yorkie (Yki). Phosphorylation of Yki results in its association with 14-3-3 and retention in the cytoplasm. Upon loss of Hpo signalling, Yki shuttles to the nucleus where it binds to the transcription factor Scalloped (Sd) and stimulates transcription of target genes like *diap1*, *cycE*, and *ex*. Figure adapted from (Zhang et al. 2008).

primary, secondary, and tertiary interactions with Hpo, Sav, and Wts. Thus, the aim was to use genetics to filter the large-scale two-hybrid data. Transposons (P-elements) inserted in the loci of the majority of the candidate genes were obtained from Genexel Inc.. Since P-element insertions potentially disrupt gene expression, the Genexel lines are putative LOF mutants. These lines were crossed to *GMR-sav,wts* and tested for their ability to suppress or enhance the rough-eye phenotype. A P-element insertion (*l(3)rG166*) in the *dmcrs2* locus (*dmcrs2^{rG166}*) was found to suppress the rough-eye phenotype.

3.1.2 The *dmcrs^{rG166}* mutant allele suppresses the rough-eye phenotype caused by elevated levels of Hpo signalling

To document the suppression of the rough-eye phenotype in *GMR-sav,wts* animals carrying one copy of the *dmcrs2^{rG166}* mutant allele, Julien Colombani, acquired scanning electron micrographs (SEMs) of wt, *GMR-sav,wts/+*, and *GMR-sav,wts/dmcrs2^{rG166}* eyes (Figure 3-2A-C'). As expected, over-expression of Sav and Wts using the eye-specific GMR driver results in a small rough-eye phenotype (compare B with A). High magnification (1x1000) SEMs of *GMR-sav,wts* eyes reveal that neighbouring ommatidia are frequently fused together and bristles are missing (Figure 3-2B'). SEMs of *GMR-sav,wts/dmcrs2^{rG166}* eyes show a rescue of the size and the roughness of the *GMR-sav,wts* eye (compare C with B). Moreover, high magnification SEMs of *GMR-sav,wts/dmcrs2^{rG166}* eyes reveal an intermediate phenotype with fewer fused ommatidia and only occasional missing bristles (Figure 3-2C'). This confirms that one copy of the *dmcrs2^{rG166}* mutant allele is sufficient to partially rescue the rough-eye phenotype of *GMR-sav,wts* animals.

3.1.3 The *l(3)rG166* P-element insertion is a *dmcrs2* LOF mutation

dMCRS2 is encoded by three exons, and the insertion point of the *l(3)rG166* P-element is predicted to be in the third exon. To verify the approximate position of the P-element, I carried out PCRs using primers that anneal to the inverted repeat of the P-element and approximately 500 bps upstream or downstream of the predicted insertion point (data not shown). Subsequent sequence analysis of the PCR products identified the exact insertion point. My analysis confirmed that the *l(3)rG166* P-element is inserted in the third exon and revealed that the exact insertion point is within a region that encodes the Forkhead associated (FHA) domain at the C-terminus

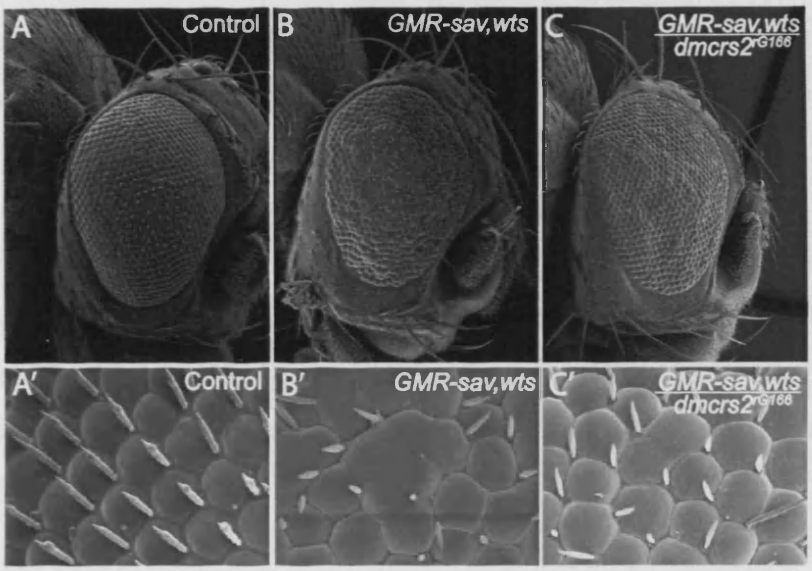

Figure 3-2: The rough-eye phenotype is suppressed in flies heterozygous for the *dmcrs2^{rG166}* mutation. (A-C') Scanning electron micrographs (SEMs) of adult control (A-A'), *GMRsav,wts* (B-B'), and *GMRsav,wts/dmcrs2^{rG166}* (C-C') eyes. GMR-driven expression of Sav and Wts in the eye results in a small rough-eye phenotype (compare B with A), which is suppressed in flies heterozygous for the *dmcrs2^{rG166}* mutation. (A') High magnification (1000x) SEM of a control eye show the regular arrangement of bristles. (B') High magnification (1000x) SEM of a *GMRsav,wts* eye reveals the fusion of neighbouring ommatidia and the loss of many bristles. (C') High magnification (1000x) SEM of a *GMRsav,wts/dmcrs2^{rG166}* eye show fewer fused ommatidia and only a few missing bristles (compare C' with B'). These images were generated by Julien Colombani.

of the dMCRS2 protein (Figure 3-3A). Moreover, Julien Colombani found that flies homozygous for the *mcrs2*^{rG166} mutation die as third instar larvae, but can be rescued to viability by GAL4/UAS-driven ubiquitous expression of dMCRS2. This demonstrates that dMCRS2 is an essential protein and that the *l(3)rG166* P-element insertion indeed represents a dMCRS2 LOF mutation.

3.1.4 dMCRS2 LOF does not affect CycE and DIAP1 protein levels or Yki activity

As previously mentioned, the Hpo signalling pathway negatively regulates the transcription of *diap1* and *cycE* to promote apoptosis and cell cycle exit (Figure 3-1). Thus, inactivation of the Hpo pathway results in derepression of Yki activity and increased levels of DIAP1 and CycE (Pantalacci et al., 2003). The ability of the *dmcrs2*^{rG166} mutant allele to suppress the rough-eye phenotype caused by hyper-activation of the Hpo signalling pathway suggests that dMCRS2 might have a pro-apoptotic function downstream of Sav and Wts. To test this idea, Julien Colombani used the FLP/FRT system to generate mitotic clones of *dmcrs2*^{rG166} mutant tissue in eye imaginal discs (the larval precursor of the adult eye) (Figure 3-3B-C'). By inducing FLP/FRT-mediated recombination in early eye-imaginal discs, it is possible to generate homozygous mutant clones (no GFP), corresponding wild-type twin-spots (two copies of GFP), while heterozygous tissue has one copy of GFP. Only small *dmcrs2*^{rG166} mutant clones could be recovered in heterozygous animals, indicating that dMCRS2 is required for normal growth and proliferation (Figures 3-3B, C). Staining of discs with anti-DIAP1 (Figure 3-3B') or anti-CycE (Figure 3-3C') antibodies revealed that DIAP1 and CycE protein levels are not affected in *dmcrs2*^{rG166} mutant clones. This suggests that dMCRS2 does not function downstream of Sav and Wts to regulate Yki activity. To confirm this observation, I studied the effect of dMCRS2 depletion on Yki activity in *Drosophila* S2 cells using previously established reporter assay as a read-out for Yki activity (Huang et al., 2005) (Figure 3-3D). In brief, Yki fused to the DNA binding domain (DB) of the yeast Gal4 transcription factor (Gal4DB-Yki) is a potent transcriptional activator, and Yki activity can be assayed by co-transfection of Gal4DB-Yki with a Gal4-responsive reporter (UAS-luciferase). Thus, transfection of S2 cells with Gal4DB-Yki results in a robust induction of luciferase activity relative to cells transfected with the DB domain alone (Huang et al., 2005). As previously reported, I found that the transcriptional activity of Gal4DB-Yki is repressed upon co-expression

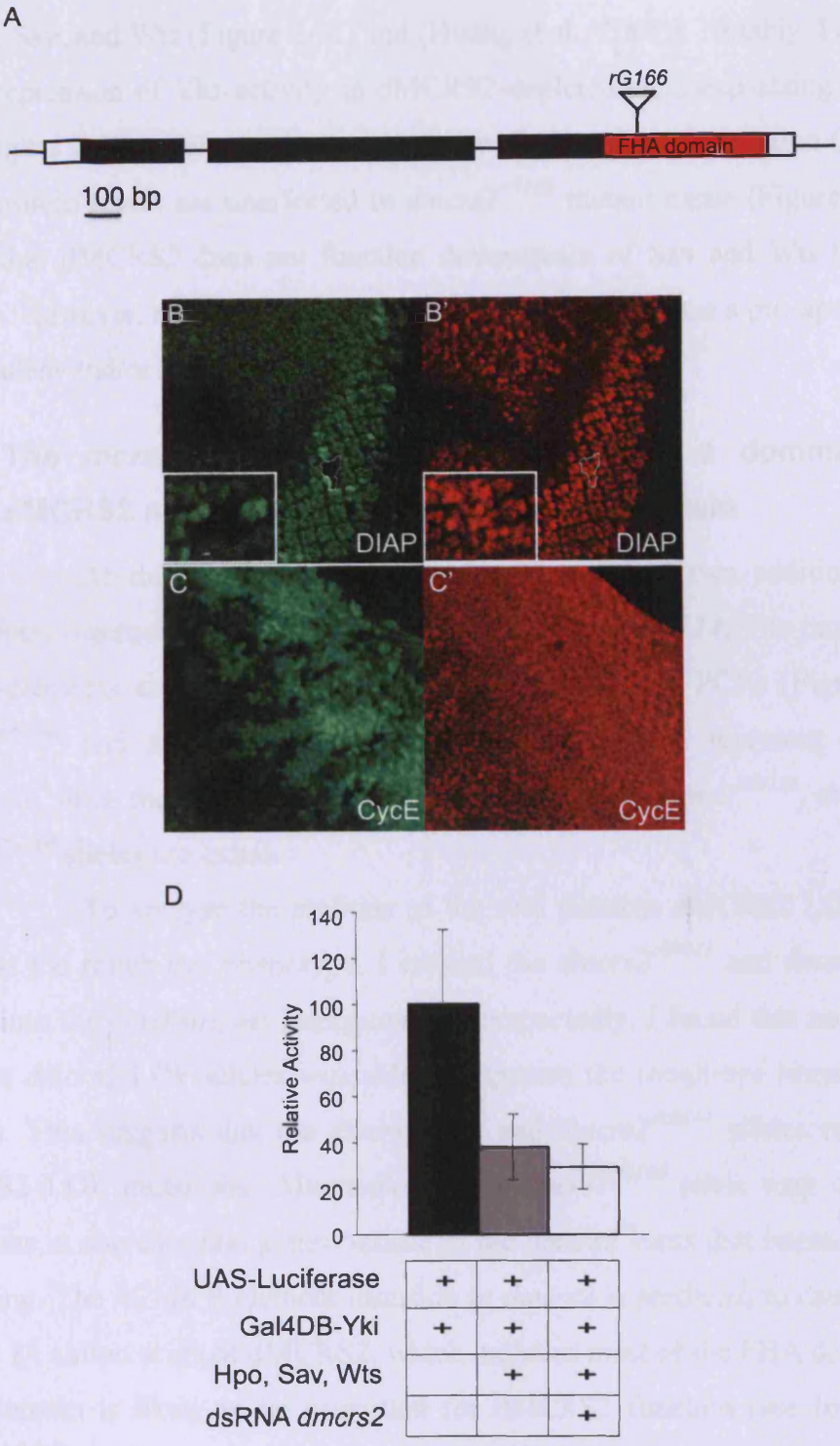

Figure 3-3: dMCRS2 LOF does not affect DIAP and CycE protein levels or Yki activity. (A) Schematic of the *dmcrs2* locus. dMCRS2 is encoded by three exons (indicated in black). The C-terminal part of the third exon encodes a Forkhead Associated (FHA) domain (indicated in red). The position of the *rG166* P-element inserted in *dmcrs2* is indicated. (B-C') High magnification of an area of the eye imaginal disc from third instar larvae. The posterior is to the right. Mitotic clones of $dmcrs2^{rG166}$ mutant tissue marked by the absense of GFP (B, C) and stained with the anti-DIAP1 (B') and anti-CycE (C') antibodies. Close up view of $dmcrs2^{rG166}$ mutant clone shows that DIAP1 levels are unchanged in the $dmcrs2^{rG166}$ mutant tissue (B-B'). (D) RNAi-mediated depletion of dMCRS2 protein levels does not derepress the loss of Gal4DB-Yki activity caused by Hpo, Sav, and Lats gain of function. S2 cells were treated with dsRNA targeting *eGFP* (black and grey bars) or *dmcrs2* (white bar). The next day, cells were transfected the indicated plasmids and 3 days later, luciferase acitivities were measured and relative activity levels were calculated.

of Hpo, Sav, and Wts (Figure 3-3D and (Huang et al., 2005)). Notably, I did not observe any derepression of Yki activity in dMCRS2-depleted cells expressing Hpo, Sav, and Wts (Figure 3-3D). This result is consistent with the initial observation that DIAP1 and CycE protein levels are unaffected in *dmcrs2*^{rG166} mutant tissue (Figure 3-3B-C'), and shows that dMCRS2 does not function downstream of Sav and Wts to regulate Yki activity. However, my results do not rule out that dMCRS2 has a pro-apoptotic function independent and/or further downstream of Yki.

3.1.5 The *mcrs2*^{rG166} allele is likely to encode a dominant negative dMCRS2 mutant protein lacking the FHA domain

At this time during the project, I acquired two additional transposon (PiggyBac) insertions in the *dmcrs2* locus, *c07041* and *c00114*. The insertion points of both P-elements at the 5'end of exon 2 were verified by PCRs (Figure 3-4A). The *dmcrs2*^{c07041} and *dmcrs2*^{c00114} mutant alleles are likely to represent dMCRS2 LOF mutations, since transheterozygous combinations of the *dmcrs2*^{c00114}, *dmcrs2*^{c07041}, and *dmcrs2*^{rG166} alleles are lethal.

To analyse the abilities of the two putative dMCRS2 LOF mutations to suppress the rough-eye phenotype, I crossed the *dmcrs2*^{c07041} and *dmcrs2*^{c00114} mutant alleles into the *GMRsav,wts* background. Unexpectedly, I found that neither of the two putative *dmcrs2* LOF alleles was able to suppress the rough-eye phenotype (data not shown). This suggests that the *dmcrs2*^{c07041} and *dmcrs2*^{c00114} alleles represent weaker dMCRS2 LOF mutations. Alternatively, the *dmcrs2*^{rG166} allele may carry additional mutations in non-essential genes outside of the *dmcrs2* locus that interact with Sav/Wts signalling. The *rG166* P-element insertion in *dmcrs2* is predicted to cause a deletion of the last 84 amino acids of dMCRS2, which includes most of the FHA domain. Since the FHA domain is likely to be important for dMCRS2 function (see Introduction), the *dmcrs2*^{rG166} mutant allele could potentially encode a dominant negative dMCRS2 mutant protein. In contrast, the *c07041* and *c00114* P-element insertions are predicted to cause a deletion of approximately 84% of the dMCRS2 protein and are more likely to represent null mutations. To study the nature of the *dmcrs2*^{c00114}, *dmcrs2*^{c07041}, and *dmcrs2*^{rG166} mutations in more details, I generated an antibody that recognises a stretch of amino acids in the central part of the dMCRS2 protein. I used the FLP/FRT system to generate mitotic clones of *dmcrs2*^{c00114}, *dmcrs2*^{c07041}, and *dmcrs2*^{rG166} mutant tissue in eye imaginal discs. Consistent with previous results (Figure 3B-C'), I found that only

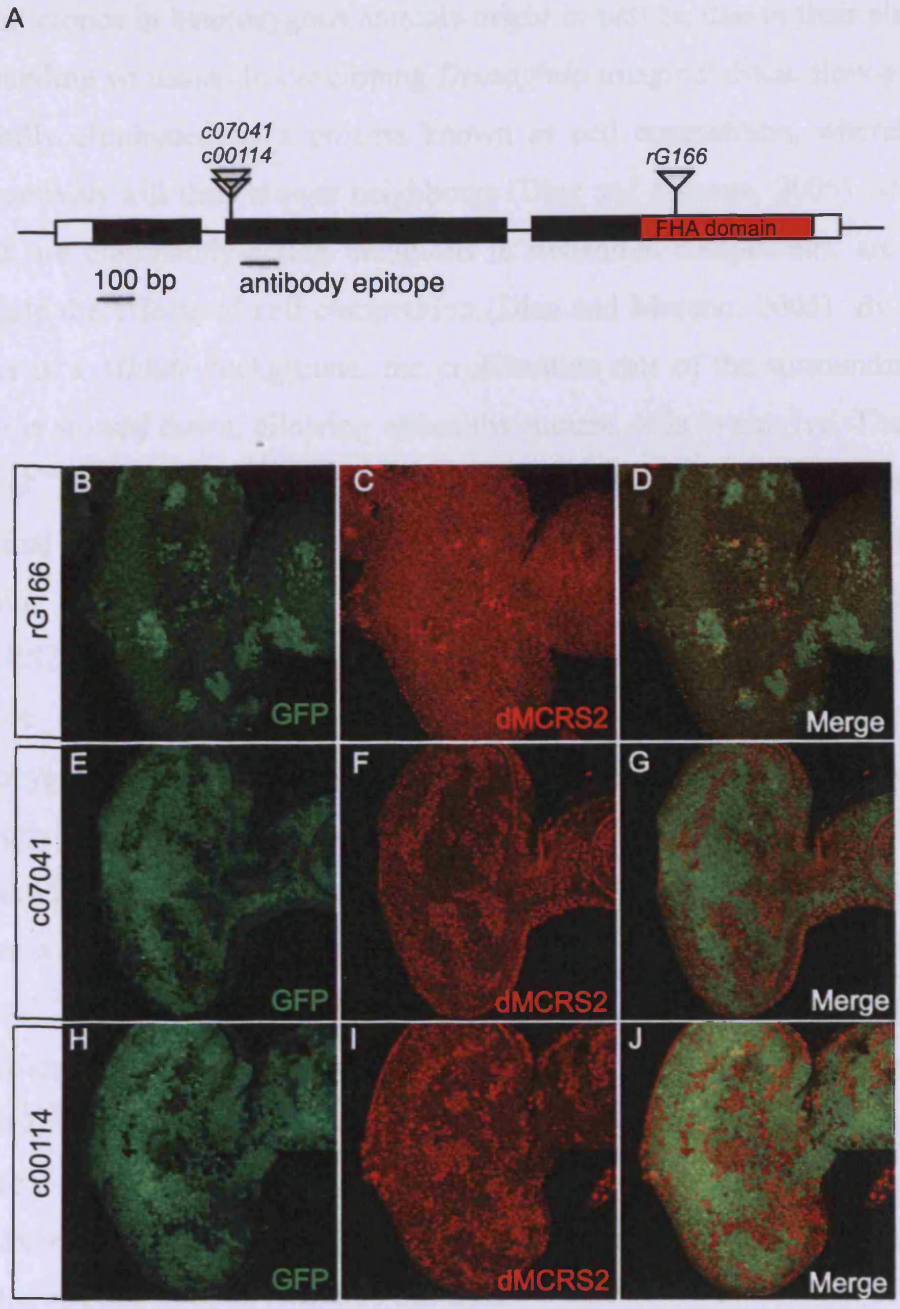

Figure 3-4: The *dmcrs2*^{rG166} allele is likely to encode a truncated dMCRS2 product. (A) Schematic of the *dmcrs2* locus. The positions of the c07041, c00114, and *rG166* P-elements inserted in *dmcrs2* are indicated. (B-J) dMCRS2 protein levels are significantly reduced mitotic clones of *dmcrs2*^{c00114} (B-D) and *dmcrs2*^{c07041} (E-G), but not *dmcrs2*^{rG166} (H-I) mutant tissue. Eye imaginal discs from third instar larvae. Posterior is to the left. Mitotic clones of *dmcrs2*^{rG166} (B-D), *dmcrs2*^{c07041} (E-G), and *dmcrs2*^{c00114} (H-I) mutant tissue marked by two copies of GFP (B, E, H) and stained with the anti-dMCRS2 antibody (C, F, I).

small *dmcrs2*^{c00114}, *dmcrs2*^{c07041}, and *dmcrs2*^{rG166} mutant clones could be recovered in heterozygous animals (data not shown). The difficulty of obtaining dMCRS2 LOF mutant clones in heterozygous animals might in part be due to their elimination by the surrounding wt tissue. In developing *Drosophila* imaginal discs, slow-growing cells are generally eliminated by a process known as cell competition, whereby fast-growing cells actively kill their slower neighbours (Diaz and Moreno, 2005). *Minute* mutations, which are dominantly-acting mutations in ribosomal components, are widely used to alleviate the effects of cell competition (Diaz and Moreno, 2005). By creating mutant clones in a *Minute* background, the proliferation rate of the surrounding heterozygous tissue is slowed down, allowing unhealthy mutant cells to survive. Thus, GFP-labelled *dmcrs2*^{c00114}, *dmcrs2*^{c07041}, and *dmcrs2*^{rG166} mutant clones were generated in eye imaginal discs that are heterozygous for a mutation in a *Minute* gene (Figure 3-4B-J). Staining discs with the anti-dMCRS2 antibody revealed a significant reduction in dMCRS2 protein levels in mitotic clones of *dmcrs2*^{c00114} and *dmcrs2*^{c07041} mutant tissue (Figure 3-4F, I). In contrast, I observed no reduction in dMCRS2 protein levels in homozygous *dmcrs2*^{rG166} mutant clones (Figure 3-4B). Since the anti-dMCRS2 antibody recognises a stretch of amino acids encoded by a region 5' to the *l(3)rG166* P-element insertion point (amino acids 119-133), this shows that the *dmcrs2*^{rG166} mutation causes a truncation rather than an ablation of the *dmcrs2*-encoded product. Thus, the *dmcrs2*^{rG166} mutation could potentially behave as a dominant negative mutation. Consistent with this idea, *dmcrs2*^{rG166} mutant tissue grows and proliferates slower than *dmcrs2*^{c00114} and *dmcrs2*^{c07041} mutant tissue (compare the sizes of GFP-labelled clones in Figure 3-4B with those in 4E and 4H). This might explain the difference in the ability of the *dmcrs2*^{rG166} versus the *dmcrs2*^{c00114} and *dmcrs2*^{c07041} mutant alleles to rescue the rough-eye phenotype in *GMRsav,wts* flies.

3.1.6 dMCRS2 might not be physically linked with the Hpo pathway

According to the data derived from the *Drosophila* genome-wide yeast 2-hybrid screen (Curagen Inc.), dMCRS2 is predicted to form a tertiary interaction with Hpo via its primary and secondary interactions with the *CG1017*-encoded product and Rep2, respectively (Figure 3-5A). To verify these interactions, recombinant Rep2-HA, CG1017-myc and dMCRS2-Flag proteins were expressed in *Drosophila* cells, and the predicted interactions were tested by co-immunoprecipitation experiments (Figure 3-5B-C). I found that whereas a small fraction of dMCRS2-Flag protein was recovered in

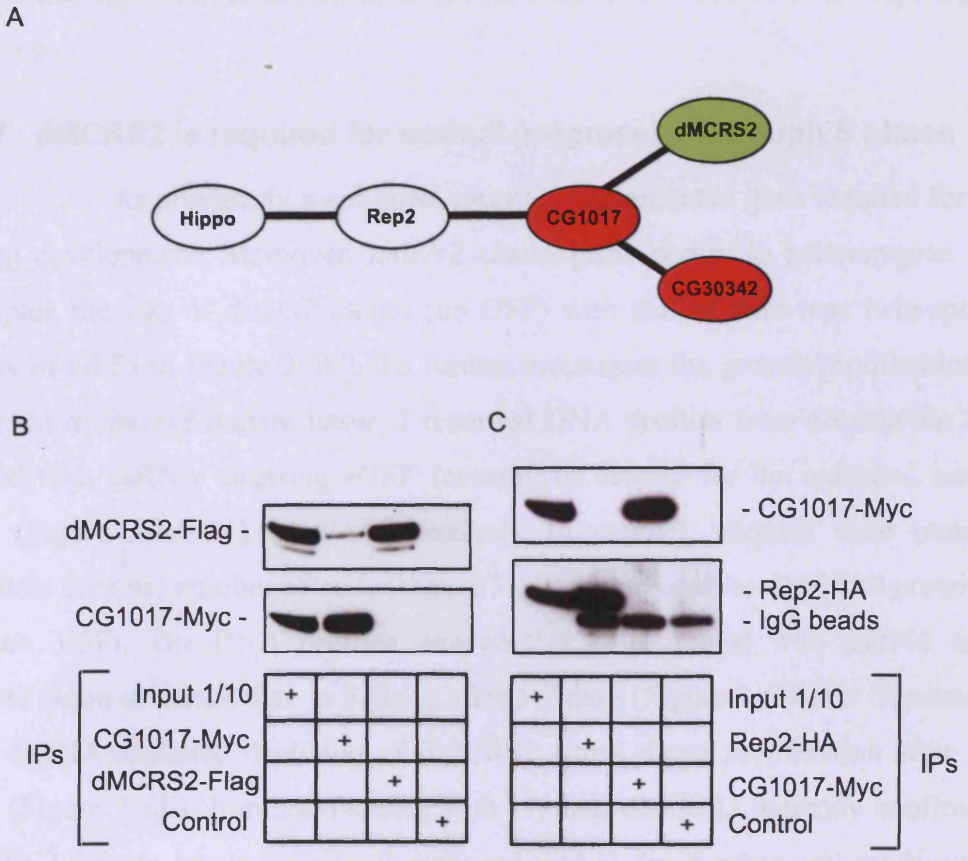

Figure 3-5: dMCRS2 might not be physically linked with Hpo pathway. (A) Schematic of protein-protein interactions based on the data derived from the genome-wide yeast 2-hybrid screen in *Drosophila* (Curagen Inc.). (B) Small amounts of dMCRS2 co-immunoprecipitates with the CG1017-encoded protein. dMCRS2-Flag, CG1017-Myc, and control immunoprecipitates were blotted for the presense of dMCRS2-Flag using an anti-Flag antibody (top panel) and CG1017-Myc using an anti-Myc antibody (bottom panel). (C) CG1017-Myc does not co-immunoprecipiate with Rep2-HA. CG1017-Myc, Rep2-HA and control immunoprecipitates were blotted for the presence of CG1017-Myc using an anti-Myc antibody (top panel) and Rep2-HA using an anti-HA antibody (bottom panel).

the CG1017-Myc precipitate (Figure 3-5B, top panel), no CG1017-Myc protein could be detected in the dMCRS2-Flag precipitate (Figure 3-5B, bottom panel) suggesting that the association of dMCRS2-Flag with CG1017-Myc is rather weak. Moreover, the *CG1017*-encoded product did not co-immunoprecipitate with Rep2-HA (Figure 3-5C). Thus, my co-immunoprecipitation data do not provide solid evidence for the predicted tertiary interaction between dMCRS2 and Hpo. Given the difficulties of interpreting the genetic interaction between dMCRS2 LOF and Sav/Wts gain of function alleles and the lack of evidence for a physical link between dMCRS2 and the Hpo pathway, I decided to continue my characterisation of dMCRS2 outside the context of the Hpo signalling pathway.

3.1.7 dMCRS2 is required for normal progression through S phase

As previously mentioned, *dmcrs2* is an essential gene required for growth during development. Moreover, *dmcrs2* clones grow poorly in heterozygous animals (compare the size of *dmcrs2* clones (no GFP) with that of wild-type twin-spots (two copies of GFP) in Figure 3-3C). To further investigate the growth/proliferation defect observed in *dmcrs2* mutant tissue, I recorded DNA profiles from *Drosophila* S2 cells treated with dsRNA targeting *eGFP* (control) or *dmcrs2* for the indicated number of days (Figure 3-6A-D') by FACS analysis. In parallel, aliquots were removed to calculate the total number of cells (Figure 3-6E) and to analyse dMCRS2 protein levels (Figure 3-6F). The DNA profiles showed that cells treated with dsRNA targeting *dmcrs2* begin to accumulate in S phase after 5-7 days (Figure 3-6B-D'). Consistent with this, dsRNA-mediated depletion of dMCRS2 slows down proliferation after about 5 days (Figure 3-6E). Immuno-blotting with my anti-dMCRS2 antibody confirmed that dMCRS2 protein levels are significantly reduced at day 6 when cell proliferation has slowed down and cells have started accumulating in S phase (Figure 3-6F). Thus, dMCRS2 is required for normal S phase progression and for proliferation and growth during development.

3.1.7.1 dMCRS2-depleted cells spend longer time in S phase

DNA profiles offer a snapshot of the percentage of cells in a particular phase of the cell cycle at a given time point, but do not provide any information regarding the kinetics of cell cycle progression. A BrdU pulse can be used to specifically label S-phase cells within an asynchronous growing population of S2 cells,

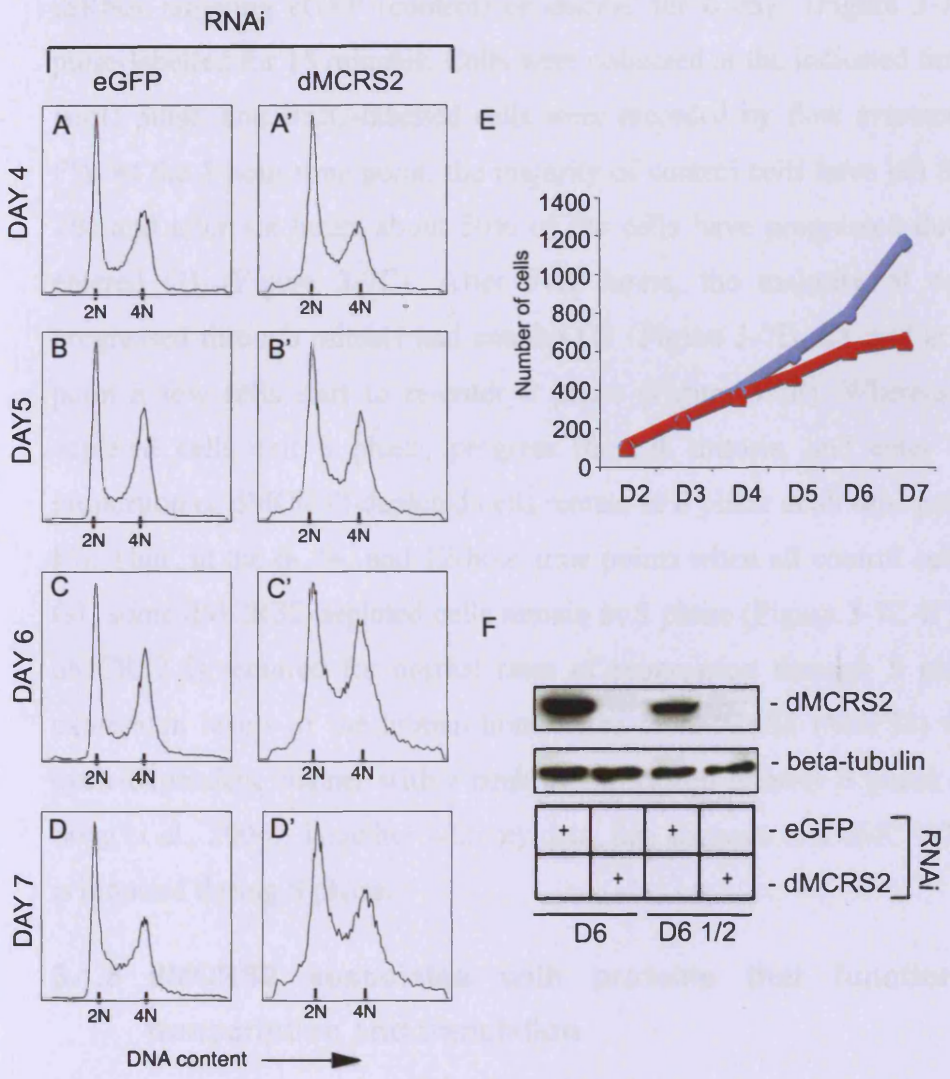

Figure 3-6: dMCRS2 is required for proliferation and normal progression through S phase. (A-D') Cells depleted of dMCRS2 accumulate in S phase. S2 cells were treated with dsRNA targeting *GFP* (control) or *dmcrs2* for the indicated number of days. Cells were fixed, stained with propidium iodide, and analysed by flow cytometry. The peaks corresponding to the G1 (2N) and G2/M (4N) populations are indicated on the X-axis. (E-F) Cells were counted and dMCRS2 protein levels measured in a parallel set-up. (E) Proliferation of dMCRS2-depleted cells (red) slows down after 5-6 days. Control treated (blue) or dMCRS2-depleted (red) cells were counted once a day from day 2-7 (D2-D7). (F) Immuno-blotting confirms that dMCRS2 protein levels are reduced in cells in S2 cells treated with dsRNA corresponding to *dmcrs2* after 6-61/2 days. Cell extracts prepared from S2 cells treated with dsRNA corresponding to *GFP* (control) or *dmcrs2* for 6 and 61/2 days and immuno-blotted for dMCRS2. Anti-β-tubulin was used as a loading control.

and BrdU-positive cells can then be followed by flow cytometry through the different phases of the cell cycle. This provides a method for estimating the rate at which cells progress through each phase of the cell cycle. To study the kinetics of dMCRS2-depleted cells as they progress through the cell cycle, an aliquot of cells treated with dsRNA targeting *eGFP* (control) or *dmcrs2* for 6 days (Figure 3-7C-C') was BrdU pulse-labelled for 15 minutes. Cells were collected at the indicated time points after the BrdU pulse, and BrdU-labelled cells were recorded by flow cytometry (Figure 3-7A-F'). At the 3-hour time point, the majority of control cells have left S phase (Figure 3-7B) and after six hours about 50% of the cells have progressed through mitosis and entered G1 (Figure 3-7C). After 9-12 hours, the majority of control cells have progressed through mitosis and entered G1 (Figure 3-7D, E), and at the 15-hour time point a few cells start to re-enter S phase (Figure 3-7F). Whereas some dMCRS2-depleted cells exit S phase, progress through mitosis, and enter G1, a significant proportion of dMCRS2-depleted cells remain in S phase at all time point (Figure 3-7A'-F'). Thus, at the 6-, 9-, and 12-hour time points when all control cells are in G2/M or G1, some dMCRS2-depleted cells remain in S phase (Figure 3-7C-E'). This shows that dMCRS2 is required for normal rates of progression through S phase. Interestingly, expression levels of the human homologue of dMCRS2 (MSP58) fluctuate in a cell cycle-dependent manner with a peak of expression in early S phase (Ren et al., 1998; Song et al., 2004). Together with my data, this suggests that dMCRS2/MSP58 function is required during S phase.

3.1.8 dMCRS2 associates with proteins that function in RNAP II transcription and translation

As an approach to place dMCRS2 in a functional context, I next sought to identify proteins that form a complex with tandem affinity-purified Glutionine S transferase (GST)-Tobacco etch virus (TEV)-Calmodulin binding peptide (CBP)-tagged dMCRS2 (GTC-dMCRS2) protein. For this purpose, I generated S2 cells stably expressing GTC-dMCRS2 under the control of the inducible methallothionein (MT) promoter (Figure 3-8A). The tandem affinity purification (TAP) technique, which was originally developed in yeast and later adapted to metazoan cells, involves two sequential purifications steps and aims to minimise contamination by abundant or "sticky" proteins in the final eluate. In the first purification step, GTC-dMCRS2 is purified on glutathione-sepharose beads and eluted by cleavage with TEV protease. In

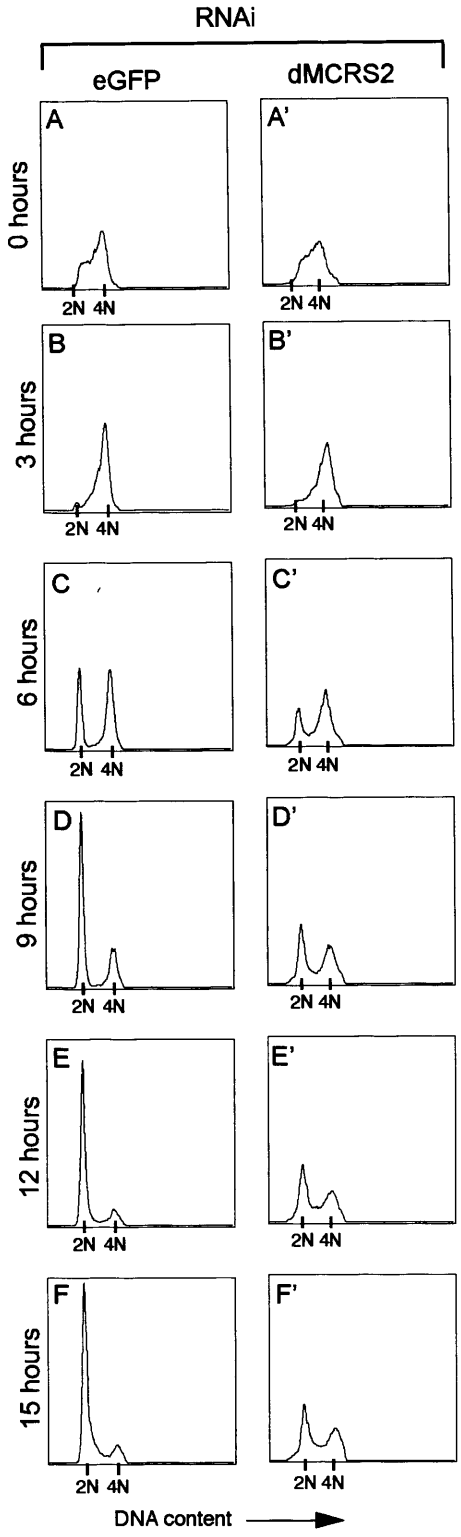

Figure 3-7: dMCRS2-depleted cells progress through S phase with slower kinetics. (A-F') S2 cells were treated with dsRNA targeting *GFP* (control, A-F) or *dmcrs2* (A'-F') for 6 days. Cells were reseeded at a density of $1x10^6$ cells/ml and pulse-labelled with BrdU for 15 min. Cells were fixed, stained with propidium iodide, and analysed by flow cytometry at the indicated time points after the BrdU pulse. The peaks corresponding to the G1 (2N) and G2/M (4N) populations are indicated on the X-axis.

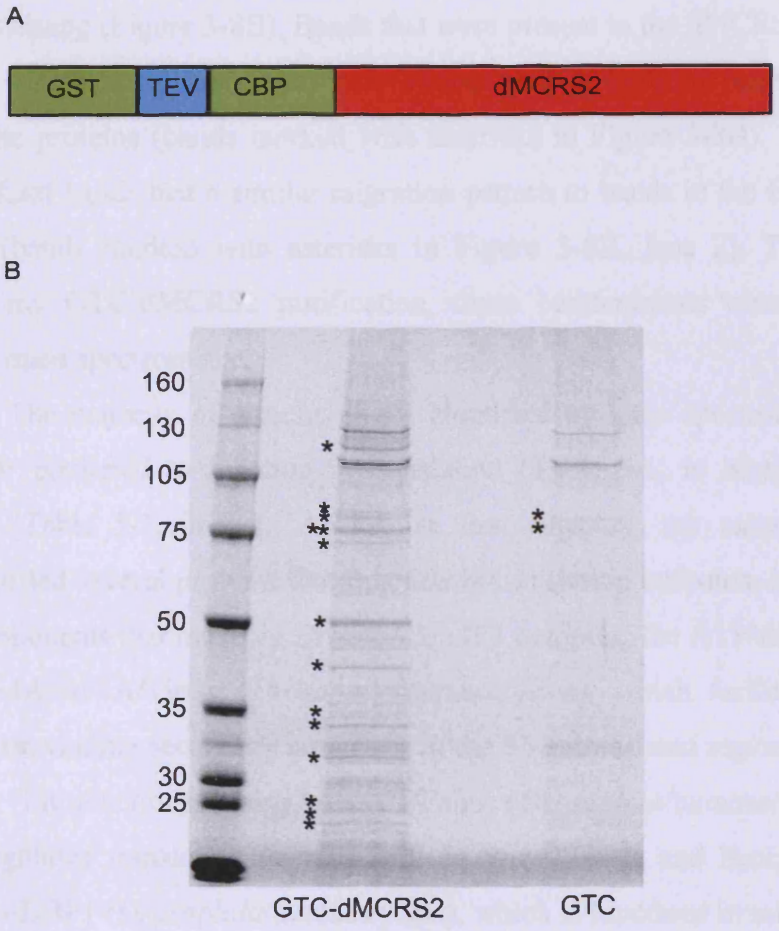

Figure 3-8: dMCRS2 associates with several proteins that function in transcription and translation. (A) Schematic of GTC-dMCRS2. (B) To identify dMCRS2-associated proteins, a two-step purification was performed from approximately $1x10^{10}$ S2 cells expressing GTC-dMCRS2 or the GTC-tag alone. The final eluates were resolved on a 4-12% Nupage Bis-Tris gel and stained with Brilliant Blue G-colloidal concentrate. Visible bands (indicated by asterisks) were excised and identified by MALDI-TOF mass spectrometry. The band corresponding to dMCRS2 is indicated by two asterisks.

the second step, cleaved CBP-dMCRS2 and any associated proteins are bound to calmodulin beads, washed and eluted (see Materials and Methods). I carried out large-scale purification from approximately $1x10^{10}$ S2 cells expressing GTC-dMRS2 or the GTC tag alone (control). The samples from the purification procedures were subjected to SDS-PAGE, and individual protein bands were visualised by blue G-colloidal concentrate staining (Figure 3-8B). Bands that were present in the dMCRS2 sample, but absent in the control sample, were carefully excised and subjected to mass spectrometry to identify the proteins (bands marked with asterisks in Figure 3-8B). In the control sample two faint bands had a similar migration pattern to bands in the GTC-dMCRS2 purification (bands marked with asterisks in Figure 3-8B, lane 2). To avoid false positives in my GTC-dMCRS2 purification, those contaminants were cut out and identified by mass spectrometry.

The majority of proteins that I identified by mass spectrometry analysis are known or predicted to function in translation (Table 3-1, in blue) or RNAP II transcription (Table 3-1, in red). As for the first category, my mass spectrometry analysis identified several proteins that function in translation initiation, including 5 out of the 13 components that make up *Drosophila* eIF3 complex, the ATP-dependent RNA helicase eIF-4A/eIF4A/Tip2p (*Drosophila*/humans/yeast), which facilitates 48S PIC assembly by unwinding secondary structures in the 5'-untranslated region (UTR) of the mRNA (see Introduction), Pabp/PABPC1/Pabp (*Drosophila*/humans/yeast), which positively regulates translation *in vitro* and *in vivo* (Tarun and Sachs, 1995), and Belle/DHX15/DBP1 (*Drosophila*/humans/yeast), which is functions in mRNA scanning in yeast (Berthelot et al., 2004) (Figure 3-9A). In addition, several small and large ribosomal subunit proteins co-purified with GTC-dMCRS2 (Table 3-1, in blue). This suggests that dMCRS2 might have a function in translation initiation.

As for the second category, my mass spectrometry analysis identified both subunits of the GTF, TFIIF, the FACT component SSRP/SSRP1/Pob3p (*Drosophila*/humans/yeast), Pitslre/ $Cdk11^{p110}$ (*Drosophila*/humans), CKIIα/CK2α/Cka2p (*Drosophila*/humans/yeast), and Psr/JMJD6 (*Drosophila*/humans). Interestingly, many of these proteins have previously been reported to co-purify with each other and with RNAP II in humans (Figure 3-9B). Thus, $Cdk11^{p110}$ has been found to associate with both subunits of TFIIF, CK2, the FACT complex, and hyper-phosphorylated RNAP II (Trembley et al., 2002), and CK2 has been isolated in complex with TFIIF, $Cdk11^{p110}$, RNAP II, and SSRP1, all of which it is capable of

Table 3-1

ID (Drosophila/Humans/Yeast[1])	Predicted function
dMCRS2/p58	Chromatin remodeling/RNAP I transcription
Pitslre/Cdk11^{p110}	Transcription/splicing
TFIIFα/GTF2F1/Rap74	Transcription
TFIIFβ/GTFII2F2/Rap30	Transcription
SSRP/SSRP1/Pob3p	Chromatin remodeling/transcription regulation
Psr/JMJD6	Chromatin remodeling/transcription regulation
CKIIα/CK2α/Cka2p	Survival/Transcription
eIF3-S9/eIF3S9/Prt1	Translation initiation
eIF3-S8/eIF3S8/Nip1	Translation initiation
Int6/eIF3S6	Translation initiation/nonsense mediated decay
eIF3-S2/eIF3S2/Tif34	Translation initiation
eIF3-S12/eIF3S12	Translation initiation
eIF-4A/eIF4A2/Tif2p	Translation initiation
Pabp/PABPC1/pabp	Translation initiation
Belle/ DHX15/DBP1	mRNA scanning
RpS3/RpS3/RpS3	Translation
RpS4/RpS4/RpS4	Translation
RpS6/RpS6/RpS6Bp	Translation
RpS7/RpS7/RpS7Ap	Translation
RpS9/RpS9/RpS9Ap	Translation
RpLP0/RpLP0/Rpp0p	Translation
RpL4/RpL4/RpL4	Translation
RpL5/RpL5/RpL5	Translation
RpL13A/RpL13A/RpL13A	Translation
RpL17/RpL23/RpL17A	Translation
RpL18A/RpL18A/RpL18A	Translation
RpL23A/RpL23/RpL25	Translation
CBP80/NCBP1/STO1	RNA cap binding/nonsense mediated decay
CG8611/DDX31/DBP7	rRNA processing
Pit/DDX18/Has1p	rRNA processing
B52/Srp55	Splicing/Alternative splicing
Hfp/PUF60	Splicing/Alternative splicing
Pasha/DGCR8	miRNA biogenesis
CG7843/ARS2	Unknown
CG4887/RBM10	Unknown
Dmorc2/horc2L/Orc2p	DNA replication
RFC40/RFC2/RFC4	DNA replication
NCD/KIFC1/KAR3p	Chromosome segregation
CG6904/glycogen synthase 1/UDP-glucose-starch glucosyltransferase	Glycogen synthesis
Uch-L3/Uch-L5/Yuh1p	Deubiquitination

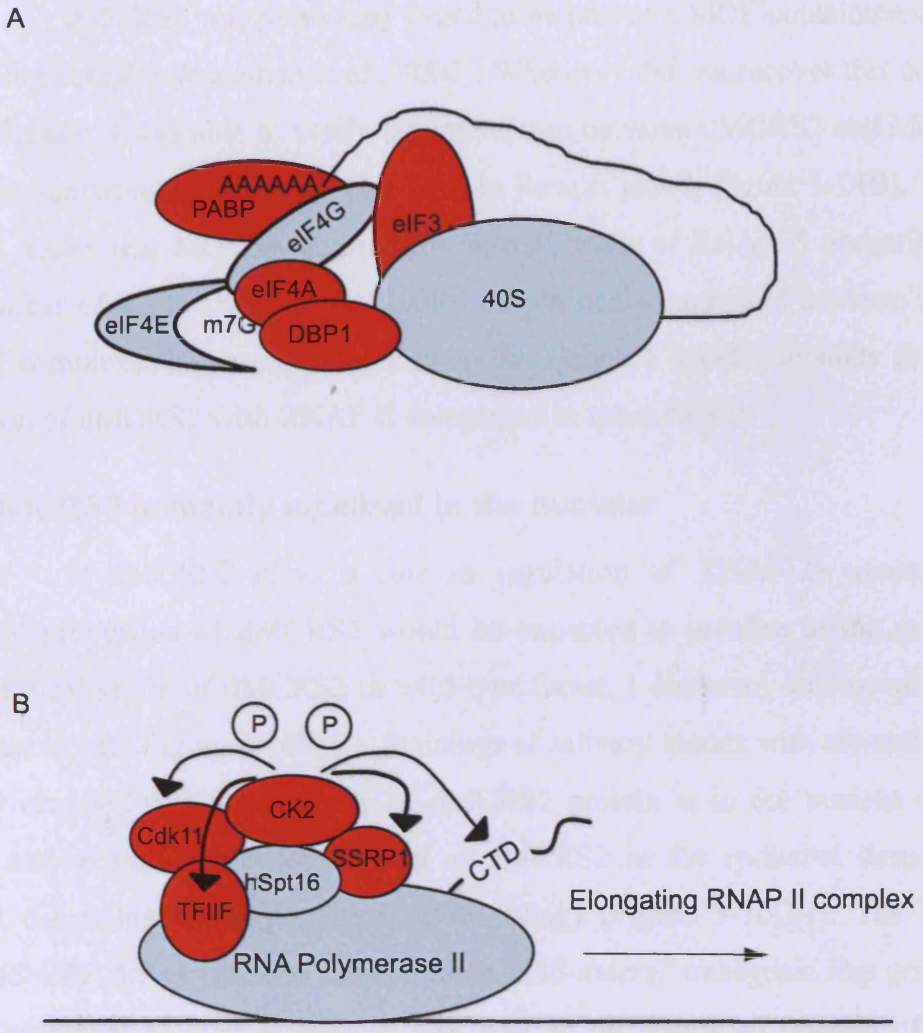

Figure 3-9: Predicted protein-protein interactions among two functional groups of proteins that co-purify with GTC-dMCRS2. (A-B) Schematics of predicted protein-protein interactions among proteins purified in complex with GTC-dMCRS2 based on previous reports in the literature. (A) Proteins purifed in complex with dMCRS2, which are predicted to function in translation initiation. (B) Proteins purifed in complex with dMCRS2, which are predicted to be associated with elongating RNAP II.

phosphorylating (Egyhazi et al., 1999; Li et al., 2005b; Payne et al., 1989; Trembley et al., 2003). The identification of several proteins in my GTC-dMCRS2 purification, which have known or predicted functions in RNAP II transcription, suggests that dMCRS2 might also have a function in regulating RNAP II transcription.

dMCRS2 was previously found to be part of a MOF-containing chromatin remodelling complex (Mendjan et al., 2006). Whereas I did not recover this complex in my purification, I was able to verify the interaction between dMCRS2 and MOF in co-immunoprecipitation experiments (see later in Results part I, Figure 3-14B). Though it has been shown that MOF is required for normal levels of RNAP II transcription of a large number of genes (Kind et al., 2008), no physical connection between MOF and RNAP II complexes has been established so far. Hence, I decided to study the putative association of dMCRS2 with RNAP II complexes in more details.

3.1.9 dMCRS2 is mainly localised in the nucleus

If dMCRS2 plays a role in regulation of RNAP II transcription, a significant proportion of dMCRS2 would be expected to localise to the nucleus. To study the localisation of dMCRS2 in wild-type tissue, I dissected salivary glands from third instar larvae (Figure 3-10A-C). Stainings of salivary glands with my anti-dMCRS2 antibody revealed that the majority of dMCRS2 protein is in the nucleus (Figure 3-10A). I also examined the localisation of dMCRS2 in the epithelial tissue of wing imaginal discs (the larval precursor of the wing) (Figure 3-10D-I). The *engrailed-Gal4,UAS-GFP* driver line was crossed to an *UAS-dmcrs2* transgenic line generated by Julien Colombani to over-express in dMCRS2 in the engrailed domain of the wing (marked by GFP in E and H). Stainings of wing imaginal discs from *engrailed-Gal4,GFP/UAS-dmcrs2* third instar larvae with my anti-dMCRS2 antibody confirmed that most dMCRS2 co-localises with nuclear GFP in the engrailed domain of the wing (compare Figure 3-10G with Figure 3-10H). These data show that the *in vivo* localisation of dMCRS2 is mostly nuclear and are consistent with a possible function of dMCRS2 in regulation of RNAP II transcription.

3.1.10 The dMCRS2 FHA domain is required for its association with Cdk11

Pitslre/Cdk11^{p110} (*Drosophila*/humans), which I recovered in my GTC-dMCRS2 purification, associates with hyper-phosphorylated RNAP II and is required for RNAP II transcription in humans (Trembley et al., 2002). To study the putative role

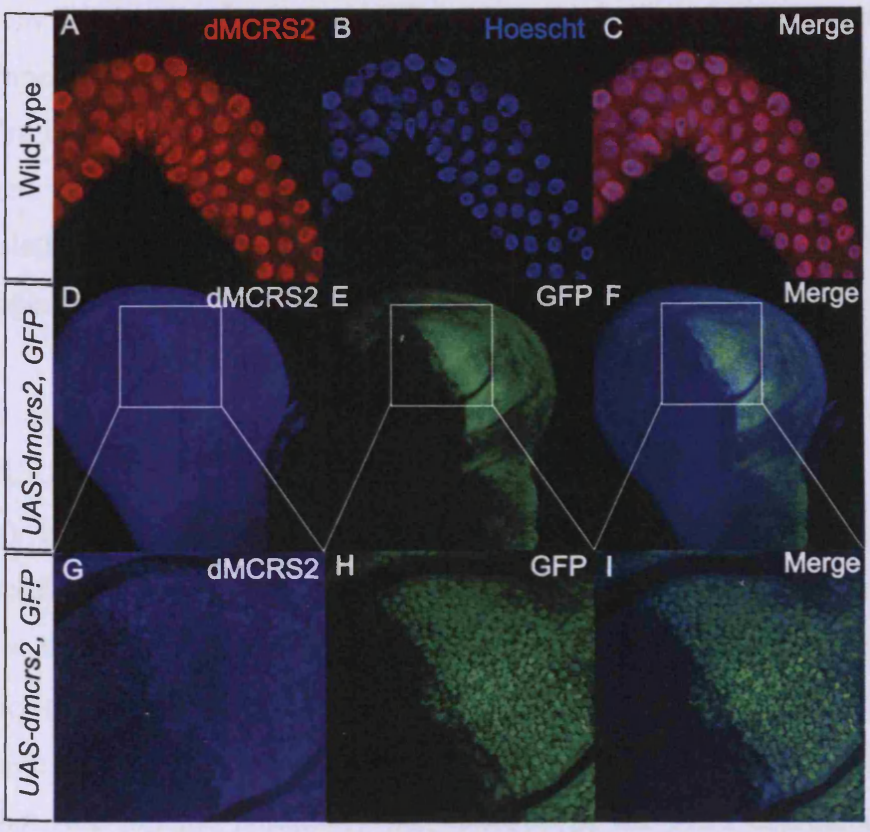

Figure 3-10: dMCRS2 is a nuclear protein. (A-C) Wild-type salivary glands from third instar larvae stained with the anti-dMCRS2 antibody in red (A) or a nuclear dye in blue (B). dMCRS2 is mainly localised in the nucleus. (D-I) Wing imaginal discs from third instar larvae. Posterior is to the right. (G-I) Close up view of area inside white square in D-F. Expression of dMCRS2 in the posterior compartment of the wing using the engrailed-Gal4 driver (marked by GFP in E and H). Wing imaginal discs stained with the anti-dMCRS2 antibody reveals that a significant fraction of dMCRS2 protein is in the nucleus (D, G).

of dMCRS2 in RNAP II transcription in more details, I initially sought to verify the association of dMCRS2 with Pitslre. I expressed recombinant HA-Pitslre protein in S2 cells, and tested its ability to co-immunoprecipitate with endogenous dMCRS2 (Figure 3-11A). Immuno-blotting of HA-Pitslre, dMCRS2, and control (anti-V5) precipitates with an anti-HA antibody revealed the presence of HA-Pitslre in the dMCRS2 precipitate (Figure 3-11A, top panel). In contrast, I was not able to detect any dMCRS2 protein in the HA-Pitslre precipitate (Figure 3-11A, bottom panel). One possible explanation for this is that binding of an antibody to the N-terminal HA-tag in HA-Pitslre interferes with its association with dMCRS2. Attempts to generate C-terminally tagged Pitslre were unsuccessful, suggesting that the C-terminus might be post-translational modified. Nevertheless, I was able to show that HA-Pitslre associates with endogenous dMCRS2.

I next wanted to analyse which part of dMCRS2 mediates its association with HA-Pitslre. For this purpose I generated full-length Flag-tagged dMCRS2 (dMCRS2-Flag) and dMCRS2 lacking its C-terminal FHA domain (dMCRS2ΔFHA-Flag). I found that deletion of the FHA domain abolished the ability of dMCRS2 to associate with HA-Pitslre (Figure 3-11C). This was not due to the presence of the Flag-tag at the C-terminus of dMCRS2ΔFHA, since full-length dMCRS2-Flag retains its ability to associate with HA-Pitslre (Figure 3-11B). These data suggest that the FHA domain of dMCRS2 is required for its association with HA-Pitslre. However, my data do not rule out the possibility that deletion of the FHA domain results in aberrant folding of the dMCRS2ΔFHA-Flag protein. Attempts to express the FHA domain alone were not successful, suggesting that high levels of the FHA domain might be lethal to the cells. I next wished to examine whether the kinase activity of HA-Pitslre is important for its interaction with dMCRS2. To generate a kinase inactive HA-Pitslre, I mutated Lysine 587 to Arginine (HA-PitslreK587R). This point mutation was selected based on previous studies of serine/threonine kinase structure and function, which have demonstrated a specific requirement for this highly conserved Lysine residue for enzymatic activity (De Bondt et al., 1993; Taylor et al., 1993). Co-immunoprecipitation studies revealed that similar amounts of HA-PitslreK587R and HA-Pitslre co-purify with dMCRS2-Flag (compare Figure 3-11D with Figure 3-11B), suggesting that the kinase activity of HA-Pitslre is not required for its association with dMCRS2.

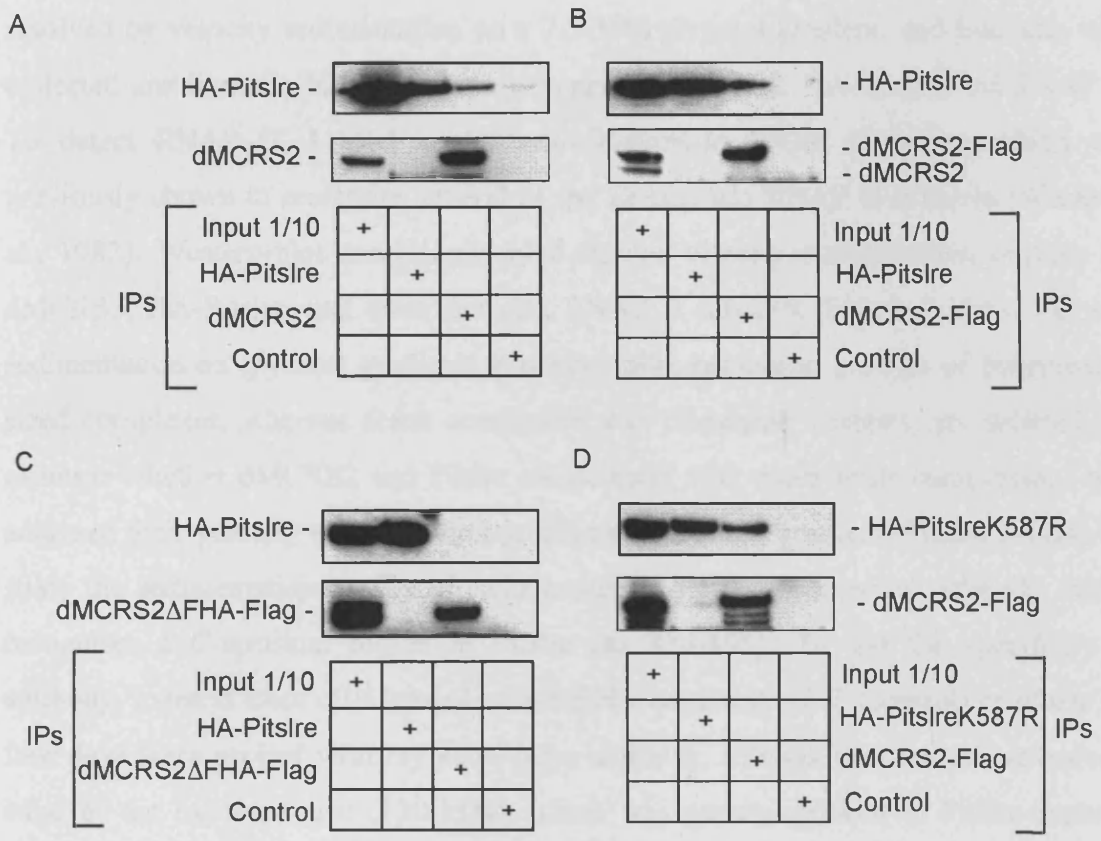

Figure 3-11: The dMCRS2 FHA domain is required for its association with PitsIre. (A) HA-PitsIre associates with endogenous dMCRS2. dMCRS2, HA-PitsIre, and control (anti-V5) immunoprecipitates were blotted for the presense of HA-PitsIre using an anti-HA antibody (top panel) and dMCRS2 using the anti-dMCRS2 antibody (bottom panel). (B-C) HA-PitsIre associates with dMCRS2-Flag, but not dMCRS2ΔFHA-Flag. HA-PitsIre, dMCRS2-Flag (B), dMCRS2ΔFHA-Flag (C), and control (anti-V5) immunoprecipitates were blotted for the presence of HA-PitsIre (top panels) using an anti-HA antibody, dMCRS2-Flag (B, bottom panel) and dMCRS2ΔFHA-Flag (C, bottom panel) using an anti-Flag antibody. (D) The HA-PitsIreK587R mutant, which is predicted to lack kinase activity, retains its ability to interact with dMCRS2-Flag. HA-PitsIreK587R, dMCRS2-Flag, and control (anti-V5) immunoprecipitates were blotted for the presence of HA-PitsIreK587R using an anti-HA antibody (top panel) or dMCRS2-Flag using an anti-Flag antibody (bottom panel).

3.1.11 dMCRS2 co-sediments with Pitslre and RNAP II on glycerol and sucrose gradients

The human Pitslre/Cdk11^{p110} (*Drosophila*/humans) protein was previously found to associate with hyper-phosphorylated RNAP II. My data show that Pitslre can be purified in complex with dMCRS2 (Table 3-1 and Figure 3-11A-B). To analyse whether dMCRS2, Pitslre, and RNAP II might exist as part of the same complex, I examined the velocity sedimentation profiles of all three proteins on sucrose and glycerol gradients (Figure 3-12A-B). Extract from S2 cells expressing HA-Pitslre was resolved by velocity sedimentation on a 7.5-35% glycerol gradient, and fractions were collected and immuno-blotted for the presence of dMCRS2, HA-Pitslre, and RNAP II. To detect RNAP II, I used a goat anti-*Drosophila* RNAP II serum, which was previously shown to recognise several of the *Drosophila* RNAP II subunits (Weeks et al., 1982). Western-blot analysis revealed similar velocity sedimentation profiles for dMCRS2, HA-Pitslre, and three different RNAP II subunits (Figure 3-12A). Velocity sedimentation on glycerol gradients generates high-resolution profiles of intermediate sized complexes, whereas dense complexes, e.g. ribosomal subunits, are pelleted. To examine whether dMCRS2 and Pitslre co-sediment with more dense complexes, I next analysed their velocity sedimentation profiles on a sucrose gradient (Figure 3-12B). To study the sedimentation profile of endogenous Pitslre, I generated an antibody, which recognises a C-terminal region of Pitslre (aa 884-898). To test the specificity of antibody, extracts from cells treated with dsRNA targeting *eGFP* (control) or *pitslre* for four days were probed with my anti-Pitslre antibody. Immunoblot analysis revealed a band of the expected size (130 kDa), which was greatly reduced in Pitslre-depleted extracts (Figure 3-12C, lane 1-2). Moreover, my antibody detected two bands in extracts from cells expressing HA-Pitslre corresponding to the sizes of endogenous and HA-Pitslre (Figure 3-12C, lane 3). Having confirmed the specificity of the anti-Pitslre antibody, I examined the profiles of endogenous dMCRS2, Pitslre, and RNAP II resolved by velocity sedimentation on a sucrose gradient (Figure 3-12B). For comparison, the 40S ribosomal subunit fractions were marked using an anti-RpS25 antibody. I found that the majority of dMCRS2 protein co-sediments with Pitslre and RNAP II in fractions slightly higher up the gradient than the 40S ribosomal subunit fractions (Figure 3-12B). These data suggest that dMCRS2 and Pitslre might both be associated with RNAP II complexes. I also noticed that a small fraction of dMCRS2 is

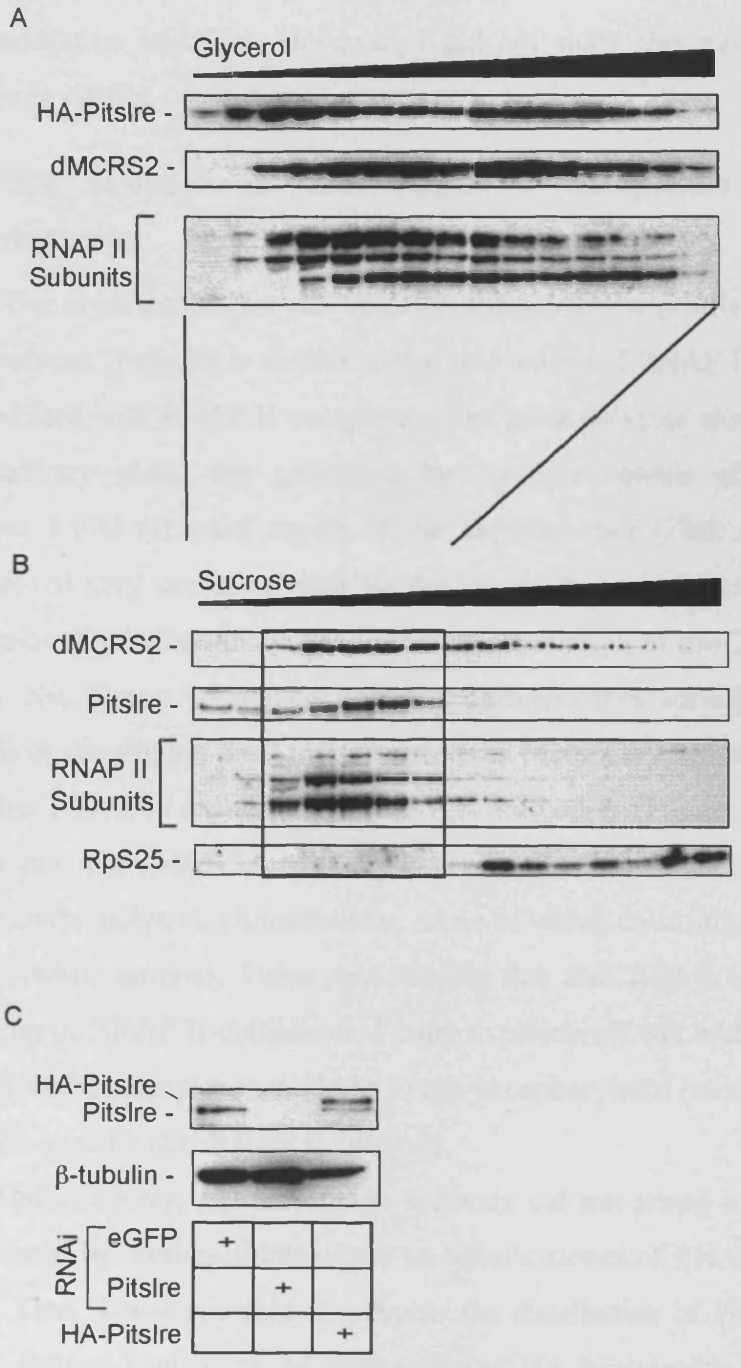

Figure 3-12: dMCRS2 co-sediments with PitsIre and RNAPII on sucrose and glycerol gradients. (A-B) Cell extracts were resolved by velocity sedimentation on a 7.5-35% glycerol gradient for 7 hours at 37.000 rpm (A) or on a 7.5-30% sucrose gradient for four hours at 39,000 rpm (B). The presence or absence of dMCRS2, PitsIre, and RNAPII in the different fractions was revealed by Western-blotting. Fractions containing the 40S subunit were identified by probing for the small ribosomal subunit protein RpS25 (B). (C) The specificity of the anti-PitsIre antibody was confirmed by immuno-blotting on cell extracts prepared from S2 cells treated with dsRNA corresponding to *eGFP* (control) or *dmcrs2* for four days. Anti-βtubulin was used as a loading control.

present in the 40S ribsosomal subunit containing fractions. This observation and the identification of translation initiation factors and small ribosomal proteins in my GTC-dMCRS2 purification (Table 3-1) suggest that dMCRS2 might have an additional function in translation initiation. However, I did not study this putative function of dMCRS2 in more details.

3.1.12 dMCRS2 co-localises with RNAP II complexes on polytene chromosomes

The observation that the velocity sedimentation profile of dMCRS2 on glycerol and sucrose gradients is similar to that of Pitslre and RNAP II, suggests that it might be associated with RNAP II complexes. The giant polytene chromosomes of the *Drosophila* salivary gland are generated by multiple rounds of endoreplication generating over 1,000 synapsed copies of the chromosomes (Zink and Paro, 1989). These have proved very useful to visualise the localisation of transcription factors on the chromosomes. To further analyse the putative association of dMCRS2 with RNAP II complexes, Nic Tapon co-stained polytene chromosomes spreads prepared from salivary glands of developing third instar larvae (see Materials and methods) with anti-dMCR2 (Figure 3-13A, in red) and anti-RNAP II antibodies (Figure 3-13B, in green). Staining with my anti-dMCRS2 antibody revealed the localisation of dMCRS2 in distinct bands on the polytene chromosomes, some of which co-localised with RNAP II (Figure 3-13C, white arrows). These data suggest that dMCRS2 is indeed associated with a sub-group of RNAP II complexes. Future experiments will address whether this sub-group of RNAP II complexes might be hyper-phosphorylated (elongating) RNAP II using a phospho-specific anti-RNAP II antibody.

Unfortunately, my anti-Pitslre antibody did not reveal a specific staining pattern when tested by immunofluorescence on mitotic clones of RNAi-depleted *pitslre* mutant tissue. Thus, I was not able to examine the distribution of Pitslre on polytene chromosomes. Instead I analysed the association of HA-Pitslre with RNAP II by co-immunoprecipitation experiments (Figure 3-12D). Immuno-blot analysis of HA-Pitslre, RNAP II, and control (anti-V5) precipitates using an anti-HA antibody revealed that a fraction of HA-Pitslre is associated with RNAP II (Figure 3-12D, top panel). I was not able to detect any RNAP II protein in the HA-Pitslre precipitate, suggesting that binding of an antibody to the N-terminal HA-tag might interfere with the association of RNAP II with HA-Pitslre (Figure 3-12D, top panel). Alternatively, only a minor and non-

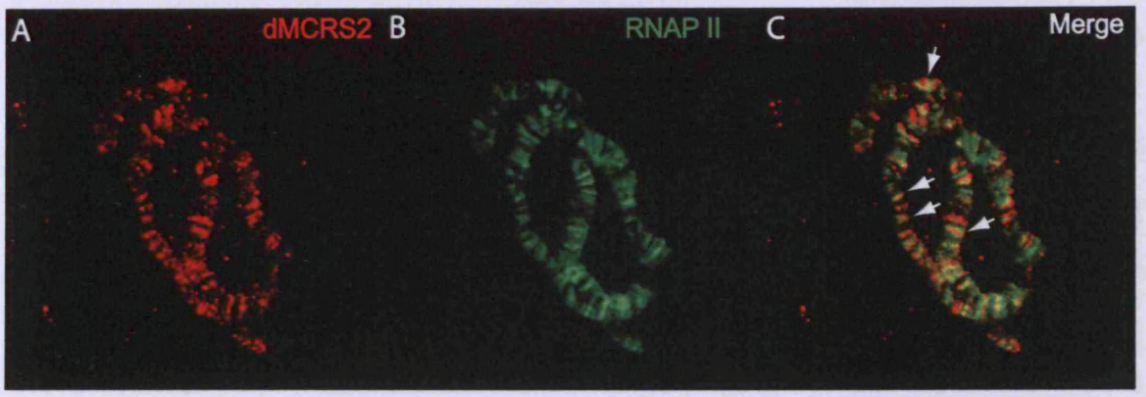

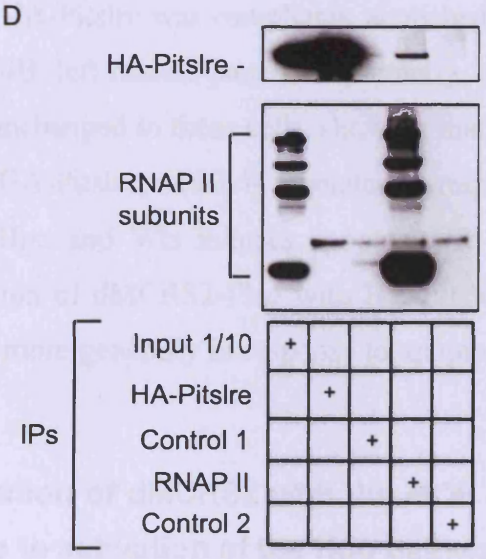

Figure 3-13: dMCRS2 co-localises with RNAP II on polytene chromosomes. (A-C) A fraction of dMCRS2 co-localise with a sub-group of RNAP II complexes. Polytene chromosome spreads prepared from third instar larvae and stained with anti-dMCRS2 (A, in red) and anti-RNAP II (B, in green) antibodies. White arrows indicate regions of co-localisation of dMCRS2 and RNAP II complexes (C). (D) HA-PitsIre, RNAP II, control 1 (anti-V5, Protein A beads), and control 2 (anti-V5, Protein G beads) immunoprecipitates were blotted for the presense of HA-PitsIre using an anti-HA antibody (top panel) and RNAP II subunits using the goat anti-*Drosophila* RNAP II serum (bottom panel).

detectable fraction of RNAP II, e.g. hyper-phosphorylated RNAP II, may associate with HA-Pitslre. However, attempts to immunoprecipitate hyper-phosporylated RNAP II using a commercial antibody were unsuccessful (data not shown).

3.1.13 The association of dMCRS2 with Pitslre is regulated in response to activation of the Hpo pathway

The initial observation that introduction of one copy of the *dmcrs2*^{rG166} mutant allele into a *GMRsav,wts* background suppressed the rough-eye phenotype of those animals, prompted my to investigate the whether Hpo signalling might regulate the association of dMCRS2 with Pitslre. I examined the ability of dMCRS2-Flag to co-immunoprecipitate with HA-Pitslre in control cells (Figure 3-14A, left panels) and cells expressing Hpo-Myc and Wts-Myc (Figure 3-14A, right panels). As previously, I found that a significant proportion of HA-Pitslre co-purified with dMCRS2-Flag in control cells (Figures 3-11B and 3-14A, left middle panel). Interestingly, the association of dMCRS2-Flag with HA-Pitslre was completely abolished in cells over-expressing Hpo and Wts (Figure 3-14B, left middle panel). Importantly, dMCRS2-Flag and HA-Pitslre protein levels were unchanged in these cells, showing that it is indeed the association of dMCRS2-Flag with HA-Pitslre, which is regulated in response to Hpo signalling. Since over-expression of Hpo and Wts induces apoptosis, it is not clear from these data whether the association of dMCRS2-Flag with HA-Pitslre is regulated specifically by Hpo signalling or in more generally in response to apoptosis. Future studies will aim to resolve this issue.

3.1.14 The association of dMCRS2 with the MOF complex is not regulated in response to activation of the Hpo pathway

dMCRS2 was previously shown to be part of a chromatin-remodelling complex containing NSL1-3, MBDR2, and the histone methylase MOF (I will refer to this complex as the MOF complex) (Mendjan et al., 2006). Unexpectedly, I did not recover any of those components in my purification (Table 3-1). Since one potential role of dMCRS2 could be to link chromatin remodelling with regulation of RNAP II transcription via its ability to associate with Pitslre/RNAP II and the MOF complex, I wished to confirm the association of dMCRS2 with the MOF complex. For this purpose, I generated HA-tagged MOF and analysed its ability to co-immunoprecipitate with dMCRS2 (Figure 3-14B, left panels). As previously described, I found that a

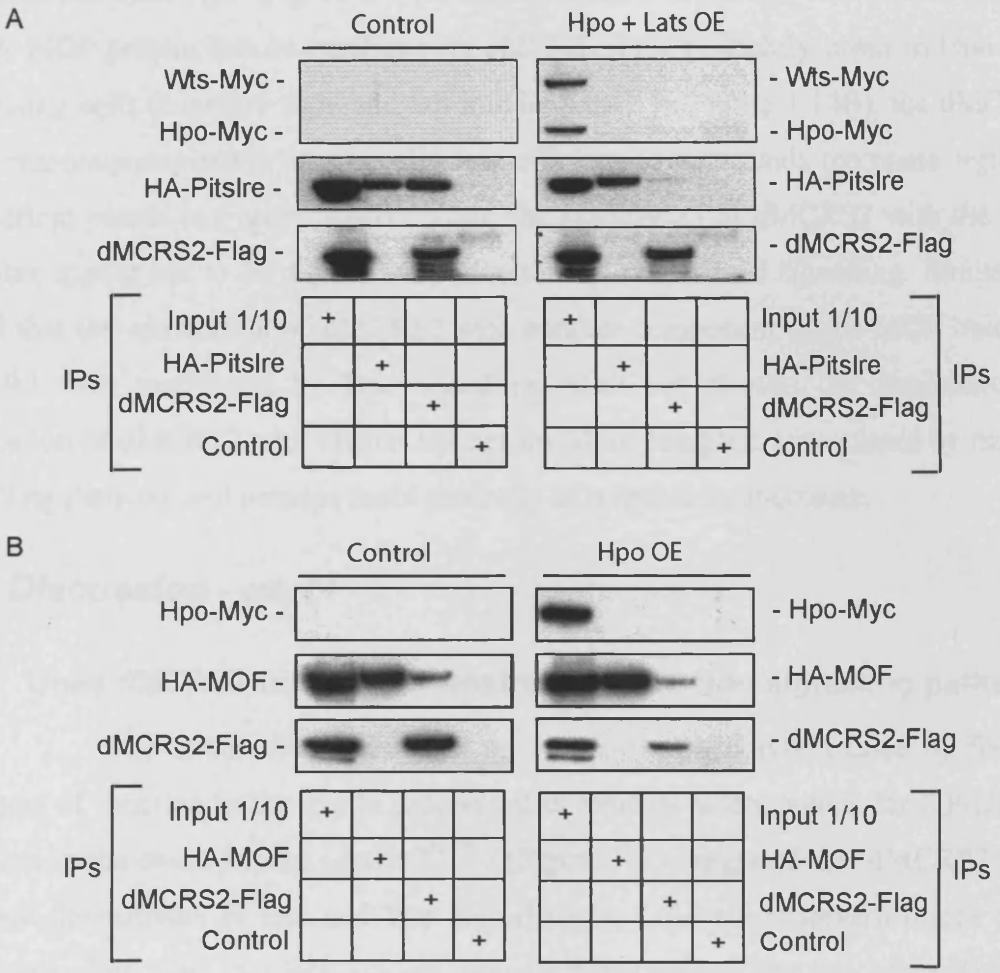

Figure 3-14: The association of dMCRS2 with PitsIre, but not MOF, is regulated in response to excess Hpo signalling. (A) The association of HA-PitsIre with dMCRS2-Flag is disrupted in response to Hpo and Lats gain of function. (A) dMCRS2-Flag, HA-PitsIre, and control (anti-V5) immunoprecipitates from control cells (left) or cells transfected with Hpo and Wts (right) were blotted for the presence of HA-PitsIre using an anti-HA antibody (top panels) and dMCRS2-Flag using an anti-Flag antibody (bottom panels). (B) The association of dMCRS2-Flag with MOF-HA is not affected by Hpo gain of function. dMCRS2-Flag, HA-MOF, and control (anti-V5) immunoprecipitates from control cells (left) or cells transfected with Hpo (right) were blotted for the presence of HA-MOF using an anti-HA antibody (top panels) and dMCRS2-Flag using an anti-Flag antibody (bottom panels).

fraction of HA-MOF co-purifies with dMCRS2-Flag (Figure 3-14B, left middle panel). I was not able to detect any HA-MOF protein in the dMCRS2-Flag immunoprecipitate (Figure 3-14B, left bottom panel). One possible explanation for this is that only a small fraction of dMCRS2 is associated with HA-MOF under these conditions. I next wished to examine whether the association of dMCRS2 with MOF is regulated in response to over-expression of Hpo (Figure 3-14B, right panels). I found that whereas the amount of HA-MOF protein that co-purifies with dMCRS2-Flag is slightly lower in Hpo over-expressing cells (compare right and left middle panels in Figure 3-14B), the dMCRS2-Flag immunoprecipitation was equally less efficient in these cells (compare right and left bottom panels in Figure 3-14B). Thus, the association of dMCRS2 with the MOF complex appear not to be significantly affected by excess Hpo signalling. Similarly, I found that the association of dMCRS2 with another component of the MOF complex, MBDR2, was unaffected by Hpo signalling (data not shown). In conclusion, the association of dMCRS2 with Pitslre, but not the MOF complex, is regulated by the Hpo signalling pathway and perhaps more generally in response to apoptosis.

3.2 Discussion - part I

3.2.1 Does dMCRS2 function downstream of the Hpo signalling pathway?

The initial observation that the rough-eye phenotype caused by Sav and Wts gain of function in the eye is suppressed in animals heterozygous for a P-element insertion in the *dmcrs2* locus (*dmcrs2*^{rG166}) (Figure 3-1) suggested that dMCRS2 might function downstream of Sav and Wts. Surprisingly, I did not observe a rescue of the rough-eye phenotype in *GMR-sav,wts* animals heterozygous for two other dMCRS2 LOF mutations, *dmcrs2*^{c07041} and *dmcrs2*^{c00114} (data not shown). My *in vivo* analysis revealed that dMCRS2 protein levels are significantly reduced in mitotic clones of *dmcrs2*^{c07041} and *dmcrs2*^{c00114} mutant tissue, but unchanged in clones of *dmcrs2*^{rG166} mutant tissue (Figure 3-4). This indicates that the *dmcrs2*^{rG166} mutation causes a truncation rather than an ablation of the *dmcrs2*-encoded product. Consistent with this, the *l(3)rG166* P-element insertion is predicted to cause a truncation of dMCRS2, which retains the epitope of dMCRS2 recognised by my anti-dMCRS2 antibody, but lacks most of the FHA domain (Figure 3-3A). Since the FHA domain is likely to be essential for dMCRS2 function, *dmcrs2*^{rG166} might encode a dominant negative form of dMCRS2. Consistent with this idea, mitotic clones of *dmcrs2*^{rG166} mutant tissue exhibit

a more severe growth defect than those of *dmcrs2*^{c07041} and *dmcrs2*^{c00114} mutant tissue (compare Figure 3-4B with 3-4E and 3-4H). Thus, *dmcrs2*^{rG166} is likely to represent a strong dMCRS2 LOF mutation. This might explain the observed rescue of the rough-eye phenotype in *GMRsav,wts* animals heterozygous for the *dmcrs2*^{rG166}, but not the *dmcrs2*^{c07041} and *dmcrs2*^{c00114}, mutant alleles (Figure 3-2 and data not shown).

The ability of one copy of *dmcrs2*^{rG166} to partially rescue the rough-eye phenotype of *GMRsav,wts* animals suggests that dMCRS2 has a pro-apoptotic function downstream of Sav and Wts. However, Julien Colombani found that CycE and DIAP protein levels were unchanged in clones of *dmcrs2*^{rG166} mutant tissue (Figure 3-3B-C'), indicating that dMCRS2 does not function immediately downstream of Sav and Wts. Consistent with this, RNAi-mediated depletion of dMCRS2 does not restore Yki activity in cells expressing Hpo, Sav, and Wts (Figure 3-3D). Thus, if dMCRS2 is required for apoptotic signalling downstream of Sav and Wts, it appears to be in parallel with or further downstream of Yki. Since the data presented here suggest that dMCRS2 might have a function in regulation of RNAP II transcription, it is tempting to speculate that dMCRS2 is required for Yki-independent transcription of pro-apoptotic genes. Alternatively, dMRCS2 may have a general rather than Hpo-specific pro-apoptotic function. This could be analysed genetically by testing the ability of *dmcrs2*^{rG166} to modifiy other apoptosis-related phenotypes, such as that elicited by expression of the IAP inhibitors Hid, Grim of Reaper.

3.2.2 dMCRS2 is required for normal rates of S phase progression and for growth during development

My *in vivo* characterisation of *dmcrs2* revealed that it is an essential gene required for normal growth during development. Thus, larvae homozygous lethal for mutations in *dmcrs2* exhibit severe growth defects and die as third instar larvae (data not shown). A more detailed analysis of the growth defect in cultured cells revealed that dMCRS2-depleted cells progress through S phase with slower kinetics than control cells. Consistent with dMCRS2 function being required in S phase, expression levels of the human homologue of dMCRS2 (MSP58) fluctuate in a cell cycle dependent manner with a peak of expression in early S phase (Ren et al., 1998; Song et al., 2004).

3.2.3 dMCRS2 can be purified in complex with proteins that function in translation initiation and RNAP II transcription

To place dMCRS2 in a functional context, I carried out a large-scale tandem affinity purification of GTC-dMCRS2 followed by mass spectrometry analysis to identify dMCRS2-associated proteins (Figure 3-8 and Table 3-1). My mass spectrometry analysis revealed a number of proteins, most of which fell into one of two groups of functionally related proteins. The first group contained several proteins that are predicted to function in translation initiation including five components of the eIF3 complex, eIF4-A/eIF4A2/Tif2p, Pabp/PABPC1/Pabp, Belle/DHX15/DBP1 (*Drosophila*/humans/yeast), and small ribosomal 40S subunit proteins. Interestingly, MSP58, the human homologue of dMCRS2, was previously found to associate with fragile mental retardation protein (FMRP) and polyribosomal poly(A)+ messenger ribonucleoprotein (mRNPs) in the cytoplasmic compartment of neurons (Davidovic et al., 2006). FMRP is a component of mRNPs complexes (Feng et al., 1997; Khandjian et al., 2004; Stefani et al., 2004) and is required for both transport (Estes et al., 2008) and translation of target mRNAs (Zalfa et al., 2003). The purification of GTC-dMCRS2 in complex with translation initiation factors and ribosomal proteins suggests that dMCRS2, like MSP58, might be associated with mRNPs. Consistent with this idea, my velocity sedimentation data revealed that a small fraction of dMCRS2 might be associated with the translation machinery (Figure 3-12B). However, I did not study this putative function of dMCRS2 in more details.

The second group of proteins recovered in my GTC-dMCRS2 purification are known or predicted to function in RNAP II transcription and/or chromatin remodelling. These included, both subunits of the GTF, TFIIF, CKIIα/CK2αCka2p, Pitslre/Cdk11^{p110}, Psr/JMJD6, and the FACT component, SSRP/SSRP1/Pob3p (*Drosophila*/humans/yeast) (Table 3-1). Several of these have previously been functionally linked. Thus, Cdk11^{p110} has been found to associate with both subunits of TFIIF, CK2, the FACT complex, and RNAP II (Trembley et al., 2002), and CK2 has been isolated in complex with TFIIF, Cdk11^{p110}, RNAP II, and SSRP1, all of which it phosphorylates (Egyhazi et al., 1999; Li et al., 2005b; Payne et al., 1989; Trembley et al., 2003). This suggests that dMCRS2 might also have a function in RNAP II transcription. Consistent with this, I found that the majority of dMCRS2 protein is

localised in the nucleus in various tissues from developing third instar larvae (Figure 4-10).

3.2.4 dMCRS2 associates with the Pitslre/ Cdk11^{p110} protein kinase

The Pitslre/Cdk11^{p110} protein kinase (*Drosophila*/humans), which I recovered in my large-scale purification of GTC-dMCRS2 (Table 3-1), was previously shown to be required for RNAP II transcription in humans (Trembley et al., 2002). To further analyse a putative function of dMCRS2 in RNAP II transcription, I characterised the association of dMCRS2 with Pitslre. My co-immunoprecipitation analyses showed that Pitslre associates with full-length dMCRS2, but not dMCRS2 lacking the C-terminal FHA domain (Figure 3-11A-C). This suggests that dMCRS2 rely on its FHA domain for its association with Pitslre. Future experiments will include GST pull-downs of bacterial produced dMCRS2 and Pitslre proteins to establish whether the interaction between dMCRS2 and Pitslre is direct. I also found that a putative kinase dead version of Pitslre, PitslreK587R, retained its ability to associate with dMCRS2, indicating that intrinsic kinase activity of Pitslre might not be not required for its association with dMCRS2 (Figure 3-11D). However, additional experiments will be required to determine whether the PitslreK587R mutant is indeed inactive.

3.2.5 dMCRS2 co-localises with a sub-group of RNAP II complexes on polytene chromosomes *in vivo*

My co-immunoprecipitation analyses revealed that Pitslre, like its human homologue Cdk11^{p110}, associates with RNAP II (Figure 3-13D and (Trembley et al., 2002)). The observation that Pitslre associates with both dMCRS2 and RNAP II suggests that dMCRS2 might also be associated with RNAP II complexes. Consistent with this idea, my velocity sedimentation experiments showed that dMCRS2 and Pitslre co-sediment with RNAP II complexes on glycerol and sucrose gradients (Figure 3-12A-B). Moreover, co-staining of polytene chromosome spreads with anti-RNAP II and anti-dMCRS2 antibodies revealed that dMCRS2 co-localises with a sub-group of RNAP II complexes on polytene chromosomes *in vivo* (Figure 3-13A-C). Since the anti-RNAP II antibody recognises both phosphorylated (elongating) and hypo-phosphorylated RNAP II complexes (Figure 3-12B), it is possible that this sub-group of RNAP II complexes represents elongating RNAP II. Consistent with this idea, CK2 and TFIIF, which were recovered in my GTC-dMCRS2 purification, co-localise with elongating RNAP II

complexes on polytene chromosomes *in vivo* (Egyhazi et al., 1999). The presence of TFIIF and absence of other GTFs in my GTC-dMCRS2 purification is also consistent with a role of dMCRS2 in RNAP II elongation, since TFIIF is the only GTF, which re-associates with RNAP II complexes following their release from the initiation complex (Zawel et al., 1995). Future experiments will address whether dMCRS2 associates with elongating RNAP II complexes by co-stainings of polytene chromosome spreads with antibodies that recognise phosphorylated RNAP II and dMCRS2. Moreover, I have acquired antibodies against several of the proteins that I identified in my GTC-dMCRS2 purification including CKII and TFIIFα, and I am currently generating a new anti-Cdk11 antibody. This will allow me to examine the distribution of these proteins along polytene chromosomes and their co-localisation with dMCRS2.

3.2.6 dMCRS2 might provide a link between the MOF complex and RNAP II

dMCRS2 was previously isolated in complex with NLS1-3, MBDR2, and MOF (Mendjan et al., 2006), suggesting that it might function in chromatin remodelling. Whereas I did not recover any of the components of the MOF complex in my GTC-dMCRS2 purification, I was able to confirm the association of dMCRS2 with MOF (Figure 3-14B) and MBDR2 (data not shown) by co-immunoprecipitation analysis. Whereas microarray analyses have shown that MOF activity is required for normal levels of RNAP II transcription of a wide range of genes (Kind et al., 2008), a molecular link between MOF and RNAP II has yet to be established. The observations that dMCRS2 associates with Pitslre/Cdk11^{p110} (Figure 3-11A-B) and co-localises with RNAP II complexes on polytene chromosomes (Figure 3-13A-C), suggest that dMCRS2 might bridge an interaction between the chromatin remodelling MOF complex (Figures 3-14 and (Mendjan et al., 2006)) and Pitslre/RNAP II complexes (Table 3-1 and Figures 3-11-14). Whereas this model is consistent with the data presented here, it needs further validation. Future experiments will aim at establishing a connection between dMCRS2, the MOF complex, and Pitlsre/RNAP II complexes by examining their distribution along polytene chromosomes and by chromatin immunoprecipitation (ChIP) experiments. In particular, it will be interesting to test whether dMCRS2, Pitslre and MOF are associated with the same genes, or whether dMCRS2 is present in separate pools associated with either partner. If Pitslre and MOF are present in the same complex, what are their relative contributions to gene

transcription? This can be analysed both using microarray analysis in cultured cells depleted of dMCRS2, Pitslre and MOF, and *in vivo* by examining the expression of enhancer trap lines in mutant clones. How the MOF complex is recruited to sites of transcription remains mysterious. It is tempting to speculate that dMCRS2, through its ability to bind RNAP II components, may act as a docking site for the MOF complex.

3.2.7 dMCRS2 might regulate RNAP II transcription in response to Hpo signalling and/or apoptosis

Interestingly, I found that the association of dMCRS2 with Pitslre, but not the MOF complex, is disrupted in response to excess Hpo signalling (Figure 3-14). This might suggest that the link between MOF-dMCRS2 and Pitslre/RNAP II complexes is disrupted in response to activation of the Hpo pathway, and could provide a mechanism for down-regulation of RNAP II transcription in response to Hpo signalling and/or apoptosis. One possible way of testing this idea will be to analyse the extent of co-localisation between dMCRS2/MOF and RNAP II in Hpo gain of function salivary glands. Since the association of dMCRS2 with the MOF complex appear to be unaffected in response to Hpo signalling (Figure 3-14B and data not shown), their co-localisation could potentially serve as an internal negative control for these analyses.

3.2.8 Does dMCRS2 have an additional function in DNA damage repair?

dMCRS2 contains a FHA domain, which is found almost exclusively in nuclear proteins that function in transcription regulation, DNA repair, and/or cell cycle progression (Durocher et al., 1999; Hofmann and Bucher, 1995; Li et al., 2000). Consistent with this, my data show that dMCRS2 is mainly nuclear and might play a role in regulation of RNAP II transcription. Interestingly, some of the GTC-dMCRS2-associated proteins identified in my large-scale purification are thought to have dual functions in RNAP II transcription and DNA damage repair. These include CKIIα/CK2α/Cka2p and the FACT component SSRP1. Thus, a complex consisting of CK2 and the two FACT components, SSRP1 and Spt16, was found to stimulate p53 activity in response to UV-induced DNA damage (Keller et al., 2001). Due to the crucial role of the FACT complex in chromatin remodelling, it has been suggested that the activated CK2-FACT complex functions as a sensor of DNA damage. Consistent with this idea, CK2-mediated phosphorylation of maize SSRP1 enhances the association of SSRP1 with UV irradiation damaged DNA (Krohn et al., 2003). The

chromatin remodelling factor, hMOF/MOF, is another MSP58/dMCRS2-associated protein, which has been reported to function in DNA damage repair (Mendjan et al., 2006). Thus, hMOF-depleted cells exhibit a delay in the kinetics of the DNA repair process (Taipale et al., 2005), and expression of dominant negative MOF results in less efficient repair of double-strand breaks (Gupta et al., 2005). Moreover, it has been suggested that hMOF-mediated H4K16 acetylation, which increases upon IR-induced DNA damage, might label sites of DNA damage and activate and/or recruit the DNA repair machinery (Gupta et al., 2005). Thus, it is possible that dMCRS2 could have an additional function in DNA damage repair. Consistent with this idea, I noticed that dMCRS2 protein levels were stabilised in S2 cells exposed to IR-induced DNA damage (data not shown). However, I did not further pursue a role of dMCRS2 in DNA damage repair.

Chapter 4 – Results and discussion part II

4.1 *dPrp38 and dMFAP1 are required for pre-mRNA processing and G2/M progression*

4.1.1 The starting point of the project

As previously discussed, we were originally interested in the *CG30342*- and *CG1017*-encoded proteins due to their potential link with the Hpo pathway (Figure 3-5A and (Giot et al., 2003)). Data from the *Drosophila* genome-wide yeast two-hybrid screen suggested that the protein encoded by the *CG1017* gene might be linked with the Hpo pathway via its interaction with Rep2 (Figure 3-5 and (Giot et al., 2003)). However, my initial protein-protein interaction data did not confirm the reported interaction between the *CG1017*-encoded protein and Rep2 (Figure 3-5B-C). Consistent with the yeast 2-hybrid data, I did find that the proteins encoded by the *CG1017* and *CG30342* genes associate with each other as discussed later (Figure 4-6). For that reason, a link between the *CG1017*- and *CG30342*-encoded proteins and the Hpo pathway was not further pursued. Instead, I focused on the characterisations of the *CG30342*- and *CG1017*-encoded products outside the context of the Hpo signalling pathway.

4.1.2 The *CG30342* gene encodes the *Drosophila* Prp38 protein

My project initially focused on the *CG30342*-encoded protein. Since this protein has not previously been studied, I carried out homology searches against other genomes to identify functional domains or homologues that might provide a clue to the function of the *CG30342*-encoded protein. Homology searches revealed that the protein encoded by the *CG30342* gene is homologous to the yeast Prp38p splicing factor and the human Prp38 protein (Prpf38). Thus, the *Drosophila* protein is 75% identical to the human Prp38 protein (Prpf38a) and 22% identical to yeast Prp38p (Chen et al., 2006b). Moreover, the *CG30342*-encoded protein contains a conserved 180 amino acid Prp38 homology domain at its N-terminus, which is found in both Prpf38 and Prp38p, and 150 additional amino acids that are found in the human, but not the yeast, Prp38 protein (Figure 4-1A). I will therefore refer to the *CG30342*-encoded protein as dPrp38 for *Drosophila* Prp38.

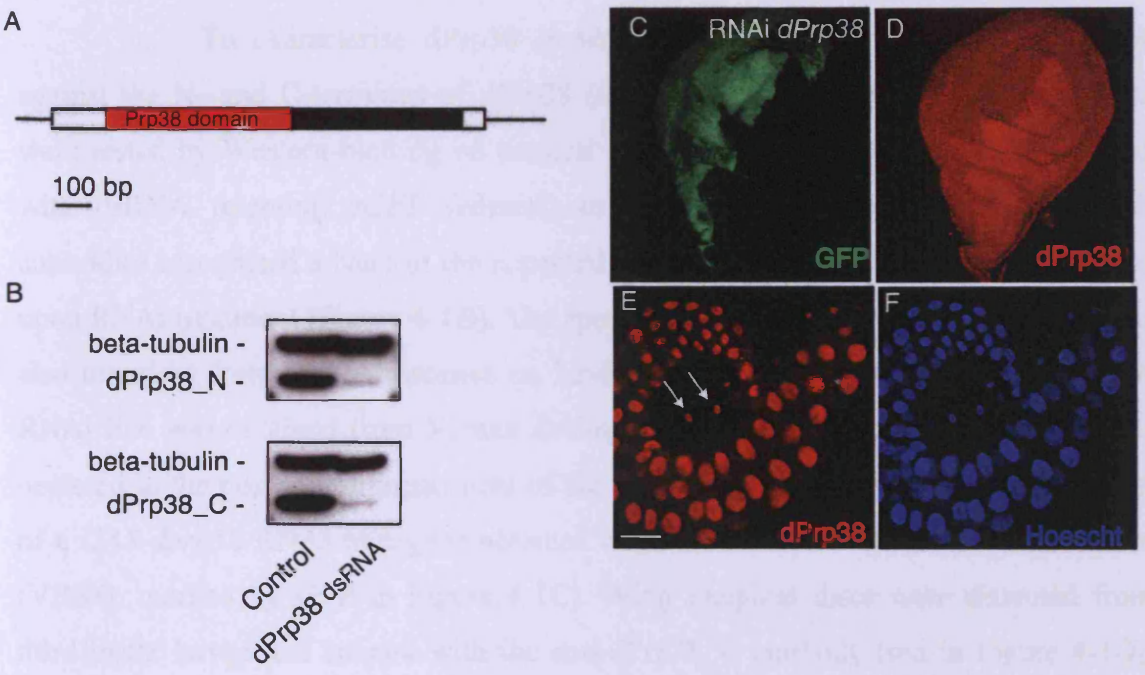

Figure 4-1: dPrp38 is a nuclear protein. (A) Schematic of the *dprp38* locus. dPrp38 is encoded by a single exon. The N-terminal part encodes a region with homology to Prp38 (red). (B) Immuno-blots on cell extracts prepared from S2 cells treated with dsRNA corresponding to *GFP* (control) or *dprp38* with antibodies recognising the C- (dPrp38_C) and N-terminal (dPrp38_N) part of dPrp38. (C-D) RNAi-mediated depletion of dPrp38 in wing imaginal discs from third instar larvae. Posterior is to the left. Expression of a *dprp38* inverted repeat in the posterior compartment of the wing using the engrailed-Gal4 driver (marked by GFP in C) results in reduced levels of dPrp38 as detected with the anti-dPrp38_C antibody (D). (E-F) dPrp38 is localised in the nucleus. Wild-type salivary glands from third instar larvae stained with the anti-dPrp38_C antibody in red (E) or a nuclear dye (F). The anti-dPrp38_C antibody also revealed a nuclear localisation of dPrp38 in the fat body (indicated by white arrows E).

As mentioned in the introduction, budding yeast Prp38p is an U4/U6.U5-tri-snRNP component that plays an important role in the maturation of the spliceosome. Prp38p activity is dispensable for the initial assembly of the spliceosome, but is required in a later step for the release of U4 snRNP and activation of the spliceosome (Xie et al., 1998). Intriguingly, the mammalian Prp38p homologue does not appear to be stably associated with the tri-snRNPs and has been recovered in surprisingly few spliceosomal purifications (Jurica and Moore, 2003). This apparent discrepancy between yeast and higher eukaryotes prompted me to study dPrp38 in more details.

4.1.3 dPrp38 is a nuclear protein

To characterise dPrp38 *in vitro* and *in vivo*, I raised two antibodies against the N- and C-terminus of dPrp38 (dPrp38_N and dPrp38_C). The antibodies were tested by Western-blotting on extracts from cultured *Drosophila* S2 cells treated with dsRNA targeting *eGFP* (control) or *dprp38*. In control treated cells, both antibodies recognised a band of the expected size (35 kDa), which was greatly reduced upon RNAi treatment (Figure 4-1B). The specificity of the anti-dPrp38_C antibody was also tested by immuno-fluorescence on larval tissue. For this purpose a UAS-*dprp38* RNAi line was obtained from Vienna *Drosophila* RNAi Centre (VDRC). dPrp38 was depleted in the posterior compartment of the wing by engrailed-Gal4 driven expression of a *UAS-dprp38* RNAi transgene obtained from the Vienna *Drosophila* RNAi Centre (VDRC, marked by GFP in Figure 4-1C). Wing imaginal discs were dissected from third instar larvae and stained with the anti-dPrp38_C antibody (red in Figure 4-1D). Reduced staining in the posterior compartment of the wing confirmed the specificity of the antibody. Next, I wished to determine the cellular localisation of dPrp38. The salivary gland provides a convenient tissue to study cellular localisation, because of the large size of the cells. Staining of cells in the salivary glands or fat body tissue dissected with the salivary glands (marked by white arrows in Figure 4-1E) of a wild-type animal revealed that dPrp38 is localised exclusively in the nucleus (Figure 4-1E-F). This is the expected localisation for a splicing factor and consistent with a conserved function of yeast Prp38p in flies.

4.1.4 dPrp38 is required for developmental growth and proliferation

4.1.4.1 Molecular and biochemical characterisation of the P(G19491) insertion

In vivo studies of core splicing factors have mostly been carried out in unicellular organisms like yeast. *Drosophila* provides a convenient system for studying loss-of-function phenotypes in a multi-cellular organism. To study *dprp38* loss-of-function, I obtained a stock bearing a P-element insertion in the open reading frame of *dprp38* (*dprp38*^{G19491}) (Figure 4-2A). The position of the P-element was verified by PCRs using primers that anneal to the inverted repeat of the P-element and approximately 500 bps upstream or downstream of the predicted insertion point (data not shown). Subsequent sequence analysis of the obtained PCR products identified the exact insertion point. The P-element insertion is predicted to give rise to a deletion of the last 65 amino acids of dPrp38, and a replacement of this region with two amino acids encoded by the P-element. To examine the nature of the product encoded by the *dPrp38*^{G19491} mutant allele, fly extracts from *dprp38*^{G19491} animals were generated and immuno-blotted with the anti-dPrp38_N and anti-dPrp38_C antibodies. As a control, extracts were generated from animals where the P-element had been precisely excised. Both antibodies detected a band of the expected size (35 kDa) in extracts from control animals (Figure 4-2B, top and middle panel). Consistent with the P-element insertion causing a deletion of the C-terminal part of dPrp38, immuno-blotting of extracts from *dprp38*^{G19491} animals with my anti-dPrp38_C antibody did not reveal any product (Figure 4-2B, middle panel). Western-blots of the same extracts using the anti-dPrp38_N antibody detected a product migrating slightly above the wild-type band (Figure 4-2B, top panel). This suggests that the *dprp38*^{G19491} mutation is not a protein null.

4.1.4.2 Characterisation of the P(G19491) insertion in dPrp38 in vivo

To study the *dprp38*^{G19491} mutation *in vivo*, I used the FLP/FRT system (Xu and Rubin, 1993) to induce mitotic clones of *dprp38*^{G19491} mutant tissue in the eye-imaginal discs of heterozygous animals (Figure 4-2C-D). Staining discs with the anti-dPrp38_C antibody revealed that dPrp38 expression levels are affected by gene dosage. Thus, the anti-dPrp38_C staining was brighter in homozygous wild-type (two copies of GFP) than heterozygous tissue (one copy of GFP), while mutant tissue (no GFP) had little detectable staining (Figure 4-2D). Since the homozygous mutant and wild-type

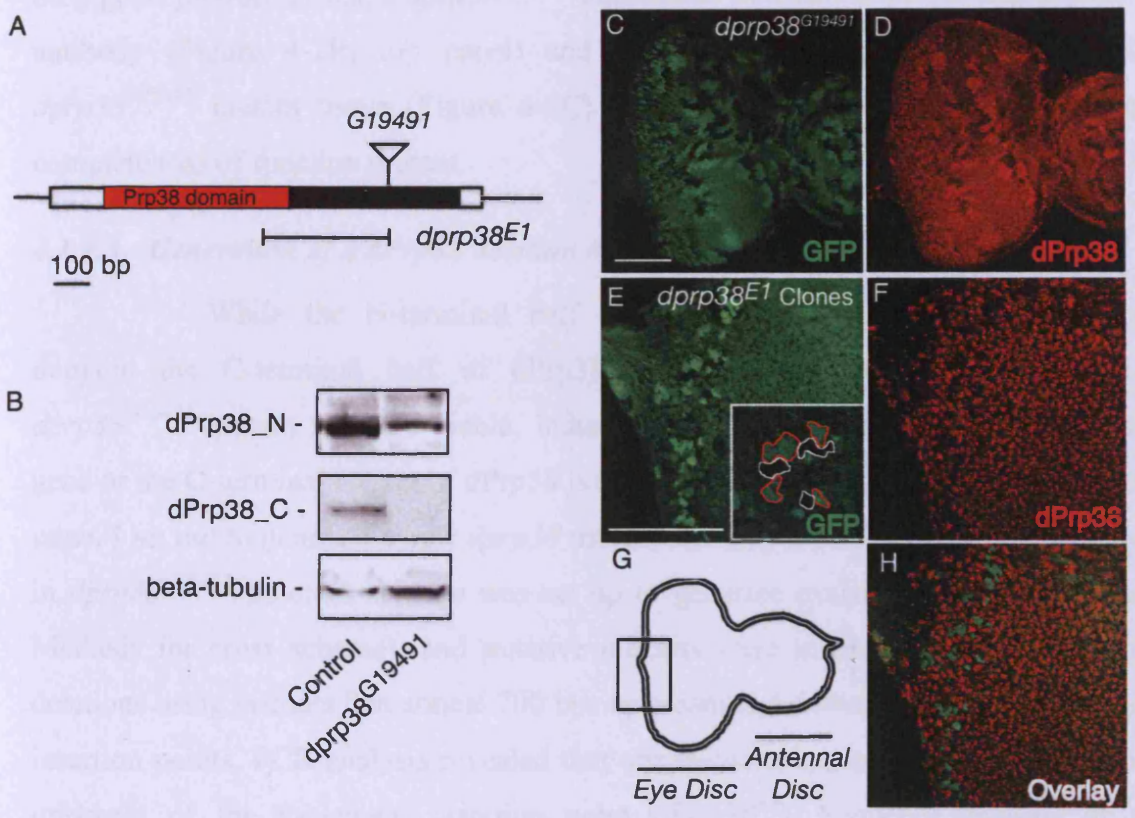

Figure 4-2: dPrp38 is required for developmental growth and proliferation. (A) Schematic of the *dprp38* locus. The position of the P-element inserted in $dprp38^{G19491}$ and the imprecise excision deletion mutant ($dprp38^{E1}$) are indicated. (B) Whole extracts from control adult flies or flies homozygous mutant for $dprp38^{G19491}$ were used for immuno-blotting with anti-dPrp38_N (top panel), anti-dPrp38_C (middle panel), and anti-β-tubulin (bottom panel). (C-F, H) Eye imaginal discs from third instar larvae. Posterior is to the left. Mitotic clones of $dprp38^{G19491}$ (C-D) or $dprp38^{E1}$(E-F, H) mutant tissue marked by the absence of GFP (C) or two copies of GFP (E, H) and stained with the dPrp38_C antibody in red (D, F, H). The inset in E is a blow-up of a region of the image, with *dprp38*-mutant areas circled in red and homozygous *Minute* clones in white. (G) is a schematic representation of the eye-antennal disc with the area in E-F, H boxed.

clones are generated simultaneously from the same mitotic recombination event, the relative growth rates of mutant and wild-type tissues can be inferred from the relative size of the clones. Notably, the *dprp38*^{G19491} insertion has no detectable effect on clone growth (compare the size of bright green and black areas in Figure 4-2C). The presence of a gene product in adult *dprp38*^{G19491} animals as detected with the anti-dPrp38_N antibody (Figure 4-2B, top panel) and the wild-type growth behaviour of the *dprp38*^{G19491} mutant tissue (Figure 4-2C) suggest that *dprp38*^{G19491} might not be a complete loss of function mutant.

4.1.4.3 Generation of a dPrp38 deletion mutant

While the N-terminal half of dPrp38 contains the Prp38 homology domain, the C-terminal half of dPrp38 is much less conserved. Homozygous *dprp38*^{G19491} mutant flies are viable, indicating that either *dprp38* is not an essential gene or the C-terminal region of dPrp38 is not essential for its function. To resolve this issue, I set out to generate a new *dprp38* mutant allele by mobilisation of the P-element in *dprp38*^{G19491}. A cross scheme was set up to generate excisions (see Materials and Methods for cross scheme), and putative mutants were screened by PCRs for small deletions using primers that anneal 700 bps upstream and downstream of the P-element insertion points. PCR analysis revealed that one excision causes a deletion of a region upstream of the P-element insertion point (*dprp38*^{E1}). Sequence analysis of the shortened PCR product revealed that in *dprp38*^{E1}, a region of 370 bp is deleted from the *dprp38* locus (Figure 4-2A). This deletion removes part of the Prp38 homology domain. Flies homozygous for *dprp38*^{E1} die as first instar larvae, but can be rescued to viability by Gal4-UAS-driven ubiquitous expression of dPrp38 (Brand et al., 1994). This demonstrates that *dprp38* loss of function is indeed lethal. Due to the early stage of lethality, I was not able to determine whether *dprp38*^{E1} is a true protein null mutation, but the severity of the phenotype suggests that *dprp38*^{E1} is a functional null or a strong hypomorph.

4.1.4.4 Clonal analysis of the dprp38^{E1} *mutant*

To study the *dprp38*^{E1} mutant phenotype *in vivo*, I used the FLP/FRT system to generate mitotic clones of *dprp38*^{E1} mutant tissue in wing and eye imaginal discs. Attempts to recover *dprp38*^{E1} mutant clones in heterozygous animals were unsuccessful, indicating that dPrp38 is required for normal growth and/or proliferation

(data not shown). Thus, GFP-labelled *dprp38*^{E1} mutant clones were generated in eye imaginal discs that are heterozygous for a mutation in a *Minute* gene (Figure 4-2E-F, H, and materials and methods). Even in this context, only small *dprp38*^{E1} mutant clones could be recovered posterior to the mitotic furrow where cell proliferation has ceased (Figure 4-2E, mutant cells are labelled by two copies of GFP, red circles). Notably, the mutant clones were similar in size to clones homozygous for the *Minute* mutation (marked by absence of GFP, white circles). Since homozygous *Minute* clones are severely growth defective due to lack of functional ribosomes, this demonstrates that dPrp38 function is indeed essential for cell growth and proliferation.

4.1.5 dPrp38 is required for proliferation and G2/M progression

4.1.5.1 Cells depleted of dPrp38 accumulate in G2/M

To further investigate the growth/proliferation defect observed in *dprp38* mutant tissue, DNA profiles were recorded from *Drosophila* S2 cells treated with dsRNAs targeting *eGFP* (control) or *dprp38* for the indicated number of days (Figure 4-3A-D'). In parallel, aliquots were removed to calculate the total number of cells (Figure 4-3E) and to analyse dPrp38 protein levels (Figure 4-3F). The DNA profiles showed that cells treated with dsRNAs targeting *dprp38* begin to accumulate in G2/M after three to four days (Figure 4-3A-B'). After five to six days, an increase in the sub-G1 (SG1) peak is evident, indicating that cells are becoming apoptotic (Figure 4-3C-D'). Consistent with this and the *in vivo* results (Figure 4-2), dsRNA-mediated depletion of dPrp38 slows down and eventually blocks proliferation after about four days (Figure 4-3E). Immuno-blotting confirmed that this correlates with a gradual decrease in dPrp38 protein levels (Figure 4-3F). Thus, dPrp38 required for G2/M progression and for proliferation and growth during development.

4.1.5.2 dPrp38-depleted cells progress through S phase with normal kinetics, but slow down in G2/M

To study the kinetics of dPrp38-depleted cells as they progress through the cell cycle, an aliquot of cells treated with dsRNA targeting *eGFP* (control) or *dPrp38* for four days (Figure 4-3B-B') was BrdU pulse-labelled for 15 minutes. Cells were collected at the indicated time points after the BrdU pulse, and BrdU-labelled cells were recorded by flow cytometry (Figure 4-4A-F'). After three hours, most dPrp38-depleted and control cells seem to have left S phase (Figure 4-4B-B'), indicating that cells

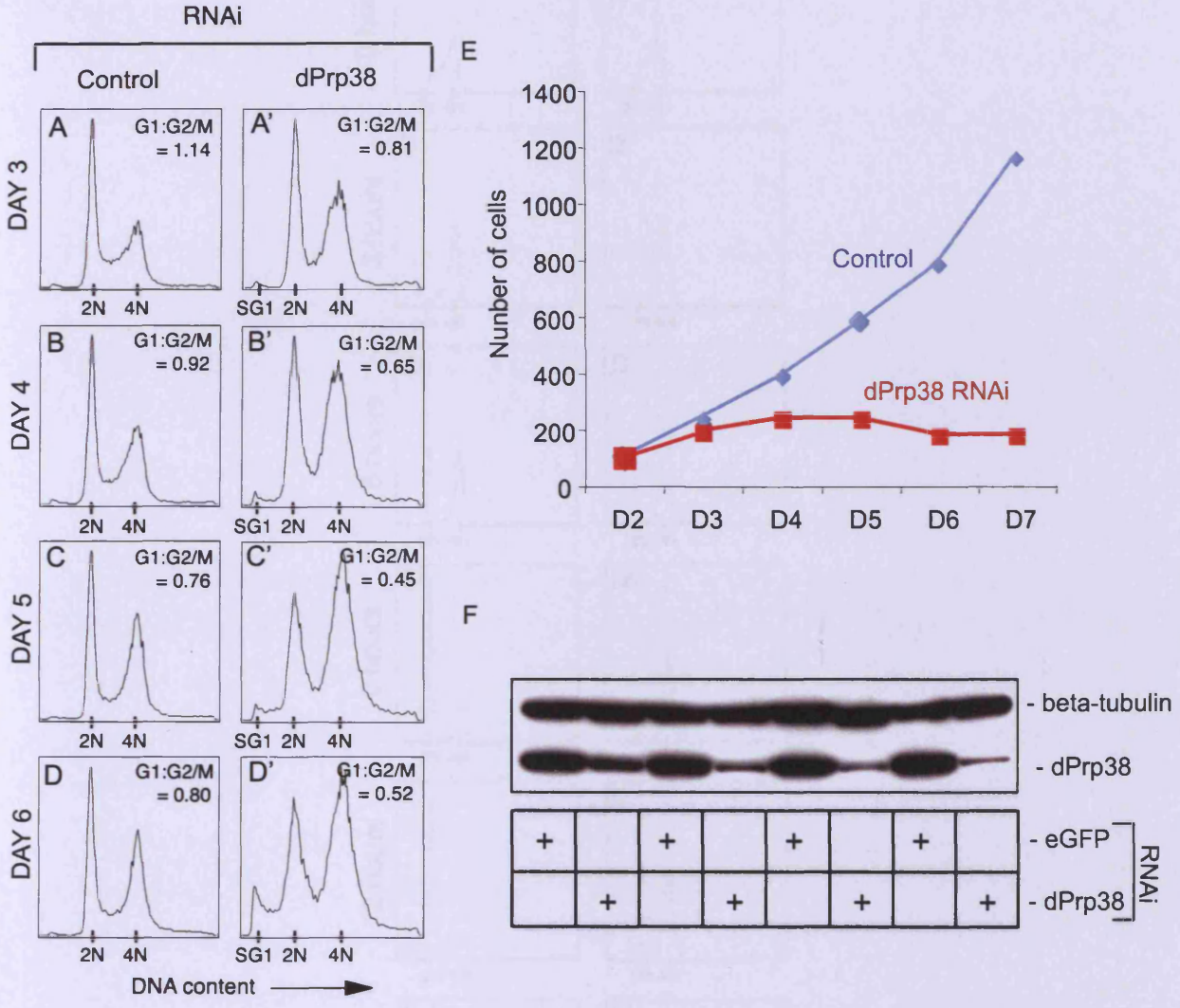

Figure 4-3: dPrp38 is required for proliferation and G2/M progression. (A-D') Cells depleted of dPrp38 accumulate in G2/M and eventually become apoptotic. S2 cells were treated with dsRNA targeting *GFP* (control) or *dPrp38* for the indicated number of days. Cells were fixed, stained with propidium iodide, and analysed by flow cytometry. The ratio of cells in the G2/M relative to G1 phase is indicated for each treatment (G1:G2/M). The peaks corresponding to the sub-G1 (SG1), G1 (2N), and G2 (4N) populations are indicated on the X-axis. (E-F) Cells were counted and dPrp38 protein levels measured in a parallel set-up. (E) Control treated (blue) or dPrp38-depleted (red) cells were counted once a day from day 2-7 (D2-D7). (F) Immuno-blotting confirms that dPrp38 protein levels are progressively reduced in cells in S2 cells treated with dsRNA corresponding to *dprp38* compared to control cells. Cell extracts prepared from S2 cells treated with dsRNA corresponding to *GFP* (control) or *dprp38* after the indicated number of days and immuno-blotted for dPrp38. Anti-β-tubulin was used as a loading control.

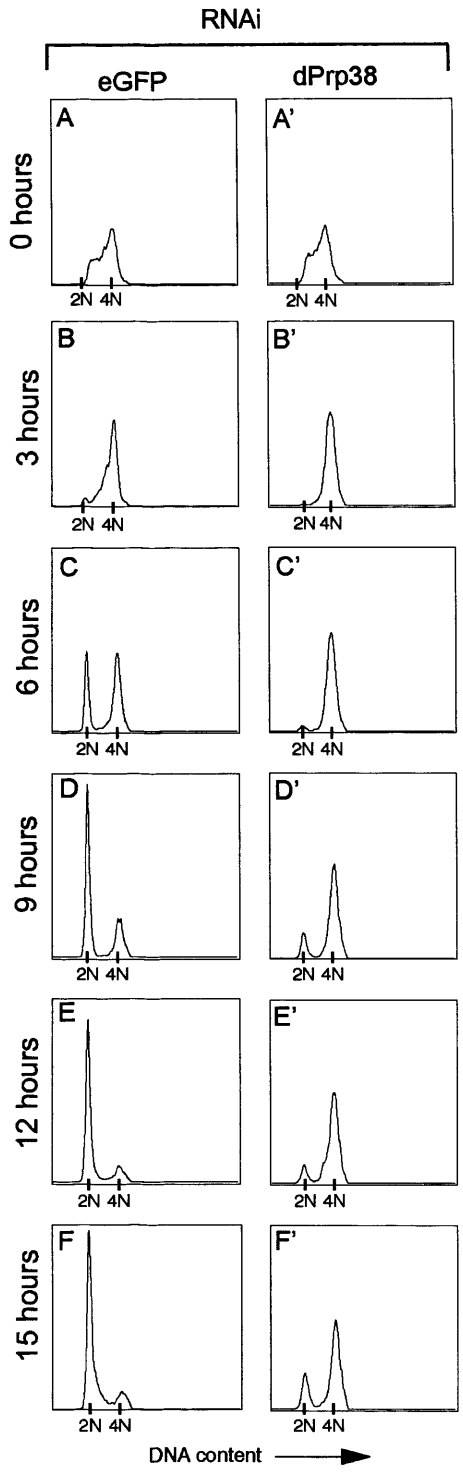

Figure 4-4: dPrp38-depleted cells progress through S phase with normal kinetics, but are slowed down in G/M. (A-F') S2 cells were treated with dsRNA targeting *GFP* (control, A-F) or *dPrp38* (A'-F') for four days. Cells were reseeded at a density of $1x10^6$ cells/ml and pulse-labelled with BrdU for 15 min. Cells were fixed, stained with propidium iodide, and analysed by flow cytometry at the indicated time points after the BrdU pulse. dPrp38-depleted cells progress through S phase with similar kinetics as control cells, but accumulate in G2/M (compare C' with C). Only a small proportion of dPrp38-depleted cells undergo mitosis and enter G1 compared with control cells (compare D'-F' with D-F).

depleted of dPrp38 progress through S phase with normal kinetics. After 6 hours, approximately 50% of control cells have entered G1, whereas the majority of dPrp38-depleted cells are still in G2/M. At the 12-hour time point, the majority of control cells are in G1 and after 15 hours some start to re-enter S phase. In contrast, the majority of dPrp38-depleted cells remain in G2/M even at the 15-hour time point (Figure 4-4C'-F'). A small proportion of cells appear to enter G1 after 9-12 hours, but with severely delayed kinetics (Figure 4-4C'-F'). Thus, dPrp38 is required for normal rates of entry into and/or progression through mitosis.

4.1.6 dPrp38 forms a complex with multiple splicing factor homologues

Having characterised the requirement for dPrp38 in growth and proliferation *in vitro* and *in vivo*, I next wished to study the molecular function of dPrp38. While yeast Prp38p is an integral component of the tri-snRNP, its mammalian homologue remains poorly characterised and has been isolated in comparatively few spliceosome preparations (Jurica and Moore, 2003). I therefore wished to identify dPrp38 binding partners in order to shed light on its function in higher eukaryotes. Two large-scale affinity purifications of endogenous dPrp38 from *Drosophila* S2 cells were performed using my anti-dPrp38_N and anti-dPrp38_C antibodies. The samples from the purification procedures were subjected to SDS-PAGE, and individual protein bands were visualised by blue G-colloidal concentrate staining (Figure 4-5A). Bands that were present in one or both of the dPrp38 samples, but absent in the control sample, were carefully excised and subjected to mass spectrometry to identify the proteins (bands marked with asterisks in Figure 4-5A).

Consistent with a role of dPrp38 in splicing, more than half of the proteins identified by mass spectrometry represent homologues of yeast splicing factors (Table 4-1). In agreement with the reported function of yeast Prp38p (Xie et al., 1998), several of the proteins identified as dPrp38 binding partners are homologues of proteins required for late maturation of the spliceosome in yeast. These include the two U5 snRNP proteins CG8877/U5-220kD/Prp8p and CG10333/U5-100kD/Prp28p and the three NTc/Cdc5-Prp19 components CG6905/Cdc5/Cef1p, CG5519/hPrp19/Prp19p, and CG6197/XAB2/Syf1p (Drosophila/Humans/Yeast). The DEAD box helicase, Prp28, is essential for the displacement of U1 snRNP by U6 snRNP at the 5'-splice site (Chen et al., 2001b; Staley and Guthrie, 1998). Prp8 is a constituent component of the U5 snRNP (Lossky et al., 1987; Stevens et al., 2001) and like Prp38, it is required for release of U4

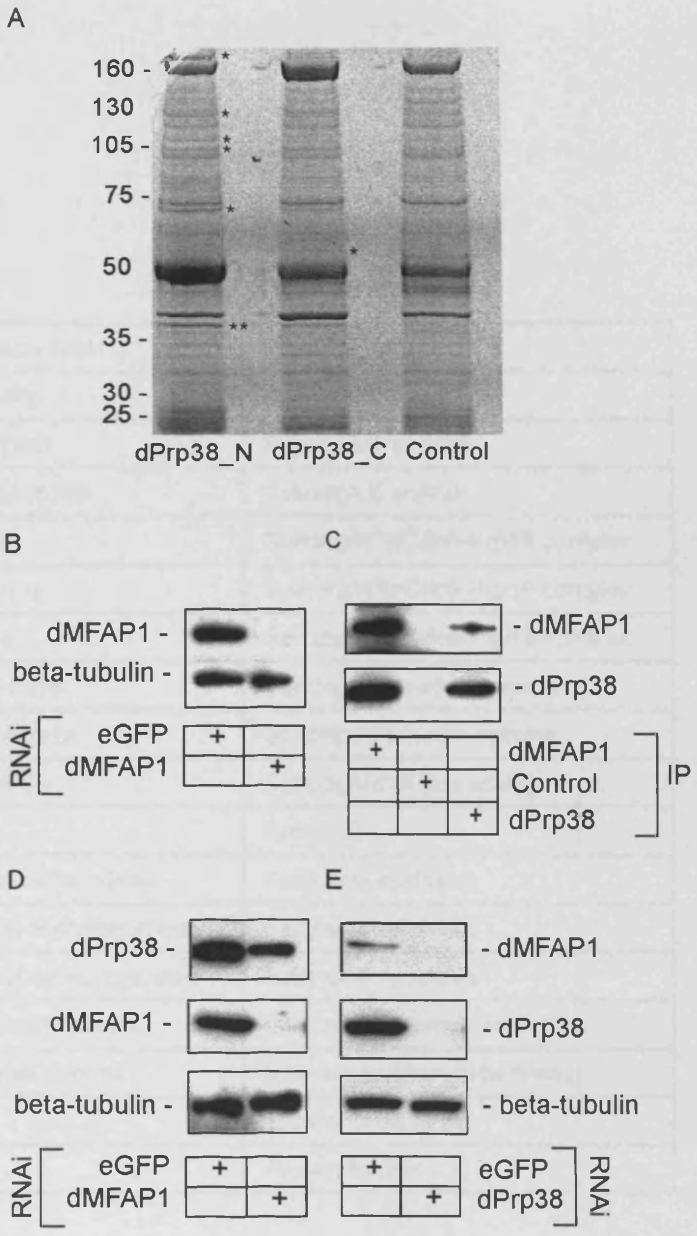

Figure 4-5: dPrp38 associates with several splicing factors and a previously uncharacterised protein dMFAP1. (A) To identify dPrp38-associated proteins, purifications were performed form S2 cells using anti-dPrp38_N, anti-dPrp38_C or anti-GFP (control) antibodies. The final eluates were resolved on a 4-12% Nupage Bis-Tris gel, and stained with Brilliant Blue G-colloidal concentrate. Visible bands (indicated by asterisks) were excised and identified by MALDI-TOF mass spectrometry. The band corresponding to dPrp38 is indicated by two asterisks. The proteins isolated in complex with endogenous dPrp38 are summarised in Table 4-1. (B) The specificity of the anti-dMFAP1 antibody was confirmed by immuno-blotting on cell extracts prepared from S2 cells treated with dsRNA corresponding to *GFP* (control) or *dmfap1* for three days. Anti-β-tubulin was used as a loading control. (C) dMFAP1 co-immunoprecipitates with dPrp38. dPrp38, dMFAP1, and control (anti-GFP) immunoprecipitates from S2 cells were blotted for dMFAP1 (top panel) and dPrp38 (bottom panel). (D-E) dMFAP1 depletion destabilises dPrp38 and vice versa. Cell extracts prepared from S2 cells treated with dsRNA corresponding to *GFP* (control, D-E), *dmfap1* (D), or *dprp38* (E) for three days were blotted for dPrp38 and dMFAP1 as indicated. Anti-β-tubulin was used as a loading control.

Table 4-1

ID (Drosophila/Humans/Yeast[1])	Predicted function
dPrp38/Prpf38a/Prp38p	Splicing/tri snRNP
CG8877/U5-220kD/Prp8	Splicing/U5 snRNP
CG10333/U5-100kD/Prp28p	Splicing/U5 snRNP
CG6905/Cdc5/Cef1p	Splicing/NTc/Cdc5-Prp19 complex
CG5519/hPrp19/Prp19p	Splicing/NTc/Cdc5-Prp19 complex
CG9143/XAB2/Syf1p	Splicing/NTc/Cdc5-Prp19 complex
CG9983/hnRNPA1/Hrp1p	Splicing/Alternative splicing
CG12749/hnRNPA1/Hrp1p	Splicing/Alternative splicing
CG6197/DDX24/MAK5	Splicing/rRNA processing
dMFAP1/MFAP1	Splicing?
CG11198/Acetyl CoA carboxylase	Fatty acid synthesis
CG5261/Dihydrolipoyl acetyltransferase	Fatty acid synthesis
CG7430/Dihydrolipoyl dehydrogenase	Fatty acid synthesis
CG7961/alpha-coatomer subunit	Intercompartmental trafficking
CG6699/beta-coatomer subunit	Intercompartmental trafficking
CG8264/Bx42	Transcription factor
CG8983/ERp60	Protein folding

[1]Protein does not have an obvious homologue in yeast, and the fly and the human IDs are indicated.

snRNP (Kuhn et al., 1999; Kuhn et al., 2002). Prp19 and Cef1 both belong to the NTc, which plays an important role in the activation step of the spliceosome by stabilising the interaction of U5 and U6 snRNPs with the pre-mRNA after the release of U1 and U4 snRNPs (Chan and Cheng, 2005; Chan et al., 2003). Additional splicing factor homologues purified in complex with dPrp38 included CG9983, and CG12749. CG9983 and CG12749 are the two closest homologues of Hrp1p/hnRNPA1 (yeast/humans) in the *Drosophila* genome. Proteins belonging to this family have been reported to function as negative regulators of pre-mRNA splicing (Zhu et al., 2001).

In addition to splicing factors, I also identified a number of proteins involved in vesicle trafficking and fatty acid synthesis. Interestingly, mouse Prp19p was recently found to be associated with lipid droplets and to have a putative role in lipid droplet biogenesis (Cho et al., 2007). It is possible that other splicing factors could have a similar additional function in lipid biogenesis. However, I did not further investigate a function of dPrp38 in lipid biogenesis and/or trafficking.

4.1.7 The *CG1017*-encoded protein, dMFAP1, forms a complex with dPrp38

As well as homologues of proteins with well-characterised functions, the mass spectrometry analysis identified the product of the predicted gene *CG1017*, which was previously found to interact with dPrp38 in a genome-wide yeast 2-hybrid screen (Table 4-1, and (Giot et al., 2003)). This protein is 52% identical to the human Microfibrillar-associated protein 1 (MFAP1). MFAP1 and its homologues contain no recognisable domain; the name refers to the fact that chicken MFAP1 (also known as AMP for Associated Microfibril protein) was initially identified through a screen for proteins detected by an antiserum raised against a crude microfibril preparation (Horrigan et al., 1992). MFAP1 was recovered in a number of purifications of various spliceosomal complexes (Bessonov et al., 2008; Deckert et al., 2006; Makarov et al., 2002; Makarova et al., 2004; Neubauer et al., 1998) although its presumed function as an extracellular matrix component initially led to its classification as a purification artefact (Neubauer, 2005; Neubauer et al., 1998). However, my observation that dMFAP1 forms a complex with dPrp38 and the *Drosophila* yeast 2-hybrid data, which suggests that the interaction might be direct, prompted me to further characterise the function of dMFAP1.

To verify the interaction between dPrp38 and dMFAP1, I generated an antibody against dMFAP1 (see Materials and Methods). The antibody was tested on extracts from cells treated with dsRNA targeting *eGFP* (control) or *dmfap1* (Figure 4-5B). The antibody detects a band in control extracts that migrates at the expected size of 75 kDa. The intensity of this band is strongly reduced in extracts from cells depleted of dMFAP1, confirming the specificity of the antibody (Figure 4-5B). This antibody and an anti-dPrp38 antibody were used to immunoprecipitate endogenous dMFAP1 and dPrp38. Western blotting revealed the presence of dPrp38 in the dMFAP1 immuno-precipitate and *vice versa* (Figure 4-5C). These data confirm that dMFAP1 forms a complex with dPrp38.

The stabilities of many proteins are increased upon their incorporation into complexes. Consistent with this idea, I found that depletion of dMFAP1 affects dPrp38 protein levels (Figure 4-5D) and vice versa (Figure 4-5E). Thus, dPrp38 proteins levels are substantially decreased in cells depleted of dMFAP1 (Figure 4-5D), and *vice versa* (Figure 4-5E). Importantly, β-tubulin levels were not affected in either sample, suggesting that dPrp38 and dMFAP1 indeed stabilise each other by forming a complex (Figure 4-5D-E).

4.1.8 dPrp38 interacts directly with dMFAP1

To examine whether the interaction between dPrp38 and dMFAP1 is direct, I used bacterial produced GST-dMFAP1 and His-dPrp38 proteins (Figure 4-6A-B). GST pull-downs of GST-dMFAP1 or GST alone (control) were carried out in the presence of His-dPrp38 (Figure 4-6A). I found that His-dPrp38 is present in the GST-dMFAP1, but not the GST precipitate (Figure 4-6A). Similarly, cleaved GST-dMFAP1 co-purifies with His-dPrp38, but not an unrelated His-tagged peptide (Figure 4-6B). This shows that the interaction between dPrp38 and dMFAP1 is direct.

Next, I wished to determine the domain in dMFAP1, which mediates its interaction with dPrp38 and *vice versa*. dMFAP1 does not contain any recognisable functional domains, though the C-terminal half of dMFAP1 is highly conserved in humans. Thus, I tested the ability of N-terminal (amino acids 1-229, HA-dMFAP1ΔC) and C-terminal (amino acid 229-478, HA-dMFAP1ΔN) domains of dMFAP1 to interact with endogenous dPrp38 (Figure 4-6C-D). I found that HA-dMFAP1ΔN (Figure 4-6C), but not HA-dMFAP1ΔC (Figure 4-6D), co-immunoprecipitates with dPrp38. This shows that the dMFAP1 interacts with dPrp38 via its conserved C-terminal part. As

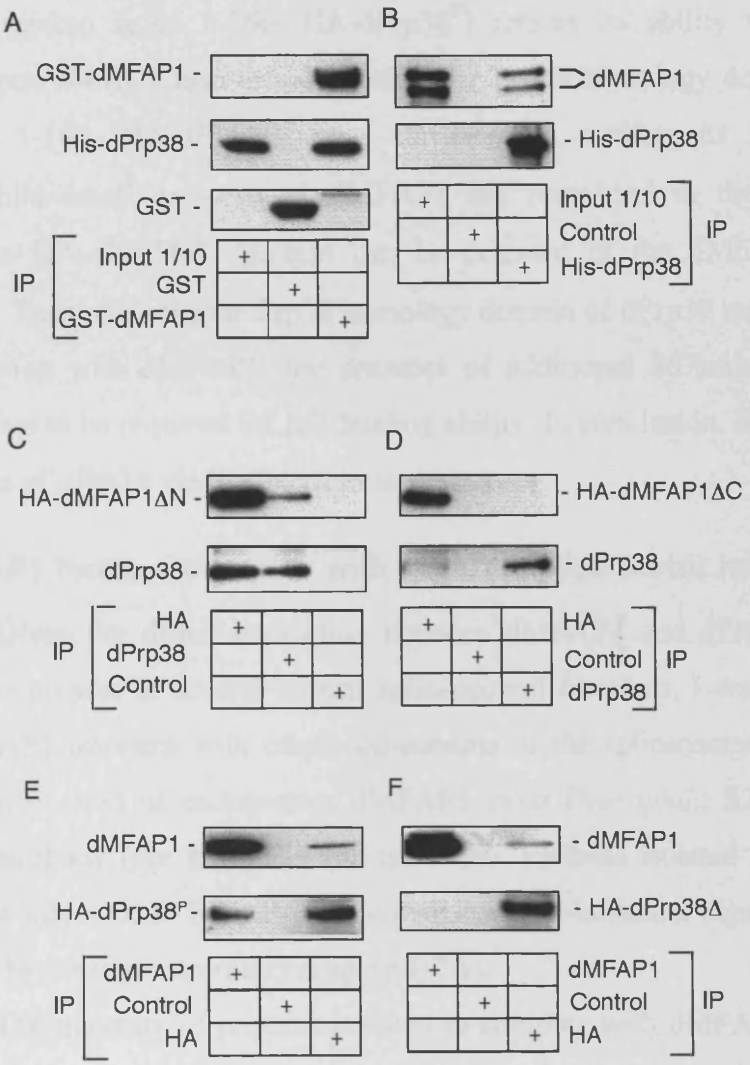

Figure 4-6: dPrp38 interacts directly with dMFAP1. (A) Bacterially expressed GST-dMFAP1 or GST alone was incubated with bacterially expressed His-dPrp38, and GST pull-downs were probed for the presence of His-dPrp38 using one of my dPrp38 antibodies (middle lane) or GST-dMFAP1 (top panel) and GST (bottom panel) using and anti-GST antibody. (B) Bacterially expressed His-dPrp38 or an unrelated His-tagged peptide (control) was incubated with cleaved GST-dMFAP1, and His pull-downs were probed for the presence of dMFAP1 using my anti-dMFAP1 antibody (top panel) or His-dPrp38 using one of my dPrp38 antibodies (bottom lane). (C-D) dPrp38 interacts with the C-terminal part of dMFAP1. dPrp38 (C-D), HA-dMFAP1ΔN (C), HA-dMFAP1ΔC (D), and control (C-D, anti-V5) immunoprecipitates from S2 cells were blotted for dMFAP1 (top panel) and dPrp38 (bottom panel). (E-F) dMFAP1 interacts with the N-terminal part of dPrp38. dMFAP1 (E-F), HA-dPrp38^{P} (E), HA-dPrp38Δ (F), and control (E-F, anti-V5) immunoprecipitates from S2 cells were blotted for dMFAP1 (top panel) and dPrp38 (bottom panel).

previously discussed, the *dprp38*^{G19491} mutation, which is predicted to cause a deletion of the last 65 amino acids of dPrp38, has no effect on growth and proliferation in vivo (Figure 4-2C-D). If the ability of dPrp38 to interact with dMFAP1 is linked with its essential function, deletion of the C-terminal part of dPrp38 would not be predicted to disrupt its interaction with dMFAP1. Indeed, I found that dPrp38 lacking the last 65 amino acids (amino acids 1-266, HA-dPrp38^{P}) retains its ability to interact with dMFAP1 (Figure 4-6E). I also tested whether the Prp38 homology domain of dPrp38 (amino acids 1-180, HA-dPrp38Δ) was sufficient to mediate its interaction with dMFAP1. While small amounts of dMFAP1 are recovered in the HA-dPrp38PΔ precipitate, no HA-dPrp38PΔ protein can be detected in the dMFAP1 precipitate (Figure 4-6F). Thus, whereas the Prp38 homology domain of dPrp38 might be sufficient for its interaction with dMFAP1, the presence of additional 86 amino acids in HA-dPrp38P appears to be required for full binding ability. In conclusion, dMFAP1 binds to the N-terminus of dPrp38 via its C-terminus.

4.1.9 dMFAP1 forms a complex with several splice factor homologues

Given the direct interaction between dMFAP1 and dPrp38 and the fact that MFAP1 is present in several human spliceosomal fractions, I wanted to establish whether dMFAP1 interacts with other components of the spliceosome. I performed a large-scale purification of endogenous dMFAP1 from *Drosophila* S2 cells using the anti-MFAP1 antibody (see materials and methods). Proteins isolated in complex with dMFAP1 were subjected to SDS-PAGE, visualised by G-colloidal concentrate staining, and identified by mass spectrometry (Figure 4-7A).

The majority of proteins isolated in complex with dMFAP1 are predicted or known to function in splicing (Table 4-2). These include dPrp38/Prpf38a/Prp38p, three U5 snRNP proteins CG8877/U5-220kD/Prp8p, CG5931/U5-200kD/Brr2p and CG3436/U5-40kD/Rsa4p, one component of the NTc/Cdc5-Prp19 complex, CG6905/Cdc5/Cef1p, and CG2173/DDX27/Drs1p (Drosophila/Humans/Yeast), which are conserved in yeast, and Hfp/Puf60, CG4602/Srp54, and CG6995/Safb2 (flies/humans) that are conserved among higher eukaryotes. Notably, CG8877/U5-220kD/Prp8p and CG6905/Cdc5/Cef1p, which function in the activation step of the yeast spliceosome (Chan and Cheng, 2005; Chan et al., 2003; Kuhn et al., 1999; Kuhn et al., 2002), were isolated in complex with both dPrp38 and dMFAP1. Also recovered in the dMFAP1 purification was the DExD/H-box RNA helicase CG5931/U5-

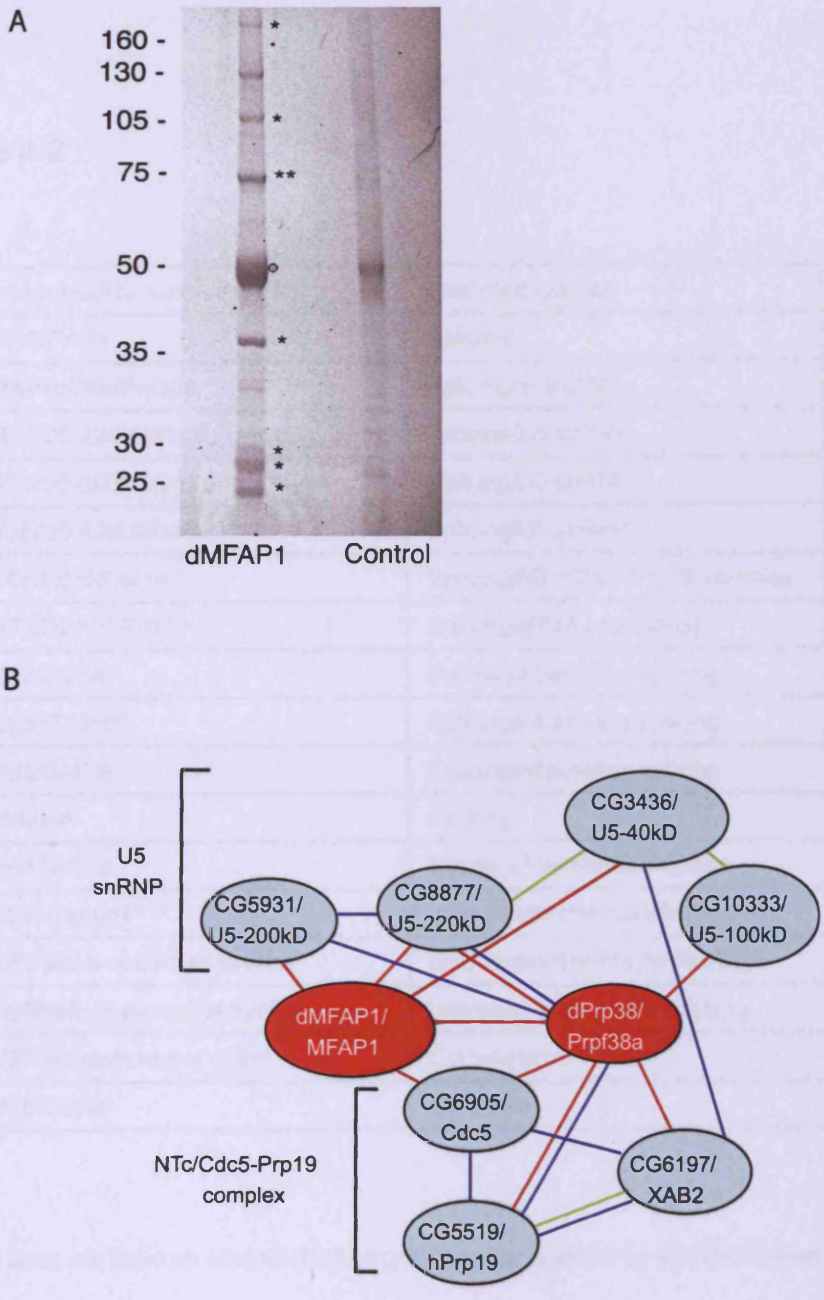

Figure 4-7: dMFAP1 associates with several splicing factors that are implicated in spliceosome activation. (A) To identify dMFAP1-associated proteins, purifications were performed form S2 cells using anti-dMFAP1 or anti-GFP (control) antibodies. The final eluates were resolved on a SDS-PAGE gel, and stained with Brilliant Blue G-colloidal concentrate. Visible bands (indicated by asterisks) were excised and identified by MALDI-TOF mass spectrometry. The band corresponding to dMFAP1 is indicated by two asterisks. Proteins isolated in complex with endogenous dMFAP1 are summarised in Table 4-2. (B) Schematic overview of some of the proteins isolated in comlex with dPrp38 and/or dMFAP1 (red) and previously reported interactions of the homologues in yeast (blue) or humans (green) (www.thebiogrid.org). Both the *Drosophila* and human IDs are indicated in the schematic. A line connecting two proteins indicates that they have been purified together using one or both of them as bait.

Table 4-2

ID (Drosophila/Humans/Yeast[1])	Predicted function
dMFAP/MFAP1	Splicing
dPrp38/Prpf38a/Prp38p	Splicing/tri-snRNP
CG8877/U5-220kD/Prp8	Splicing/U5 snRNP
CG5931/U5-200kD/Brr2p	Splicing/U5 snRNP
CG3436/U5-40kD/Rsa4p	Splicing/U5 snRNP
CG6905/Cdc5/Cef1p	Splicing/NTc/Cdc5-Prp19 complex
CG2173/DDX27/Drs1p	Splicing/rRNA processing
CG4602/Srp54	Splicing/Alternative splicing
CG12085/PUF60	Splicing/Alternative splicing
CG6995/SAF-B	Splicing/Alternative splicing
Pinin/MemA	Splicing
Abstrakt/Ded1p	Splicing/Translation initiation
CG11098/Tango1	Intercompartmental trafficking
CG7961/alpha-coatomer subunit	Intercompartmental trafficking
CG6699/beta-coatomer subunit	Intercompartmental trafficking
CG17927/Myosin heavy chain	Cytoskeleton
CG1676/Cactin	Unknown

[1]Protein does not have an obvious homologue in yeast, and the fly and the human IDs are indicated.

200kD/Brr2p, which in yeast is required for release of the U4 snRNP and activation of the spliceosome (Raghunathan and Guthrie, 1998). This suggests that dPrp38 and dMFAP1 might both function during the activation step of the spliceosome cycle.

Based on my results (Table 4-1 and Table 4-2) and data in the literature, I have generated a schematic overview of putative protein-protein interactions between some of the proteins that were purified in complex with dPrp38 and/or dMFAP1 (Figure 4-7B). Interestingly, dPrp38 and dMFAP1 are both associated with multiple U5 snRNP proteins and one or several components of the NTc/Cdc5-Prp19 complex, suggesting that they might bridge an interaction between the two complexes.

4.1.10 dMFAP1 is required for pre-mRNA processing

The observations that dMFAP1 interacts directly with dPrp38 (Figure 4-6A-B) and can be isolated in complex with several splicing factor homologues (Table 4-2) suggest that dMFAP1 might function in pre-mRNA processing. To further investigate this, I used the *γ-tubulin* transcript as a read-out to study the requirement for dMFAP1 in pre-mRNA processing. Using quantitative RT-PCR to measure *γ-tubulin* pre-mRNA and mRNA levels, I observed a 70-84% decrease in *γ-tubulin* mRNA levels accompanied by a 3.4-7.3-fold increase in *γ-tubulin* pre-mRNA levels in cells depleted of dMFAP1, dPrp38 or the well-characterised splicing factor CG8877/Prp8p (Drosophila/yeast) compared with control cells (Figure 4-8A). I also examined the effect of reducing dMFAP1 protein levels on pre-mRNA processing of other transcripts including *hippo*, *dmcrs2*, and *eIF3-S10* (Figure 4-8B-C). For these transcripts, I observed an about 40% reduction in mRNA levels (Figure 4-8B) accompanied by a 7-10-fold increase in pre-mRNA levels (Figure 4-8C) in dMFAP1-depleted cells compared with control cells. Thus, dMFAP1 is indeed required for pre-mRNA processing.

4.1.11 *dmfap1* is an essential gene

Having confirmed that dMFAP1 is a spliceosome-associated protein, I next wanted to study the *in vivo* requirement for dMFAP1. Initially, I set out to generate a *dmfap1* deletion mutant by mobilisation of a P-element (GE5102) inserted approximately 1 kb upstream of the coding region of *dmfap1*. About one thousand putative *dmfap1* mutants were screened for imprecise excisions by PCRs, but no imprecise excisions of the P-element were recovered (data not shown). Instead I used a

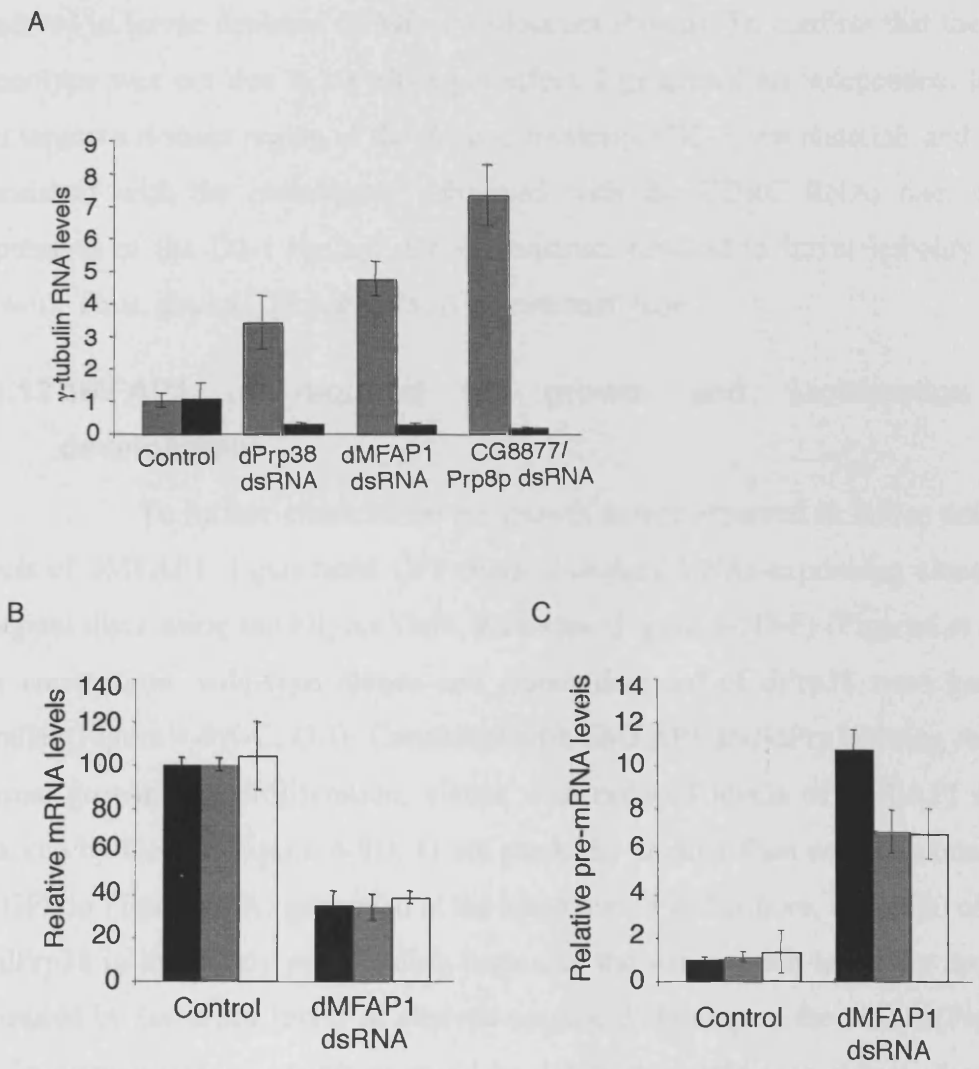

Figure 4-8: dMFAP1 is required for pre-mRNA processing. (A) Total RNA was extracted from S2 cells treated with dsRNA targeting *eGFP* (control), *dprp38*, *dmfap1*, or *CG8877/prp8* for four days, and *γ-tubulin* mRNA (black) and pre-mRNA (grey) levels were measured after 1st strand synthesis by qPCRs (see materials and methods). (B-C) Total RNA was extracted from S2 cells treated with dsRNA targeting *eGFP* (control) or *dmfap1*, and *hippo* (black), *dmcrs2* (grey), or *eIF3-S10* (white) mRNA (B) and pre-mRNA (C) levels were measured after 1st strand synthesis by qPCRs. (A-C) mRNA and pre-mRNA levels were compared between different samples by normalisation to levels of the intronless *his3* transcript.

transgenic *dmfap1* RNAi line from VDRC to study dMFAP1 loss of function phenotypes. Ubiquitous expression of the *dmfap1* RNAi construct caused lethality at the larval stage. The lethality is likely to be a consequence of the severe growth defect observed in larvae depleted of MFAP1 (data not shown). To confirm that the observed phenotype was not due to an off-target effect, I generated an independent RNAi line that targets a distinct region of the *dmfap1* transcript (D2-1, see materials and methods). Consistent with the phenotype I observed with the VDRC RNAi line, ubiquitous expression of the D2-1 dmfap1 RNAi construct resulted in larval lethality (data not shown). Thus, *dmfap1*, like *dprp38*, is an essential gene.

4.1.12 dMFAP1 is required for growth and proliferation during development

To further characterise the growth defect observed in larvae with reduced levels of dMFAP1, I generated GFP-marked *dmfap1* RNAi-expressing clones in wing imaginal discs using the Flipout/Gal4 technique (Figure 4-9D-F) (Pignoni et al., 1997). For comparison, wild-type clones and clones depleted of dPrp38 were generated in parallel (Figure 4-9A-C, G-I). Consistent with dMFAP1 and dPrp38 being required for normal growth and proliferation, clones with reduced levels of dMFAP1 or dPrp38 (marked by GFP in Figure 4-9D, I) are markedly smaller than control clones (marked by GFP in Figure 4-9A) generated at the same time. Furthermore, depletion of dMFAP1 or dPrp38 in the highly proliferating region of the wing pouch results in apoptosis, as measured by increased levels of cleaved-caspase 3 staining in the clones (Figure 4-9E, H). In comparison, no apoptosis could be detected in wild-type clones (Figure 4-9B). Thus, normal levels of dMFAP1 and dPrp38 are required for clonal growth and survival in proliferating tissue.

4.1.12.1 dPrp38 and dMFAP1 gain of function causes an overgrowth phenotype

To study dMFAP1 and dPrp38 gain of function phenotypes, I used *UAS-dprp38* and *UAS-dmfap1* transgenic animals that had been generated by Julien Colombani (see Materials and Methods). *UAS-GFP* (control), *UAS-dprp38*, and *UAS-dmfap1* transgenic animals were crossed to flies carrying the *engrailed-Gal4* transgene to drive the expression of GFP (control), dPrp38 or dMFAP1 in the posterior compartment of the wing. The crosses were carried out under density-controlled conditions, since over-crowded conditions might affect the availability of nutrients

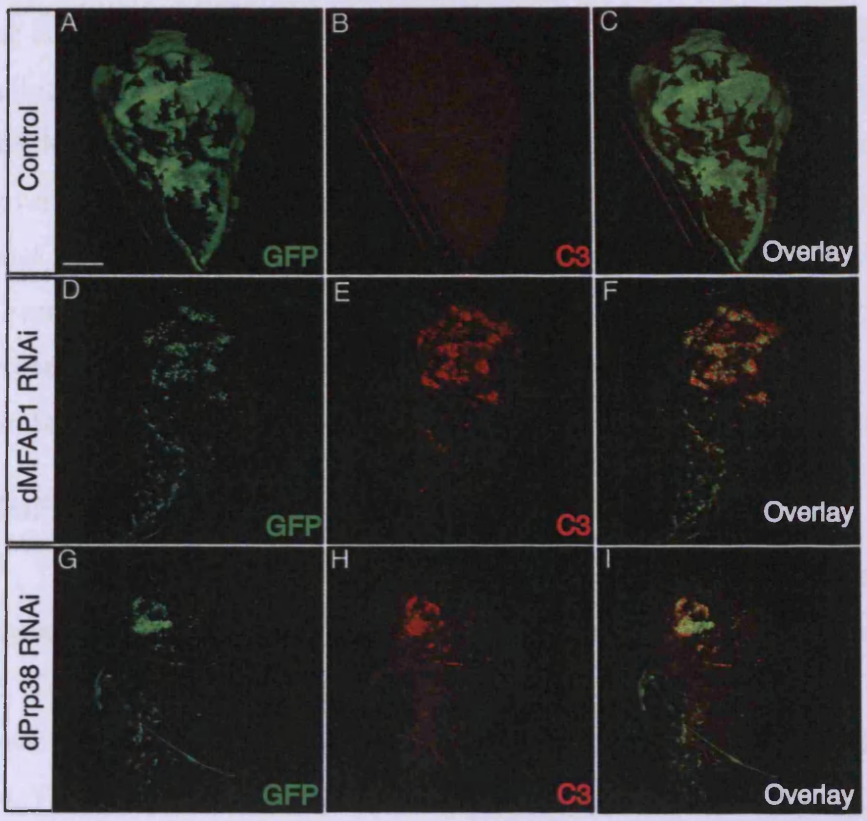

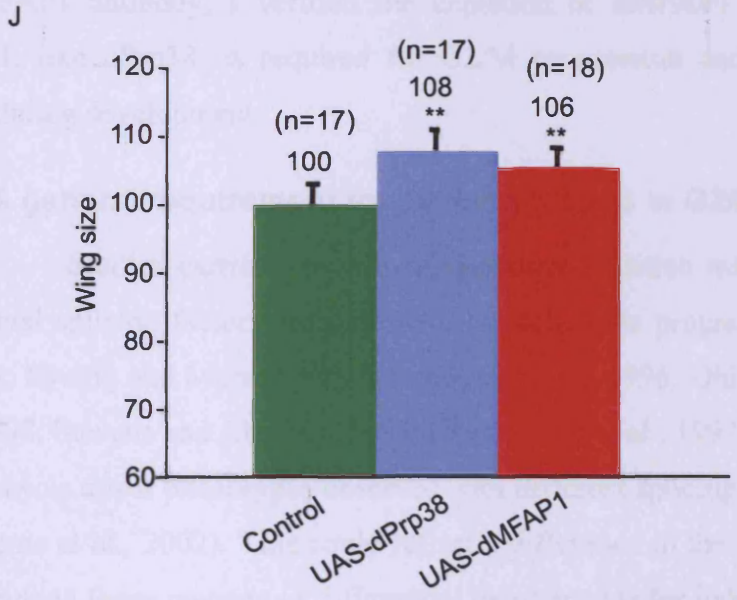

Figure 4-9: *In vivo* characterisation of dMFAP1. (A-I) Wing imaginal discs from third instar larvae. Posterior is to the right. Wild-type clones (A-C) or clones expressing *dprp38* and *dmfap1* RNAi constructs (D-I) were generated using the FLPout technique (marked by GFP in A, D, G). Clones with reduced levels of dMFAP1 (D-F) or dPrp38 (G-I) are smaller than control clones (A-C) generated at the same time and undergo apoptosis as measured by increased levels of cleaved-caspase 3 staining in the clones (red in E, H). (J) Ectopic expression of dPrp38 or dMFAP1 in the posterior compartment of the wing results in an over-growth phenotype. dPrp38, dMFAP1, or GFP (control) were expressed in the posterior compartment of the wing using the engrailed-Gal4 driver and the wing areas were measured (see Materials and methods). The number of wing used for each genotype is indicated (n). ** Indicates that $p<0.01$, using a students t-test.

during the larval growth phase and thus the final organ size in the adult fly. The area of the engrailed domain of female wings in the adult F1 progeny was quantified in each cross (see Materials and Methods). dMFAP1 and dPrp38 gain of functions cause modest overgrowth phenotypes (Figure 4-9J). Thus, Gal4-UAS-driven expression of dPrp38 and dMFAP1 results in an 8% and 6% increase in the area of the engrailed domain. From these data, it cannot be concluded if the observed overgrowth is the result of increased proliferation or growth rates or and extended period of growth/proliferation. I did not study the overgrowth phenotypes in more detail.

4.1.13 dMFAP1 is required for G2/M progression

To further investigate the growth/proliferation defect observed in *dmfap1* mutant tissue, I analysed the DNA profile from cultured *Drosophila* S2 cells depleted of dMFAP1. Consistent with my *in vivo* results, dsRNA-mediated depletion of dMFAP1 slows down proliferation (data not shown) and cells eventually arrest in G2/M (Figure 4-10A-B). Thus, in cells depleted of dMFAP1 the ratio of cells in G1 and G2/M is 0.42 (Figure 4-10B) compared with 1.20 for control treated cells (Figure 4-10A). Using my anti-dMFAP1 antibody, I verified the depletion of dMFAP1 (Figure 4-10C). Thus dMFAP1, like dPrp38, is required for G2/M progression and for proliferation and growth during development.

4.1.14 A general requirement for splicing factors in G2/M progression

Studies carried out with temperature-sensitive mutants in yeast suggest that several splicing factors are important for cell cycle progression (Boger-Nadjar et al., 1998; Hwang and Murray, 1997; Lundgren et al., 1996; Ohi et al., 1998; Potashkin et al., 1998; Stevens and Abelson, 1999; Urushiyama et al., 1997; Vaisman et al., 1995). The cell cycle arrest phenotypes observed with different splicing factor mutants seem to vary (Burns et al., 2002). This could reflect a difference in the severity of the splicing defects among those mutants or differential requirements for individual splicing factors. My data (Fig. 4J-L) and some evidence from mammalian cells suggest that in higher eukaryotes at least certain splicing factors are required for the G2/M transition (Bernstein and Coughlin, 1998; Li et al., 2005a; Pacheco et al., 2006). However, it is unclear whether this cell cycle arrest phenotype is general, or whether inactivation of different core components of the metazoan spliceosome would give rise to the same variability in cell cycle arrest phenotypes reported in yeast. To address this, I analysed

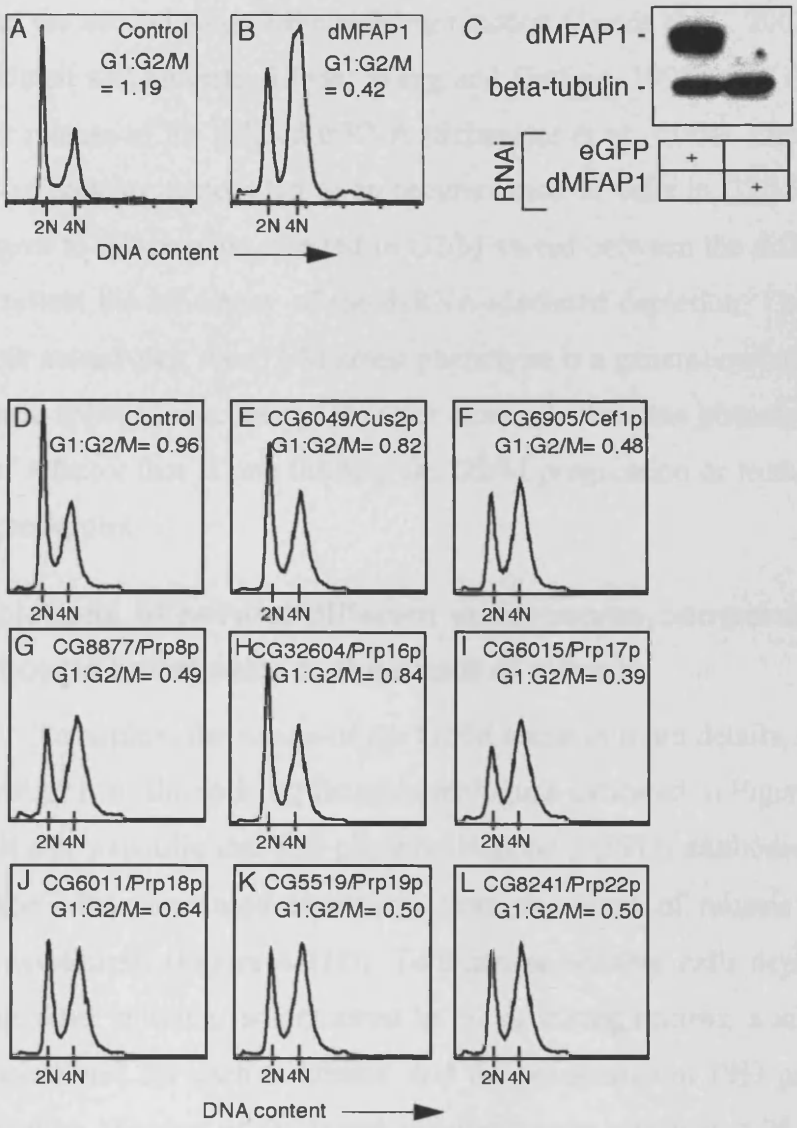

Figure 4-10: Depletion of dMFAP1 and several core components of the spliceosome results in G2/M arrest. (A-L) Cells depleted of dMFAP1 or other splicing factors arrest in G2/M. S2 cells were treated with dsRNA targeting *GFP* (control), *dmfap1*, or other splicing factors for three days. Cells were fixed, stained with propidium iodide, and analysed by flow cytometry. The ratio of cells in G2/M relative to G1 is indicated for each treatment (G1:G2/M). (C) Immunoblotting confirms that dMFAP1 protein levels are reduced in cells treated with dsRNA targeting *dmfap1* compared with control cells. Anti-β-tubulin is used as a loading control.

the DNA profile from S2 cells treated with dsRNAs targeting a range of *Drosophila* homologues of yeast splicing factor (Figure 4-10D-L). These include Cus2p, which functions in the recruitment of U2 to the branch region (Perriman and Ares, 2000), Cef1p and Prp19p, which are required for maturation of the spliceosome (Chan and Cheng, 2005; Chan et al., 2003; Tsai et al., 1999), Prp8p, Prp16p, Prp17p, and Prp18p, which act in the second step of the splicing reaction (James et al., 2002a; Schneider et al., 2002; Umen and Guthrie, 1995a; Wang and Guthrie, 1998), and Prp22p, which is required for release of the spliced mRNA (Schneider et al., 2004). Depletion of any of these putative splicing factors led to an accumulation of cells in G2/M (Figure 4-10D-L). The degree to which cells arrested in G2/M varied between the different treatments and might reflect the efficiency of the dsRNA-mediated depletion. These data suggest that in higher eukaryotes, the G2/M arrest phenotype is a general outcome of interfering with the basic splicing machinery. It is not clear whether this phenotype is due to the depletion of a factor that is rate limiting for G2/M progression or to the activation of a cell cycle checkpoint.

4.1.15 Depletions of several different spliceosome components results in cell cycle arrest prior to the onset of mitosis

To explore the nature of the G2/M arrest in more details, cells depleted of dPrp38, dMFAP1, or the splicing factor homologues indicated in Figure 4-10D-L were stained with anti-γ-tubulin and anti-phospho-Histone 3 (PH3) antibodies. The anti-PH3 antibody labels the condensed chromatin from the onset of mitosis (Figure 4-11A) through to cytokinesis (Figure 4-11D). To examine whether cells depleted of dPrp38, dMFAP1, or other splicing factors arrest in G2 or during mitosis, a minimum of 1200 cells were examined for each treatment, and the percentage of PH3 positive cells was scored. Depletion of either of the tested splicing factors results in a 26-100% reduction in the number of PH3 positive cells relative to that of control cells (Figure 4-11E). I did not note the accumulation of cells at any stage of mitosis. This suggests that these splicing factor-deficient cells are arrested in G2, prior to chromosome condensation, rather than at a later stage during mitosis.

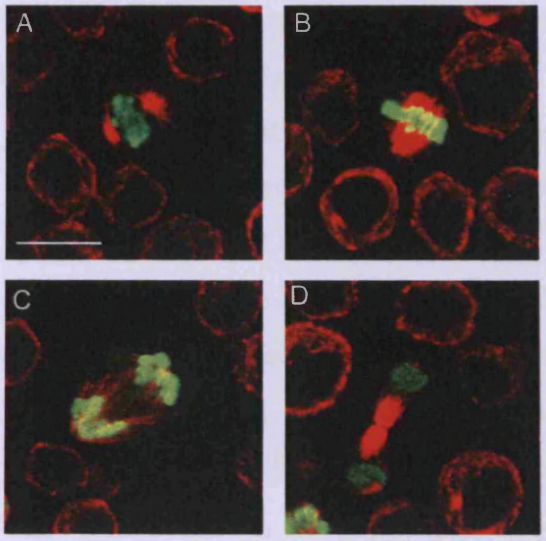

E

ID (Drosophila/Humans/Yeast[1])	Phospho-Histone 3 positive cells (%) relative to control cells
Control	100
CG6049/Cus2p/Tat-SF1	73.4
CG32604/Prp16p/DHX38	65.8
CG8241/Prp22p/DHX8	50.5
dPrp38/Prpf38a/Prp38p	36.4
CG6015/Prp17p/Cdc40	34.7
dMFAP1/MFAP1	28.3
CG8877/U5-220kD/Prp8p	17.6
CG6011/Prp18p/Prpf18	12.5
CG5519/hPrp19/Prp19p	4.1
CG6905/Cdc5/Cef1p	0

Figure 4-11: Depletion of several components of the spliceosome results in G2/M arrest. (A-D) S2 cells stain positive for phospho-histone 3 (PH3) from the onset of mitosis (A), through metaphase (B) and anaphase (C) to cytokinesis (D). S2 cells were stained with anti-γ-tubulin (in red) and anti-PH3 (in green) antibodies. (A) The scale bar is at 100 μM. (E) Depletion of various splicing factor homologues results in a decrease in numbers of PH3-positive cells. Cells were treated with dsRNA targeting the indicated proteins for four days and stained with anti-γ-tubulin and anti-PH3 antibodies. For each set-up, the percentage of PH3-positive cells relative to that of control cells was calculated by examining a minimum of 1200 cells. [1]When a protein does not have an obvious homologue in yeast, the fly and human IDs are indicated.

4.1.16 Depletion of dPrp38 or dMFAP1 causes a reduction in *stg/cdc25* mRNA levels

In *Drosophila*, mitosis is triggered by a temporally controlled burst of *string/cdc25* (*stg*) transcription (Edgar and O'Farrell, 1989). Stg is a phosphatase, which activates the mitotic kinase Cdk1 and is essential for G2/M progression. In addition to the transcriptional regulation of *stg* mRNA levels, the presence of an intron in the *stg* transcript implies that *stg* mRNA levels are critically dependent on a functional spliceosome. Thus, the observation that depletion of dPrp38, dMFAP1, and a number of core splicing factor homologues cause cells to arrest in G2/M (Figure 4-10) suggests that *stg* mRNA levels might be affected under those conditions. To investigate this, I measured *stg* mRNA levels in cells depleted of dMFAP1, dPrp38, or the well-characterised splicing factor CG8877/Prp8p (flies/yeast). As expected, treating cells with dsRNA targeting *dmfap1*, *dprp38*, or *CG8877/prp8* caused cells to arrest in G2/M (Figure 4-12A-F). Using quantitative RT-PCR to measure *stg* mRNA levels, I observed an 83-96% decrease in *stg* mRNA in cells depleted of dMFAP1, dPrp38 or CG8877/Prp8p compared with control cells (Figure 4-12G). The observed decrease in mRNA levels could be due to a defect in processing of the *stg* pre-mRNA or could be an indirect effect caused by interference of a factor required for regulation of *stg* transcription. Attempts to measure *stg* pre-mRNA levels by quantitative RT-PCR were unsuccessful (data not shown). This is most likely due to the low level and instability of *stg* pre-mRNA. Consistent with this idea, it has previously been reported that many pre-mRNAs do not accumulate in response to a defective spliceosome, but are degraded by the exosome complex (Bousquet-Antonelli et al., 2000).

4.2 Discussion part II

4.2.1 A conserved function of Prp38p in higher eukaryotes

The essential budding yeast protein, Prp38p, was the first protein shown to function in maturation of the spliceosome. Prp38p is dispensable for the initial assembly of the spliceosome, but is required for the release of the U4 snRNP and activation of the spliceosome (Xie et al., 1998). Homologues of Prp38p have been identified in higher eukaryotes, but the conservation of the primary sequence is poor. Thus, Prp38p is only 24 and 22% identical to Prpf38a (humans) and dPrp38 (flies), respectively. In contrast,

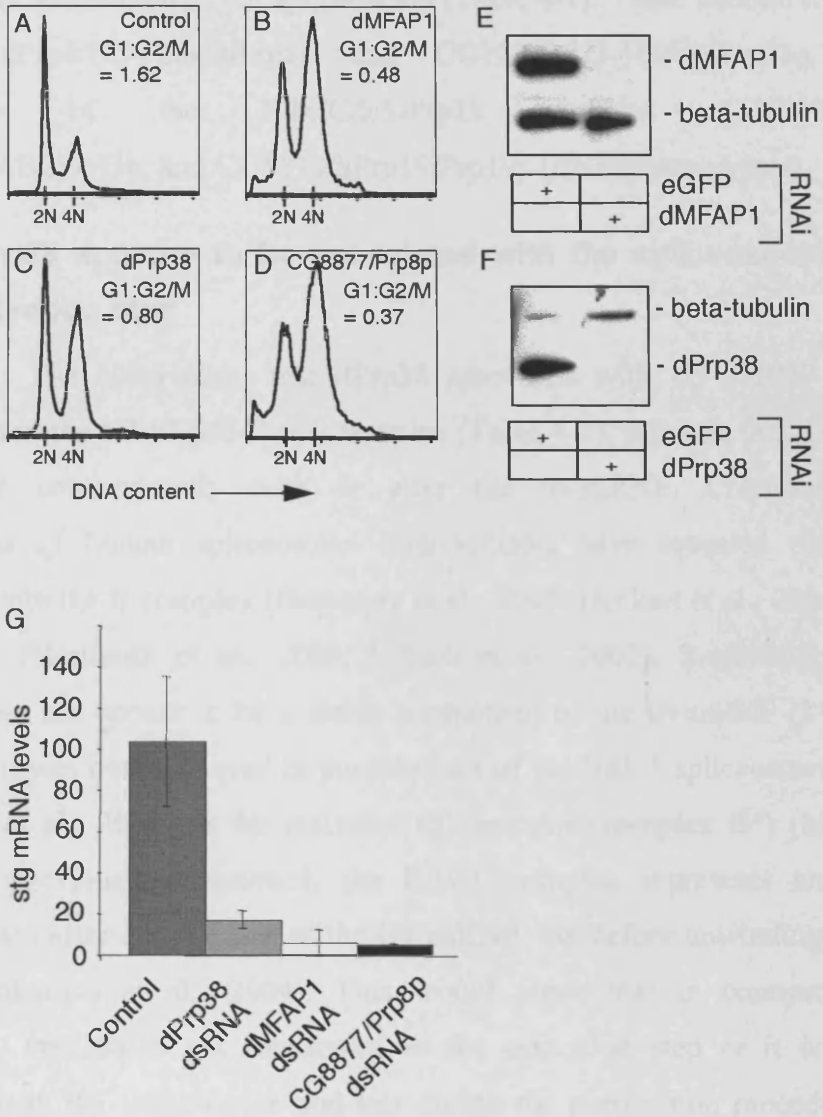

Figure 4-12: Depletion of dPrp38 or dMFAP1 causes a reduction in *stg* mRNA levels. (A-D) S2 cells were treated with dsRNA targeting *GFP* (control) or genes encoding the indicated products for three days. Cells were fixed, stained with propidium iodide, and analysed by flow cytometry. The ratio of cells in G2/M relative to G1 is indicated for each treatment. (E-F) The effectiveness of dPrp38 and dMFAP1 depletions were assayed by immuno-blotting. (G) In parallel, total RNA was extracted from cells and *stg* mRNA levels were measured after 1st strand synthesis by quantitive PCR (see materials and methods). *stg* mRNA levels were compared between the different samples by normalisation to mRNA levels of α-tubulin.

dPrp38 is 75% identical to Prpf38a. Despite the low level of homology between Prp38p and its homologues in higher eukaryotes, my data suggest that its function may be conserved in metazoans. Thus, mass spectrometry analysis of proteins isolated in complex with dPrp38 revealed a number of splicing factor homologues that have been implicated in maturation of the spliceosome (Table 4-1). These include two U5 snRNP proteins, dPrp8/U5-220kD/Prp8p and CG10333/U5-100kD/Prp28p, and three components of the NTc/Cdc5-Prp19 complex CG6905/Cdc5/Cef1p, CG9143/XAB2/Syf1p, and CG5519/hPrp19/Prp19p (flies/humans/yeast).

4.2.2 dPrp38 appears to be associated with the spliceosome during the activation step

The observation that dPrp38 associates with U5 snRNP proteins and components of the NTc/Cdc5-Prp19 complex (Table 4-1), suggests that it might join the spliceosome concomitantly with or after the tri-snRNP. Consistent with this, purifications of human spliceosome intermediates have revealed that Prpf38a is associated with the B complex (Bessonov et al., 2008; Deckert et al., 2006), but not the A complex (Hartmuth et al., 2002; Urlaub et al., 2002). Surprisingly, in humans Prpf38p does not appear to be a stable component of the tri-snRNP (Makarov et al., 2002), and it was not recovered in purifications of the BΔU1 spliceosome intermediate (Makarova et al., 2004) or the activated spliceosome (complex B*) (Makarov et al., 2002). As previously mentioned, the BΔU1 complex represents an intermediate activation step after dissociation of the U1 snRNP, but before unwinding of the U4/U6 duplex (Makarova et al., 2004). This would argue that in contrast to its yeast counterpart, Prpf38a is not implicated in the activation step or it is very loosely associated with the spliceosome and lost during the purification procedures. My data favours the latter possibility. Thus, dPrp38 associates with several components of the Cdc5-Prp19 complex, which in humans appear to be stably associated with the BΔ1U and B* complexes (Makarov et al., 2002; Makarova et al., 2004), but not the B complex (Makarova et al., 2004). Thus, my data suggest that, like yeast Prp38p, dPrp38 joins the spliceosome concomitantly with the tri-snRNP and stays associated with the spliceosome during at least part of the activation step.

4.2.3 What is the molecular function of dPrp38 in spliceosome activation?

The integral U5 snRNP protein CG8877/Prp8p (Lossky et al., 1987; Stevens et al., 2001) was recovered in both my dPrp38 (Table 4-1) and dMFAP1 (Table 4-2) purifications. Consistent with the recovery of CG8877/Prp8p in my dPrp38 purification, budding yeast *prp38* and *prp8* were previously found to interact genetically. Prp8p is the largest known nuclear yeast protein and it is thought to play a scaffold-like role in the spliceosome by forming numerous interactions with the pre-mRNA, snRNPs, and splice factors. Genetics suggest that Prp8p regulates unwinding of the U4/U6 duplex and plays a central role in the release of U4 snRNP and activation of the spliceosome. Consistent with this, Prp8p interacts physically and genetically with Brr2p, the RNA helicase that is thought to be responsible for the unwinding of the U4/U6 double helix.

Xie and co-workers have proposed a model in which Prp38p recruits (or activates) an RNA unwinding activity necessary for U4 snRNP release and U6 snRNA integration into the active site of the spliceosome. It is tempting to speculate that Brr2p might represent this RNA unwinding activity. The ability of Brr2p to interact directly with Prp8p would argue against a role of dPrp38 in recruitment of CG5931/Brr2p. However, dPrp38 could form a weak interaction with CG5931/Brr2p sufficient for its activation, or dPrp38 could recruit a factor required for activation of CG5931/Brr2p. As previously mentioned, Snu114p is thought to function upstream of Brr2p to regulate its activity required for unwinding of the U4/U6 duplex (Small et al., 2006). However, CG4849/Snu114p is most likely not recruited to the spliceosome by dPrp38 since Snu114p, like Brr2p, interacts directly with Prp8p (Achsel et al., 1998; van Nues and Beggs, 2001a). Thus, it is not clear if/how dPrp38 might facilitate U4 snRNP release during spliceosome activation.

Interestingly, the NTc/Cdc5-Prp19 complex components, CG5519/Prp19p and CG6905/Cef1p, were both isolated in complex with dPrp38 (Table 4-1). In budding yeast, the NTc joins the spliceosome after U1 and U4 snRNP release, but before the first catalytic step and is required for spliceosome activation. Thus, dPrp38 might have an additional function after U4 snRNP release to facilitate NTc/Cdc5-Prp19 complex recruitment and/or spliceosome activation.

4.2.4 dMFAP1 appears to be associated with the spliceosome during the activation step

In addition to homologues of known splicing factors, I identified a previously uncharacterised protein, dMFAP1, which binds directly to dPrp38 (Table 4-1 and Figure 4-6A-B). Human MFAP1 has been recovered in a number of spliceosome purifications, but was initially discarded as a contaminant due to its proposed extracellular localisation (Neubauer, 2005; Neubauer et al., 1998). Here I show that dMFAP1, like dPrp38, functions in pre-mRNA processing (Figure 4-8) and is associated with several conserved splicing factors including dPrp38, the U5 snRNP proteins CG8877/U5-220kD/Prp8p, CG3436/U5-40kD/Rsa4p, and CG5931/U5-200kD/Brr2p and the NTc/Cdc5-Prp19 core component, CG6905/Cdc5/Cef1p (Table 4-2). Consistent with the association of dMFAP1 with U5 snRNP proteins and a component of the NTC/Cdc5-Prp19 complex, human MFAP1 was previously recovered in purifications of B, BΔ1U and B* complexes (Bessonov et al., 2008; Deckert et al., 2006; Makarov et al., 2002; Makarova et al., 2004), but not A complexes (Hartmuth et al., 2002). Thus, dMFAP1/MFAP1 might join the spliceosome simultaneously with dPrp38/Prpf38a, but seems to be more tightly associated with the spliceosome during the activation step. Moreover, MFAP1 was not recovered in spliceosome complexes after the first catalytic step, suggesting that it functions during the activation step (Bessonov et al., 2008; Jurica et al., 2002).

4.2.5 A function of dMFAP1 in alternative splicing?

In addition to highly conserved spliceosome components, dMFAP1 also formed a complex with a number of splicing factors that have evolved more recently in metazoans. Unsurprisingly, most of these function in regulation of alternative splicing. Thus, *CG4602/srp54*, *CG6995/saf-b*, and *hfp/puf60* were all recovered in a RNAi screen for regulators of alternative splicing, which included 70% of all genes encoding known Drosophila RNA-binding proteins (Park et al., 2004). This is consistent with the idea that additional splicing factors have evolved in metazoans to accommodate more complex splice patterns. As expected, very few core splicing components were found to regulate alternative splicing. An interesting exception is CG5931/Brr2p, which I isolated in complex with dMFAP1 (Park et al., 2004). dMFAP1 is highly conserved among higher eukaryotes, but not in yeast, indicating that it has evolved more recently. Notably, dMFAP1 does not contain a conserved RNA-binding motif and was not

included in the screen carried out by Park and co-workers (Park et al., 2004). Thus, it remains to be determined whether dMFAP1 might regulate alternative splicing in higher eukaryotes.

4.2.6 dPrp38 and dMFAP1 protein levels affect growth and proliferation during development

My *in vivo* studies revealed that dPrp38 is required for growth and proliferation (Figure 4-2 and 4-9A-I). Thus, flies homozygous for the $dprp38^{E1}$ mutation die as first instar larvae, but can be rescued to viability by Gal4-UAS-driven ubiquitous expression of dPrp38 (Brand et al., 1994). Moreover, $dprp38^{E1}$ mutant tissue fail to grow in a wild-type background, suggesting that the $dprp38^{E1}$ mutation is a functional null or a strong hypomorph. The inability of $dprp38^{E1}$ mutant tissue to grow in a wild-type background is not only the due to elimination by cell competition, since only small $dprp38^{E1}$ mutant clones are recovered in a growth compromised (*Minute*) background (Figure 4-2). This shows that dPrp38 is intrinsically required for growth and proliferation and is consistent with an essential function dPrp38 in splicing. My *in vivo* studies also showed that dMFAP1 is an essential protein required for normal growth during development. Thus, flies with reduced levels of dMFAP1 are severely growth compromised and die at the larval stage. Consistent with this, clones of mutant tissue with reduced levels of dMFAP1 exhibit proliferation and growth defects and undergo apoptosis (Figure 4-9A-F). Thus, dMFAP1 and dPrp38 might both perform essential functions in pre-mRNA processing.

Interestingly, dPrp38 and dMFAP1 gain of functions result in modest overgrowth phenotypes (Figure 4-9J). It is not clear though if/how the overgrowth phenotypes are linked with a role of dPrp38 and dMFAP1 in splicing. Moreover, it cannot be concluded whether excess growth is due to an extended period of growth or to increased proliferation/growth rates (Figure 4-9J). Future experiments will provide a more detailed analysis of the overgrowth phenotypes. First, by counting the number of cells within fixed areas of wild-type and dPrp38 or dMFAP1 gain of function tissue, it can be determined whether the overgrowth phenotype is due to an increase in cell size or excess proliferation. Second, the proliferation rates of dPrp38 and dMFAP1 gain-of-function cells can be analysed by inducing Flipout-GAL4 clones at fixed time points and comparing clonal growth rates with those of control clones.

4.2.7 dPrp38 is required for G2/M progression

As mentioned above, my *in vivo* data show that dPrp38 LOF results in a severe growth and proliferation defect. A more detailed analysis in cultured cells shows that dPrp38 is required for G2/M progression (Figure 4-3). Thus, dPrp38-depleted cells gradually accumulate in G2/M in response to decreased levels of dPrp38. BrdU pulse-labelling experiments confirm that the majority of dPrp38-depleted cells fail to progress through mitosis (Figure 4-4). Importantly, dPrp38-depleted cells progress through S phase with normal kinetics, indicating that dPrp38 only becomes rate-limiting upon entry into mitosis. Though it cannot be excluded that the transition from G1 to S phase occurs with slower kinetics in cells depleted of dPrp38, the gradual accumulation of dPrp38-depleted cells in G2/M in response to decreasing levels of dPrp38 (Figure 4-3) and the severe delay or lack of progression through mitosis (Figure 4-4) strongly suggest that G2/M progression is the main rate-limiting step.

4.2.8 A general requirement for splicing factors in G2/M progression in higher eukaryotes?

In yeast, a subset of genes with known functions in splicing has also been implicated in cell cycle progression. These include *PRP3*, *PRP17*, *PRP8*, *CEF1*, *PRP22* (*S. cerevisiae*) (Boger-Nadjar et al., 1998; Hartwell et al., 1973; Hwang and Murray, 1997; Johnston and Thomas, 1982; Ohi et al., 1998; Shea et al., 1994; Vaisman et al., 1995) and *PRP1*, *PRP2*, *PRP5*, *PRP6*, *CDC28/PRP8*, *CDC5*, and *PRP12* (*S. pombe*) (Habara et al., 2001; Lundgren et al., 1996; Nurse et al., 1976; Ohi et al., 1994; Potashkin et al., 1998; Takahashi et al., 1994; Urushiyama et al., 1997). Whereas mutations in some genes encoding splicing factors cause cells to arrest heterogeneously throughout the cell cycle, *cef1-13*, *prp17Δ*, and *prp22-1* mutants arrest homogenously in G2/M (Burns et al., 2002). A model has been put forward to explain the variability of the timing of cell cycle arrest, which suggests that splicing factors are differentially required for efficient splicing of single transcripts or a subset of transcripts (Burns et al., 2002). Consistent with this idea, removal of a single intron from the α-tubulin encoding *TUB1* gene alleviates both the G2/M arrest and cell division defect observed in the *cef1-13* mutant, but only partially rescues the cell division defect observed in *prp17Δ*, and *prp22-1* (Burns et al., 2002; Chawla et al., 2003). Instead, the G2/M arrest and growth defect in the *prp17Δ* mutant can be rescued by removal of an intron from the *ANC1*

gene (Dahan and Kupiec, 2004). The molecular basis for this specificity remains unclear.

The range of cell cycle phenotypes observed with different splicing factor mutants in yeast prompted me to study the requirement for various *Drosophila* splicing factors in cell cycle progression. I analysed the effect of individual depletions of splicing factors that are predicted to function at various stages of the spliceosome cycle. Depletion of any of those splicing factors caused cells to arrest in G2/M (Figure 4-10D-L), suggesting that it is a general consequence of interfering with spliceosome activity. Consistent with this, a genome wide screen RNA interference screen in HeLa cells for factors required for mitosis identified a number of genes encoding splicing factors (Kittler et al., 2004). However, it cannot be concluded whether the observed G2/M arrest results from of a failure to splice a pre-mRNA encoding a factor that is rate limiting for entry into mitosis, or whether a defect in splicing activates a mitotic checkpoint that causes cells to arrest in G2.

4.2.9 dPrp38 and dMFAP1 are required for normal *stg* mRNA levels

As mentioned above, the G2/M arrest observed in cells depleted of dPrp38, dMFAP1, and other splicing factors might be the consequence of a failure to splice a pre-mRNA encoding a factor that is rate limiting for entry into mitosis. In *Drosophila*, Stg activity is essential for G2/M progression and seems to be regulated at the transcriptional level. Thus, mitosis is triggered by a temporally controlled burst of *stg* transcription (Edgar and O'Farrell, 1989). This fluctuation in *stg* mRNA levels suggests that *de novo* transcription and/or processing of *stg* pre-mRNA is important and possibly rate-limiting for G2/M transition. Consistent with this idea, although not excluding other explanations, I found that depletion of dPrp38, dMFAP1 or CG8877/Prp8p cause a 83-96% reduction in *stg* mRNA levels and a G2/M arrest (Figure 4-12). Importantly, this decrease in *stg* mRNA levels could be due to a defect in splicing of *stg* pre-mRNAs or reduced levels of *stg* transcription. However, the observation that dPrp38 and dMFAP1 are both required for pre-mRNA processing (Figure 4-8) favours the idea that the reduction in *stg* mRNA levels is caused directly or indirectly by a defect in pre-mRNA processing. The presence of an intron in the *stg* pre-mRNA suggests that dPrp38, dMFAP1 or CG8877/Prp8p could be directly required for splicing of *stg* pre-mRNAs. However, attempts to detect *stg* pre-mRNA products in cells depleted of dPrp38, dMFAP1 or CG8877/Prp8p by RT-PCR were unsuccessful

(data not shown). This is most likely due to the low level and instability of *stg* pre-mRNA.

Chapter 5 – Results and discussion part III

5.1 Pixie associates with the 40S ribosomal subunit in an ATP-dependent manner and functions in translation initiation

5.1.1 Background to the Pixie project

pixie (*pix*) was identified in a genetic screen for molecules that regulate growth and interact with PI3K signalling (Coelho et al., 2005b). Female flies with a small-wing phenotype elicited by *MS1096-Gal4* driven expression of a dominant negative form of the catalytic subunit of PI3K ($Dp110^{KD}$) in the wings, were crossed to male flies that had been fed Ethyl methanesulfonate (EMS) to randomly mutagenise their genomes (Figure 5-1). The resultant progeny were screened for dominant suppression or enhancement of the $Dp110^{KD}$ small wing phenotype. One group of 7 mutant chromosomes isolated as enhancers in the screen exhibited lethality or reduced body size when placed in *trans* with each other and displayed a complex complementation pattern. The gene corresponding to two of these mutations (pix^{3c2} and pix^{3c3}, Figure 5-2), which are lethal *in trans* to each other, was mapped by meiotic recombination using visible markers and Single Nucleotide Polymorphisms (SNPs), and named *pixie* (Coelho et al., 2005b).

Carmen Coelho carried out a detailed *in vivo* study of different *pixie* loss of function mutations (Figure 5-2). This study showed that mutations in *pixie* have an unusual effect on fly growth that is similar to the effect of mutations in genes encoding ribosomal proteins. For example, weak *pixie* mutant combinations (pix^{L35}/pix^{L24} and pix^{L35}/pix^{L17}) and some heterozygous ribosomal protein mutants (*Minutes)* have slender bristles and show developmental delay, yet their final adult body size is near normal (Coelho et al., 2005a; Lambertsson, 1998). In addition, *pixie* and ribosomal protein mutant wing imaginal discs show complex defects in growth and cell survival that vary spatially and temporally (Coelho et al., 2005a). This phenotypic similarity suggested that the *pixie* growth phenotype might arise via an effect on translation. Consistent with this, depletion of Pixie was found to reduce global translation as measured by levels of [^{35}S]-cysteine and -methionine incorporation (Coelho et al., 2005a).

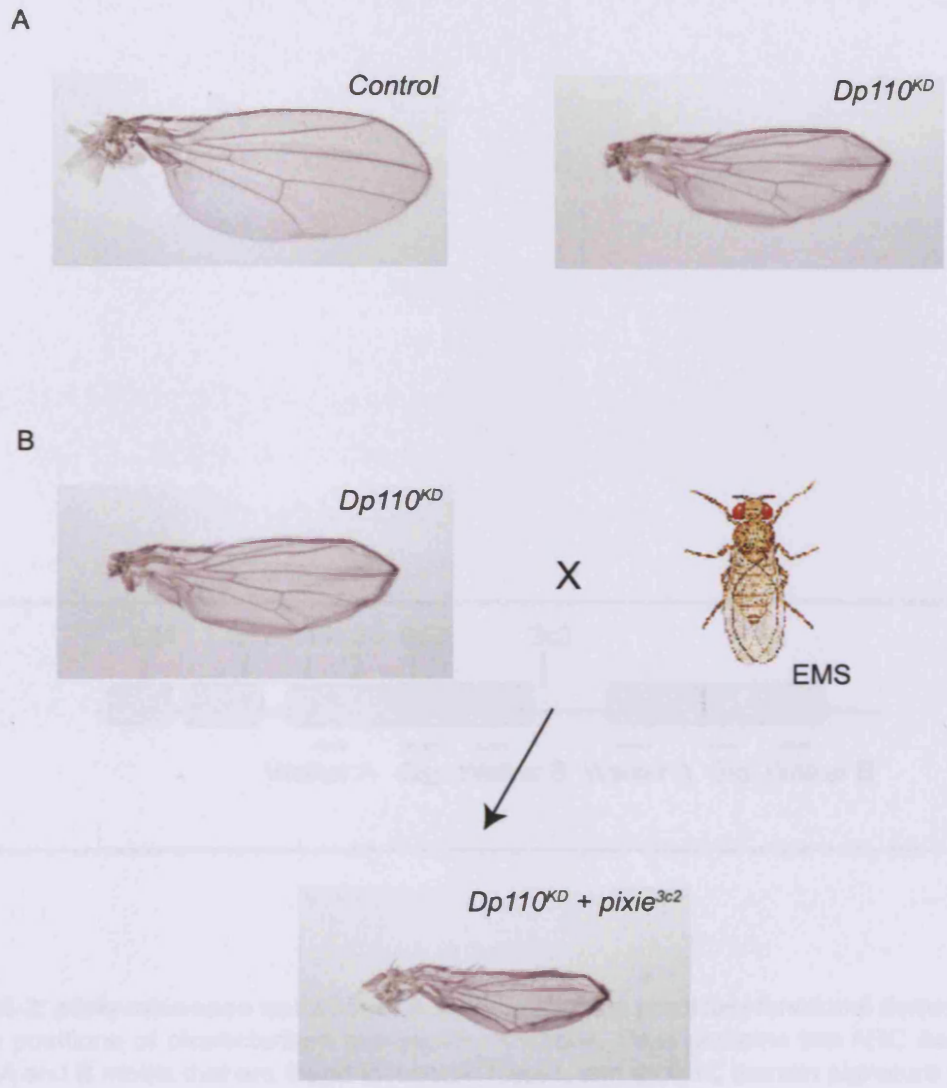

Figure 5-1: A screen for novel growth regulators identified a loss of function mutation in Pixie (*pixie*^{3c2}). (A) Expression of a kinase dead version of the catalytic subunit of PI3K (Dp110^{KD}) in the *Drosophila* wing using the *MS1096-Gal4* driver results in a small-wing phenotype. (B) The *pixie*^{3c2} mutation enhances the small-wing phenotype caused by expression of Dp110^{KD} in the wing. Flies with a small-wing phenotype due to the expression of Dp110^{KD} in the wing were crossed to flies that had been fed EMS to randomly mutagenise their genomes. The offspring were screened for flies, in which the small-wing phenotype was either enhanced or suppressed (Coelho et al, 2005b).

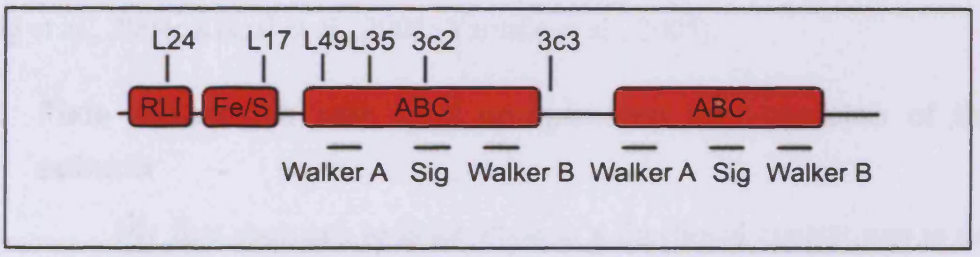

Figure 5-2: *pixie* missense mutations. A schematic of the predicted functional domains of Pixie and the positions of characterised mis-sense mutations. Pixie contains two ABC domains with Walker A and B motifs that are found in most ATPases, and an ABC domain signature motif (Sig), which distinguishes ABC domain proteins from other ATPases. At the N-terminus, Pixie has an iron-sulfur cluster domain (Fe/S), and a domain with high homology to its human homologue, RLI. The positions of previously characterised mutations in *pixie* is indicated; pix^{L24} (Pro38Leu), pix^{L17} (Ala77Thr), pix^{L35} (Pro146Leu), pix^{3c2} (Gln231Leu), and pix^{3c3} (Ala77Thr) (Coelho et al, 2005b). The pix^{3c2} and pix^{3c3} alleles, which were recovered in the screen for modifiers of the small-wing phenotype, are dominant negative, pix^{L49}, pix^{L24} and pix^{L17} are strong LOF alleles, and pix^{L35} is a hypomorphic allele (Coelho et al, 2005a; Coelho et al, 2005b).

5.1.2 The starting point of my project

At the time when I joined the Leevers laboratory, the molecular function of Pixie had not been further studied. The only Pixie ortholog that had been characterised in any details was human RNAse L inhibitor (RLI). As the name implies, RLI was identified due to its ability to inhibit the antiviral activity of RNAse L (Bisbal et al., 1995). Importantly, RNAse L is only found in mammals, whereas Pixie/RLI is conserved in all eukaryota and archaea sequenced so far (Gabaldon and Huynen, 2004). Thus, the reported function of RLI in viral infection does not account for the conservation of RLI/Pixie in non-mammalian species. The initial *in vivo* and *in vitro* data, which hinted that Pixie might function in translation (Coelho et al., 2005a), would better explain the high level of conservation of the Pixie/RLI protein. This prompted me to study the function of Pixie and its role in translation in more details. During the course of my studies, three independent studies provided evidence that the yeast homologue of Pixie, Rli1p, functions in translation initiation and ribosome biogenesis (Dong et al., 2004; Kispal et al., 2005; Yarunin et al., 2005).

5.1.3 Pixie associates with eIF3 components and proteins of the 40S subunit

My first approach to place Pixie in a functional context was to use mass spectrometry to identify proteins that co-purify with tandem affinity-purified GST-TEV-CBP-tagged Pixie (GTC-Pixie) protein. For this purpose, I generated S2 cells stably expressing GTC-Pixie under the control of the inducible methallothionein (MT) promoter (Figure 5-3A). To test GTC-Pixie expression levels, cells expressing GTC-Pixie were grown in the presence of increasing concentrations of $CuSO_4$ for 16 hours (Figure 5-3B). As expected, increasing concentrations of $CuSO_4$ induces increasing levels of GTC-Pixie expression. Moreover, in the absence of $CuSO_4$, leakage from the MT promoter results in low GTC-Pixie expression levels that are comparable with those of endogenous Pixie protein. To avoid any impact that massive over-expression of GTC-Pixie might have on cell signalling, I carried out large-scale purification from non-induced cells expressing GTC-Pixie at low levels (Figure 5-3B). GTC-Pixie was affinity-purified from approximately $1x10^{10}$ S2 cells on glutathione-sepharose beads and cleaved with TEV protease. CBP-Pixie and any associated proteins were bound to calmodulin beads were then washed and eluted (see Materials and Methods). Control

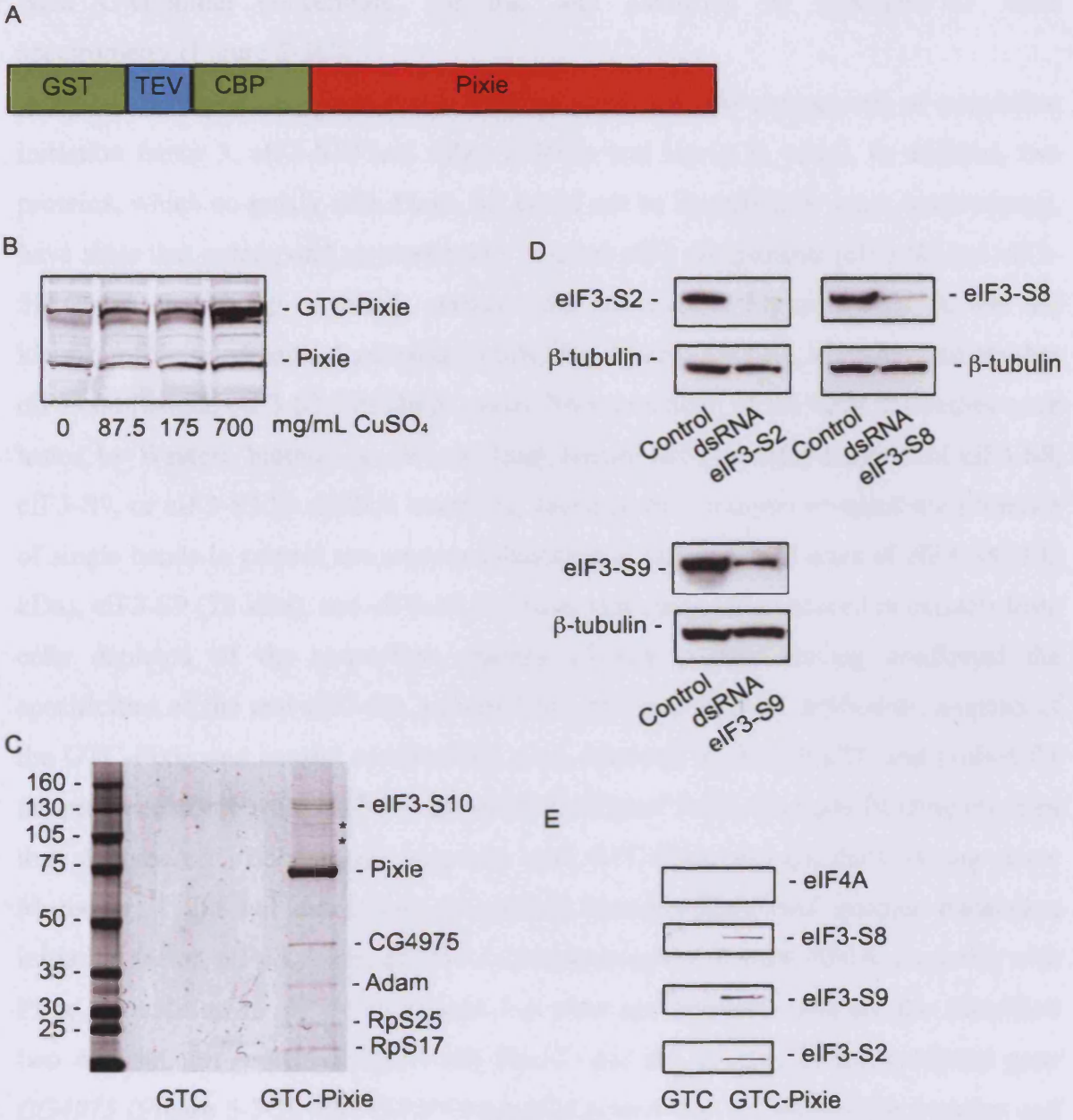

Figure 5-3: Pixie associates with eIF3 components and proteins of the 40S ribosomal subunit. (A) Schematic of GTC-Pixie. (B) Anti-Pixie immuno-blots of extracts prepared from S2 cells expressing GTC-Pixie under the control of the inducible MT promoter, incubated for 16 hours with increasing concentrations of $CuSO_4$. (C) The specificities of the anti-eIF3-S2, -eIF3_S8, and -eIF3-S9 antibodies were tested on control extracts or extracts from cells depleted of eIF3-S2, eIF3-S8 or eIF3-S9. (D-E) A two-step purification was performed from approximately $1x10^{10}$ S2 cells expressing GTC-Pixie or the GTC-tag alone. The final eluates were resolved on a 4-12% Nupage Bis-Tris gel and stained with Brilliant Blue G-colloidal concentrate (D) or blotted onto a PVDF membrane and probed with antibodies against the indicated translation initiation factors (E). Visible bands were excised and identified by MALDI-TOF mass spectrometry (C). Two bands that were visible, but could not be identified by MALDI-TOF mass spectrometry (marked with * in C), have sizes corresponding to other eIF3 components, eIF3-S9 and eIF3-S8.

purifications were carried out from cells expressing the GTC tag alone. The final eluates were resolved by SDS-PAGE, and individual protein bands were stained with Brilliant Blue G-colloidal concentrate, cut out, and identified by MALDI-TOF mass spectrometry (Figure 5-3C).

My mass spectrometry analysis identified two components of translation initiation factor 3, eIF3-S10 and Adam (Tif32p and Hcr1p in yeast). In addition, two proteins, which co-purify with Pixie, but could not be identified by mass spectrometry, have sizes that correspond approximately to other eIF3 components (eIF3-S9 and eIF3-S8 (Prt1p and Nip1p in yeast), marked with asterisks in Figure 5-3C). To test the identity of these proteins, I generated antibodies against eIF3-S8, eIF3-S9, and another eIF3 component, eIF3-S2 (Tif34p in yeast). The specificity of the three antibodies were tested by Western blotting on extracts from control cells or cells depleted of eIF3-S8, eIF3-S9, or eIF3-S2 by dsRNA treatment. Immuno-blot analysis revealed the presence of single bands in control extracts corresponding to the predicted sizes of eIF3-S8 (105 kDa), eIF3-S9 (78 kDa), and eIF3-S2 (34 kDa) that are greatly reduced in extracts from cells depleted of the respective proteins (Figure 5-3D). Having confirmed the specificities of the anti-eIF3-S8, anti-eIF3-S9, and anti-eIF3-S2 antibodies, aliquots of the GTC-Pixie and control purifications were resolved by SDS-PAGE and probed for the presence of eIF3-S8, eIF3-S9, and eIF3-S2 (Figure 5-3E). Immuno-blotting revealed that all three eIF3 components co-purify with GTC-Pixie, but not the GTC-tag alone. Moreover, I did not detect any interaction between Pixie and another translation initiation factor, eIF4A. Thus, all eIF3 components tested, but not eIF4A, co-purify with Pixie. In addition to eIF3 components, my mass spectrometry analysis also identified two 40S subunit proteins, Rps25 and Rps17, and the product of the predicted gene *CG4975* (Figure 5-3C). The *CG4975*-encoded protein has no identifiable domains and is found only in flies, so it was not studied further. The observation that Pixie interacts with eIF3 components and 40S ribosomal proteins (Figure 5-3C, E) suggests that it might function in translation initiation. Consistent with this idea, yeast Rli1p interacts with several translation initiation factors including eIF3 and is required for normal levels of translation initiation (Dong et al., 2004; Kispal et al., 2005; Yarunin et al., 2005).

5.1.4 Pixie is required for optimal stability of an eIF3 sub-core complex

The observation that Pixie can be purified in complex with various eIF3 components prompted me to examine the nature of the eIF3-Pixie interaction in more detail. For this purpose, I generated an antibody against Adam. The specificity of the antibody was tested on control extracts and extracts from Adam-depleted cells. Immuno-blot analysis revealed the presence of a single band of the predicted size (35 kD) in control extracts that is markedly reduced in Adam-depleted extracts (Figure 5-4A). Having confirmed the specificity of the Adam antibody, I examined the effect that eIF3-S10-depletion has on Pixie and various eIF3 components including Adam. I found that depletion of eIF3-S10 reduces protein levels of eIF3-S8 and eIF3-S9, but not those of the loosely associated eIF3 component Adam (Figure 5-4B). Thus, eIF3-S10, eIF3-S8 and eIF3-S9 seem to be required in stoichiometric amounts to stabilise each other and might form a sub-complex. Consistent with this, their yeast homologues, Tif32p, Nip1p, and Prt1p, have been shown to form a sub-complex, in which Tif32p bridges an interaction between Nip1p and Prt1p (Phan et al., 2001). eIF3-S10 depletion has no effect on Pixie protein levels suggesting that Pixie is not a stoichiometric component of this sub-complex (Figure 5-4B). Importantly, maximum depletion of Pixie reduces the stability of some eIF3 components (Figure 5-4C). Thus, in cells efficiently depleted of Pixie, eIF3-S10, eIF3-S9, and eIF3-S8 protein levels are significantly reduced, Adam proteins levels slightly affected, and eIF3-S2 protein levels unaffected. In contrast, partial (90%) depletion of Pixie has no impact on eIF3-S10 levels (Figure 5-5C). Thus, Pixie may play a catalytic rather than structural role in stabilizing some eIF3 core components, perhaps by promoting their assembly into translation initiation-competent complexes. Consistent with the idea, the abundance of the yeast homologue of Pixie, Rli1p, is relatively low compared with that of several translation initiation factors including eIF3 (Dong et al., 2004).

5.1.5 Pixie is required for normal levels of translation initiation

The observation that Pixie can be isolated in complex with eIF3 and proteins from the 40S subunit suggests that Pixie, like Rli1p, may have a role in translation initiation. To further analyse this, I studied the A_{254} (for absorbance at 254 nm wavelength) profiles from control cells and cells depleted of Pixie. An A_{254} (polysome) profile depicts the concentrations of RNA over the length of a gradient and consists of easily distinguishable peaks corresponding to the 40S subunit, the 60S

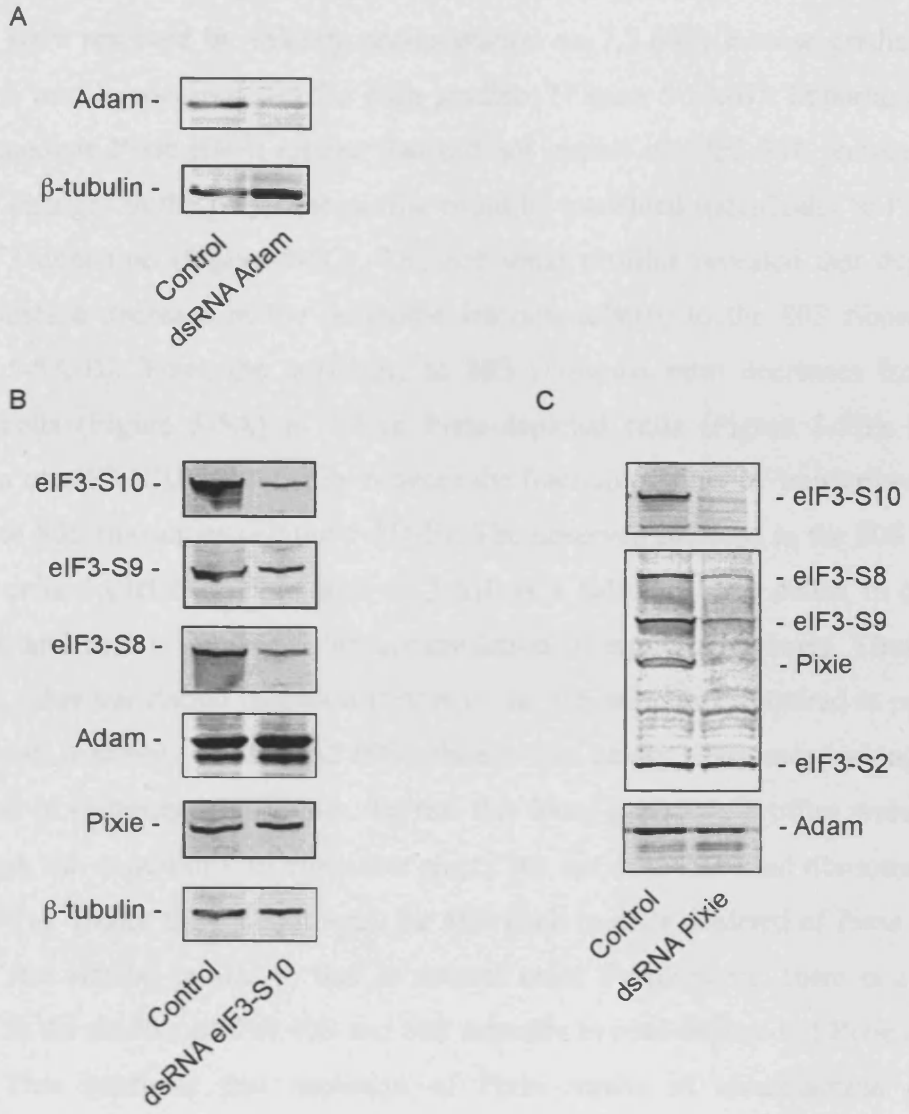

Figure 5-4: Pixie is required for optimal stability of eIF3 core components. (A) Immuno-blot analysis confirms the specificity of the anti-Adam antibody. Cytoplasmic extracts from cells treated with dsRNA targeting *eGFP* or *adam* for 8 days were probed with the anti-Adam antibody. (B) Depletion of eIF3-S10 causes a reduction in protein levels of eIF3-S8 and eIF3-S9, but not those of Pixie and Adam. Cell extracs were prepared from cells treated with dsRNA targeting *eGFP* (control) or *eIF3-S10* for five days and analysed by immuno-blotting with the indicated antibodies. (C) Depletion of Pixie causes a reduction in protein levels of eIF3-S8, eIF3-S9, and eIF3-S10, but not those of Adam or eIF3-S2.Cell lysates were prepared from cells treated with dsRNA targeting *eGFP* (control) or *pixie* for five days and analysed by immuno-blotting with the indicated antibodies.

subunits, the 80S ribosome, and mRNAs containing multiple ribosomes (polysomes) (Figure 5-5A). By measuring the areas underneath the 80S and polysome peaks, it is possible to estimate the relative abundance of 80S ribsosomes and polysomes under different conditions. To generate the polysome profiles, control and Pixie-depleted extracts were resolved by velocity sedimentation on 7.5-60% sucrose gradients, and a polysome profile was recorded for each gradient (Figure 5-5A-B). Importantly, I used an intermediate Pixie RNAi regime that did not impact on eIF3-S10 protein levels so that any changes in the polysome profile could be attributed specifically to Pixie rather than eIF3 depletion (Figure 5-5C). The polysome profiles revealed that depletion of Pixie causes a decrease in the polysome fraction relative to the 80S ribosome peak (Figure 5-5A-B). Thus, the polysome to 80S ribosome ratio decreases from 2.6 in control cells (Figure 5-5A) to 1.0 in Pixie-depleted cells (Figure 5-5B). Similarly, depletion of eIF3-S10 dramatically reduces the fraction of actively transcribed mRNAs relative to 80S ribosomes (Figure 5-5D-E). The observed increase in the 80S ribosome peak in cells depleted of Pixie and eIF3-S10 is a hallmark of a defect in translation initiation and mostly represents an accumulation of empty ribosomes. Thus, binding eIF3 and other translation initiation factors to the 40S subunit is required to prevent the spontaneous assembly of 40S and 60S subunits into empty ribosomes lacking mRNAs (reviewed in (Hinnebusch, 2006)). To test this idea, polysome profiles were resolved under high salt conditions, to dissociate empty but not mRNA-bound ribosomes (Foiani et al., 1991). Under these conditions, the 80S peak in cells depleted of Pixie is greatly reduced and similar in size to that in control cells. Furthermore, there is a dramatic increase in the amount of free 40S and 60S subunits in cells depleted of Pixie (Figure 5-5G-H). This confirms that depletion of Pixie results in accumulation of empty ribosomes. As expected, the polysome fraction is reduced in cells depleted of Pixie (Figure 5-5G-H). Thus, Pixie, like eIF3, is required for the formation of mRNA-bound ribosomes.

5.1.6 Pixie is not associated with elongating ribosomes

Next, I wished to study the association of Pixie with eIF3 and the translational machinery in more details by examining their sedimentation profiles on sucrose gradients. For this purpose, I generated an antibody against the 40S subunit ribosomal protein Rps25 that I had previously purified in complex with GTC-Pixie. The specificity of the anti-Rps25 antibody was tested on extracts from cells treated with

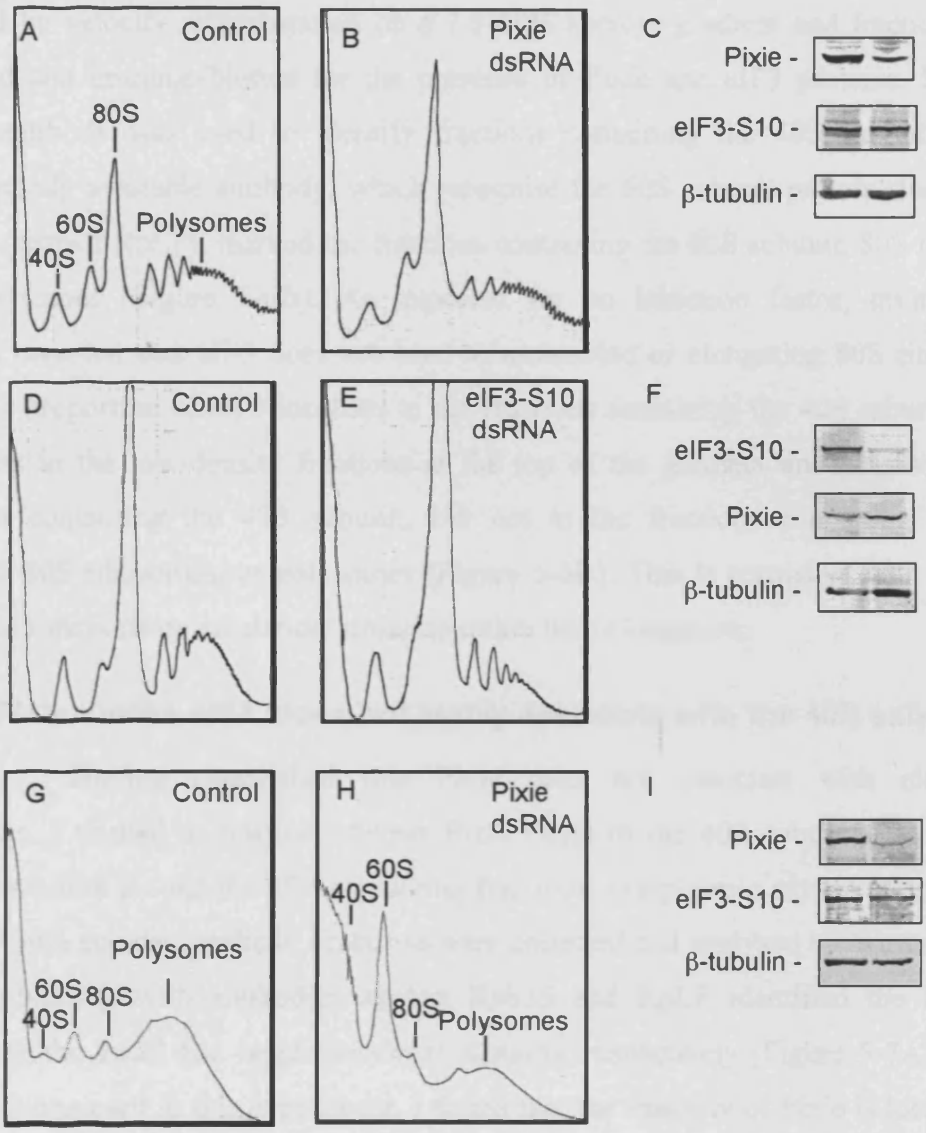

Figure 5-5: Reducing levels of Pixie inhibits translation initiation. S2 cells were treated with dsRNA targeting *eGFP* (control), *pixie*, or *eIF3-S10* for five (D-F) or eight (A-C, G-I) days. Prior to harvesting, cells were starved in PBS containing 2 mg/mL glucose for one hour, stimulated with 1 μM insulin in complete Drosophila Schneider medium for three hours, and treated with 100 μg/mL cycloheximide for 10 mins. (A-B, D-E, G-H) Cytoplasmic extracts were resolved by velocity sedimentation on 7.5-60% sucrose gradients for two hours at 39,000 rpm, then the A_{254} profile was recorded for each gradient. (G-H) cytoplasmic extracts were resolved by velocity sedimentation in the presence of 0.7M NaCl to dissociate empty 80S ribosomes lacking mRNA. The positions of different ribosomal species on the ribosomal profiles are indicated (A, G-H). (C,F,I) an aliquot of each cytoplasmic extract was resolved by SDS-PAGE and immuno-blotted with the indicated antibodies.

dsRNA targeting *eGFP* or *rps25* for five days. Immuno-blotting revealed the presence of a single band of the expected size (13 kD) in control extracts that was greatly reduced in Rps25-depleted extracts (Figure 5-6A). Next, cytoplasmic extract from S2 cells was resolved by velocity sedimentation on a 7.5-60% sucrose gradient and fractions were collected and immuno-blotted for the presence of Pixie and eIF3 proteins. My anti-Rps25 antibody was used to identify fractions containing the 40S subunit, and a commercially available antibody, which recognise the 60S subunit protein ribosome P antigen (termed RpLP), marked the fractions containing the 60S subunit, 80S ribosome and polysomes (Figure 5-6B). As expected for an initiation factor, immuno-blot analysis revealed that eIF3 does not bind to assembled or elongating 80S ribosomes. Instead a proportion of eIF3 localises to the fractions containing the 40S subunit. Pixie is present in the low-density fractions at the top of the gradient and possibly in the fractions containing the 40S subunit, but not in the fractions containing the 60S subunits, 80S ribosomes, or polysomes (Figure 5-6B). This is consistent with the idea that Pixie functions in translation initiation rather than elongation.

5.1.7 Pixie, unlike eIF3, does not stably associate with the 40S subunit

Having established that Pixie does not associate with elongating ribosomes, I wished to resolve whether Pixie binds to the 40S subunit. To obtain a better resolution around the 40S-containing fractions, cytoplasmic extract was resolved on a 7.5-30% sucrose gradient. Fractions were collected and analysed by Western blots. Immuno-blotting with antibodies against RpS25 and RpLP identified the fractions containing the small and large ribosomal subunits, respectively (Figure 5-7A). Under the conditions used in this experiment, I found that the majority of Pixie is localised in the soluble fractions at the top of the gradient rather than co-sedimenting with core eIF3 components or the 40S subunit. Instead, the distribution of Pixie is rather similar to that of Adam, which was affinity purified with Pixie (Figure 5-3C). Thus, although in large-scale affinity purifications Pixie can be isolated with small amounts of core eIF3 components and 40S subunit proteins, the association of Pixie and/or Adam with eIF3 and the 40S subunit might be too weak to withstand the velocity sedimentation conditions. Consistent with this idea, the mammalian homologue of Adam, eIF3j, is lost from the 40S subunit upon velocity sedimentation (Fraser et al., 2004; Unbehaun et al., 2004), and the interaction between Rli1p and the 40S subunit only withstands velocity

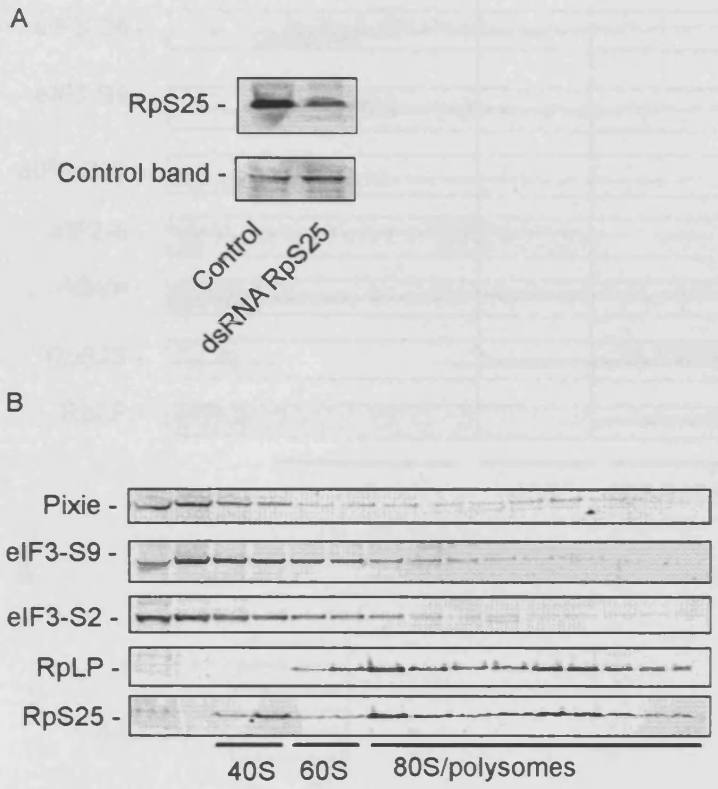

Figure 5-6: Pixie does not associate with elongating ribosomes. (A) The specificity of the anti-Rps25 andtibody was confirmed by immuno-blotting of cytoplasmic extracts prepared from cells treated with dsRNA targeting *eGFP* or *rps25* for five days. An unspecific band was used as a loading control. (B) Cytoplasmic extracts were prepared from $5x10^8$ S2 cells and resolved by velocity sedimentation on 7.5-60% sucrose gradients for two hours at 39,000 rpm. Gradients were collected and polysome profiles simultaneously recorded (data not shown). The presence or absence of Pixie and two eIF3 components in the different fractions was revealed by Western-blotting. Fractions containing the 40S and 60S subunits were identified by probing for the small and large ribosomal subunit proteins, RpS25 and RpLP.

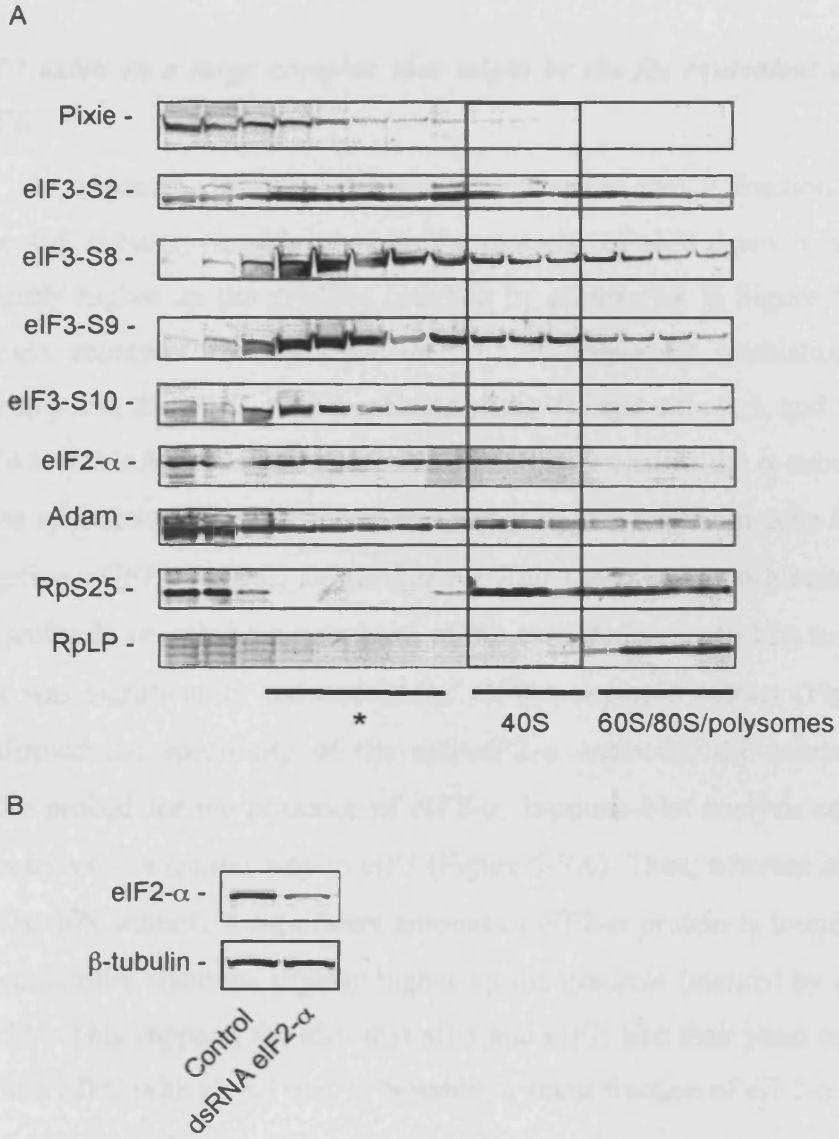

Figure 5-7: Pixie, unlike eIF3, does not associate with the 40S subunit under standard conditions. (A) Cytoplasmic extracts were prepared from $5x10^8$ S2 cells and resolved by velocity sedimentation on 7.5-30% sucrose gradients for 4.5 hours at 39,000 rpm. Gradients were collected and probed for the presence of Pixie, eIF2α, and various eIF3 components. The presence of the 40S and 60S ribsomal subunits was revealed by probing for the small and large ribosomal proteins, RpS25 and RpLP. The asterisk indicates an eIF3- and eIF2-containing complex that may correspond to the *Drosophila* equivalent of the yeast MFC.(B) The specificity of the anti-eIF2-α antibody was tested on extracts from cells treated with dsRNA targeting *eGFP* (control) or *eIF2-α* for four days. β-tubulin was used as a loading control.

sedimentation at low salt concentrations or upon cross-linking (Dong et al., 2004; Kispal et al., 2005; Yarunin et al., 2005).

5.1.7.1 eIF3 exists in a large complex that might be the fly equivalent of the yeast MFC

As expected, immuno-blot analysis revealed that a fraction of eIF3 is bound to the 40S subunit. Notably, though, the majority of eIF3 exists in a less dense complex slightly higher up the gradient (marked by an asterisk in Figure 5-7A). This complex might represent the fly equivalent of an important translation initiation intermediate in yeast, the MFC, which consists of the TC and eIFs 1, 3, and 5 (Asano et al., 2000). To test this hypothesis, I generated an antibody against the α-subunit of eIF2 (eIF2-α). The specificity of the antibody was tested on extracts from cells treated with dsRNA targeting *eGFP* (control) or *eIF2-α* for four days. Immuno-blotting with the anti-eIF2-α antibody revealed a single band of the expected size (40 kD) in the control extracts that was significantly reduced in the eIF2-α-depleted extract (Figure 5-7B). Having confirmed the specificity of the anti-eIF2-α antibody, the sucrose gradient fractions were probed for the presence of eIF2-α. Immuno-blot analysis revealed that the eIF2-α behaves in a similar way to eIF3 (Figure 5-7A). Thus, whereas some eIF2-α is bound to the 40S subunit, a significant amount of eIF2-α protein is found in the less dense eIF3-containing fractions slightly higher up the gradient (marked by an asterisks in Figure 5-7A). This supports the idea that eIF3 and eIF2, like their yeast counterparts, might exist in a MFC with eIFs 1 and 5. Notably, a small fraction of eIF2-α is found in the soluble fractions at the top of the gradient. This might represent free eIF2 or eIF2 bound Met-tRNA$_i^{Met}$ and GTP in the TC (Figure 5-7A).

5.1.8 Pixie associates with the 40S subunit in an ATP-dependent manner

Although in my large-scale purifications Pixie associates with small amounts of eIF3 and 40S subunit proteins (Figure 5-3C, E), these interactions are lost upon velocity sedimentation (Figure 5-7). This suggests that the interactions between Pixie and eIF3 and/or the 40S subunit are weak and possibly regulated in some way. The presence of two ABC domains in Pixie, which are predicted to bind and hydrolyse ATP, suggests that the association of Pixie with eIF3 and/or the 40S subunit might be regulated in an ATP-dependent manner. Consistent with these domains being important for Pixie function, several strong loss-of-function mutations in *pixie* are in conserved

residues of the ABC domains (Coelho et al., 2005a). For example, pix^{3c2} disrupts the nucleotide-binding ABC domain signature motif of the first ABC domain, and pix^{L49} (Gly123Ser) is in the third conserved glycine of the Walker A loop of the first ABC domain that is predicted to bind to the nucleotide phosphate groups (Figure 5-2) (Coelho et al., 2005a). Moreover, a mutation in yeast Rli1p that is predicted to allow ATP binding, but not hydrolysis, is non-functional and inhibits growth when over-expressed (Dong et al., 2004).

To test whether Pixie associates with eIF3 and/or the 40S subunit in an ATP-dependent manner, I examined the sedimentation profile of Pixie on 7.5-30% sucrose gradients in the presence of ADP (control), ATP or a non-hydrolysable version of ATP (ADP-N-P). Immuno-blotting showed that addition of ADP, ATP or ADP-N-P to these extracts does not dramatically alter the distribution of eIF3-S2, eIF3-S8, eIF3-S9, eIF3-S10, RpLP and RpS25 on the sucrose gradients (Figure 5-8). Similarly, the addition of ADP or ATP has no effect on the distribution of Pixie on the sucrose gradients. In contrast, in the presence of ADP-N-P, a substantial proportion of Pixie protein redistributes to the 40S subunit-containing fractions (Figure 5-8). Given the similar distribution of Pixie and Adam on the initial sucrose gradients (Figure 5-7), I also examined the effect of ADP-N-P on the distribution of Adam. However, I did not observe a consistent redistribution of Adam under these conditions (data not shown). However, this result is not conclusive, since the association of Adam/eIF3j with the 40S subunit might be too weak to withstand velocity sedimentation irrespective of whether Pixie promotes its recruitment to the 40S subunit in the first place.

The presence of Pixie in the 40S subunit-containing fractions suggests that Pixie binds to the 40S subunit under these conditions. However, it cannot be ruled out that the presence of Pixie in these fractions is the result of its association with a different complex of similar size. To distinguish between these two possibilities, I examined the effect that depletion of two 40S subunit proteins, Rps25 and Rps13, has on the ATP-dependent redistribution of Pixie into the 40S subunit-containing fractions. The rationale behind this approach was that depletion of Rps25 and Rps13 is likely to affect 40S subunit levels, since 40S subunit ribosomal proteins are required in stoichiometric amounts. Extracts from cells treated with dsRNA targeting *eGFP* (control) or *rps25* and *rps13* were resolved on 7.5-30% sucrose gradients in the presence of ADP-N-P, and fractions were collected and analysed by immuno-blotting. As expected, a significant proportion of the Pixie protein is found in the 40S subunit-

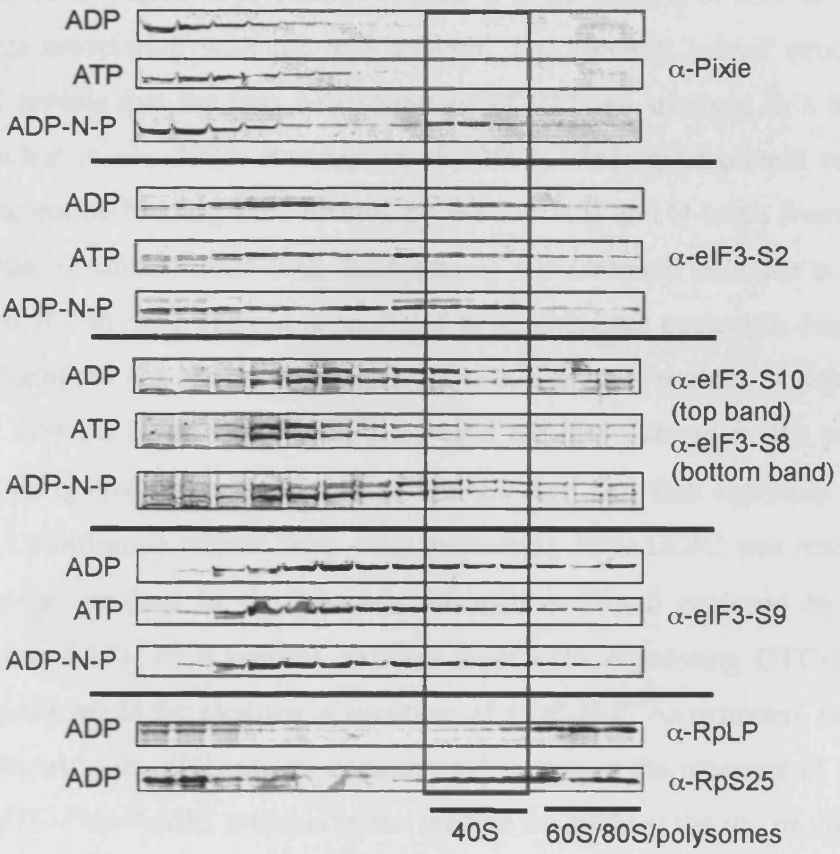

Figure 5-8: Pixie redistributes into the 40S subunit-containing fractions in the presence of ATP-N-P. The presence of ADP-N-P redistributes a significant proportion of endogenous Pixie protein into the 40S subunit-containing fractions, but does not affect the distribution of eIF3 components on the gradient. Cytoplasmic extracts were prepared $5x10^8$ S2 cells, then 5 mM ADP, ATP, or ADP-N-P was added prior to their resolution on 7.5-30% sucrose gradients for 4.5 hours at 39,000 rpm. Gradients were collected and probed for the presence of Pixie and various eIF3 components. Fractions containing the 40S and 60S subunits were identified by probing for the small and large ribosomal subunit proteins, RpS25 and RpLP.

containing fractions of the control gradient (Figure 5-9A). In contrast, depletion of Rps25 and Rps13 blocks the ATP-dependent redistribution of Pixie into more dense fractions (Figure 5-9A-B). The failure to detect Pixie in these fractions is not due to an effect on Pixie protein levels. Thus, immuno-blotting confirmed that Pixie protein levels are unaffected in cells depleted of Rps25 and Rps13 (Figure 5-9B). These data show that Pixie indeed binds to the 40S subunit in the presence of ADP-N-P.

5.1.9 The C-terminal ABC domain of Pixie is required for its association with the 40S subunit

I next wished to determine whether it is the binding of ATP to Pixie itself that allows its association with the 40S subunit. The recently solved structure of *p. furiosus* RLI reveals that the two ABC domains of RLI are arranged in a head-to-tail fashion (Karcher et al., 2005; Karcher et al., 2008). This arrangement creates two composite nucleotide-binding sites formed by Walker A/B and Q-loops from one ABC domain and the signature motifs from the opposing ABC domain (Karcher et al., 2008). Thus, deletion of one ABC domain is predicted to abolish both nucleotide-binding sites. I therefore examined the ability of a truncated Pixie mutant protein, which lacks the second ABC domain (GTC-PixieΔABC), to bind the 40S subunit in the presence of ADP-N-P. This involved the generation of a stable cell line that expresses the GTC-PixieΔABC. Cytoplasmic extract from cells expressing PixieΔABC was resolved on a 7.5-30% sucrose gradient in the presence of ADP-N-P and analysed by immuno-blotting (Figure 5-10). As a control, extracts from cells expressing GTC-Pixie were resolved on gradients in the absence or presence of ADP-N-P. As expected, endogenous Pixie redistributes to the 40S subunit-containing fractions in the presence of ADP-N-P. In contrast, GTC-PixieΔABC remains in the soluble fractions at the top of the gradient, indicating that GTC-PixieΔABC is unable to bind the 40S subunit. This is not due to the presence of the GTC-tag, since GTC-Pixie behaves similarly to endogenous Pixie. Thus, the C-terminal ABC domain of Pixie is necessary for its binding to the 40S subunit.

5.1.10 The PixieE501Q mutant is constitutively associated with the 40S subunit

The observation that GTC-PixieΔABC is unable to bind the 40S subunit is consistent with the idea that ATP-binding by Pixie itself is required for its association

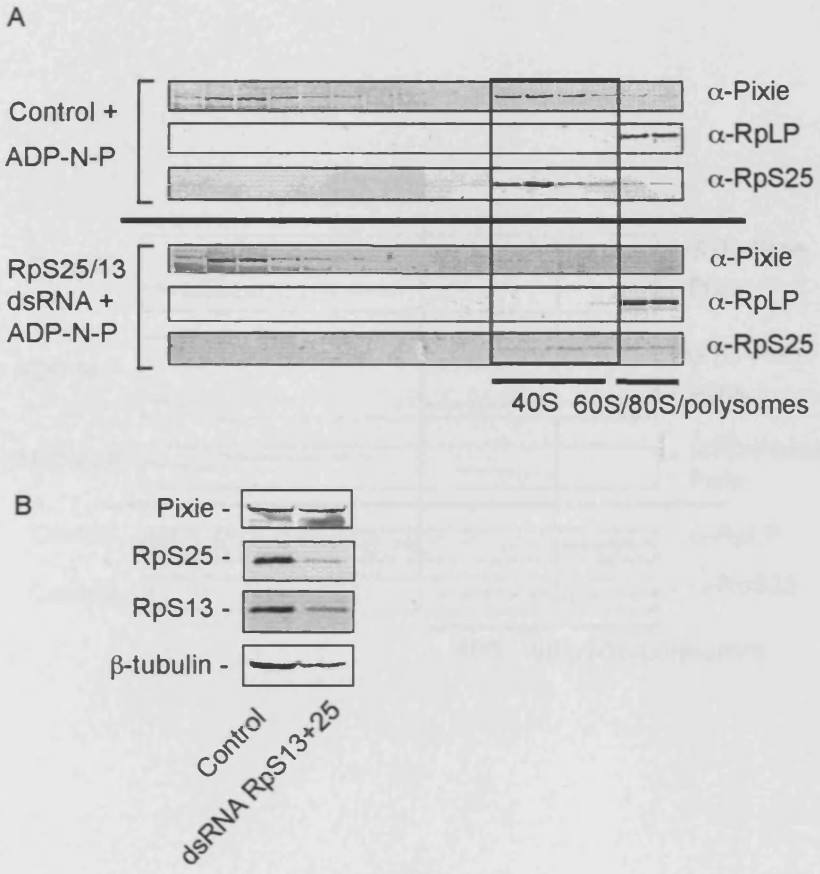

Figure 5-9: Pixie associates with the 40S subunit in an ATP-dependent manner. The ATP-dependent redistribution of Pixie into denser fractions depends on its association with the 40S subunit. (A) $5x10^8$ S2 cells treated with dsRNA targeting *eGFP* (control), or *rps25* and *rps13* for five days were collected, cytoplasmic extracts were prepared, and 5 mM ADP-N-P was added prior to their resolution on 7.5-30% sucrose gradients for 4.5 hours at 39,000 rpm. (B) An aliquot of each cytoplasmic extract as resolved by SDS-PAGE and immuo-blotted with the indicated antibodies. Immuno-blotting confirms that RpS25 and RpS13 protein levels are reduced in cells treated with dsRNA targeting *rps25* and *rps13* compared with control cells.

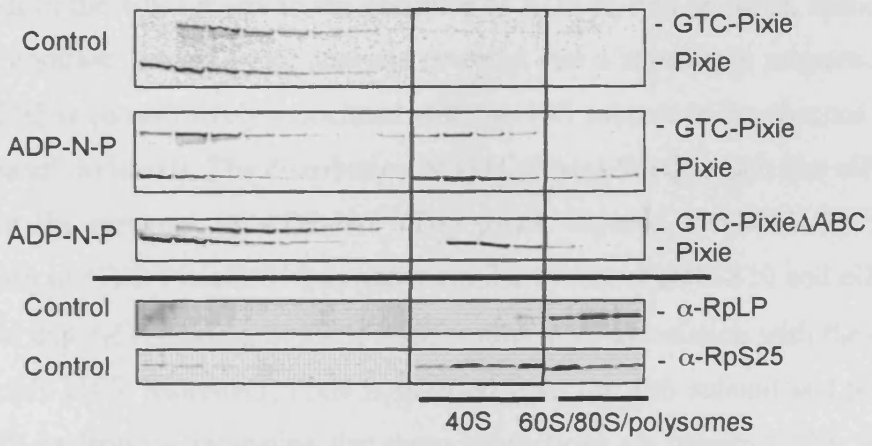

Figure 5-10: The C-terminal ABC domain of Pixie is required for its association with the 40S subunit. GTC-Pixie and endogenous Pixie, but not GTC-PixieΔABC, redistributes to the 40S subunit-containing fractions in the presence of ADP-N-P. Cytoplasmic extracts were prepared from $5x10^8$ S2 cells stably expressing GTC-Pixie or a truncated GTC-Pixie protein lacking the C-terminal ABC domain (GTC-PixieΔABC). 5 mM ADP-N-P was added to the extracts as indicated prior to their resolution on 7.5-30% sucrose gradients for 4.5 hours at 39,000 rpm. The presence of GTC-Pixie, GTC-PixieΔABC, and endogenous Pixie protein was revealed by immuno-blotting with an anti-Pixie antibody recognising the N-terminal part of Pixie.

with the 40S subunit. However, it does not rule out the possibility that the ABC domain is required for the binding of Pixie to another protein that associates with the 40S subunit in an ATP-dependent manner. Furthermore, deletion of the C-terminal ABC domain might interfere with the folding of the rest of the Pixie protein. I therefore wished to generate a gain of function mutation in Pixie that would mimic the binding of Pixie to ADP-N-P. I chose to mutagenise Glutamate 501 in the conserved Walker B motif of the second ABC domain to Glutamine (PixieE501Q). This mutation is predicted to allow ATP binding, but not hydrolysis. To study the sedimentation profile of the PixieE501Q mutant on a sucrose gradient, I generated stable cell lines expressing GTC-PixieE501Q under the control of an inducible promoter. Cytoplasmic extracts from these cells were resolved by velocity sedimentation on 7.5-30% sucrose gradients in the presence or absence of ADP-N-P (Figure 5-11A). As expected, endogenous Pixie only binds to the 40S subunit in the presence of ADP-N-P (Top panel, induced + ADP-N-P). In contrast, immuno-blot analysis revealed that a significant proportion of GTC-PixieE501Q is constitutively associated with the 40S subunit in the absence of ADP-N-P (Top panel, induced). The distribution of GTC-PixieE501Q, much like eIF3, does not change in the presence of ADP-N-P (Top panel, induced + ADP-N-P). In fact, the distribution of GTC-PixieE501Q is rather similar to that of eIF3-S10 and eIF2-α. These data show that ATP-binding by Pixie itself results in its association with the 40S subunit and possibly eIF3. Moreover, Pixie is released from the 40S subunit and possibly eIF3 upon ATP-hydrolysis, indicating that these interactions are transient. This is consistent with the idea that Pixie provides a catalytic rather than a structural function.

5.1.11 The association of Pixie with the 40S ribosome subunit is insensitive to eIF3 depletion

The observations that Pixie co-purifies with eIF3 and that a proportion of eIF3 is constitutively bound to the 40S subunit, prompted me to investigate whether eIF3 is required for the ATP-dependent recruitment of Pixie to the 40S subunit. Cytoplasmic extracts were prepared from $5x10^8$ cells treated with dsRNA targeting *eGFP* or *eIF3-S10* for five days and resolved on 7.5-30% sucrose gradients (Figure 5-12B). As expected, depletion of eIF3-S10 protein levels reduces the stability of eIF3-S9, but has no effect on Pixie levels (Figure 5-4B and 5-12B). Importantly, reduced levels of 40S subunit-bound eIF3-S10 and eIF3-S9 do not affect ATP-dependent binding of Pixie to the 40S subunit. While it is possible that the small amount of

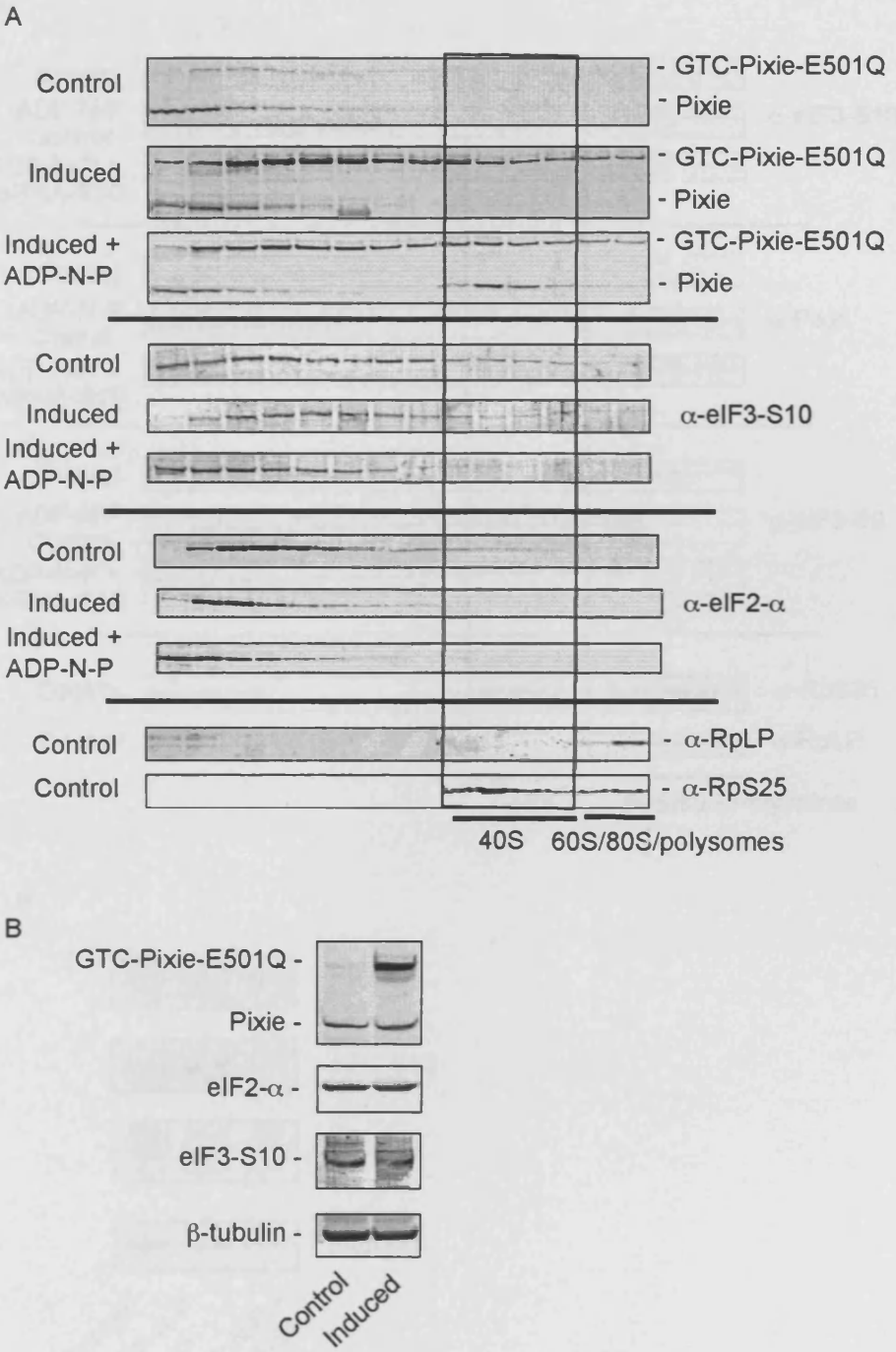

Figure 5-11: GTC-PixieE501Q, which is predicted to bind, but not hydrolyse ATP, is constitutively associated with the 40S subunit. (A) A proportion of GTC-PixieE501Q, much like eIF3-S10, is constitutively associated with the 40S subunit. Cytoplasmic extracts were prepared from $5x10^8$ S2 cells stably expressing GTC-Pixie or the GTC-PixieE501Q mutant protein, and where indicated 5 mM ADP-N-P was added to the extracts prior to their resolution on 7.5-30% sucrose gradients for 4.5 hours at 39,000 rpm. GTC-PixieE501Q expression was induced by addition of 175 μg/mL (Induced + ADP-N-P, panel 3) or 700 μg/mL (Induced, panel 2) $CuSO_4$ for 16 hours. High levels of GTC-PixieE501Q over-expression do not affect the association of eIF3-S10 and eIF2-α with the 40S subunit (Induced, panel 2). (B) Immuno-blotting revealed that high levels of GTC-PixieE501Q over-expression (induced by 700 μg/mL $CuSO_4$) do not affect the levels of endogenous Pixie, eIF2-α, or eIF3-S10 expression.

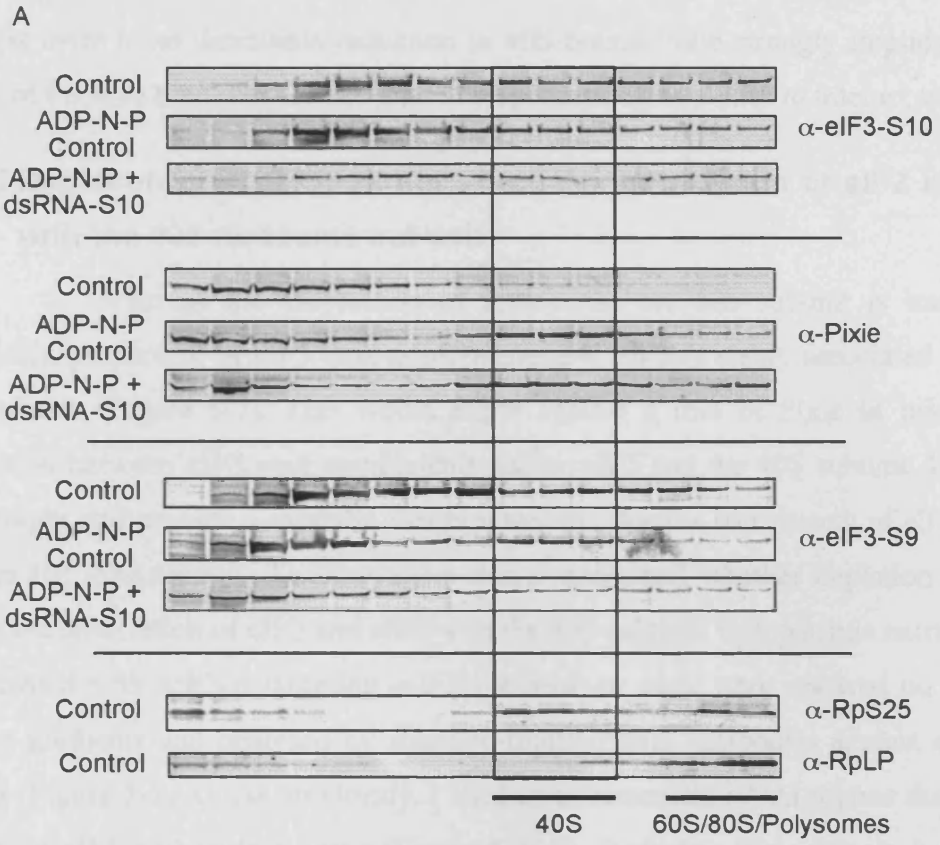

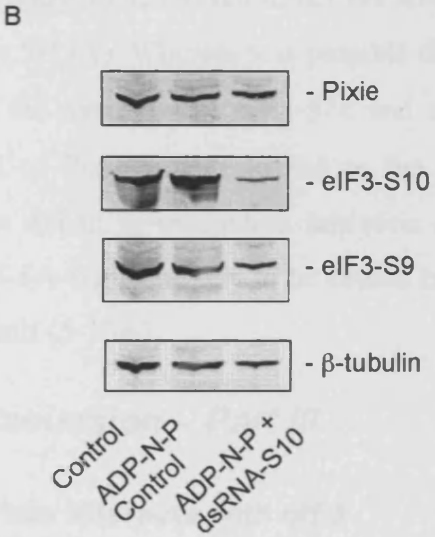

Figure 5-12: The association of Pixie with the 40S subunit is insensitive to eIF3 depletion. (A) Reduced levels of 40S subunit-bound eIF3 does not affect the ATP-dependent association of Pixie with the 40S subunit. Cells were treated with dsRNA targeting *eGFP* (control) or *eIF3-S10* for five days. Cytoplasmic extracts were prepared from $5x10^8$ control or eIF3-S10-depleted cells and resolved on 7.5-30% sucrose gradients for 4.5 hours at 39,000 rpm in the presence or absence of 5 mM ADP-N-P. (B) Immuno-blotting confirms the depletion of eIF3-S10 and shows that eIF3-S9 levels are also reduced, whereas Pixie protein levels are unaffected.

remaining eIF3-S10 is responsible for the association of Pixie with the 40S subunit, the fact that there is no detectable reduction in 40S-bound Pixie strongly implies that the ability of Pixie to bind the 40S subunit is independent of its ability to interact with eIF3.

5.1.12 Depletion of Pixie does not affect the association of eIF2 and eIF3 with the 40S ribosome subunit

Whereas the association of Pixie with the 40S subunit is transient, a significant proportion of eIF3 core components and eIF2 is stably associated with the 40S subunit (Figure 5-7). This would argue against a role of Pixie in bridging an interaction between eIF3 core components and/or eIF2 and the 40S subunit. However, Pixie might still provide a catalytic function required for the recruitment of eIF3 and/or eIF2 to the 40S subunit. To investigate this, I examined whether depletion of Pixie affects the association of eIF2 and eIF3 with the 40S subunit. Cytoplasmic extracts from cells treated with dsRNA targeting *eGFP* (control) or *pixie* were resolved on 7.5-30% sucrose gradients and analysed by immuno-blotting with antibodies against eIF3-S10 eIF2-α (Figure 5-13A). As previously, I used an intermediate RNAi regime that did not impact on eIF3-S10 protein levels (Figure 5-13B). Reducing Pixie protein levels with approximately 90%, did not affect the levels of 40S subunit-bound eIF3-S10 and eIF2-α (Figure 5-13A). Whereas it is possible that the remaining Pixie activity is sufficient to promote the assembly of eIF3-S10 and eIF2-α onto the 40S subunit, the same 90% depletion of Pixie is able to reduce the polysome content of cells (Figure 5-5A-B). Thus, the defect in translation initiation observed in cells partially depleted of Pixie (Figure 5-5A-B) is unlikely to be caused by a lack of recruitment of eIF3 or eIF2 to the 40S subunit (5-13A).

5.2 Discussion – Part III

5.2.1 Pixie interacts with eIF3

I initially carried out a large-scale TAP purification to identify proteins that co-purify with GTC-tagged Pixie. My mass spectrometry analysis of GTC-Pixie-associated proteins identified two eIF3 components, Adam and eIF3-S10, and two 40S subunit ribosomal proteins (Figure 5-3C). Subsequent immuno-blot analysis of proteins isolated in complex with GTC-Pixie revealed the identity of a further three eIF3 components, eIF3-S2, eIF3-S8, and eIF3-S9 (Figure 5-3E). Consistent with their

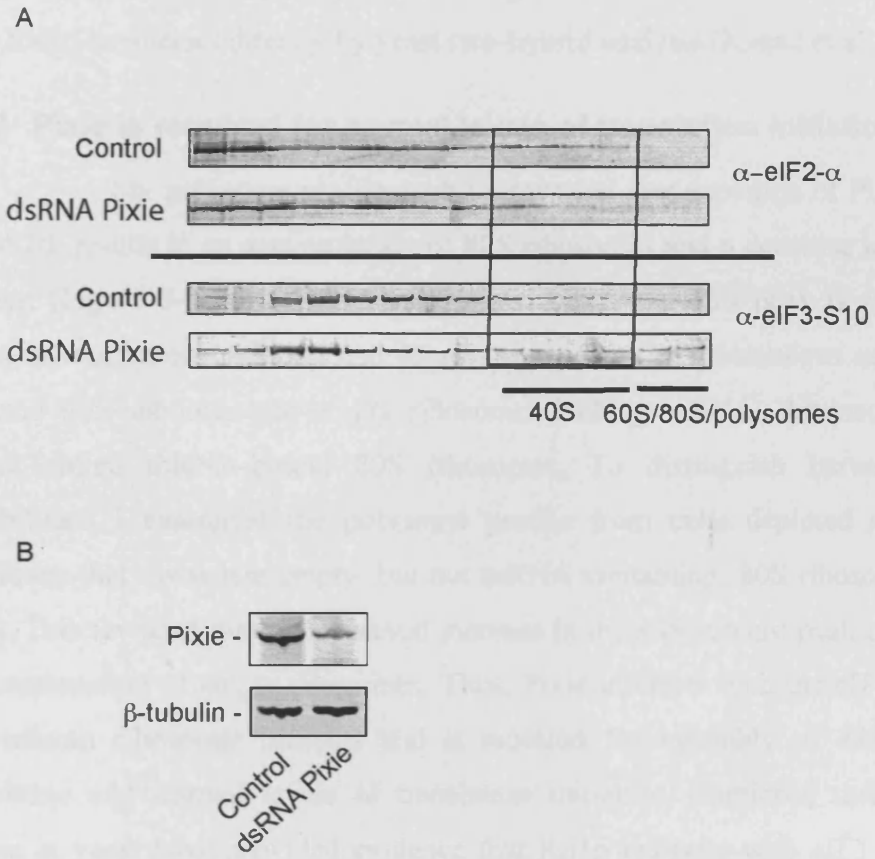

Figure 5-13: Depletion of Pixie does not affect recruitment of eIF2 and eIF3 to the 40S subunit. (A) Cytoplasmic extracts were prepared from $5x10^8$ S2 cells treated with dsRNA targeting *eGFP* or *pixie* for 8 days, and 5 mM ADP-N-P was added to the extracts prior to their resolution on 7.5-30% sucrose gradients for 4.5 hours at 39,000 rpm. (B) Immuno-blotting confirms that Pixie protein levels are 90% reduced in Pixie-depleted extracts compared with control extracts.

fundamental function in translation initiation, eIF3-S2, eIF3-S8, eIF3-S9, and eIF3-S10 are all highly conserved, and their yeast counterparts, Tif34p, Nip1p, Prt1p, and Tif32p, are essential for viability. Adam is also well conserved though its yeast homologue Hcr1p is dispensable for viability. The observation that sufficient amounts of Adam and eIF3-S10 protein were recovered in my GTC-Pixie purification to allow identification by mass spectrometry might indicate that they interact directly with Pixie (Figure 5-3C). Consistent with this idea, the yeast homologues of Pixie and Adam, Rli1p and Hcr1p, were found to interact directly by yeast two-hybrid analysis (Kispal et al., 2005).

5.2.2 Pixie is required for normal levels of translation initiation

My polysome profile analysis revealed that depletion of Pixie, like that of eIF3-S10, results in an accumulation of 80S ribosomes and a decrease in the polysome fraction (Figure 5-5A-F). The dramatic increase in the 80S peak is a hallmark of a defect in translation initiation and mostly represents the spontaneous assembly of free 40S and 60S subunits into empty ribosomes lacking mRNA. Alternatively, it could reflect stalled mRNA-bound 80S ribosomes. To distinguish between these two possibilities, I examined the polysome profile from cells depleted of Pixie under conditions that dissociate empty, but not mRNA containing, 80S ribosomes (Figure 5-5G-I). This revealed that the observed increase in the 80S subunit peak indeed is due to an accumulation of empty ribosomes. Thus, Pixie interacts with the eIF3 complex and 40S subunit ribosomal proteins and is required for assembly of 48S pre-initiation complexes and normal levels of translation initiation. Similarly, three independent studies in yeast have provided evidence that Rli1p interacts with eIF3 and ribosomal proteins and functions in translation initiation (Dong et al., 2004; Kispal et al., 2005; Yarunin et al., 2005), indicating that this function of Pixe/Rli1p is conserved from yeast to metazoans.

5.2.3 Pixie is not constitutively associated with the 40S subunit

The initial observations that Pixie binds to eIF3 (Figure 5-3C, E) and is required for normal levels of translation initiation (Figure 5-5A-C), prompted me to analyse the association of Pixie and eIF3 with the translational machinery in more details. I was initially surprised to find that most Pixie is localised in the soluble fractions at the top of the gradient rather than co-sedimenting with the core eIF3 components or the 40S subunit (Figure 5-7). This suggests that the interactions between

Pixie and eIF3 and/or the 40S subunit, which I initially identified in my GTC-Pixie purification, might be too weak to withstand the velocity sedimentation conditions or possibly regulated. Consistent with this idea, the interaction of yeast Rli1p with the 40S subunit only withstands velocity sedimentation under low salt conditions or upon cross-linking (Dong et al., 2004; Kispal et al., 2005; Yarunin et al., 2005).

Interestingly, my velocity sedimentation analyses revealed that whereas a proportion of eIF3 is bound to the 40S subunit, a significant amount of eIF3 exists in a less dense complex further up the gradient (Figure 5-7). This complex might be the fly equivalent of the yeast MFC, which consists of the TC and eIFs 1, 3, and 5 (Asano et al., 2000). Consistent with this idea, I found that a significant proportion of eIF2-α is present in these eIF3-containing fractions (Figure 5-7).

5.2.4 Pixie associates with the 40S subunit in an ATP-dependent manner

Pixie possesses two ABC domains, the integrity of which is essential for its biological function (Coelho et al., 2005a). This, prompted me to examine whether the binding of Pixie to the 40S subunit might be ATP-dependent. Indeed, I found that binding of Pixie to the 40S subunit is transient and ATP-dependent (Figures 5-8 and 5-9). Thus, Pixie is detected in the 40S subunit fractions only in the presence of ADP-N-P. Moreover, a point mutation in the ATP-binding center of Pixie, which is predicted to allow Pixie to bind, but not hydrolyse, ATP, results in constitutive association of Pixie with the 40S subunit (Figure 5-11). This indicates that Pixie associates with the 40S subunit in its ATP-bound form and is released upon ATP hydrolysis. Given the similar distribution of Pixie and Adam on sucrose gradients, I examined whether redistribution of Pixie to the 40S subunit fractions in the presence of ADP-N-P had an effect on the sedimentation profile of Adam. ATP-dependent binding of Pixie to the 40S subunit did not increase levels of 40S subunit-bound Adam protein (data not shown). This might not be expected, since Pixie is likely to provide a catalytic function rather than bridging an interaction between Adam and the 40S subunit. Given the direct interaction between the yeast homologues of Pixie and Adam, Rli1p and Hcr1p, it is still possible that Pixie promotes recruitment of Adam to the 40S subunit (Kispal et al., 2005). However, due to the loose association of Adam with the 40S subunit, it is not possible to address this by velocity sedimentation analysis.

5.2.5 Pixie binds to the 40S subunit independent of core components of eIF3

The ability of Pixie to interact with eIF3 and the observation that a proportion of eIF3 is constitutively bound to the 40S subunit prompted me to examine whether ATP-dependent interaction of Pixie with the 40S subunit is mediated by eIF3. Treatment of cells with dsRNA targeting eIF3-S10 reduced levels of 40S subunit-bound eIF3-S10 and eIF3-S9, but had no impact on ATP-dependent binding of Pixie to the 40S subunit (Figure 5-12). These data suggests that Pixie binds to the 40S subunit independent of core eIF3 components. My data do not exclude that binding of Pixie to the 40S subunit could be mediated by other eIF3 components that are not affected by eIF3-S10 depletion. However, the mammalian homologue of Adam, eIF3j, is the only eIF3 component that is thought to bind to the 40S subunit independent of the rest of the eIF3 complex (Fraser et al., 2007; Fraser et al., 2004; Nielsen et al., 2006; Unbehaun et al., 2004). Given that a substantial fraction of Pixie is recruited to the 40S subunit under conditions where only a small proportion of Adam is 40S subunit-bound, my data favour the idea that Pixie binds the 40S subunit independent of eIF3.

5.2.6 Pixie might promote the assembly of eIF3 core components into translation initiation competent complexes

Interestingly, I found that dsRNA-mediated depletion of eIF3-S10 reduces levels of eIF3-S8 and eIF3-S9, but has no impact on Adam and Pixie levels (Figure 5-4A). This observation suggests that the optimal stability of eIF3-S8, eIF3-S9 and eIF3-S10 depends on the presence of all three proteins in stoichiometric amounts and their assembly into a complex. Consistent with this, the yeast homologues of eIF3-S8, eIF3-S9 and eIF3-S10, Nip1p, Prt1p, and Tif32p, form an eIF3 sub-complex, in which Tif32p bridges an interaction between Nip1p and Prt1p (Phan et al., 2001). I also found that extensive dsRNA-mediated depletion of Pixie causes a reduction in the protein levels of eIF3-S8, eIF3-S9, and eIF3-S10, whereas levels of Adam are slightly affected and those of eIF3-S2 are unaffected (Figure 5-4B). Thus, Pixie may aid the assembly of the eIF3-S8-eIF3-S10-eIF3-S9 sub-complex into stable translation initiation competent complexes. The observation that partial (90%) depletion of Pixie has no impact on eIF3-S10 protein levels suggests that Pixie provides a catalytic rather than a structural function. Consistent with this idea, I only detected significant amounts of Pixie in the eIF3-containing fractions of the gradient in the presence of ADP-N-P.

5.2.7 Pixie depletion results in reduced translation initiation, but does not affect recruitment of eIFs 2 and 3

Given the fact that Pixie can bind both to both eIF3 and ribosomal proteins, and the effect that ADP-N-P has on its distribution on sucrose gradients, Pixie may play a catalytic role in the assembly of translation pre-initiation complexes onto the 40S subunit. To investigate whether Pixie promotes the recruitment of eIF3 to the 40S subunit, I compared levels of 40S-bound eIF3-S10 in cells depleted of Pixie with that in control cells. I found that a 90% depletion of Pixie does not affect levels of 40S subunit-bound eIF3-S10 (Figure 5-13), either because Pixie is not essential for its recruitment to the 40S subunit, or because the remaining Pixie is still able to provide that catalytic function. Consistent with my data, depletion of Rli1p also has no impact on the proportion of 40S subunit-bound eIF3 in yeast (Dong et al., 2004). Instead, Rli1p depletion reduces levels of 40S subunit-bound eIF1, eIF2, and eIF5 (Dong et al., 2004). In contrast, I found that depletion of 90% of Pixie has no impact on recruitment of eIF2-α to the 40S subunit (Figure 5-13). This discrepancy between my data and the data published by Dong and co-workers might reflect a difference in the efficiency of the Pixie versus the Rli1p depletion. Notably, though, the same 90% depletion of Pixie is able to reduce the polysome content of cells (Figure 5-5A-C), indicating that the observed defect in translation initiation is unlikely to be caused by a lack of recruitment of eIF2-α or eIF3 core components to the 40S subunit.

5.2.8 A function of Pixie between 43S and 48S pre-initiation complex assembly

As previously mentioned, the eIF3 complex functions as a platform that coordinates multiple events during translation initiation. For instance, activation of the insulin-signalling pathway results in the replacement of eIF3-bound S6K by mTOR and the recruitment of eIF4B to the eIF3 complex (Holz et al., 2005). Moreover, mTOR-dependent signalling stimulates the assembly of 48S pre-initiation complexes by promoting the association of 40S subunit-bound eIF3 with mRNA-bound eIF4G (Harris et al., 2006). Thus, it is possible that Pixie, rather than recruiting eIF3 to the 40S subunit, interacts with 40S subunit-bound eIF3 at a later step of translation initiation to promote assembly of 48S pre-initiation complexes.

Interestingly, the mammalian homologue of Adam, eIF3j, was recently found to reduce the affinity of the 40S subunit for mRNA by binding to the mRNA

entry channel. Thus, high affinity for mRNA is only restored upon recruitment of the TC to the 40S subunit and positioning of Met-tRNA$_i^{Met}$ in the P site (Fraser et al., 2007). Given the potential direct interaction between Pixie and Adam (Kispal et al., 2005), Pixie might modulate Adam activity at this stage of translation initiation to promote 48S pre-initiation complex assembly.

5.2.9 *pixie* mutant flies have *a Minute*-like phenotype, suggesting that ribosome levels might be affected.

Insulin signalling regulates several aspects of translation including translation initiation and elongation. In addition to mutations in the *pixie* gene, the screen carried out in the Leevers laboratory also identified mutations genes encoding ribosomal proteins (Coelho et al., 2005b). This indicates that mutations in the genes encoding the building blocks of the translational machinery interact genetically with mutations that reduce insulin signalling. Interestingly, phenotypic analyses carried out by Carmen Coelho showed that the *pixie* mutant phenotype is similar to that displayed by the *Minute* class of mutations, several of which have been shown to correspond to mutations in ribosomal genes (Coelho et al., 2005a; Lambertsson, 1998). Like flies heterozygous for *Minute* mutations, flies trans-heterozygous for weak *pixie* mutant combinations or flies carrying a dominant negative *pixie* allele show developmental delay and have slender bristles (Coelho et al., 2005a). Thus, *pixie* has a 'Minute-like' phenotype, consistent with it being required for normal levels of translation. To date, no translation initiation factors have been reported to have *Minute*-like phenotypes and eIF4A mutations do not have the same effect on clonal growth as *pixie* mutations (Coelho et al., 2005a). Thus, although my biochemical data demonstrate that Pixie plays a role in translation initiation, its mutant phenotypes are more akin to those of ribosomal protein mutants than those of translation initiation factors. The *Minute*-like aspects of the *pixie* mutant phenotype may reflect the fact that Pixie, like yeast Rli1p, has an additional role in ribosome biogenesis (Dong et al., 2004; Kispal et al., 2005; Yarunin et al., 2005). Consistent with this idea, my data demonstrate that Pixie can bind the 40S ribosomal subunit (Figure 5-3C), and that it does so in dependently of core eIF3 components (Figure 5-13). Future experiments might shed light on whether the reported function of Rli1p in ribosome biogenesis is conserved in flies. In yeast, conditional knockout of Rlip results in nuclear accumulation of recombinant GFP-tagged small and large ribosomal subunit proteins, and this is likely to be caused by a defect in ribosome

biogenesis (Kispal et al., 2005; Yarunin et al., 2005). To address the putative function of Pixie in ribosome biogenesis, the cellular localisation of GFP-tagged small and large ribosomal proteins could be examined in control and Pixie-depleted cells. The small and large ribosomal subunit rRNAs are generated from the same pre-rRNA by multiple consecutive cleavage events. Since a defect in pre-rRNA processing is likely to result in the accumulation of pre-rRNA or partially processed pre-rRNA intermediates, the requirement for Pixie in rRNA maturation could be addressed by Nortern-blot analysis, using probes that recognise different rRNA intermediates, in control and Pixie-depleted cells.

Chapter 6 - Concluding Remarks

Gene expression is regulated at multiple stages including transcription, pre-mRNA processing, and translation. The first regulated step in gene expression is transcription. For all protein-encoding genes, this is initiated by the recruitment of RNAP II and a number of general and gene-specific transcription factors to the promoter region of the gene. Once the RNAP II PIC has assembled onto the promoter region, phosphorylation of RNAP II on its CTD is required for transcription elongation to take place. This is carried out by various kinases including Cdks 7 and 9. Efficient RNAP II transcription elongation also relies on the coordinated action of positive elongation factors and chromatin remodelling factors. The data presented here suggest that the FHA domain protein dMCRS2 might have a previously uncharacterised function in RNAP II transcription. Thus, dMCRS2 can be purified in complex with RNAP II-associated proteins and co-localises with a subset of RNAP II complexes on polytene chromosomes. However, it is not clear which role dMCRS2 might play in RNAP II transcription. The association of dMCRS2 with TFIIF, Pitslre, CK2, and the FACT component SSRP1 suggests that dMCRS2 might function in early and/or late transcription elongation. dMCRS2 was previously shown to form a complex with the histone acetyl transferase MOF (Mendjan et al., 2006), which mediates H4K16Ac at the 5'-end of genes and has been shown to regulate RNAP II-dependent transcription of a number of genes (Kind et al., 2008). How the MOF complex is recruited to sites of active transcription remains mysterious, and a physical link between the chromatin remodelling MOF-complex and RNAP II has yet to be established. It is tempting to speculate that dMCRS2 might provide a physical link between the MOF-complex and RNAP II via its ability to associate with Pitslre. Thus, RNAP II-associated dMCRS2 and/or Pitslre could function as a docking site for the remainder of the MOF complex, which in turn might stimulate early or late RNAP II elongation by modulating the chromatin structure. Interestingly, the association of dMCRS2 with Pitslre is abolished in response to hyper-activation of the Hpo signalling pathway. Thus, the association of dMCRS2 and/or the MOF complex with RNAP II could be regulated in response to apoptotic stimuli. Whereas the above model is consistent with the data presented here, it requires further validation. First, it remains to be determined whether dMCRS2 function

is indeed required for normal levels of RNAP II transcription. Second, it will be interesting to resolve whether dMCRS2 associates with initiating or elongating RNAP II complexes. Third, it will be important to clarify whether dMCRS2 and/or Pitslre are required for the recruitment of the MOF complex to sites of active transcription. Finally, if RNAP II-associated dMCRS2 functions as a docking site for the MOF complex, it will be interesting to determine whether association of dMCRS2 and/or the MOF complex with RNAP II regulated in response to apoptosis?

Once a gene has been transcribed, the next step in gene expression is splicing of the pre-mRNA to generate mature mRNA. This process is carried out by the spliceosome, a highly conserved ribonucleoprotein complex that consists of five snRNAs and more than 200 proteins. Whereas much of the mechanistic insight into the spliceosome has been derived from yeast genetics, the isolation and comparison of different mammalian spliceosome intermediates have revealed that excision of an intron from a pre-mRNA occurs largely by the same sequential path in yeast and higher eukaryotes (Bessonov et al., 2008; Jurica et al., 2002; Makarov et al., 2002; Makarova et al., 2004). Importantly, purifications of mammalian spliceosomes have added a vast array of elements to the pre-existing list of conserved core splicing factors. Many of these have no previous connection to splicing and require functional validation (Jurica and Moore, 2003). One example is MFAP1, which was recovered in a number of purifications of various mammalian spliceosomal complexes (Bessonov et al., 2008; Deckert et al., 2006; Makarov et al., 2002; Makarova et al., 2004; Neubauer et al., 1998). The supposed function of MFAP1 as an extra-cellular matrix component initially led to its classification as a purification artefact (Neubauer, 2005; Neubauer et al., 1998). Here I provide evidence that the *Drosophila* homologue MFAP1, dMFAP1, is indeed required for pre-mRNA processing (Andersen and Tapon, 2008). Moreover, I show that dMFAP1 binds directly to dPrp38 (Andersen and Tapon, 2008), the *Drosophila* homologue of the yeast tri-snRNP protein Prp38p that was previously shown to be dispensable for spliceosome assembly, but required for spliceosome activation (Xie et al., 1998). In addition to dPrp38, dMFAP1 is associated with several other splicing factors that function during the activation step, suggesting that dMFAP1, like dPrp38, plays a role in the activation step of the spliceosome (Andersen and Tapon, 2008). Consistent with this, human MFAP1 associates with fully assembled and activated spliceosomes, but is absent from spliceosomes purified after the first catalytic reaction (Bessonov et al., 2008; Deckert et al., 2006; Makarov et al., 2002; Makarova et

al., 2004; Neubauer et al., 1998). dMFAP1 is well conserved among higher eukaryotes, but has no recognisable homologue in yeast, indicating that it has evolved more recently in metazoans. This might suggest that dMFAP1, like many other metazoan-specific splicing factors, plays a role in alternative splicing. It would be interesting to include dMFAP1 in future RNAi screens for regulators of alternative splicing.

In agreement with their fundamental functions, I found that dPrp38 and dMFAP1 are essential proteins required for growth and proliferation during development (Andersen and Tapon, 2008). A more detailed analysis of this growth defect shows that dMFAP1 and dPrp38 are required for G2/M progression (Andersen and Tapon, 2008). Interestingly, dsRNA-mediated depletion of a wide range of core splicing factors elicits a similar phenotype, suggesting that the observed G2/M arrest might be a general consequence of interfering with spliceosome function (Andersen and Tapon, 2008). In agreement with this, a genome-wide screen RNA interference screen in HeLa cells for factors required for mitosis identified a number of genes encoding splicing factors (Kittler et al., 2004). Future studies might resolve whether the observed G2/M arrest results from of a failure to splice a pre-mRNA encoding a factor that is rate limiting for entry into mitosis (e.g. *stg/cdc25)*, or whether a defect in splicing activates a mitotic checkpoint that causes cells to arrest in G2.

Once pre-mRNAs have been processed into mRNAs, they are exported into the cytoplasm where they engage with translation initiation factors and ribosomal subunits to form translation initiation competent complexes. This is another step in gene expression, which is tightly regulated in accordance with extra-cellular insulin levels and intra-cellular energy and amino acid levels. Leevers and co-workers carried out a genetic screen to identify molecules that regulate growth and interact with PI3K-signalling (Coelho et al., 2005b). One of the genes identified in this screen, *pixie*, was found to enhance the small-wing phenotype elicited by expression of a dominant negative form of the catalytic subunit of PI3K in the wing. Subsequently, Pixie was found to be required for normal global levels of translation (Coelho et al., 2005a). The data presented here provide a more detailed characterisation of role of Pixie in translation. I show that Pixie associates with eIF3 and small ribosomal proteins and is required for the assembly of translation initiation competent complexes (Andersen and Leevers, 2007). Thus, depletion of Pixie results in the accumulation of empty 80S ribosomes lacking mRNAs and reduces translation initiation levels (Andersen and Leevers, 2007). Moreover, Pixie associates with the 40S subunit in an ATP-dependent

manner, suggesting that Pixie plays a catalytic role in the assembly of complexes required for translation initiation (Andersen and Leevers, 2007). It is not clear at which stage of translation initiation Pixie is required. Thus, depletion of Pixie does not appear to affect the recruitment of eIF3 and eIF2 to the 40S subunit (shown here and (Andersen and Leevers, 2007)). This suggests that Pixie is dispensable for 43S PIC assembly and might be required at a later stage of translation initiation, e.g. for assembly of 48S PICs. Interestingly, eIF3, which Pixie was co-purified with, seems to provide a platform to coordinate a dynamic sequence of events required for 48S PIC assembly in response to insulin signalling (Holz et al., 2005). Thus, insulin signalling recruits the mTORC1 complex to eIF3, which results in the activation and release of S6K1 (Holz et al., 2005). Following activation and dissociation from the translational machinery, S6K1 phosphorylates and activates eIF4B. Phosphorylation of eIF4B promotes its recruitment to the translational machinery via its association with eIF3 (Holz et al., 2005). Insulin signalling also stimulates the association of eIF4G with eIF3 and thereby promotes 48S PIC assembly. It is tempting to speculate that Pixie provides a catalytic function downstream of insulin signalling to assist and/or coordinate the association of some of these factors with eIF3. It would be interesting to examine the effect of Pixie depletion on the association of mTOR, S6K, eIF4B, and eIF4G with 40S-bound eIF3. This might provide a better understanding of the mechanism by which Pixie promotes 48S PIC assembly and translation initiation.

Although my biochemical analysis demonstrates a role of Pixie in translation initiation (Andersen and Leevers, 2007), the *pixie* mutant phenotypes are more akin those of ribosomal protein mutants than those of translation initiation factors (Coelho et al., 2005a). This suggests that Pixie might have an additional function required to maintain normal levels of ribosomes. Consistent with this idea, the yeast homologue Rli1p has dual functions in translation initiation and ribosome biogenesis (Kispal et al., 2005; Yarunin et al., 2005). Whereas the function of Pixie/Rli1p in translation initiation seems to be well conserved, it remains to be determined whether the function of Rli1p in ribosome biogenesis is also conserved in higher eukaryotes.

Organism growth relies on gene expression and is therefore crucially dependent on the basic cellular machineries that are responsible for gene transcription, pre-mRNA processing, nuclear export, and protein synthesis. Moreover, each step of gene expression must be tightly regulated in accordance with nutrient availability and developmental programming. In multicellular organisms, developmental programming

ensures that the transcription of specific subsets of genes is triggered at the appropriate stage of development. During early development, growth is often exponential, and genes encoding molecules required for protein synthesis and organelle biogenesis are actively transcribed. At later stages of development different subsets of genes are turned on to restrict proliferation and promote differentiation of progenitor cells into specialised cells. This shift in gene expression is mainly achieved by highly controlled epigenetic mechanisms including covalent modifications of histones such as acetylation, phosphorylation, and methylation (Agger et al., 2008; Berger, 2007; Panning and Taatjes, 2008; Thomas and Voss, 2007). The importance of keeping those mechanisms in check is evident from the observation that many human cancers are caused by changes in the epigenetic landscape that result in silencing of tumour suppressor genes. Thus, loss of hMOF, which specifically acetylates histone 4 on lysine 16, leads to nucleosome repositioning and silencing of the *TMS1* (*target of methylation-mediated silencing*) tumour suppressor gene (Kapoor-Vazirani et al., 2008). In contrast to other histone modifications, H4K16Ac is restricted to a more select set of target genes, suggesting that the dMCRS2-MOF complex might regulate a limited subset of genes required for specific cellular processes, e.g., apoptosis.

Regulation of alternative splicing is another mechanism by which gene expression is fine-tuned to meet cellular needs at different stages of development in multicellular organisms. In contrast to unicellular organisms, where alternative splicing is almost non-existent, alternative splicing represents a key regulatory step in higher eukaryotes. Thus, a recent study estimates that at least 74% of multi-exon transcripts are alternatively spliced in humans (Johnson et al., 2003). To accommodate more complex splice patterns, additional splicing factors have evolved in metazoans. These include the family of SR proteins, which function in splice site selection. Genes encoding SR proteins are frequently mutated in various types of cancer (Ghigna et al., 2005; Karni et al., 2007; Sjoblom et al., 2006). One possible explanation for this is that mutations in SR proteins are likely to affect the expression of only a subset of genes and could potentially target oncogenes or tumour suppressor genes specifically. The finding that dMFAP1 is required for pre-mRNA processing adds another protein to the list of splicing factors that have evolved more recently in metazoans. It will be interesting to learn more about the contribution of dMFAP1 to alternative splicing and whether mutations in the dmfap1 gene is associated with human diseases.

Protein synthesis is the last step in gene expression and is subject to regulation by multiple signalling pathways. During early development mass accumulation is often exponential and this puts a high demand on the translational machinery to synthesise proteins required for organelle biogenesis. Importantly, protein synthesis and ribosome biogenesis are among the most energetically demanding cellular processes and must be kept in check and coordinated with nutrient availability. The TOR kinase represents a major node for the integration of multiple signals representing the metabolic state of the cell and regulates protein synthesis according to amino acid and energy levels. The observation that mutations in *pixie* interact genetically with mutations altering the activity of the insulin signalling pathway suggests that Pixie could function as a downstream effector of insulin signalling to regulate translation levels (Coelho et al., 2005). Interestingly, the presence of two iron-sulfur clusters (ISCs) at the N-terminus of Pixie implies that Pixie activity could be regulated by other means, e.g., in response to reactive oxygen species (ROS). Thus, Nitric Oxide (NO) is known to alter the activity of iron regulatory protein 1 (IRP1) by promoting disassembly of its ISCs in response to immunological or inflammatory stimuli (reviewed in (Bouton and Drapier, 2003)). Similarly, Pixie activity might be modulated in response to stress. It is tempting to speculate that Pixie could function as a sensor of ROS to regulate protein synthesis and growth in response to various types of environmental stress. In addition, the main source of ROS in the cell is the mitochondria, where ROS are generated as part of the respiratory process. Thus, Pixie could sense the energy status of the cell and thus couple mitochondrial ATP generation with the energy-intensive process of protein synthesis. Since Pixie/RLI proteins are extraordinarily conserved, this might represent an ancient mechanism for regulating growth of unicellular organisms in response to environmental clues (Gabaldon and Huynen, 2004). Interestingly, the human homologue of Pixie, RLI, was originally identified as an inhibitor of the antiviral 2-5A/RNAse L system, which is induced by interferon in response to viral infection (Bisbal et al., 1995). Interferon signalling increases levels of NO, which in turn might alter the activity of RLI to promote the antiviral action of the 2-5A/RNAse L system. Thus, it is possible that in mammals, deregulation of RLI activity in response to immunological and/or inflammatory stimuli would support immune defence processes by simultaneously slowing down metabolism and promoting antiviral action.

References

Abovich, N., and Rosbash, M. (1997). Cross-intron bridging interactions in the yeast commitment complex are conserved in mammals. Cell *89*, 403-412.

Abramson, R.D., Dever, T.E., and Merrick, W.C. (1988). Biochemical evidence supporting a mechanism for cap-independent and internal initiation of eukaryotic mRNA. J Biol Chem *263*, 6016-6019.

Achsel, T., Ahrens, K., Brahms, H., Teigelkamp, S., and Luhrmann, R. (1998). The human U5-220kD protein (hPrp8) forms a stable RNA-free complex with several U5-specific proteins, including an RNA unwindase, a homologue of ribosomal elongation factor EF-2, and a novel WD-40 protein. Mol Cell Biol *18*, 6756-6766.

Adelman, K., Wei, W., Ardehali, M.B., Werner, J., Zhu, B., Reinberg, D., and Lis, J.T. (2006). Drosophila Paf1 modulates chromatin structure at actively transcribed genes. Mol Cell Biol *26*, 250-260.

Agger, K., Christensen, J., Cloos, P.A., and Helin, K. (2008). The emerging functions of histone demethylases. Curr Opin Genet Dev *18*, 159-168.

Ahmed, K., Gerber, D.A., and Cochet, C. (2002). Joining the cell survival squad: an emerging role for protein kinase CK2. Trends Cell Biol *12*, 226-230.

Ahn, S.H., Kim, M., and Buratowski, S. (2004). Phosphorylation of serine 2 within the RNA polymerase II C-terminal domain couples transcription and 3' end processing. Mol Cell *13*, 67-76.

Ajuh, P., Kuster, B., Panov, K., Zomerdijk, J.C., Mann, M., and Lamond, A.I. (2000). Functional analysis of the human CDC5L complex and identification of its components by mass spectrometry. EMBO J *19*, 6569-6581.

Akhtar, A., and Becker, P.B. (2000). Activation of transcription through histone H4 acetylation by MOF, an acetyltransferase essential for dosage compensation in Drosophila. Mol Cell *5*, 367-375.

Akoulitchev, S., Chuikov, S., and Reinberg, D. (2000). TFIIH is negatively regulated by cdk8-containing mediator complexes. Nature *407*, 102-106.

Albright, S.R., and Tjian, R. (2000). TAFs revisited: more data reveal new twists and confirm old ideas. Gene *242*, 1-13.

Alessi, D.R., Deak, M., Casamayor, A., Caudwell, F.B., Morrice, N., Norman, D.G., Gaffney, P., Reese, C.B., MacDougall, C.N., Harbison, D., *et al.* (1997). 3-Phosphoinositide-dependent protein kinase-1 (PDK1): structural and functional homology with the Drosophila DSTPK61 kinase. Curr Biol *7*, 776-789.

Alessi, D.R., Kozlowski, M.T., Weng, Q.P., Morrice, N., and Avruch, J. (1998). 3-Phosphoinositide-dependent protein kinase 1 (PDK1) phosphorylates and activates the p70 S6 kinase in vivo and in vitro. Curr Biol *8*, 69-81.

Algire, M.A., Maag, D., and Lorsch, J.R. (2005). Pi release from eIF2, not GTP hydrolysis, is the step controlled by start-site selection during eukaryotic translation initiation. Mol Cell *20*, 251-262.

Algire, M.A., Maag, D., Savio, P., Acker, M.G., Tarun, S.Z., Jr., Sachs, A.B., Asano, K., Nielsen, K.H., Olsen, D.S., Phan, L., *et al.* (2002). Development and characterization of a reconstituted yeast translation initiation system. RNA *8*, 382-397.

Alkalaeva, E.Z., Pisarev, A.V., Frolova, L.Y., Kisselev, L.L., and Pestova, T.V. (2006). In vitro reconstitution of eukaryotic translation reveals cooperativity between release factors eRF1 and eRF3. Cell *125*, 1125-1136.

Andersen, D.S., and Leevers, S.J. (2007). The essential Drosophila ATP-binding cassette domain protein, pixie, binds the 40 S ribosome in an ATP-dependent manner and is required for translation initiation. J Biol Chem *282*, 14752-14760.

Andersen, D.S., and Tapon, N. (2008). Drosophila MFAP1 is required for pre-mRNA processing and G2/M progression. J Biol Chem.

Andrulis, E.D., Guzman, E., Doring, P., Werner, J., and Lis, J.T. (2000). High-resolution localization of Drosophila Spt5 and Spt6 at heat shock genes in vivo: roles in promoter proximal pausing and transcription elongation. Genes Dev *14*, 2635-2649.

Arenas, J.E., and Abelson, J.N. (1997). Prp43: An RNA helicase-like factor involved in spliceosome disassembly. Proc Natl Acad Sci U S A *94*, 11798-11802.

Ariza, M.E., Broome-Powell, M., Lahti, J.M., Kidd, V.J., and Nelson, M.A. (1999). Fas-induced apoptosis in human malignant melanoma cell lines is associated with the activation of the p34(cdc2)-related PITSLRE protein kinases. J Biol Chem *274*, 28505-28513.

Arning, S., Gruter, P., Bilbe, G., and Kramer, A. (1996). Mammalian splicing factor SF1 is encoded by variant cDNAs and binds to RNA. RNA *2*, 794-810.

Aronova, A., Bacikova, D., Crotti, L.B., Horowitz, D.S., and Schwer, B. (2007). Functional interactions between Prp8, Prp18, Slu7, and U5 snRNA during the second step of pre-mRNA splicing. RNA *13*, 1437-1444.

Asano, K., Clayton, J., Shalev, A., and Hinnebusch, A.G. (2000). A multifactor complex of eukaryotic initiation factors, eIF1, eIF2, eIF3, eIF5, and initiator tRNA(Met) is an important translation initiation intermediate in vivo. Genes Dev *14*, 2534-2546.

Auble, D.T., and Hahn, S. (1993). An ATP-dependent inhibitor of TBP binding to DNA. Genes Dev *7*, 844-856.

Averous, J., and Proud, C.G. (2006). When translation meets transformation: the mTOR story. Oncogene *25*, 6423-6435.

Avruch, J., Belham, C., Weng, Q., Hara, K., and Yonezawa, K. (2001). The p70 S6 kinase integrates nutrient and growth signals to control translational capacity. Prog Mol Subcell Biol *26*, 115-154.

Bacikova, D., and Horowitz, D.S. (2005). Genetic and functional interaction of evolutionarily conserved regions of the Prp18 protein and the U5 snRNA. Mol Cell Biol *25*, 2107-2116.

Bartels, C., Klatt, C., Luhrmann, R., and Fabrizio, P. (2002). The ribosomal translocase homologue Snu114p is involved in unwinding U4/U6 RNA during activation of the spliceosome. EMBO Rep *3*, 875-880.

Battiste, J.L., Pestova, T.V., Hellen, C.U., and Wagner, G. (2000). The eIF1A solution structure reveals a large RNA-binding surface important for scanning function. Mol Cell *5*, 109-119.

Behzadnia, N., Hartmuth, K., Will, C.L., and Luhrmann, R. (2006). Functional spliceosomal A complexes can be assembled in vitro in the absence of a penta-snRNP. RNA *12*, 1738-1746.

Bellen, H.J., Levis, R.W., Liao, G., He, Y., Carlson, J.W., Tsang, G., Evans-Holm, M., Hiesinger, P.R., Schulze, K.L., Rubin, G.M., *et al.* (2004). The BDGP gene disruption project: single transposon insertions associated with 40% of Drosophila genes. Genetics *167*, 761-781.

Belotserkovskaya, R., Oh, S., Bondarenko, V.A., Orphanides, G., Studitsky, V.M., and Reinberg, D. (2003). FACT facilitates transcription-dependent nucleosome alteration. Science *301*, 1090-1093.

Benne, R., and Hershey, J.W. (1976). Purification and characterization of initiation factor IF-E3 from rabbit reticulocytes. Proc Natl Acad Sci U S A *73*, 3005-3009.

Benne, R., and Hershey, J.W. (1978). The mechanism of action of protein synthesis initiation factors from rabbit reticulocytes. J Biol Chem *253*, 3078-3087.

Bennett, F.C., and Harvey, K.F. (2006). Fat cadherin modulates organ size in Drosophila via the Salvador/Warts/Hippo signaling pathway. Curr Biol *16*, 2101-2110.

Bentley, D.L. (2005). Rules of engagement: co-transcriptional recruitment of pre-mRNA processing factors. Curr Opin Cell Biol *17*, 251-256.

Berger, S.L. (2007). The complex language of chromatin regulation during transcription. Nature *447*, 407-412.

Bernstein, H.S., and Coughlin, S.R. (1998). A mammalian homolog of fission yeast Cdc5 regulates G2 progression and mitotic entry. J Biol Chem *273*, 4666-4671.

Berthelot, K., Muldoon, M., Rajkowitsch, L., Hughes, J., and McCarthy, J.E. (2004). Dynamics and processivity of 40S ribosome scanning on mRNA in yeast. Mol Microbiol *51*, 987-1001.

Bertolotti, A., Zhang, Y., Hendershot, L.M., Harding, H.P., and Ron, D. (2000). Dynamic interaction of BiP and ER stress transducers in the unfolded-protein response. Nat Cell Biol *2*, 326-332.

Bessonov, S., Anokhina, M., Will, C.L., Urlaub, H., and Luhrmann, R. (2008). Isolation of an active step I spliceosome and composition of its RNP core. Nature.

Bi, X., Ren, J., and Goss, D.J. (2000). Wheat germ translation initiation factor eIF4B affects eIF4A and eIFiso4F helicase activity by increasing the ATP binding affinity of eIF4A. Biochemistry *39*, 5758-5765.

Bienkiewicz, E.A., Moon Woody, A., and Woody, R.W. (2000). Conformation of the RNA polymerase II C-terminal domain: circular dichroism of long and short fragments. J Mol Biol *297*, 119-133.

Bisbal, C., Martinand, C., Silhol, M., Lebleu, B., and Salehzada, T. (1995). Cloning and characterization of a RNAse L inhibitor. A new component of the interferon-regulated 2-5A pathway. J Biol Chem *270*, 13308-13317.

Bjorklund, S., and Gustafsson, C.M. (2005). The yeast Mediator complex and its regulation. Trends Biochem Sci *30*, 240-244.

Blair, S.S. (2003). Genetic mosaic techniques for studying Drosophila development. Development *130*, 5065-5072.

Bleichert, F., and Baserga, S.J. (2007). The long unwinding road of RNA helicases. Mol Cell *27*, 339-352.

Blum, S., Schmid, S.R., Pause, A., Buser, P., Linder, P., Sonenberg, N., and Trachsel, H. (1992). ATP hydrolysis by initiation factor 4A is required for translation initiation in Saccharomyces cerevisiae. Proc Natl Acad Sci U S A *89*, 7664-7668.

Boger-Nadjar, E., Vaisman, N., Ben-Yehuda, S., Kassir, Y., and Kupiec, M. (1998). Efficient initiation of S-phase in yeast requires Cdc40p, a protein involved in pre-mRNA splicing. Mol Gen Genet *260*, 232-241.

Borggrefe, T., Davis, R., Erdjument-Bromage, H., Tempst, P., and Kornberg, R.D. (2002). A complex of the Srb8, -9, -10, and -11 transcriptional regulatory proteins from yeast. J Biol Chem *277*, 44202-44207.

Bortvin, A., and Winston, F. (1996). Evidence that Spt6p controls chromatin structure by a direct interaction with histones. Science *272*, 1473-1476.

Boube, M., Joulia, L., Cribbs, D.L., and Bourbon, H.M. (2002). Evidence for a mediator of RNA polymerase II transcriptional regulation conserved from yeast to man. Cell *110*, 143-151.

Boukis, L.A., Liu, N., Furuyama, S., and Bruzik, J.P. (2004). Ser/Arg-rich protein-mediated communication between U1 and U2 small nuclear ribonucleoprotein particles. J Biol Chem *279*, 29647-29653.

Bousquet-Antonelli, C., Presutti, C., and Tollervey, D. (2000). Identification of a regulated pathway for nuclear pre-mRNA turnover. Cell *102*, 765-775.

Bouton, C., and Drapier, J.C. (2003). Iron regulatory proteins as NO signal transducers. Sci STKE *2003*, pe17.

Bradsher, J., Coin, F., and Egly, J.M. (2000). Distinct roles for the helicases of TFIIH in transcript initiation and promoter escape. J Biol Chem *275*, 2532-2538.

Brand, A.H., Manoukian, A.S., and Perrimon, N. (1994). Ectopic expression in Drosophila. Methods Cell Biol *44*, 635-654.

Brand, A.H., and Perrimon, N. (1993). Targeted gene expression as a means of altering cell fates and generating dominant phenotypes. Development *118*, 401-415.

Bregman, D.B., Pestell, R.G., and Kidd, V.J. (2000). Cell cycle regulation and RNA polymerase II. Front Biosci *5*, D244-257.

Brenner, T.J., and Guthrie, C. (2005). Genetic analysis reveals a role for the C terminus of the Saccharomyces cerevisiae GTPase Snu114 during spliceosome activation. Genetics *170*, 1063-1080.

Briggs, S.D., Xiao, T., Sun, Z.W., Caldwell, J.A., Shabanowitz, J., Hunt, D.F., Allis, C.D., and Strahl, B.D. (2002). Gene silencing: trans-histone regulatory pathway in chromatin. Nature *418*, 498.

Brow, D.A. (2002). Allosteric cascade of spliceosome activation. Annu Rev Genet *36*, 333-360.

Brow, D.A., and Vidaver, R.M. (1995). An element in human U6 RNA destabilizes the U4/U6 spliceosomal RNA complex. RNA *1*, 122-131.

Browne, G.J., and Proud, C.G. (2004). A novel mTOR-regulated phosphorylation site in elongation factor 2 kinase modulates the activity of the kinase and its binding to calmodulin. Mol Cell Biol *24*, 2986-2997.

Brush, M.H., Weiser, D.C., and Shenolikar, S. (2003). Growth arrest and DNA damage-inducible protein GADD34 targets protein phosphatase 1 alpha to the endoplasmic reticulum and promotes dephosphorylation of the alpha subunit of eukaryotic translation initiation factor 2. Mol Cell Biol *23*, 1292-1303.

Bunnell, B.A., Heath, L.S., Adams, D.E., Lahti, J.M., and Kidd, V.J. (1990). Increased expression of a 58-kDa protein kinase leads to changes in the CHO cell cycle. Proc Natl Acad Sci U S A *87*, 7467-7471.

Buratowski, S. (2005). Connections between mRNA 3' end processing and transcription termination. Curr Opin Cell Biol *17*, 257-261.

Buratowski, S., Hahn, S., Guarente, L., and Sharp, P.A. (1989). Five intermediate complexes in transcription initiation by RNA polymerase II. Cell *56*, 549-561.

Burgess, S.M., and Guthrie, C. (1993). A mechanism to enhance mRNA splicing fidelity: the RNA-dependent ATPase Prp16 governs usage of a discard pathway for aberrant lariat intermediates. Cell *73*, 1377-1391.

Burke, T.W., and Kadonaga, J.T. (1996). Drosophila TFIID binds to a conserved downstream basal promoter element that is present in many TATA-box-deficient promoters. Genes Dev *10*, 711-724.

Burke, T.W., and Kadonaga, J.T. (1997). The downstream core promoter element, DPE, is conserved from Drosophila to humans and is recognized by TAFII60 of Drosophila. Genes Dev *11*, 3020-3031.

Burns, C., Ohi, R., Mehta, S., O'Toole, E., Winey, M., Clark, T., Sugnet, C., Ares, M., and Gould, K. (2002). Removal of a single alpha-tubulin gene intron suppresses cell cycle arrest phenotypes of splicing factor mutations in Saccharomyces cerevisiae. Mol Cell Biol *22*, 801-815.

Caceres, J.F., Misteli, T., Screaton, G.R., Spector, D.L., and Krainer, A.R. (1997). Role of the modular domains of SR proteins in subnuclear localization and alternative splicing specificity. J Cell Biol *138*, 225-238.

Cagas, P.M., and Corden, J.L. (1995). Structural studies of a synthetic peptide derived from the carboxyl-terminal domain of RNA polymerase II. Proteins *21*, 149-160.

Campbell, S.G., Hoyle, N.P., and Ashe, M.P. (2005). Dynamic cycling of eIF2 through a large eIF2B-containing cytoplasmic body: implications for translation control. J Cell Biol *170*, 925-934.

Carlberg, U., Nilsson, A., and Nygard, O. (1990). Functional properties of phosphorylated elongation factor 2. Eur J Biochem *191*, 639-645.

Carlson, M. (1997). Genetics of transcriptional regulation in yeast: connections to the RNA polymerase II CTD. Annu Rev Cell Dev Biol *13*, 1-23.

Caruthers, J.M., and McKay, D.B. (2002). Helicase structure and mechanism. Curr Opin Struct Biol *12*, 123-133.

Chadick, J.Z., and Asturias, F.J. (2005). Structure of eukaryotic Mediator complexes. Trends Biochem Sci *30*, 264-271.

Chakarova, C.F., Hims, M.M., Bolz, H., Abu-Safieh, L., Patel, R.J., Papaioannou, M.G., Inglehearn, C.F., Keen, T.J., Willis, C., Moore, A.T., *et al.* (2002). Mutations in HPRP3, a third member of pre-mRNA splicing factor genes, implicated in autosomal dominant retinitis pigmentosa. Hum Mol Genet *11*, 87-92.

Chambers, R.S., Wang, B.Q., Burton, Z.F., and Dahmus, M.E. (1995). The activity of COOH-terminal domain phosphatase is regulated by a docking site on RNA polymerase II and by the general transcription factors IIF and IIB. J Biol Chem *270*, 14962-14969.

Chan, C.C., Dostie, J., Diem, M.D., Feng, W., Mann, M., Rappsilber, J., and Dreyfuss, G. (2004). eIF4A3 is a novel component of the exon junction complex. RNA *10*, 200-209.

Chan, S.P., and Cheng, S.C. (2005). The Prp19-associated complex is required for specifying interactions of U5 and U6 with pre-mRNA during spliceosome activation. J Biol Chem *280*, 31190-31199.

Chan, S.P., Kao, D.I., Tsai, W.Y., and Cheng, S.C. (2003). The Prp19p-associated complex in spliceosome activation. Science *302*, 279-282.

Chaudhuri, J., Chowdhury, D., and Maitra, U. (1999). Distinct functions of eukaryotic translation initiation factors eIF1A and eIF3 in the formation of the 40 S ribosomal preinitiation complex. J Biol Chem *274*, 17975-17980.

Chauvin, C., Salhi, S., Le Goff, C., Viranaicken, W., Diop, D., and Jean-Jean, O. (2005). Involvement of human release factors eRF3a and eRF3b in translation termination and regulation of the termination complex formation. Mol Cell Biol *25*, 5801-5811.

Chawla, G., Sapra, A., Surana, U., and Vijayraghavan, U. (2003). Dependence of pre-mRNA introns on PRP17, a non-essential splicing factor: implications for efficient progression through cell cycle transitions. Nucleic Acids Res *31*, 2333-2343.

Chen, C.H., Kao, D.I., Chan, S.P., Kao, T.C., Lin, J.Y., and Cheng, S.C. (2006a). Functional links between the Prp19-associated complex, U4/U6 biogenesis, and spliceosome recycling. RNA *12*, 765-774.

Chen, C.H., Tsai, W.Y., Chen, H.R., Wang, C.H., and Cheng, S.C. (2001a). Identification and characterization of two novel components of the Prp19p-associated complex, Ntc30p and Ntc20p. J Biol Chem *276*, 488-494.

Chen, C.H., Yu, W.C., Tsao, T.Y., Wang, L.Y., Chen, H.R., Lin, J.Y., Tsai, W.Y., and Cheng, S.C. (2002). Functional and physical interactions between components of the Prp19p-associated complex. Nucleic Acids Res *30*, 1029-1037.

Chen, H.R., Jan, S.P., Tsao, T.Y., Sheu, Y.J., Banroques, J., and Cheng, S.C. (1998). Snt309p, a component of the Prp19p-associated complex that interacts with Prp19p and associates with the spliceosome simultaneously with or immediately after dissociation of U4 in the same manner as Prp19p. Mol Cell Biol *18*, 2196-2204.

Chen, J.-J. (2000). Heme-regulated eIF2α kinase. In translational Control of Gene expression, N. Sonenberg, J.W.B. Hershey, and M.B. Mathews, eds. Cold Spring Harbor, New York: Cold Spring Harbor Laboratory Press 529-546.

Chen, J.Y., Stands, L., Staley, J.P., Jackups, R.R., Jr., Latus, L.J., and Chang, T.H. (2001b). Specific alterations of U1-C protein or U1 small nuclear RNA can eliminate the requirement of Prp28p, an essential DEAD box splicing factor. Mol Cell *7*, 227-232.

Chen, Y.I., Maika, S.D., and Stevens, S.W. (2006b). Epitope tagging of proteins at the native chromosomal loci of genes in mice and in cultured vertebrate cells. J Mol Biol *361*, 412-419.

Chen, Z.Q., Dong, J., Ishimura, A., Daar, I., Hinnebusch, A.G., and Dean, M. (2006c). The essential vertebrate ABCE1 protein interacts with eukaryotic initiation factors. J Biol Chem *281*, 7452-7457.

Cheng, B., and Price, D.H. (2007). Properties of RNA polymerase II elongation complexes before and after the P-TEFb-mediated transition into productive elongation. J Biol Chem *282*, 21901-21912.

Cheung, Y.N., Maag, D., Mitchell, S.F., Fekete, C.A., Algire, M.A., Takacs, J.E., Shirokikh, N., Pestova, T., Lorsch, J.R., and Hinnebusch, A.G. (2007). Dissociation of

eIF1 from the 40S ribosomal subunit is a key step in start codon selection in vivo. Genes Dev *21*, 1217-1230.

Chi, Y., Huddleston, M.J., Zhang, X., Young, R.A., Annan, R.S., Carr, S.A., and Deshaies, R.J. (2001). Negative regulation of Gcn4 and Msn2 transcription factors by Srb10 cyclin-dependent kinase. Genes Dev *15*, 1078-1092.

Cho, E., Feng, Y., Rauskolb, C., Maitra, S., Fehon, R., and Irvine, K.D. (2006). Delineation of a Fat tumor suppressor pathway. Nat Genet *38*, 1142-1150.

Cho, E., and Irvine, K.D. (2004). Action of fat, four-jointed, dachsous and dachs in distal-to-proximal wing signaling. Development *131*, 4489-4500.

Cho, E.J., Kobor, M.S., Kim, M., Greenblatt, J., and Buratowski, S. (2001). Opposing effects of Ctk1 kinase and Fcp1 phosphatase at Ser 2 of the RNA polymerase II C-terminal domain. Genes Dev *15*, 3319-3329.

Cho, E.J., Rodriguez, C.R., Takagi, T., and Buratowski, S. (1998). Allosteric interactions between capping enzyme subunits and the RNA polymerase II carboxy-terminal domain. Genes Dev *12*, 3482-3487.

Cho, S.Y., Shin, E.S., Park, P.J., Shin, D.W., Chang, H.K., Kim, D., Lee, H.H., Lee, J.H., Kim, S.H., Song, M.J., *et al.* (2007). Identification of mouse Prp19p as a lipid droplet-associated protein and its possible involvement in the biogenesis of lipid droplets. J Biol Chem *282*, 2456-2465.

Choi, S.K., Lee, J.H., Zoll, W.L., Merrick, W.C., and Dever, T.E. (1998). Promotion of met-tRNAiMet binding to ribosomes by yIF2, a bacterial IF2 homolog in yeast. Science *280*, 1757-1760.

Choi, S.K., Olsen, D.S., Roll-Mecak, A., Martung, A., Remo, K.L., Burley, S.K., Hinnebusch, A.G., and Dever, T.E. (2000). Physical and functional interaction between the eukaryotic orthologs of prokaryotic translation initiation factors IF1 and IF2. Mol Cell Biol *20*, 7183-7191.

Chua, K., and Reed, R. (1999). The RNA splicing factor hSlu7 is required for correct 3' splice-site choice. Nature *402*, 207-210.

Close, P., Hawkes, N., Cornez, I., Creppe, C., Lambert, C.A., Rogister, B., Siebenlist, U., Merville, M.P., Slaugenhaupt, S.A., Bours, V., *et al.* (2006). Transcription impairment and cell migration defects in elongator-depleted cells: implication for familial dysautonomia. Mol Cell *22*, 521-531.

Coelho, C.M., Kolevski, B., Bunn, C., Walker, C., Dahanukar, A., and Leevers, S.J. (2005a). Growth and cell survival are unevenly impaired in pixie mutant wing discs. Development *132*, 5411-5424.

Coelho, C.M., Kolevski, B., Walker, C.D., Lavagi, I., Shaw, T., Ebert, A., Leevers, S.J., and Marygold, S.J. (2005b). A genetic screen for dominant modifiers of a small-wing phenotype in Drosophila melanogaster identifies proteins involved in splicing and translation. Genetics *171*, 597-614.

Cohen, P., and Frame, S. (2001). The renaissance of GSK3. Nat Rev Mol Cell Biol *2*, 769-776.

Coin, F., Marinoni, J.C., Rodolfo, C., Fribourg, S., Pedrini, A.M., and Egly, J.M. (1998). Mutations in the XPD helicase gene result in XP and TTD phenotypes, preventing interaction between XPD and the p44 subunit of TFIIH. Nat Genet *20*, 184-188.

Colwill, K., Pawson, T., Andrews, B., Prasad, J., Manley, J.L., Bell, J.C., and Duncan, P.I. (1996). The Clk/Sty protein kinase phosphorylates SR splicing factors and regulates their intranuclear distribution. EMBO J *15*, 265-275.

Company, M., Arenas, J., and Abelson, J. (1991). Requirement of the RNA helicase-like protein PRP22 for release of messenger RNA from spliceosomes. Nature *349*, 487-493.

Conaway, J.W., and Conaway, R.C. (1999). Transcription elongation and human disease. Annu Rev Biochem *68*, 301-319.

Conaway, J.W., Florens, L., Sato, S., Tomomori-Sato, C., Parmely, T.J., Yao, T., Swanson, S.K., Banks, C.A., Washburn, M.P., and Conaway, R.C. (2005a). The mammalian Mediator complex. FEBS Lett *579*, 904-908.

Conaway, R.C., Sato, S., Tomomori-Sato, C., Yao, T., and Conaway, J.W. (2005b). The mammalian Mediator complex and its role in transcriptional regulation. Trends Biochem Sci *30*, 250-255.

Corden, J.L., and Patturajan, M. (1997). A CTD function linking transcription to splicing. Trends Biochem Sci *22*, 413-416.

Cordin, O., Banroques, J., Tanner, N.K., and Linder, P. (2006). The DEAD-box protein family of RNA helicases. Gene *367*, 17-37.

Cornelis, S., Bruynooghe, Y., Denecker, G., Van Huffel, S., Tinton, S., and Beyaert, R. (2000). Identification and characterization of a novel cell cycle-regulated internal ribosome entry site. Mol Cell *5*, 597-605.

Corradetti, M.N., and Guan, K.L. (2006). Upstream of the mammalian target of rapamycin: do all roads pass through mTOR? Oncogene *25*, 6347-6360.

Crispino, J.D., Blencowe, B.J., and Sharp, P.A. (1994). Complementation by SR proteins of pre-mRNA splicing reactions depleted of U1 snRNP. Science *265*, 1866-1869.

Cristofari, G., and Darlix, J.L. (2002). The ubiquitous nature of RNA chaperone proteins. Prog Nucleic Acid Res Mol Biol *72*, 223-268.

Crotti, L.B., Bacikova, D., and Horowitz, D.S. (2007). The Prp18 protein stabilizes the interaction of both exons with the U5 snRNA during the second step of pre-mRNA splicing. Genes Dev *21*, 1204-1216.

Dahan, O., and Kupiec, M. (2004). The Saccharomyces cerevisiae gene CDC40/PRP17 controls cell cycle progression through splicing of the ANC1 gene. Nucleic Acids Res *32*, 2529-2540.

Dahmus, M.E. (1995). Phosphorylation of the C-terminal domain of RNA polymerase II. Biochim Biophys Acta *1261*, 171-182.

Dahmus, M.E. (1996). Reversible phosphorylation of the C-terminal domain of RNA polymerase II. J Biol Chem *271*, 19009-19012.

Danaie, P., Wittmer, B., Altmann, M., and Trachsel, H. (1995). Isolation of a protein complex containing translation initiation factor Prt1 from Saccharomyces cerevisiae. J Biol Chem *270*, 4288-4292.

Das, S., Ghosh, R., and Maitra, U. (2001). Eukaryotic translation initiation factor 5 functions as a GTPase-activating protein. J Biol Chem *276*, 6720-6726.

Das, S., and Maitra, U. (2001). Functional significance and mechanism of eIF5-promoted GTP hydrolysis in eukaryotic translation initiation. Prog Nucleic Acid Res Mol Biol *70*, 207-231.

Davidovic, L., Bechara, E., Gravel, M., Jaglin, X.H., Tremblay, S., Sik, A., Bardoni, B., and Khandjian, E.W. (2006). The nuclear microspherule protein 58 is a novel RNA-binding protein that interacts with fragile X mental retardation protein in polyribosomal mRNPs from neurons. Hum Mol Genet *15*, 1525-1538.

De Bondt, H.L., Rosenblatt, J., Jancarik, J., Jones, H.D., Morgan, D.O., and Kim, S.H. (1993). Crystal structure of cyclin-dependent kinase 2. Nature *363*, 595-602.

de la Cruz, J., Kressler, D., and Linder, P. (1999). Unwinding RNA in Saccharomyces cerevisiae: DEAD-box proteins and related families. Trends Biochem Sci *24*, 192-198.

de la Mata, M., and Kornblihtt, A.R. (2006). RNA polymerase II C-terminal domain mediates regulation of alternative splicing by SRp20. Nat Struct Mol Biol *13*, 973-980.

Deckert, J., Hartmuth, K., Boehringer, D., Behzadnia, N., Will, C.L., Kastner, B., Stark, H., Urlaub, H., and Luhrmann, R. (2006). Protein composition and electron microscopy structure of affinity-purified human spliceosomal B complexes isolated under physiological conditions. Mol Cell Biol *26*, 5528-5543.

DeJong, J., and Roeder, R.G. (1993). A single cDNA, hTFIIA/alpha, encodes both the p35 and p19 subunits of human TFIIA. Genes Dev *7*, 2220-2234.

Deng, W., and Roberts, S.G. (2005). A core promoter element downstream of the TATA box that is recognized by TFIIB. Genes Dev *19*, 2418-2423.

Deng, W., and Roberts, S.G. (2006). Core promoter elements recognized by transcription factor IIB. Biochem Soc Trans *34*, 1051-1053.

Deng, W., and Roberts, S.G. (2007). TFIIB and the regulation of transcription by RNA polymerase II. Chromosoma *116*, 417-429.

Devault, A., Martinez, A.M., Fesquet, D., Labbe, J.C., Morin, N., Tassan, J.P., Nigg, E.A., Cavadore, J.C., and Doree, M. (1995). MAT1 ('menage a trois') a new RING finger protein subunit stabilizing cyclin H-cdk7 complexes in starfish and Xenopus CAK. EMBO J *14*, 5027-5036.

Dever, T.E. (2002). Gene-specific regulation by general translation factors. Cell *108*, 545-556.

Diaz, B., and Moreno, E. (2005). The competitive nature of cells. Exp Cell Res *306*, 317-322.

Dietzl, G., Chen, D., Schnorrer, F., Su, K.C., Barinova, Y., Fellner, M., Gasser, B., Kinsey, K., Oppel, S., Scheiblauer, S., *et al.* (2007). A genome-wide transgenic RNAi library for conditional gene inactivation in Drosophila. Nature *448*, 151-156.

Dillon, S.C., Zhang, X., Trievel, R.C., and Cheng, X. (2005). The SET-domain protein superfamily: protein lysine methyltransferases. Genome Biol *6*, 227.

Dong, J., Lai, R., Nielsen, K., Fekete, C.A., Qiu, H., and Hinnebusch, A.G. (2004). The essential ATP-binding cassette protein RLI1 functions in translation by promoting preinitiation complex assembly. J Biol Chem *279*, 42157-42168.

Dou, Y., Milne, T.A., Tackett, A.J., Smith, E.R., Fukuda, A., Wysocka, J., Allis, C.D., Chait, B.T., Hess, J.L., and Roeder, R.G. (2005). Physical association and coordinate function of the H3 K4 methyltransferase MLL1 and the H4 K16 acetyltransferase MOF. Cell *121*, 873-885.

Drapkin, R., Reardon, J.T., Ansari, A., Huang, J.C., Zawel, L., Ahn, K., Sancar, A., and Reinberg, D. (1994). Dual role of TFIIH in DNA excision repair and in transcription by RNA polymerase II. Nature *368*, 769-772.

Dubaele, S., Proietti De Santis, L., Bienstock, R.J., Keriel, A., Stefanini, M., Van Houten, B., and Egly, J.M. (2003). Basal transcription defect discriminates between xeroderma pigmentosum and trichothiodystrophy in XPD patients. Mol Cell *11*, 1635-1646.

Dumont-Miscopein, A., Lavergne, J.P., Guillot, D., Sontag, B., and Reboud, J.P. (1994). Interaction of phosphorylated elongation factor EF-2 with nucleotides and ribosomes. FEBS Lett *356*, 283-286.

Duncan, P.I., Stojdl, D.F., Marius, R.M., and Bell, J.C. (1997). In vivo regulation of alternative pre-mRNA splicing by the Clk1 protein kinase. Mol Cell Biol *17*, 5996-6001.

Duncan, P.I., Stojdl, D.F., Marius, R.M., Scheit, K.H., and Bell, J.C. (1998). The Clk2 and Clk3 dual-specificity protein kinases regulate the intranuclear distribution of SR proteins and influence pre-mRNA splicing. Exp Cell Res *241*, 300-308.

Duncan, R., Milburn, S.C., and Hershey, J.W. (1987). Regulated phosphorylation and low abundance of HeLa cell initiation factor eIF-4F suggest a role in translational control. Heat shock effects on eIF-4F. J Biol Chem *262*, 380-388.

Durocher, D., Henckel, J., Fersht, A.R., and Jackson, S.P. (1999). The FHA domain is a modular phosphopeptide recognition motif. Mol Cell *4*, 387-394.

Dvir, A., Conaway, R.C., and Conaway, J.W. (1996). Promoter escape by RNA polymerase II. A role for an ATP cofactor in suppression of arrest by polymerase at promoter-proximal sites. J Biol Chem *271*, 23352-23356.

Dynlacht, B.D., Hoey, T., and Tjian, R. (1991). Isolation of coactivators associated with the TATA-binding protein that mediate transcriptional activation. Cell *66*, 563-576.

Edgar, B.A., and O'Farrell, P.H. (1989). Genetic control of cell division patterns in the Drosophila embryo. Cell *57*, 177-187.

Egyhazi, E., Ossoinak, A., Filhol-Cochet, O., Cochet, C., and Pigon, A. (1999). The binding of the alpha subunit of protein kinase CK2 and RAP74 subunit of TFIIF to protein-coding genes in living cells is DRB sensitive. Mol Cell Biochem *191*, 149-159.

Eipers, P.G., Barnoski, B.L., Han, J., Carroll, A.J., and Kidd, V.J. (1991). Localization of the expressed human p58 protein kinase chromosomal gene to chromosome 1p36 and a highly related sequence to chromosome 15. Genomics *11*, 621-629.

Engels, W.R. (1992). The origin of P elements in Drosophila melanogaster. Bioessays *14*, 681-686.

Eperon, I.C., Ireland, D.C., Smith, R.A., Mayeda, A., and Krainer, A.R. (1993). Pathways for selection of 5' splice sites by U1 snRNPs and SF2/ASF. EMBO J *12*, 3607-3617.

Eperon, I.C., Makarova, O.V., Mayeda, A., Munroe, S.H., Caceres, J.F., Hayward, D.G., and Krainer, A.R. (2000). Selection of alternative 5' splice sites: role of U1 snRNP and models for the antagonistic effects of SF2/ASF and hnRNP A1. Mol Cell Biol *20*, 8303-8318.

Estes, P.S., O'Shea, M., Clasen, S., and Zarnescu, D.C. (2008). Fragile X protein controls the efficacy of mRNA transport in Drosophila neurons. Mol Cell Neurosci.

Expert-Bezancon, A., Sureau, A., Durosay, P., Salesse, R., Groeneveld, H., Lecaer, J.P., and Marie, J. (2004). hnRNP A1 and the SR proteins ASF/SF2 and SC35 have antagonistic functions in splicing of beta-tropomyosin exon 6B. J Biol Chem *279*, 38249-38259.

Falvey, A.K., and Staehelin, T. (1970). Structure and function of mammalian ribosomes. II. Exchange of ribosomal subunits at various stages of in vitro polypeptide synthesis. J Mol Biol *53*, 21-34.

Feaver, W.J., Svejstrup, J.Q., Henry, N.L., and Kornberg, R.D. (1994). Relationship of CDK-activating kinase and RNA polymerase II CTD kinase TFIIH/TFIIK. Cell *79*, 1103-1109.

Fekete, C.A., Applefield, D.J., Blakely, S.A., Shirokikh, N., Pestova, T., Lorsch, J.R., and Hinnebusch, A.G. (2005). The eIF1A C-terminal domain promotes initiation complex assembly, scanning and AUG selection in vivo. EMBO J *24*, 3588-3601.

Feng, Y., Gutekunst, C.A., Eberhart, D.E., Yi, H., Warren, S.T., and Hersch, S.M. (1997). Fragile X mental retardation protein: nucleocytoplasmic shuttling and association with somatodendritic ribosomes. J Neurosci *17*, 1539-1547.

Fesquet, D., Labbe, J.C., Derancourt, J., Capony, J.P., Galas, S., Girard, F., Lorca, T., Shuttleworth, J., Doree, M., and Cavadore, J.C. (1993). The MO15 gene encodes the catalytic subunit of a protein kinase that activates cdc2 and other cyclin-dependent kinases (CDKs) through phosphorylation of Thr161 and its homologues. EMBO J *12*, 3111-3121.

Fisher, R.P., and Morgan, D.O. (1994). A novel cyclin associates with MO15/CDK7 to form the CDK-activating kinase. Cell *78*, 713-724.

Flores, O., Lu, H., Killeen, M., Greenblatt, J., Burton, Z.F., and Reinberg, D. (1991). The small subunit of transcription factor IIF recruits RNA polymerase II into the preinitiation complex. Proc Natl Acad Sci U S A *88*, 9999-10003.

Foiani, M., Cigan, A.M., Paddon, C.J., Harashima, S., and Hinnebusch, A.G. (1991). GCD2, a translational repressor of the GCN4 gene, has a general function in the initiation of protein synthesis in Saccharomyces cerevisiae. Mol Cell Biol *11*, 3203-3216.

Fortes, P., Bilbao-Cortes, D., Fornerod, M., Rigaut, G., Raymond, W., Seraphin, B., and Mattaj, I.W. (1999). Luc7p, a novel yeast U1 snRNP protein with a role in 5' splice site recognition. Genes Dev *13*, 2425-2438.

Frank, D., and Guthrie, C. (1992). An essential splicing factor, SLU7, mediates 3' splice site choice in yeast. Genes Dev *6*, 2112-2124.

Fraser, C.S., Berry, K.E., Hershey, J.W., and Doudna, J.A. (2007). eIF3j is located in the decoding center of the human 40S ribosomal subunit. Mol Cell *26*, 811-819.

Fraser, C.S., Lee, J.Y., Mayeur, G.L., Bushell, M., Doudna, J.A., and Hershey, J.W. (2004). The j-subunit of human translation initiation factor eIF3 is required for the stable binding of eIF3 and its subcomplexes to 40 S ribosomal subunits in vitro. J Biol Chem *279*, 8946-8956.

Frias, M.A., Thoreen, C.C., Jaffe, J.D., Schroder, W., Sculley, T., Carr, S.A., and Sabatini, D.M. (2006). mSin1 is necessary for Akt/PKB phosphorylation, and its isoforms define three distinct mTORC2s. Curr Biol *16*, 1865-1870.

Fringer, J.M., Acker, M.G., Fekete, C.A., Lorsch, J.R., and Dever, T.E. (2007). Coupled release of eukaryotic translation initiation factors 5B and 1A from 80S ribosomes following subunit joining. Mol Cell Biol *27*, 2384-2397.

Frolova, L., Le Goff, X., Zhouravleva, G., Davydova, E., Philippe, M., and Kisselev, L. (1996). Eukaryotic polypeptide chain release factor eRF3 is an eRF1- and ribosome-dependent guanosine triphosphatase. RNA *2*, 334-341.

Frolova, L., Seit-Nebi, A., and Kisselev, L. (2002). Highly conserved NIKS tetrapeptide is functionally essential in eukaryotic translation termination factor eRF1. RNA *8*, 129-136.

Frolova, L.Y., Merkulova, T.I., and Kisselev, L.L. (2000). Translation termination in eukaryotes: polypeptide release factor eRF1 is composed of functionally and structurally distinct domains. RNA *6*, 381-390.

Frolova, L.Y., Tsivkovskii, R.Y., Sivolobova, G.F., Oparina, N.Y., Serpinsky, O.I., Blinov, V.M., Tatkov, S.I., and Kisselev, L.L. (1999). Mutations in the highly conserved GGQ motif of class 1 polypeptide release factors abolish ability of human eRF1 to trigger peptidyl-tRNA hydrolysis. RNA *5*, 1014-1020.

Fromont-Racine, M., Rain, J.C., and Legrain, P. (1997). Toward a functional analysis of the yeast genome through exhaustive two-hybrid screens. Nat Genet *16*, 277-282.

Fryer, C.J., White, J.B., and Jones, K.A. (2004). Mastermind recruits CycC:CDK8 to phosphorylate the Notch ICD and coordinate activation with turnover. Mol Cell *16*, 509-520.

Fujinaga, K., Irwin, D., Huang, Y., Taube, R., Kurosu, T., and Peterlin, B.M. (2004). Dynamics of human immunodeficiency virus transcription: P-TEFb phosphorylates RD and dissociates negative effectors from the transactivation response element. Mol Cell Biol *24*, 787-795.

Gabaldon, T., and Huynen, M.A. (2004). Prediction of protein function and pathways in the genome era. Cell Mol Life Sci *61*, 930-944.

Gallie, D.R. (1991). The cap and poly(A) tail function synergistically to regulate mRNA translational efficiency. Genes Dev *5*, 2108-2116.

Garami, A., Zwartkruis, F.J., Nobukuni, T., Joaquin, M., Roccio, M., Stocker, H., Kozma, S.C., Hafen, E., Bos, J.L., and Thomas, G. (2003). Insulin activation of Rheb, a mediator of mTOR/S6K/4E-BP signaling, is inhibited by TSC1 and 2. Mol Cell *11*, 1457-1466.

Gerber, M., Ma, J., Dean, K., Eissenberg, J.C., and Shilatifard, A. (2001). Drosophila ELL is associated with actively elongating RNA polymerase II on transcriptionally active sites in vivo. EMBO J *20*, 6104-6114.

Gerber, M., Tenney, K., Conaway, J.W., Conaway, R.C., Eissenberg, J.C., and Shilatifard, A. (2005). Regulation of heat shock gene expression by RNA polymerase II elongation factor, Elongin A. J Biol Chem *280*, 4017-4020.

Gershenzon, N.I., and Ioshikhes, I.P. (2005). Synergy of human Pol II core promoter elements revealed by statistical sequence analysis. Bioinformatics *21*, 1295-1300.

Ghigna, C., Giordano, S., Shen, H., Benvenuto, F., Castiglioni, F., Comoglio, P.M., Green, M.R., Riva, S., and Biamonti, G. (2005). Cell motility is controlled by SF2/ASF through alternative splicing of the Ron protooncogene. Mol Cell *20*, 881-890.

Gill, G., Pascal, E., Tseng, Z.H., and Tjian, R. (1994). A glutamine-rich hydrophobic patch in transcription factor Sp1 contacts the dTAFII110 component of the Drosophila TFIID complex and mediates transcriptional activation. Proc Natl Acad Sci U S A *91*, 192-196.

Gingras, A.C., Raught, B., Gygi, S.P., Niedzwiecka, A., Miron, M., Burley, S.K., Polakiewicz, R.D., Wyslouch-Cieszynska, A., Aebersold, R., and Sonenberg, N. (2001). Hierarchical phosphorylation of the translation inhibitor 4E-BP1. Genes Dev *15*, 2852-2864.

Gingras, A.C., Raught, B., and Sonenberg, N. (1999). eIF4 initiation factors: effectors of mRNA recruitment to ribosomes and regulators of translation. Annu Rev Biochem *68*, 913-963.

Giot, L., Bader, J., Brouwer, C., Chaudhuri, A., Kuang, B., Li, Y., Hao, Y., Ooi, C., Godwin, B., Vitols, E., *et al.* (2003). A protein interaction map of Drosophila melanogaster. Science *302*, 1727-1736.

Goldstrohm, A.C., Greenleaf, A.L., and Garcia-Blanco, M.A. (2001). Co-transcriptional splicing of pre-messenger RNAs: considerations for the mechanism of alternative splicing. Gene *277*, 31-47.

Gottschalk, A., Tang, J., Puig, O., Salgado, J., Neubauer, G., Colot, H.V., Mann, M., Seraphin, B., Rosbash, M., Luhrmann, R., *et al.* (1998). A comprehensive biochemical and genetic analysis of the yeast U1 snRNP reveals five novel proteins. RNA *4*, 374-393.

Goulev, Y., Fauny, J.D., Gonzalez-Marti, B., Flagiello, D., Silber, J., and Zider, A. (2008). SCALLOPED interacts with YORKIE, the nuclear effector of the hippo tumor-suppressor pathway in Drosophila. Curr Biol *18*, 435-441.

Gozani, O., Feld, R., and Reed, R. (1996). Evidence that sequence-independent binding of highly conserved U2 snRNP proteins upstream of the branch site is required for assembly of spliceosomal complex A. Genes Dev *10*, 233-243.

Grainger, R., and Beggs, J. (2005). Prp8 protein: at the heart of the spliceosome. RNA *11*, 533-557.

Gromak, N., West, S., and Proudfoot, N.J. (2006). Pause sites promote transcriptional termination of mammalian RNA polymerase II. Mol Cell Biol *26*, 3986-3996.

Gui, J.F., Lane, W.S., and Fu, X.D. (1994). A serine kinase regulates intracellular localization of splicing factors in the cell cycle. Nature *369*, 678-682.

Gupta, A., Sharma, G.G., Young, C.S., Agarwal, M., Smith, E.R., Paull, T.T., Lucchesi, J.C., Khanna, K.K., Ludwig, T., and Pandita, T.K. (2005). Involvement of human MOF in ATM function. Mol Cell Biol *25*, 5292-5305.

Guth, S., Martinez, C., Gaur, R.K., and Valcarcel, J. (1999). Evidence for substrate-specific requirement of the splicing factor U2AF(35) and for its function after polypyrimidine tract recognition by U2AF(65). Mol Cell Biol *19*, 8263-8271.

Ha, I., Roberts, S., Maldonado, E., Sun, X., Kim, L.U., Green, M., and Reinberg, D. (1993). Multiple functional domains of human transcription factor IIB: distinct interactions with two general transcription factors and RNA polymerase II. Genes Dev *7*, 1021-1032.

Habara, Y., Urushiyama, S., Shibuya, T., Ohshima, Y., and Tani, T. (2001). Mutation in the prp12+ gene encoding a homolog of SAP130/SF3b130 causes differential inhibition of pre-mRNA splicing and arrest of cell-cycle progression in Schizosaccharomyces pombe. Rna *7*, 671-681.

Hamaratoglu, F., Willecke, M., Kango-Singh, M., Nolo, R., Hyun, E., Tao, C., Jafar-Nejad, H., and Halder, G. (2006). The tumour-suppressor genes NF2/Merlin and Expanded act through Hippo signalling to regulate cell proliferation and apoptosis. Nat Cell Biol *8*, 27-36.

Harding, H.P., Novoa, I., Zhang, Y., Zeng, H., Wek, R., Schapira, M., and Ron, D. (2000a). Regulated translation initiation controls stress-induced gene expression in mammalian cells. Mol Cell *6*, 1099-1108.

Harding, H.P., Zhang, Y., Bertolotti, A., Zeng, H., and Ron, D. (2000b). Perk is essential for translational regulation and cell survival during the unfolded protein response. Mol Cell *5*, 897-904.

Harper, J.W., and Elledge, S.J. (1998). The role of Cdk7 in CAK function, a retro-retrospective. Genes Dev *12*, 285-289.

Harrington, L.S., Findlay, G.M., Gray, A., Tolkacheva, T., Wigfield, S., Rebholz, H., Barnett, J., Leslie, N.R., Cheng, S., Shepherd, P.R., *et al.* (2004). The TSC1-2 tumor suppressor controls insulin-PI3K signaling via regulation of IRS proteins. J Cell Biol *166*, 213-223.

Harris, T.E., Chi, A., Shabanowitz, J., Hunt, D.F., Rhoads, R.E., and Lawrence, J.C., Jr. (2006). mTOR-dependent stimulation of the association of eIF4G and eIF3 by insulin. EMBO J *25*, 1659-1668.

Hartmuth, K., Urlaub, H., Vornlocher, H.P., Will, C.L., Gentzel, M., Wilm, M., and Luhrmann, R. (2002). Protein composition of human prespliceosomes isolated by a tobramycin affinity-selection method. Proc Natl Acad Sci U S A *99*, 16719-16724.

Hartwell, L.H., Mortimer, R.K., Culotti, J., and Culotti, M. (1973). Genetic Control of the Cell Division Cycle in Yeast: V. Genetic Analysis of cdc Mutants. Genetics *74*, 267-286.

Hartzog, G.A., Wada, T., Handa, H., and Winston, F. (1998). Evidence that Spt4, Spt5, and Spt6 control transcription elongation by RNA polymerase II in Saccharomyces cerevisiae. Genes Dev *12*, 357-369.

Haruta, T., Uno, T., Kawahara, J., Takano, A., Egawa, K., Sharma, P.M., Olefsky, J.M., and Kobayashi, M. (2000). A rapamycin-sensitive pathway down-regulates insulin signaling via phosphorylation and proteasomal degradation of insulin receptor substrate-1. Mol Endocrinol *14*, 783-794.

Harvey, K., and Tapon, N. (2007). The Salvador-Warts-Hippo pathway - an emerging tumour-suppressor network. Nat Rev Cancer *7*, 182-191.

Harvey, K.F., Pfleger, C.M., and Hariharan, I.K. (2003). The Drosophila Mst ortholog, hippo, restricts growth and cell proliferation and promotes apoptosis. Cell *114*, 457-467.

Hauryliuk, V., Zavialov, A., Kisselev, L., and Ehrenberg, M. (2006). Class-1 release factor eRF1 promotes GTP binding by class-2 release factor eRF3. Biochimie *88*, 747-757.

Henshaw, E.C., Guiney, D.G., and Hirsch, C.A. (1973). The ribosome cycle in mammalian protein synthesis. I. The place of monomeric ribosomes and ribosomal subunits in the cycle. J Biol Chem *248*, 4367-4376.

Herbert, T.P., Tee, A.R., and Proud, C.G. (2002). The extracellular signal-regulated kinase pathway regulates the phosphorylation of 4E-BP1 at multiple sites. J Biol Chem *277*, 11591-11596.

Hieb, A.R., Baran, S., Goodrich, J.A., and Kugel, J.F. (2006). An 8 nt RNA triggers a rate-limiting shift of RNA polymerase II complexes into elongation. EMBO J *25*, 3100-3109.

Hilfiker, A., Hilfiker-Kleiner, D., Pannuti, A., and Lucchesi, J.C. (1997). mof, a putative acetyl transferase gene related to the Tip60 and MOZ human genes and to the SAS genes of yeast, is required for dosage compensation in Drosophila. EMBO J *16*, 2054-2060.

Hinnebusch, A.G. (2000). Mechanism and regulation of initiator methionyl-tRNA binding to ribosomes. In Translational Control of Gene Expression, N. Sonenberg, J.W.B. Hershey, and M.B. Mathews, eds. Cold Spring Harbor, New York: Cold Spring Harbor Laboratory Press, 185-243.

Hinnebusch, A.G. (2006). eIF3: a versatile scaffold for translation initiation complexes. Trends Biochem Sci *31*, 553-562.

Hirohashi, Y., Wang, Q., Liu, Q., Du, X., Zhang, H., Sato, N., and Greene, M.I. (2006a). p78/MCRS1 forms a complex with centrosomal protein Nde1 and is essential for cell viability. Oncogene *25*, 4937-4946.

Hirohashi, Y., Wang, Q., Liu, Q., Li, B., Du, X., Zhang, H., Furuuchi, K., Masuda, K., Sato, N., and Greene, M.I. (2006b). Centrosomal proteins Nde1 and Su48 form a complex regulated by phosphorylation. Oncogene *25*, 6048-6055.

Hirose, F., Ohshima, N., Kwon, E.J., Yoshida, H., and Yamaguchi, M. (2002). Drosophila Mi-2 negatively regulates dDREF by inhibiting its DNA-binding activity. Mol Cell Biol *22*, 5182-5193.

Hirose, Y., and Manley, J.L. (2000). RNA polymerase II and the integration of nuclear events. Genes Dev *14*, 1415-1429.

Ho, C.K., and Shuman, S. (1999). Distinct roles for CTD Ser-2 and Ser-5 phosphorylation in the recruitment and allosteric activation of mammalian mRNA capping enzyme. Mol Cell *3*, 405-411.

Hofmann, K., and Bucher, P. (1995). The FHA domain: a putative nuclear signalling domain found in protein kinases and transcription factors. Trends Biochem Sci *20*, 347-349.

Holstege, F.C., Fiedler, U., and Timmers, H.T. (1997). Three transitions in the RNA polymerase II transcription complex during initiation. EMBO J *16*, 7468-7480.

Holstege, F.C., Jennings, E.G., Wyrick, J.J., Lee, T.I., Hengartner, C.J., Green, M.R., Golub, T.R., Lander, E.S., and Young, R.A. (1998). Dissecting the regulatory circuitry of a eukaryotic genome. Cell *95*, 717-728.

Holstege, F.C., van der Vliet, P.C., and Timmers, H.T. (1996). Opening of an RNA polymerase II promoter occurs in two distinct steps and requires the basal transcription factors IIE and IIH. EMBO J *15*, 1666-1677.

Holz, M.K., Ballif, B.A., Gygi, S.P., and Blenis, J. (2005). mTOR and S6K1 mediate assembly of the translation preinitiation complex through dynamic protein interchange and ordered phosphorylation events. Cell *123*, 569-580.

Horowitz, D.S., and Krainer, A.R. (1997). A human protein required for the second step of pre-mRNA splicing is functionally related to a yeast splicing factor. Genes Dev *11*, 139-151.

Horrigan, S.K., Rich, C.B., Streeten, B.W., Li, Z.Y., and Foster, J.A. (1992). Characterization of an associated microfibril protein through recombinant DNA techniques. J Biol Chem *267*, 10087-10095.

Hu, D., Mayeda, A., Trembley, J.H., Lahti, J.M., and Kidd, V.J. (2003). CDK11 complexes promote pre-mRNA splicing. J Biol Chem *278*, 8623-8629.

Huang, H.K., Yoon, H., Hannig, E.M., and Donahue, T.F. (1997). GTP hydrolysis controls stringent selection of the AUG start codon during translation initiation in Saccharomyces cerevisiae. Genes Dev *11*, 2396-2413.

Huang, J., Wu, S., Barrera, J., Matthews, K., and Pan, D. (2005). The Hippo signaling pathway coordinately regulates cell proliferation and apoptosis by inactivating Yorkie, the Drosophila Homolog of YAP. Cell *122*, 421-434.

Hwang, L.H., and Murray, A.W. (1997). A novel yeast screen for mitotic arrest mutants identifies DOC1, a new gene involved in cyclin proteolysis. Mol Biol Cell *8*, 1877-1887.

Iizuka, N., Najita, L., Franzusoff, A., and Sarnow, P. (1994). Cap-dependent and cap-independent translation by internal initiation of mRNAs in cell extracts prepared from Saccharomyces cerevisiae. Mol Cell Biol *14*, 7322-7330.

Imbalzano, A.N., Zaret, K.S., and Kingston, R.E. (1994). Transcription factor (TF) IIB and TFIIA can independently increase the affinity of the TATA-binding protein for DNA. J Biol Chem *269*, 8280-8286.

Inoki, K., Li, Y., Xu, T., and Guan, K.L. (2003a). Rheb GTPase is a direct target of TSC2 GAP activity and regulates mTOR signaling. Genes Dev *17*, 1829-1834.

Inoki, K., Li, Y., Zhu, T., Wu, J., and Guan, K.L. (2002). TSC2 is phosphorylated and inhibited by Akt and suppresses mTOR signalling. Nat Cell Biol *4*, 648-657.

Inoki, K., Zhu, T., and Guan, K.L. (2003b). TSC2 mediates cellular energy response to control cell growth and survival. Cell *115*, 577-590.

Ito, K., Frolova, L., Seit-Nebi, A., Karamyshev, A., Kisselev, L., and Nakamura, Y. (2002). Omnipotent decoding potential resides in eukaryotic translation termination factor eRF1 of variant-code organisms and is modulated by the interactions of amino acid sequences within domain 1. Proc Natl Acad Sci U S A *99*, 8494-8499.

Jacinto, E., Facchinetti, V., Liu, D., Soto, N., Wei, S., Jung, S.Y., Huang, Q., Qin, J., and Su, B. (2006). SIN1/MIP1 maintains rictor-mTOR complex integrity and regulates Akt phosphorylation and substrate specificity. Cell *127*, 125-137.

Jackson, R.J. (2005). Alternative mechanisms of initiating translation of mammalian mRNAs. Biochem Soc Trans *33*, 1231-1241.

James, S., Turner, W., and Schwer, B. (2002a). How Slu7 and Prp18 cooperate in the second step of yeast pre-mRNA splicing. RNA *8*, 1068-1077.

James, S.A., Turner, W., and Schwer, B. (2002b). How Slu7 and Prp18 cooperate in the second step of yeast pre-mRNA splicing. RNA *8*, 1068-1077.

Jeronimo, C., Forget, D., Bouchard, A., Li, Q., Chua, G., Poitras, C., Therien, C., Bergeron, D., Bourassa, S., Greenblatt, J., *et al.* (2007). Systematic analysis of the protein interaction network for the human transcription machinery reveals the identity of the 7SK capping enzyme. Mol Cell *27*, 262-274.

Jia, J., Zhang, W., Wang, B., Trinko, R., and Jiang, J. (2003). The Drosophila Ste20 family kinase dMST functions as a tumor suppressor by restricting cell proliferation and promoting apoptosis. Genes Dev *17*, 2514-2519.

Jiang, H.Y., Wek, S.A., McGrath, B.C., Lu, D., Hai, T., Harding, H.P., Wang, X., Ron, D., Cavener, D.R., and Wek, R.C. (2004). Activating transcription factor 3 is integral to the eukaryotic initiation factor 2 kinase stress response. Mol Cell Biol *24*, 1365-1377.

Johnson, J.M., Castle, J., Garrett-Engele, P., Kan, Z., Loerch, P.M., Armour, C.D., Santos, R., Schadt, E.E., Stoughton, R., and Shoemaker, D.D. (2003). Genome-wide survey of human alternative pre-mRNA splicing with exon junction microarrays. Science *302*, 2141-2144.

Johnson, K.M., and Carey, M. (2003). Assembly of a mediator/TFIID/TFIIA complex bypasses the need for an activator. Curr Biol *13*, 772-777.

Johnson, K.M., Wang, J., Smallwood, A., Arayata, C., and Carey, M. (2002). TFIID and human mediator coactivator complexes assemble cooperatively on promoter DNA. Genes Dev *16*, 1852-1863.

Johnston, L.H., and Thomas, A.P. (1982). The isolation of new DNA synthesis mutants in the yeast Saccharomyces cerevisiae. Mol Gen Genet *186*, 439-444.

Jones, M.H., Frank, D.N., and Guthrie, C. (1995). Characterization and functional ordering of Slu7p and Prp17p during the second step of pre-mRNA splicing in yeast. Proc Natl Acad Sci U S A *92*, 9687-9691.

Jurica, M.S., Licklider, L.J., Gygi, S.R., Grigorieff, N., and Moore, M.J. (2002). Purification and characterization of native spliceosomes suitable for three-dimensional structural analysis. RNA *8*, 426-439.

Jurica, M.S., and Moore, M.J. (2003). Pre-mRNA splicing: awash in a sea of proteins. Mol Cell *12*, 5-14.

Jurica, M.S., Sousa, D., Moore, M.J., and Grigorieff, N. (2004). Three-dimensional structure of C complex spliceosomes by electron microscopy. Nat Struct Mol Biol *11*, 265-269.

Justice, R.W., Zilian, O., Woods, D.F., Noll, M., and Bryant, P.J. (1995). The Drosophila tumor suppressor gene warts encodes a homolog of human myotonic dystrophy kinase and is required for the control of cell shape and proliferation. Genes Dev *9*, 534-546.

Kango-Singh, M., Nolo, R., Tao, C., Verstreken, P., Hiesinger, P.R., Bellen, H.J., and Halder, G. (2002). Shar-pei mediates cell proliferation arrest during imaginal disc growth in Drosophila. Development *129*, 5719-5730.

Kao, C.F., Hillyer, C., Tsukuda, T., Henry, K., Berger, S., and Osley, M.A. (2004). Rad6 plays a role in transcriptional activation through ubiquitylation of histone H2B. Genes Dev *18*, 184-195.

Kaplan, C.D., Holland, M.J., and Winston, F. (2005). Interaction between transcription elongation factors and mRNA 3'-end formation at the Saccharomyces cerevisiae GAL10-GAL7 locus. J Biol Chem *280*, 913-922.

Kaplan, C.D., Laprade, L., and Winston, F. (2003). Transcription elongation factors repress transcription initiation from cryptic sites. Science *301*, 1096-1099.

Kapoor-Vazirani, P., Kagey, J.D., Powell, D.R., and Vertino, P.M. (2008). Role of hMOF-dependent histone H4 lysine 16 acetylation in the maintenance of TMS1/ASC gene activity. Cancer Res *68*, 6810-6821.

Kapp, L.D., and Lorsch, J.R. (2004). The molecular mechanics of eukaryotic translation. Annu Rev Biochem *73*, 657-704.

Karcher, A., Buttner, K., Martens, B., Jansen, R.P., and Hopfner, K.P. (2005). X-ray structure of RLI, an essential twin cassette ABC ATPase involved in ribosome biogenesis and HIV capsid assembly. Structure *13*, 649-659.

Karcher, A., Schele, A., and Hopfner, K.P. (2008). X-ray structure of the complete ABC enzyme ABCE1 from Pyrococcus abyssi. J Biol Chem *283*, 7962-7971.

Karni, R., de Stanchina, E., Lowe, S.W., Sinha, R., Mu, D., and Krainer, A.R. (2007). The gene encoding the splicing factor SF2/ASF is a proto-oncogene. Nat Struct Mol Biol *14*, 185-193.

Kaufman, R.J. (1999). Stress signaling from the lumen of the endoplasmic reticulum: coordination of gene transcriptional and translational controls. Genes Dev *13*, 1211-1233.

Kaufmann, J., Ahrens, K., Koop, R., Smale, S.T., and Muller, R. (1998). CIF150, a human cofactor for transcription factor IID-dependent initiator function. Mol Cell Biol *18*, 233-239.

Kaufmann, J., and Smale, S.T. (1994). Direct recognition of initiator elements by a component of the transcription factor IID complex. Genes Dev *8*, 821-829.

Kawauchi, J., Mischo, H., Braglia, P., Rondon, A., and Proudfoot, N.J. (2008). Budding yeast RNA polymerases I and II employ parallel mechanisms of transcriptional termination. Genes Dev *22*, 1082-1092.

Keller, D.M., Zeng, X., Wang, Y., Zhang, Q.H., Kapoor, M., Shu, H., Goodman, R., Lozano, G., Zhao, Y., and Lu, H. (2001). A DNA damage-induced p53 serine 392 kinase complex contains CK2, hSpt16, and SSRP1. Mol Cell *7*, 283-292.

Kerr, I.D. (2004). Sequence analysis of twin ATP binding cassette proteins involved in translational control, antibiotic resistance, and ribonuclease L inhibition. Biochem Biophys Res Commun *315*, 166-173.

Khandjian, E.W., Huot, M.E., Tremblay, S., Davidovic, L., Mazroui, R., and Bardoni, B. (2004). Biochemical evidence for the association of fragile X mental retardation protein with brain polyribosomal ribonucleoparticles. Proc Natl Acad Sci U S A *101*, 13357-13362.

Killeen, M.T., and Greenblatt, J.F. (1992). The general transcription factor RAP30 binds to RNA polymerase II and prevents it from binding nonspecifically to DNA. Mol Cell Biol *12*, 30-37.

Kim, J.L., Nikolov, D.B., and Burley, S.K. (1993a). Co-crystal structure of TBP recognizing the minor groove of a TATA element. Nature *365*, 520-527.

Kim, S.H., and Lin, R.J. (1996). Spliceosome activation by PRP2 ATPase prior to the first transesterification reaction of pre-mRNA splicing. Mol Cell Biol *16*, 6810-6819.

Kim, Y., Geiger, J.H., Hahn, S., and Sigler, P.B. (1993b). Crystal structure of a yeast TBP/TATA-box complex. Nature *365*, 512-520.

Kind, J., Vaquerizas, J.M., Gebhardt, P., Gentzel, M., Luscombe, N.M., Bertone, P., and Akhtar, A. (2008). Genome-wide analysis reveals MOF as a key regulator of dosage compensation and gene expression in Drosophila. Cell *133*, 813-828.

Kispal, G., Sipos, K., Lange, H., Fekete, Z., Bedekovics, T., Janaky, T., Bassler, J., Aguilar Netz, D.J., Balk, J., Rotte, C., *et al.* (2005). Biogenesis of cytosolic ribosomes requires the essential iron-sulphur protein Rli1p and mitochondria. EMBO J *24*, 589-598.

Kisselev, L.L., and Buckingham, R.H. (2000). Translational termination comes of age. Trends Biochem Sci *25*, 561-566.

Kistler, A.L., and Guthrie, C. (2001). Deletion of MUD2, the yeast homolog of U2AF65, can bypass the requirement for sub2, an essential spliceosomal ATPase. Genes Dev *15*, 42-49.

Kittler, R., Putz, G., Pelletier, L., Poser, I., Heninger, A.K., Drechsel, D., Fischer, S., Konstantinova, I., Habermann, B., Grabner, H., *et al.* (2004). An endoribonuclease-prepared siRNA screen in human cells identifies genes essential for cell division. Nature *432*, 1036-1040.

Knebel, A., Morrice, N., and Cohen, P. (2001). A novel method to identify protein kinase substrates: eEF2 kinase is phosphorylated and inhibited by SAPK4/p38delta. EMBO J *20*, 4360-4369.

Kobor, M.S., Archambault, J., Lester, W., Holstege, F.C., Gileadi, O., Jansma, D.B., Jennings, E.G., Kouyoumdjian, F., Davidson, A.R., Young, R.A., *et al.* (1999). An unusual eukaryotic protein phosphatase required for transcription by RNA polymerase II and CTD dephosphorylation in S. cerevisiae. Mol Cell *4*, 55-62.

Kohtz, J.D., Jamison, S.F., Will, C.L., Zuo, P., Luhrmann, R., Garcia-Blanco, M.A., and Manley, J.L. (1994). Protein-protein interactions and 5'-splice-site recognition in mammalian mRNA precursors. Nature *368*, 119-124.

Kokubo, T., Gong, D.W., Yamashita, S., Horikoshi, M., Roeder, R.G., and Nakatani, Y. (1993). Drosophila 230-kD TFIID subunit, a functional homolog of the human cell cycle gene product, negatively regulates DNA binding of the TATA box-binding subunit of TFIID. Genes Dev *7*, 1033-1046.

Kokubo, T., Swanson, M.J., Nishikawa, J.I., Hinnebusch, A.G., and Nakatani, Y. (1998). The yeast TAF145 inhibitory domain and TFIIA competitively bind to TATA-binding protein. Mol Cell Biol *18*, 1003-1012.

Kolosov, P., Frolova, L., Seit-Nebi, A., Dubovaya, V., Kononenko, A., Oparina, N., Justesen, J., Efimov, A., and Kisselev, L. (2005). Invariant amino acids essential for decoding function of polypeptide release factor eRF1. Nucleic Acids Res *33*, 6418-6425.

Kolupaeva, V.G., Unbehaun, A., Lomakin, I.B., Hellen, C.U., and Pestova, T.V. (2005). Binding of eukaryotic initiation factor 3 to ribosomal 40S subunits and its role in ribosomal dissociation and anti-association. RNA *11*, 470-486.

Komarnitsky, P., Cho, E.J., and Buratowski, S. (2000). Different phosphorylated forms of RNA polymerase II and associated mRNA processing factors during transcription. Genes Dev *14*, 2452-2460.

Konarska, M.M., and Sharp, P.A. (1988). Association of U2, U4, U5, and U6 small nuclear ribonucleoproteins in a spliceosome-type complex in absence of precursor RNA. Proc Natl Acad Sci U S A *85*, 5459-5462.

Kong, S.E., Kobor, M.S., Krogan, N.J., Somesh, B.P., Sogaard, T.M., Greenblatt, J.F., and Svejstrup, J.Q. (2005). Interaction of Fcp1 phosphatase with elongating RNA polymerase II holoenzyme, enzymatic mechanism of action, and genetic interaction with elongator. J Biol Chem *280*, 4299-4306.

Kornberg, R.D. (2005). Mediator and the mechanism of transcriptional activation. Trends Biochem Sci *30*, 235-239.

Kornblihtt, A.R. (2004). Shortcuts to the end. Nat Struct Mol Biol *11*, 1156-1157.

Krishnamurthy, S., He, X., Reyes-Reyes, M., Moore, C., and Hampsey, M. (2004). Ssu72 Is an RNA polymerase II CTD phosphatase. Mol Cell *14*, 387-394.

Krogan, N.J., Dover, J., Wood, A., Schneider, J., Heidt, J., Boateng, M.A., Dean, K., Ryan, O.W., Golshani, A., Johnston, M., *et al.* (2003a). The Paf1 complex is required for histone H3 methylation by COMPASS and Dot1p: linking transcriptional elongation to histone methylation. Mol Cell *11*, 721-729.

Krogan, N.J., Kim, M., Ahn, S.H., Zhong, G., Kobor, M.S., Cagney, G., Emili, A., Shilatifard, A., Buratowski, S., and Greenblatt, J.F. (2002). RNA polymerase II elongation factors of Saccharomyces cerevisiae: a targeted proteomics approach. Mol Cell Biol *22*, 6979-6992.

Krogan, N.J., Kim, M., Tong, A., Golshani, A., Cagney, G., Canadien, V., Richards, D.P., Beattie, B.K., Emili, A., Boone, C., *et al.* (2003b). Methylation of histone H3 by Set2 in Saccharomyces cerevisiae is linked to transcriptional elongation by RNA polymerase II. Mol Cell Biol *23*, 4207-4218.

Krohn, N.M., Stemmer, C., Fojan, P., Grimm, R., and Grasser, K.D. (2003). Protein kinase CK2 phosphorylates the high mobility group domain protein SSRP1, inducing the recognition of UV-damaged DNA. J Biol Chem *278*, 12710-12715.

Kugel, J.F., and Goodrich, J.A. (1998). Promoter escape limits the rate of RNA polymerase II transcription and is enhanced by TFIIE, TFIIH, and ATP on negatively supercoiled DNA. Proc Natl Acad Sci U S A *95*, 9232-9237.

Kugel, J.F., and Goodrich, J.A. (2000). A kinetic model for the early steps of RNA synthesis by human RNA polymerase II. J Biol Chem *275*, 40483-40491.

Kuhn, A.N., and Brow, D.A. (2000). Suppressors of a cold-sensitive mutation in yeast U4 RNA define five domains in the splicing factor Prp8 that influence spliceosome activation. Genetics *155*, 1667-1682.

Kuhn, A.N., Li, Z., and Brow, D.A. (1999). Splicing factor Prp8 governs U4/U6 RNA unwinding during activation of the spliceosome. Mol Cell *3*, 65-75.

Kuhn, A.N., Reichl, E.M., and Brow, D.A. (2002). Distinct domains of splicing factor Prp8 mediate different aspects of spliceosome activation. Proc Natl Acad Sci U S A *99*, 9145-9149.

Kuldell, N.H., and Buratowski, S. (1997). Genetic analysis of the large subunit of yeast transcription factor IIE reveals two regions with distinct functions. Mol Cell Biol *17*, 5288-5298.

Kumar, K.P., Akoulitchev, S., and Reinberg, D. (1998). Promoter-proximal stalling results from the inability to recruit transcription factor IIH to the transcription complex and is a regulated event. Proc Natl Acad Sci U S A *95*, 9767-9772.

Kuras, L., Kosa, P., Mencia, M., and Struhl, K. (2000). TAF-Containing and TAF-independent forms of transcriptionally active TBP in vivo. Science *288*, 1244-1248.

Kuras, L., and Struhl, K. (1999). Binding of TBP to promoters in vivo is stimulated by activators and requires Pol II holoenzyme. Nature *399*, 609-613.

Kuroyanagi, N., Onogi, H., Wakabayashi, T., and Hagiwara, M. (1998). Novel SR-protein-specific kinase, SRPK2, disassembles nuclear speckles. Biochem Biophys Res Commun *242*, 357-364.

Kutach, A.K., and Kadonaga, J.T. (2000). The downstream promoter element DPE appears to be as widely used as the TATA box in Drosophila core promoters. Mol Cell Biol *20*, 4754-4764.

Laggerbauer, B., Achsel, T., and Luhrmann, R. (1998). The human U5-200kD DEXH-box protein unwinds U4/U6 RNA duplices in vitro. Proc Natl Acad Sci U S A *95*, 4188-4192.

Lagrange, T., Kapanidis, A.N., Tang, H., Reinberg, D., and Ebright, R.H. (1998). New core promoter element in RNA polymerase II-dependent transcription: sequence-specific DNA binding by transcription factor IIB. Genes Dev *12*, 34-44.

Lahti, J.M., Xiang, J., Heath, L.S., Campana, D., and Kidd, V.J. (1995). PITSLRE protein kinase activity is associated with apoptosis. Mol Cell Biol *15*, 1-11.

Lai, M.C., Lin, R.I., and Tarn, W.Y. (2003). Differential effects of hyperphosphorylation on splicing factor SRp55. Biochem J *371*, 937-945.

Lai, Z.C., Wei, X., Shimizu, T., Ramos, E., Rohrbaugh, M., Nikolaidis, N., Ho, L.L., and Li, Y. (2005). Control of cell proliferation and apoptosis by mob as tumor suppressor, mats. Cell *120*, 675-685.

Lambertsson, A. (1998). The minute genes in Drosophila and their molecular functions. Adv Genet *38*, 69-134.

Larochelle, S., Pandur, J., Fisher, R.P., Salz, H.K., and Suter, B. (1998). Cdk7 is essential for mitosis and for in vivo Cdk-activating kinase activity. Genes Dev *12*, 370-381.

Lasko, P. (2000). The drosophila melanogaster genome: translation factors and RNA binding proteins. J Cell Biol *150*, F51-56.

Lawson, T.G., Lee, K.A., Maimone, M.M., Abramson, R.D., Dever, T.E., Merrick, W.C., and Thach, R.E. (1989). Dissociation of double-stranded polynucleotide helical structures by eukaryotic initiation factors, as revealed by a novel assay. Biochemistry *28*, 4729-4734.

Le Roy, F., Salehzada, T., Bisbal, C., Dougherty, J.P., and Peltz, S.W. (2005). A newly discovered function for RNase L in regulating translation termination. Nat Struct Mol Biol *12*, 505-512.

Lebaron, S., Froment, C., Fromont-Racine, M., Rain, J.C., Monsarrat, B., Caizergues-Ferrer, M., and Henry, Y. (2005). The splicing ATPase prp43p is a component of multiple preribosomal particles. Mol Cell Biol *25*, 9269-9282.

Lee, J.M., and Greenleaf, A.L. (1997). Modulation of RNA polymerase II elongation efficiency by C-terminal heptapeptide repeat domain kinase I. J Biol Chem *272*, 10990-10993.

Lee, T.I., and Young, R.A. (2000). Transcription of eukaryotic protein-coding genes. Annu Rev Genet *34*, 77-137.

Li, J., Lee, G.I., Van Doren, S.R., and Walker, J.C. (2000). The FHA domain mediates phosphoprotein interactions. J Cell Sci *113 Pt 23*, 4143-4149.

Li, T., Inoue, A., Lahti, J.M., and Kidd, V.J. (2004). Failure to proliferate and mitotic arrest of CDK11(p110/p58)-null mutant mice at the blastocyst stage of embryonic cell development. Mol Cell Biol *24*, 3188-3197.

Li, X., Wang, J., and Manley, J.L. (2005a). Loss of splicing factor ASF/SF2 induces G2 cell cycle arrest and apoptosis, but inhibits internucleosomal DNA fragmentation. Genes Dev *19*, 2705-2714.

Li, X.Y., Virbasius, A., Zhu, X., and Green, M.R. (1999). Enhancement of TBP binding by activators and general transcription factors. Nature *399*, 605-609.

Li, Y., Keller, D.M., Scott, J.D., and Lu, H. (2005b). CK2 phosphorylates SSRP1 and inhibits its DNA-binding activity. J Biol Chem *280*, 11869-11875.

Li, Z., and Brow, D.A. (1996). A spontaneous duplication in U6 spliceosomal RNA uncouples the early and late functions of the ACAGA element in vivo. RNA *2*, 879-894.

Licatalosi, D.D., Geiger, G., Minet, M., Schroeder, S., Cilli, K., McNeil, J.B., and Bentley, D.L. (2002). Functional interaction of yeast pre-mRNA 3' end processing factors with RNA polymerase II. Mol Cell *9*, 1101-1111.

Lieberman, P.M., and Berk, A.J. (1994). A mechanism for TAFs in transcriptional activation: activation domain enhancement of TFIID-TFIIA--promoter DNA complex formation. Genes Dev *8*, 995-1006.

Lin, D.Y., and Shih, H.M. (2002). Essential role of the 58-kDa microspherule protein in the modulation of Daxx-dependent transcriptional repression as revealed by nucleolar sequestration. J Biol Chem *277*, 25446-25456.

Lin, S., Xiao, R., Sun, P., Xu, X., and Fu, X.D. (2005). Dephosphorylation-dependent sorting of SR splicing factors during mRNP maturation. Mol Cell *20*, 413-425.

Lin, Y.C., and Gralla, J.D. (2005). Stimulation of the XPB ATP-dependent helicase by the beta subunit of TFIIE. Nucleic Acids Res *33*, 3072-3081.

Lindqvist, L., Imataka, H., and Pelletier, J. (2008). Cap-dependent eukaryotic initiation factor-mRNA interactions probed by cross-linking. RNA *14*, 960-969.

Lis, J.T., Mason, P., Peng, J., Price, D.H., and Werner, J. (2000). P-TEFb kinase recruitment and function at heat shock loci. Genes Dev *14*, 792-803.

Listerman, I., Sapra, A.K., and Neugebauer, K.M. (2006). Cotranscriptional coupling of splicing factor recruitment and precursor messenger RNA splicing in mammalian cells. Nat Struct Mol Biol *13*, 815-822.

Little, J.T., and Jurica, M.S. (2008). Splicing Factor SPF30 Bridges an Interaction between the Prespliceosome Protein U2AF35 and Tri-small Nuclear Ribonucleoprotein Protein hPrp3. J Biol Chem *283*, 8145-8152.

Liu, Y.C., Chen, H.C., Wu, N.Y., and Cheng, S.C. (2007). A novel splicing factor, Yju2, is associated with NTC and acts after Prp2 in promoting the first catalytic reaction of pre-mRNA splicing. Mol Cell Biol *27*, 5403-5413.

Long, X., Lin, Y., Ortiz-Vega, S., Yonezawa, K., and Avruch, J. (2005a). Rheb binds and regulates the mTOR kinase. Curr Biol *15*, 702-713.

Long, X., Ortiz-Vega, S., Lin, Y., and Avruch, J. (2005b). Rheb binding to mammalian target of rapamycin (mTOR) is regulated by amino acid sufficiency. J Biol Chem *280*, 23433-23436.

Lopez-Bigas, N., Audit, B., Ouzounis, C., Parra, G., and Guigo, R. (2005). Are splicing mutations the most frequent cause of hereditary disease? FEBS Lett *579*, 1900-1903.

Lopez-Lastra, M., Rivas, A., and Barria, M.I. (2005). Protein synthesis in eukaryotes: the growing biological relevance of cap-independent translation initiation. Biol Res *38*, 121-146.

Lorsch, J.R., and Herschlag, D. (1999). Kinetic dissection of fundamental processes of eukaryotic translation initiation in vitro. EMBO J *18*, 6705-6717.

Lossky, M., Anderson, G.J., Jackson, S.P., and Beggs, J. (1987). Identification of a yeast snRNP protein and detection of snRNP-snRNP interactions. Cell *51*, 1019-1026.

Loyer, P., Trembley, J.H., Grenet, J.A., Busson, A., Corlu, A., Zhao, W., Kocak, M., Kidd, V.J., and Lahti, J.M. (2008). Characterization of cyclin L1 and L2 interactions with CDK11 and splicing factors: influence of cyclin L isoforms on splice site selection. J Biol Chem *283*, 7721-7732.

Lu, H., Zawel, L., Fisher, L., Egly, J.M., and Reinberg, D. (1992). Human general transcription factor IIH phosphorylates the C-terminal domain of RNA polymerase II. Nature *358*, 641-645.

Lu, L., Han, A.P., and Chen, J.J. (2001). Translation initiation control by heme-regulated eukaryotic initiation factor 2alpha kinase in erythroid cells under cytoplasmic stresses. Mol Cell Biol *21*, 7971-7980.

Lund, M., and Kjems, J. (2002). Defining a 5' splice site by functional selection in the presence and absence of U1 snRNA 5' end. RNA *8*, 166-179.

Lundgren, K., Allan, S., Urushiyama, S., Tani, T., Ohshima, Y., Frendewey, D., and Beach, D. (1996). A connection between pre-mRNA splicing and the cell cycle in fission yeast: cdc28+ is allelic with prp8+ and encodes an RNA-dependent ATPase/helicase. Mol Biol Cell *7*, 1083-1094.

Lusser, A., and Kadonaga, J.T. (2003). Chromatin remodeling by ATP-dependent molecular machines. Bioessays *25*, 1192-1200.

Lybarger, S., Beickman, K., Brown, V., Dembla-Rajpal, N., Morey, K., Seipelt, R., and Rymond, B.C. (1999). Elevated levels of a U4/U6.U5 snRNP-associated protein, Spp381p, rescue a mutant defective in spliceosome maturation. Mol Cell Biol *19*, 577-584.

Ma, C.T., Velazquez-Dones, A., Hagopian, J.C., Ghosh, G., Fu, X.D., and Adams, J.A. (2008). Ordered multi-site phosphorylation of the splicing factor ASF/SF2 by SRPK1. J Mol Biol *376*, 55-68.

Ma, D., Watanabe, H., Mermelstein, F., Admon, A., Oguri, K., Sun, X., Wada, T., Imai, T., Shiroya, T., Reinberg, D., *et al.* (1993). Isolation of a cDNA encoding the largest subunit of TFIIA reveals functions important for activated transcription. Genes Dev *7*, 2246-2257.

Ma, Y., and Hendershot, L.M. (2003). Delineation of a negative feedback regulatory loop that controls protein translation during endoplasmic reticulum stress. J Biol Chem *278*, 34864-34873.

Maag, D., Fekete, C.A., Gryczynski, Z., and Lorsch, J.R. (2005). A conformational change in the eukaryotic translation preinitiation complex and release of eIF1 signal recognition of the start codon. Mol Cell *17*, 265-275.

Mabon, S.A., and Misteli, T. (2005). Differential recruitment of pre-mRNA splicing factors to alternatively spliced transcripts in vivo. PLoS Biol *3*, e374.

Madhani, H.D., and Guthrie, C. (1994). Dynamic RNA-RNA interactions in the spliceosome. Annu Rev Genet *28*, 1-26.

Majumdar, R., Bandyopadhyay, A., and Maitra, U. (2003). Mammalian translation initiation factor eIF1 functions with eIF1A and eIF3 in the formation of a stable 40 S preinitiation complex. J Biol Chem *278*, 6580-6587.

Majumdar, R., and Maitra, U. (2005). Regulation of GTP hydrolysis prior to ribosomal AUG selection during eukaryotic translation initiation. EMBO J *24*, 3737-3746.

Makarov, E.M., Makarova, O.V., Urlaub, H., Gentzel, M., Will, C.L., Wilm, M., and Luhrmann, R. (2002). Small nuclear ribonucleoprotein remodeling during catalytic activation of the spliceosome. Science *298*, 2205-2208.

Makarova, O.V., Makarov, E.M., Urlaub, H., Will, C.L., Gentzel, M., Wilm, M., and Luhrmann, R. (2004). A subset of human 35S U5 proteins, including Prp19, function prior to catalytic step 1 of splicing. EMBO J *23*, 2381-2391.

Malecova, B., Gross, P., Boyer-Guittaut, M., Yavuz, S., and Oelgeschlager, T. (2007). The initiator core promoter element antagonizes repression of TATA-directed transcription by negative cofactor NC2. J Biol Chem *282*, 24767-24776.

Malumbres, M., and Barbacid, M. (2005). Mammalian cyclin-dependent kinases. Trends Biochem Sci *30*, 630-641.

Mamane, Y., Petroulakis, E., LeBacquer, O., and Sonenberg, N. (2006). mTOR, translation initiation and cancer. Oncogene *25*, 6416-6422.

Mandal, S.S., Cho, H., Kim, S., Cabane, K., and Reinberg, D. (2002). FCP1, a phosphatase specific for the heptapeptide repeat of the largest subunit of RNA polymerase II, stimulates transcription elongation. Mol Cell Biol *22*, 7543-7552.

Maniatis, T., and Reed, R. (2002). An extensive network of coupling among gene expression machines. Nature *416*, 499-506.

Maniatis, T., and Tasic, B. (2002). Alternative pre-mRNA splicing and proteome expansion in metazoans. Nature *418*, 236-243.

Marshall, N.F., Peng, J., Xie, Z., and Price, D.H. (1996). Control of RNA polymerase II elongation potential by a novel carboxyl-terminal domain kinase. J Biol Chem *271*, 27176-27183.

Martin, A., Schneider, S., and Schwer, B. (2002). Prp43 is an essential RNA-dependent ATPase required for release of lariat-intron from the spliceosome. J Biol Chem *277*, 17743-17750.

Martinand, C., Montavon, C., Salehzada, T., Silhol, M., Lebleu, B., and Bisbal, C. (1999). RNase L inhibitor is induced during human immunodeficiency virus type 1 infection and down regulates the 2-5A/RNase L pathway in human T cells. J Virol *73*, 290-296.

Martinand, C., Salehzada, T., Silhol, M., Lebleu, B., and Bisbal, C. (1998). RNase L inhibitor (RLI) antisense constructions block partially the down regulation of the 2-5A/RNase L pathway in encephalomyocarditis-virus-(EMCV)-infected cells. Eur J Biochem *254*, 248-255.

Marygold, S.J., Roote, J., Reuter, G., Lambertsson, A., Ashburner, M., Millburn, G.H., Harrison, P.M., Yu, Z., Kenmochi, N., Kaufman, T.C., *et al.* (2007). The ribosomal protein genes and Minute loci of Drosophila melanogaster. Genome Biol *8*, R216.

Matlin, A.J., Clark, F., and Smith, C.W. (2005). Understanding alternative splicing: towards a cellular code. Nat Rev Mol Cell Biol *6*, 386-398.

Maxon, M.E., Goodrich, J.A., and Tjian, R. (1994). Transcription factor IIE binds preferentially to RNA polymerase IIa and recruits TFIIH: a model for promoter clearance. Genes Dev *8*, 515-524.

Mayas, R.M., Maita, H., and Staley, J.P. (2006). Exon ligation is proofread by the DExD/H-box ATPase Prp22p. Nat Struct Mol Biol *13*, 482-490.

McCracken, S., and Greenblatt, J. (1991). Related RNA polymerase-binding regions in human RAP30/74 and Escherichia coli sigma 70. Science *253*, 900-902.

McKie, A.B., McHale, J.C., Keen, T.J., Tarttelin, E.E., Goliath, R., van Lith-Verhoeven, J.J., Greenberg, J., Ramesar, R.S., Hoyng, C.B., Cremers, F.P., *et al.* (2001). Mutations in the pre-mRNA splicing factor gene PRPC8 in autosomal dominant retinitis pigmentosa (RP13). Hum Mol Genet *10*, 1555-1562.

Meinhart, A., Kamenski, T., Hoeppner, S., Baumli, S., and Cramer, P. (2005). A structural perspective of CTD function. Genes Dev *19*, 1401-1415.

Meininghaus, M., Chapman, R.D., Horndasch, M., and Eick, D. (2000). Conditional expression of RNA polymerase II in mammalian cells. Deletion of the carboxyl-terminal domain of the large subunit affects early steps in transcription. J Biol Chem *275*, 24375-24382.

Meisterernst, M., and Roeder, R.G. (1991). Family of proteins that interact with TFIID and regulate promoter activity. Cell *67*, 557-567.

Mendjan, S., Taipale, M., Kind, J., Holz, H., Gebhardt, P., Schelder, M., Vermeulen, M., Buscaino, A., Duncan, K., Mueller, J., *et al.* (2006). Nuclear pore components are involved in the transcriptional regulation of dosage compensation in Drosophila. Mol Cell *21*, 811-823.

Merendino, L., Guth, S., Bilbao, D., Martinez, C., and Valcarcel, J. (1999). Inhibition of msl-2 splicing by Sex-lethal reveals interaction between U2AF35 and the 3' splice site AG. Nature *402*, 838-841.

Merkulova, T.I., Frolova, L.Y., Lazar, M., Camonis, J., and Kisselev, L.L. (1999). C-terminal domains of human translation termination factors eRF1 and eRF3 mediate their in vivo interaction. FEBS Lett *443*, 41-47.

Methot, N., Song, M.S., and Sonenberg, N. (1996). A region rich in aspartic acid, arginine, tyrosine, and glycine (DRYG) mediates eukaryotic initiation factor 4B (eIF4B) self-association and interaction with eIF3. Mol Cell Biol *16*, 5328-5334.

Michel, Y.M., Poncet, D., Piron, M., Kean, K.M., and Borman, A.M. (2000). Cap-Poly(A) synergy in mammalian cell-free extracts. Investigation of the requirements for poly(A)-mediated stimulation of translation initiation. J Biol Chem *275*, 32268-32276.

Misteli, T., and Spector, D.L. (1996). Serine/threonine phosphatase 1 modulates the subnuclear distribution of pre-mRNA splicing factors. Mol Biol Cell *7*, 1559-1572.

Misteli, T., and Spector, D.L. (1999). RNA polymerase II targets pre-mRNA splicing factors to transcription sites in vivo. Mol Cell *3*, 697-705.

Miyamoto, S., Patel, P., and Hershey, J.W. (2005). Changes in ribosomal binding activity of eIF3 correlate with increased translation rates during activation of T lymphocytes. J Biol Chem *280*, 28251-28264.

Mordes, D., Luo, X., Kar, A., Kuo, D., Xu, L., Fushimi, K., Yu, G., Sternberg, P., Jr., and Wu, J.Y. (2006). Pre-mRNA splicing and retinitis pigmentosa. Mol Vis *12*, 1259-1271.

Moreland, R.J., Tirode, F., Yan, Q., Conaway, J.W., Egly, J.M., and Conaway, R.C. (1999). A role for the TFIIH XPB DNA helicase in promoter escape by RNA polymerase II. J Biol Chem *274*, 22127-22130.

Morris, D.P., and Greenleaf, A.L. (2000). The splicing factor, Prp40, binds the phosphorylated carboxyl-terminal domain of RNA polymerase II. J Biol Chem *275*, 39935-39943.

Mothe-Satney, I., Brunn, G.J., McMahon, L.P., Capaldo, C.T., Abraham, R.T., and Lawrence, J.C., Jr. (2000). Mammalian target of rapamycin-dependent phosphorylation of PHAS-I in four (S/T)P sites detected by phospho-specific antibodies. J Biol Chem *275*, 33836-33843.

Murray, H.L., and Jarrell, K.A. (1999). Flipping the switch to an active spliceosome. Cell *96*, 599-602.

Naar, A.M., Taatjes, D.J., Zhai, W., Nogales, E., and Tjian, R. (2002). Human CRSP interacts with RNA polymerase II CTD and adopts a specific CTD-bound conformation. Genes Dev *16*, 1339-1344.

Nanduri, S., Rahman, F., Williams, B.R., and Qin, J. (2000). A dynamically tuned double-stranded RNA binding mechanism for the activation of antiviral kinase PKR. EMBO J *19*, 5567-5574.

Nasmyth, K., and Nurse, P. (1981). Cell division cycle mutants altered in DNA replication and mitosis in the fission yeast Schizosaccharomyces pombe. Mol Gen Genet *182*, 119-124.

Nayler, O., Stratling, W., Bourquin, J.P., Stagljar, I., Lindemann, L., Jasper, H., Hartmann, A.M., Fackelmayer, F.O., Ullrich, A., and Stamm, S. (1998). SAF-B protein couples transcription and pre-mRNA splicing to SAR/MAR elements. Nucleic Acids Res *26*, 3542-3549.

Nelson, C., Goto, S., Lund, K., Hung, W., and Sadowski, I. (2003). Srb10/Cdk8 regulates yeast filamentous growth by phosphorylating the transcription factor Ste12. Nature *421*, 187-190.

Neubauer, G. (2005). The analysis of multiprotein complexes: the yeast and the human spliceosome as case studies. Methods Enzymol *405*, 236-263.

Neubauer, G., King, A., Rappsilber, J., Calvio, C., Watson, M., Ajuh, P., Sleeman, J., Lamond, A., and Mann, M. (1998). Mass spectrometry and EST-database searching allows characterization of the multi-protein spliceosome complex. Nat Genet *20*, 46-50.

Newsome, T.P., Asling, B., and Dickson, B.J. (2000). Analysis of Drosophila photoreceptor axon guidance in eye-specific mosaics. Development *127*, 851-860.

Ng, H.H., Robert, F., Young, R.A., and Struhl, K. (2003). Targeted recruitment of Set1 histone methylase by elongating Pol II provides a localized mark and memory of recent transcriptional activity. Mol Cell *11*, 709-719.

Ngo, J.C., Chakrabarti, S., Ding, J.H., Velazquez-Dones, A., Nolen, B., Aubol, B.E., Adams, J.A., Fu, X.D., and Ghosh, G. (2005). Interplay between SRPK and Clk/Sty kinases in phosphorylation of the splicing factor ASF/SF2 is regulated by a docking motif in ASF/SF2. Mol Cell *20*, 77-89.

Ni, Z., Schwartz, B.E., Werner, J., Suarez, J.R., and Lis, J.T. (2004). Coordination of transcription, RNA processing, and surveillance by P-TEFb kinase on heat shock genes. Mol Cell *13*, 55-65.

Nielsen, K.H., Valasek, L., Sykes, C., Jivotovskaya, A., and Hinnebusch, A.G. (2006). Interaction of the RNP1 motif in PRT1 with HCR1 promotes 40S binding of eukaryotic initiation factor 3 in yeast. Mol Cell Biol *26*, 2984-2998.

Nojima, H., Tokunaga, C., Eguchi, S., Oshiro, N., Hidayat, S., Yoshino, K., Hara, K., Tanaka, N., Avruch, J., and Yonezawa, K. (2003). The mammalian target of rapamycin (mTOR) partner, raptor, binds the mTOR substrates p70 S6 kinase and 4E-BP1 through their TOR signaling (TOS) motif. J Biol Chem *278*, 15461-15464.

Novoa, I., Zhang, Y., Zeng, H., Jungreis, R., Harding, H.P., and Ron, D. (2003). Stress-induced gene expression requires programmed recovery from translational repression. EMBO J *22*, 1180-1187.

Nurse, P., Thuriaux, P., and Nasmyth, K. (1976). Genetic control of the cell division cycle in the fission yeast Schizosaccharomyces pombe. Mol Gen Genet *146*, 167-178.

O'Brien, T., Hardin, S., Greenleaf, A., and Lis, J.T. (1994). Phosphorylation of RNA polymerase II C-terminal domain and transcriptional elongation. Nature *370*, 75-77.

O'Day, C.L., Dalbadie-McFarland, G., and Abelson, J. (1996). The Saccharomyces cerevisiae Prp5 protein has RNA-dependent ATPase activity with specificity for U2 small nuclear RNA. J Biol Chem *271*, 33261-33267.

Oelgeschlager, T. (2002). Regulation of RNA polymerase II activity by CTD phosphorylation and cell cycle control. J Cell Physiol *190*, 160-169.

Ohi, M., and Gould, K. (2002). Characterization of interactions among the Cef1p-Prp19p-associated splicing complex. RNA *8*, 798-815.

Ohi, M.D., Link, A.J., Ren, L., Jennings, J.L., McDonald, W.H., and Gould, K.L. (2002). Proteomics analysis reveals stable multiprotein complexes in both fission and budding yeasts containing Myb-related Cdc5p/Cef1p, novel pre-mRNA splicing factors, and snRNAs. Mol Cell Biol *22*, 2011-2024.

Ohi, M.D., Vander Kooi, C.W., Rosenberg, J.A., Chazin, W.J., and Gould, K.L. (2003). Structural insights into the U-box, a domain associated with multi-ubiquitination. Nat Struct Biol *10*, 250-255.

Ohi, M.D., Vander Kooi, C.W., Rosenberg, J.A., Ren, L., Hirsch, J.P., Chazin, W.J., Walz, T., and Gould, K.L. (2005). Structural and functional analysis of essential pre-mRNA splicing factor Prp19p. Mol Cell Biol *25*, 451-460.

Ohi, R., Feoktistova, A., McCann, S., Valentine, V., Look, A.T., Lipsick, J.S., and Gould, K.L. (1998). Myb-related Schizosaccharomyces pombe cdc5p is structurally and functionally conserved in eukaryotes. Mol Cell Biol *18*, 4097-4108.

Ohi, R., McCollum, D., Hirani, B., Den Haese, G.J., Zhang, X., Burke, J.D., Turner, K., and Gould, K.L. (1994). The Schizosaccharomyces pombe cdc5+ gene encodes an essential protein with homology to c-Myb. EMBO J *13*, 471-483.

Ohkuma, Y., and Roeder, R.G. (1994). Regulation of TFIIH ATPase and kinase activities by TFIIE during active initiation complex formation. Nature *368*, 160-163.

Ohkuma, Y., Sumimoto, H., Horikoshi, M., and Roeder, R.G. (1990). Factors involved in specific transcription by mammalian RNA polymerase II: purification and characterization of general transcription factor TFIIE. Proc Natl Acad Sci U S A *87*, 9163-9167.

Orphanides, G., Lagrange, T., and Reinberg, D. (1996). The general transcription factors of RNA polymerase II. Genes Dev *10*, 2657-2683.

Ozer, J., Mitsouras, K., Zerby, D., Carey, M., and Lieberman, P.M. (1998). Transcription factor IIA derepresses TATA-binding protein (TBP)-associated factor inhibition of TBP-DNA binding. J Biol Chem *273*, 14293-14300.

Ozer, J., Moore, P.A., Bolden, A.H., Lee, A., Rosen, C.A., and Lieberman, P.M. (1994). Molecular cloning of the small (gamma) subunit of human TFIIA reveals functions critical for activated transcription. Genes Dev *8*, 2324-2335.

Pacheco, T.R., Moita, L.F., Gomes, A.Q., Hacohen, N., and Carmo-Fonseca, M. (2006). RNA interference knockdown of hU2AF35 impairs cell cycle progression and modulates alternative splicing of Cdc25 transcripts. Mol Biol Cell *17*, 4187-4199.

Pal, M., and Luse, D.S. (2003). The initiation-elongation transition: lateral mobility of RNA in RNA polymerase II complexes is greatly reduced at +8/+9 and absent by +23. Proc Natl Acad Sci U S A *100*, 5700-5705.

Pan, G., and Greenblatt, J. (1994). Initiation of transcription by RNA polymerase II is limited by melting of the promoter DNA in the region immediately upstream of the initiation site. J Biol Chem *269*, 30101-30104.

Panning, B., and Taatjes, D.J. (2008). Transcriptional regulation: it takes a village. Mol Cell *31*, 622-629.

Pantalacci, S., Tapon, N., and Leopold, P. (2003). The Salvador partner Hippo promotes apoptosis and cell-cycle exit in Drosophila. Nat Cell Biol *5*, 921-927.

Park, J.W., Parisky, K., Celotto, A.M., Reenan, R.A., and Graveley, B.R. (2004). Identification of alternative splicing regulators by RNA interference in Drosophila. Proc Natl Acad Sci U S A *101*, 15974-15979.

Pause, A., Methot, N., and Sonenberg, N. (1993). The HRIGRXXR region of the DEAD box RNA helicase eukaryotic translation initiation factor 4A is required for RNA binding and ATP hydrolysis. Mol Cell Biol *13*, 6789-6798.

Pause, A., and Sonenberg, N. (1992). Mutational analysis of a DEAD box RNA helicase: the mammalian translation initiation factor eIF-4A. EMBO J *11*, 2643-2654.

Pavri, R., Lewis, B., Kim, T.K., Dilworth, F.J., Erdjument-Bromage, H., Tempst, P., de Murcia, G., Evans, R., Chambon, P., and Reinberg, D. (2005). PARP-1 determines specificity in a retinoid signaling pathway via direct modulation of mediator. Mol Cell *18*, 83-96.

Pavri, R., Zhu, B., Li, G., Trojer, P., Mandal, S., Shilatifard, A., and Reinberg, D. (2006). Histone H2B monoubiquitination functions cooperatively with FACT to regulate elongation by RNA polymerase II. Cell *125*, 703-717.

Payne, J.M., Laybourn, P.J., and Dahmus, M.E. (1989). The transition of RNA polymerase II from initiation to elongation is associated with phosphorylation of the carboxyl-terminal domain of subunit IIa. J Biol Chem *264*, 19621-19629.

Peng, J., Schwartz, D., Elias, J.E., Thoreen, C.C., Cheng, D., Marsischky, G., Roelofs, J., Finley, D., and Gygi, S.P. (2003). A proteomics approach to understanding protein ubiquitination. Nat Biotechnol *21*, 921-926.

Perriman, R., and Ares, M. (2000). ATP can be dispensable for prespliceosome formation in yeast. Genes Dev *14*, 97-107.

Perriman, R., Barta, I., Voeltz, G.K., Abelson, J., and Ares, M., Jr. (2003). ATP requirement for Prp5p function is determined by Cus2p and the structure of U2 small nuclear RNA. Proc Natl Acad Sci U S A *100*, 13857-13862.

Perrimon, N. (1998). Creating mosaics in Drosophila. Int J Dev Biol *42*, 243-247.

Pestova, T.V., Borukhov, S.I., and Hellen, C.U. (1998). Eukaryotic ribosomes require initiation factors 1 and 1A to locate initiation codons. Nature *394*, 854-859.

Pestova, T.V., and Kolupaeva, V.G. (2002). The roles of individual eukaryotic translation initiation factors in ribosomal scanning and initiation codon selection. Genes Dev *16*, 2906-2922.

Pestova, T.V., Lomakin, I.B., Lee, J.H., Choi, S.K., Dever, T.E., and Hellen, C.U. (2000). The joining of ribosomal subunits in eukaryotes requires eIF5B. Nature *403*, 332-335.

Peterlin, B.M., and Price, D.H. (2006). Controlling the elongation phase of transcription with P-TEFb. Mol Cell *23*, 297-305.

Peterson, M.G., Tanese, N., Pugh, B.F., and Tjian, R. (1990). Functional domains and upstream activation properties of cloned human TATA binding protein. Science *248*, 1625-1630.

Petretti, C., Savoian, M., Montembault, E., Glover, D.M., Prigent, C., and Giet, R. (2006). The PITSLRE/CDK11p58 protein kinase promotes centrosome maturation and bipolar spindle formation. EMBO Rep *7*, 418-424.

Phan, L., Schoenfeld, L.W., Valasek, L., Nielsen, K.H., and Hinnebusch, A.G. (2001). A subcomplex of three eIF3 subunits binds eIF1 and eIF5 and stimulates ribosome binding of mRNA and tRNA(i)Met. EMBO J *20*, 2954-2965.

Phan, L., Zhang, X., Asano, K., Anderson, J., Vornlocher, H.P., Greenberg, J.R., Qin, J., and Hinnebusch, A.G. (1998). Identification of a translation initiation factor 3 (eIF3) core complex, conserved in yeast and mammals, that interacts with eIF5. Mol Cell Biol *18*, 4935-4946.

Pignoni, F., Hu, B., and Zipursky, S. (1997). Identification of genes required for Drosophila eye development using a phenotypic enhancer-trap. Proc Natl Acad Sci USA *94*, 9220-9225.

Pisareva, V.P., Pisarev, A.V., Hellen, C.U., Rodnina, M.V., and Pestova, T.V. (2006). Kinetic analysis of interaction of eukaryotic release factor 3 with guanine nucleotides. J Biol Chem *281*, 40224-40235.

Pokholok, D.K., Hannett, N.M., and Young, R.A. (2002). Exchange of RNA polymerase II initiation and elongation factors during gene expression in vivo. Mol Cell *9*, 799-809.

Pokholok, D.K., Harbison, C.T., Levine, S., Cole, M., Hannett, N.M., Lee, T.I., Bell, G.W., Walker, K., Rolfe, P.A., Herbolsheimer, E., *et al.* (2005). Genome-wide map of nucleosome acetylation and methylation in yeast. Cell *122*, 517-527.

Potashkin, J., Kim, D., Fons, M., Humphrey, T., and Frendewey, D. (1998). Cell-division-cycle defects associated with fission yeast pre-mRNA splicing mutants. Curr Genet *34*, 153-163.

Potter, C.J., Pedraza, L.G., and Xu, T. (2002). Akt regulates growth by directly phosphorylating Tsc2. Nat Cell Biol *4*, 658-665.

Prasad, J., Colwill, K., Pawson, T., and Manley, J.L. (1999). The protein kinase Clk/Sty directly modulates SR protein activity: both hyper- and hypophosphorylation inhibit splicing. Mol Cell Biol *19*, 6991-7000.

Preiss, T., and Hentze, M.W. (1998). Dual function of the messenger RNA cap structure in poly(A)-tail-promoted translation in yeast. Nature *392*, 516-520.

Price, D.H. (2000). P-TEFb, a cyclin-dependent kinase controlling elongation by RNA polymerase II. Mol Cell Biol *20*, 2629-2634.

Price, D.H. (2008). Poised polymerases: on your mark...get set...go! Mol Cell *30*, 7-10.

Proud, C.G. (2005). eIF2 and the control of cell physiology. Semin Cell Dev Biol *16*, 3-12.

Proud, C.G. (2006). Regulation of protein synthesis by insulin. Biochem Soc Trans *34*, 213-216.

Proudfoot, N.J., Furger, A., and Dye, M.J. (2002). Integrating mRNA processing with transcription. Cell *108*, 501-512.

Pugh, B.F., and Tjian, R. (1990). Mechanism of transcriptional activation by Sp1: evidence for coactivators. Cell *61*, 1187-1197.

Pullen, N., Dennis, P.B., Andjelkovic, M., Dufner, A., Kozma, S.C., Hemmings, B.A., and Thomas, G. (1998). Phosphorylation and activation of p70s6k by PDK1. Science *279*, 707-710.

Purnell, B.A., Emanuel, P.A., and Gilmour, D.S. (1994). TFIID sequence recognition of the initiator and sequences farther downstream in Drosophila class II genes. Genes Dev *8*, 830-842.

Raghunathan, P.L., and Guthrie, C. (1998). RNA unwinding in U4/U6 snRNPs requires ATP hydrolysis and the DEIH-box splicing factor Brr2. Curr Biol *8*, 847-855.

Ranish, J.A., Lane, W.S., and Hahn, S. (1992). Isolation of two genes that encode subunits of the yeast transcription factor IIA. Science *255*, 1127-1129.

Ranish, J.A., Yudkovsky, N., and Hahn, S. (1999). Intermediates in formation and activity of the RNA polymerase II preinitiation complex: holoenzyme recruitment and a postrecruitment role for the TATA box and TFIIB. Genes Dev *13*, 49-63.

Raught, B., Gingras, A.C., Gygi, S.P., Imataka, H., Morino, S., Gradi, A., Aebersold, R., and Sonenberg, N. (2000). Serum-stimulated, rapamycin-sensitive phosphorylation sites in the eukaryotic translation initiation factor 4GI. EMBO J *19*, 434-444.

Raught, B., Peiretti, F., Gingras, A.C., Livingstone, M., Shahbazian, D., Mayeur, G.L., Polakiewicz, R.D., Sonenberg, N., and Hershey, J.W. (2004). Phosphorylation of eucaryotic translation initiation factor 4B Ser422 is modulated by S6 kinases. EMBO J *23*, 1761-1769.

Ray, B.K., Lawson, T.G., Kramer, J.C., Cladaras, M.H., Grifo, J.A., Abramson, R.D., Merrick, W.C., and Thach, R.E. (1985). ATP-dependent unwinding of messenger RNA structure by eukaryotic initiation factors. J Biol Chem *260*, 7651-7658.

Raychaudhuri, P., Chaudhuri, A., and Maitra, U. (1985). Eukaryotic initiation factor 5 from calf liver is a single polypeptide chain protein of Mr = 62,000. J Biol Chem *260*, 2132-2139.

Rea, S., Xouri, G., and Akhtar, A. (2007). Males absent on the first (MOF): from flies to humans. Oncogene *26*, 5385-5394.

Redpath, N.T., Foulstone, E.J., and Proud, C.G. (1996). Regulation of translation elongation factor-2 by insulin via a rapamycin-sensitive signalling pathway. EMBO J *15*, 2291-2297.

Reinberg, D., and Roeder, R.G. (1987). Factors involved in specific transcription by mammalian RNA polymerase II. Purification and functional analysis of initiation factors IIB and IIE. J Biol Chem *262*, 3310-3321.

Ren, Y., Busch, R.K., Perlaky, L., and Busch, H. (1998). The 58-kDa microspherule protein (MSP58), a nucleolar protein, interacts with nucleolar protein p120. Eur J Biochem *253*, 734-742.

Richter-Cook, N.J., Dever, T.E., Hensold, J.O., and Merrick, W.C. (1998). Purification and characterization of a new eukaryotic protein translation factor. Eukaryotic initiation factor 4H. J Biol Chem *273*, 7579-7587.

Robert, F., Douziech, M., Forget, D., Egly, J.M., Greenblatt, J., Burton, Z.F., and Coulombe, B. (1998). Wrapping of promoter DNA around the RNA polymerase II initiation complex induced by TFIIF. Mol Cell *2*, 341-351.

Roberts, S.G., Choy, B., Walker, S.S., Lin, Y.S., and Green, M.R. (1995). A role for activator-mediated TFIIB recruitment in diverse aspects of transcriptional regulation. Curr Biol *5*, 508-516.

Robertson, H.M., Preston, C.R., Phillis, R.W., Johnson-Schlitz, D.M., Benz, W.K., and Engels, W.R. (1988). A stable genomic source of P element transposase in Drosophila melanogaster. Genetics *118*, 461-470.

Rocak, S., and Linder, P. (2004). DEAD-box proteins: the driving forces behind RNA metabolism. Nat Rev Mol Cell Biol *5*, 232-241.

Rodriguez, C.R., Cho, E.J., Keogh, M.C., Moore, C.L., Greenleaf, A.L., and Buratowski, S. (2000). Kin28, the TFIIH-associated carboxy-terminal domain kinase, facilitates the recruitment of mRNA processing machinery to RNA polymerase II. Mol Cell Biol *20*, 104-112.

Roeder, R.G. (1996). The role of general initiation factors in transcription by RNA polymerase II. Trends Biochem Sci *21*, 327-335.

Rogers, G.W., Jr., Richter, N.J., Lima, W.F., and Merrick, W.C. (2001). Modulation of the helicase activity of eIF4A by eIF4B, eIF4H, and eIF4F. J Biol Chem *276*, 30914-30922.

Rogers, G.W., Jr., Richter, N.J., and Merrick, W.C. (1999). Biochemical and kinetic characterization of the RNA helicase activity of eukaryotic initiation factor 4A. J Biol Chem *274*, 12236-12244.

Rosbash, M., and Seraphin, B. (1991). Who's on first? The U1 snRNP-5' splice site interaction and splicing. Trends Biochem Sci *16*, 187-190.

Rowlands, A.G., Panniers, R., and Henshaw, E.C. (1988). The catalytic mechanism of guanine nucleotide exchange factor action and competitive inhibition by phosphorylated eukaryotic initiation factor 2. J Biol Chem *263*, 5526-5533.

Rozen, F., Edery, I., Meerovitch, K., Dever, T.E., Merrick, W.C., and Sonenberg, N. (1990). Bidirectional RNA helicase activity of eucaryotic translation initiation factors 4A and 4F. Mol Cell Biol *10*, 1134-1144.

Rubin, G.M., and Spradling, A.C. (1982). Genetic transformation of Drosophila with transposable element vectors. Science *218*, 348-353.

Ruby, S.W., and Abelson, J. (1988). An early hierarchic role of U1 small nuclear ribonucleoprotein in spliceosome assembly. Science *242*, 1028-1035.

Ruvinsky, I., and Meyuhas, O. (2006). Ribosomal protein S6 phosphorylation: from protein synthesis to cell size. Trends Biochem Sci *31*, 342-348.

Ruvinsky, I., Sharon, N., Lerer, T., Cohen, H., Stolovich-Rain, M., Nir, T., Dor, Y., Zisman, P., and Meyuhas, O. (2005). Ribosomal protein S6 phosphorylation is a determinant of cell size and glucose homeostasis. Genes Dev *19*, 2199-2211.

Rymond, B.C., and Rosbash, M. (1985). Cleavage of 5' splice site and lariat formation are independent of 3' splice site in yeast mRNA splicing. Nature *317*, 735-737.

Salas-Marco, J., and Bedwell, D.M. (2004). GTP hydrolysis by eRF3 facilitates stop codon decoding during eukaryotic translation termination. Mol Cell Biol *24*, 7769-7778.

Salz, H.K., Cline, T.W., and Schedl, P. (1987). Functional changes associated with structural alterations induced by mobilization of a P element inserted in the Sex-lethal gene of Drosophila. Genetics *117*, 221-231.

Samuelsen, C.O., Baraznenok, V., Khorosjutina, O., Spahr, H., Kieselbach, T., Holmberg, S., and Gustafsson, C.M. (2003). TRAP230/ARC240 and TRAP240/ARC250 Mediator subunits are functionally conserved through evolution. Proc Natl Acad Sci U S A *100*, 6422-6427.

Sancak, Y., Peterson, T.R., Shaul, Y.D., Lindquist, R.A., Thoreen, C.C., Bar-Peled, L., and Sabatini, D.M. (2008). The Rag GTPases bind raptor and mediate amino acid signaling to mTORC1. Science *320*, 1496-1501.

Sander, B., Golas, M.M., Makarov, E.M., Brahms, H., Kastner, B., Luhrmann, R., and Stark, H. (2006). Organization of core spliceosomal components U5 snRNA loop I and U4/U6 Di-snRNP within U4/U6.U5 Tri-snRNP as revealed by electron cryomicroscopy. Mol Cell *24*, 267-278.

Sarbassov, D.D., Ali, S.M., and Sabatini, D.M. (2005a). Growing roles for the mTOR pathway. Curr Opin Cell Biol *17*, 596-603.

Sarbassov, D.D., Guertin, D.A., Ali, S.M., and Sabatini, D.M. (2005b). Phosphorylation and regulation of Akt/PKB by the rictor-mTOR complex. Science *307*, 1098-1101.

Sato, S., Tomomori-Sato, C., Parmely, T.J., Florens, L., Zybailov, B., Swanson, S.K., Banks, C.A., Jin, J., Cai, Y., Washburn, M.P., *et al.* (2004). A set of consensus mammalian mediator subunits identified by multidimensional protein identification technology. Mol Cell *14*, 685-691.

Saucedo, L.J., Gao, X., Chiarelli, D.A., Li, L., Pan, D., and Edgar, B.A. (2003). Rheb promotes cell growth as a component of the insulin/TOR signalling network. Nat Cell Biol *5*, 566-571.

Sauer, F., and Tjian, R. (1997). Mechanisms of transcriptional activation: differences and similarities between yeast, Drosophila, and man. Curr Opin Genet Dev *7*, 176-181.

Saunders, A., Core, L.J., and Lis, J.T. (2006). Breaking barriers to transcription elongation. Nat Rev Mol Cell Biol *7*, 557-567.

Saunders, A., Werner, J., Andrulis, E.D., Nakayama, T., Hirose, S., Reinberg, D., and Lis, J.T. (2003). Tracking FACT and the RNA polymerase II elongation complex through chromatin in vivo. Science *301*, 1094-1096.

Sawadogo, M., and Roeder, R.G. (1985). Interaction of a gene-specific transcription factor with the adenovirus major late promoter upstream of the TATA box region. Cell *43*, 165-175.

Schalm, S.S., Fingar, D.C., Sabatini, D.M., and Blenis, J. (2003). TOS motif-mediated raptor binding regulates 4E-BP1 multisite phosphorylation and function. Curr Biol *13*, 797-806.

Schellenberg, M.J., Edwards, R.A., Ritchie, D.B., Kent, O.A., Golas, M.M., Stark, H., Luhrmann, R., Glover, J.N., and MacMillan, A.M. (2006). Crystal structure of a core spliceosomal protein interface. Proc Natl Acad Sci U S A *103*, 1266-1271.

Schneider, S., Campodonico, E., and Schwer, B. (2004). Motifs IV and V in the DEAH box splicing factor Prp22 are important for RNA unwinding, and helicase-defective Prp22 mutants are suppressed by Prp8. J Biol Chem *279*, 8617-8626.

Schneider, S., Hotz, H., and Schwer, B. (2002). Characterization of dominant-negative mutants of the DEAH-box splicing factors Prp22 and Prp16. J Biol Chem *277*, 15452-15458.

Schroeder, R., Barta, A., and Semrad, K. (2004). Strategies for RNA folding and assembly. Nat Rev Mol Cell Biol *5*, 908-919.

Schroeder, S.C., Schwer, B., Shuman, S., and Bentley, D. (2000). Dynamic association of capping enzymes with transcribing RNA polymerase II. Genes Dev *14*, 2435-2440.

Schwer, B., and Gross, C.H. (1998). Prp22, a DExH-box RNA helicase, plays two distinct roles in yeast pre-mRNA splicing. EMBO J *17*, 2086-2094.

Schwer, B., and Guthrie, C. (1991). PRP16 is an RNA-dependent ATPase that interacts transiently with the spliceosome. Nature *349*, 494-499.

Schwer, B., and Guthrie, C. (1992). A conformational rearrangement in the spliceosome is dependent on PRP16 and ATP hydrolysis. EMBO J *11*, 5033-5039.

Sedore, S.C., Byers, S.A., Biglione, S., Price, J.P., Maury, W.J., and Price, D.H. (2007). Manipulation of P-TEFb control machinery by HIV: recruitment of P-TEFb from the large form by Tat and binding of HEXIM1 to TAR. Nucleic Acids Res *35*, 4347-4358.

Shah, O.J., Wang, Z., and Hunter, T. (2004). Inappropriate activation of the TSC/Rheb/mTOR/S6K cassette induces IRS1/2 depletion, insulin resistance, and cell survival deficiencies. Curr Biol *14*, 1650-1656.

Shao, H., Revach, M., Moshonov, S., Tzuman, Y., Gazit, K., Albeck, S., Unger, T., and Dikstein, R. (2005). Core promoter binding by histone-like TAF complexes. Mol Cell Biol *25*, 206-219.

Shea, J.E., Toyn, J.H., and Johnston, L.H. (1994). The budding yeast U5 snRNP Prp8 is a highly conserved protein which links RNA splicing with cell cycle progression. Nucleic Acids Res *22*, 5555-5564.

Shen, H., and Green, M.R. (2004). A pathway of sequential arginine-serine-rich domain-splicing signal interactions during mammalian spliceosome assembly. Mol Cell *16*, 363-373.

Shen, H., Kan, J.L., and Green, M.R. (2004). Arginine-serine-rich domains bound at splicing enhancers contact the branchpoint to promote prespliceosome assembly. Mol Cell *13*, 367-376.

Sheu, G.T., and Traugh, J.A. (1997). Recombinant subunits of mammalian elongation factor 1 expressed in Escherichia coli. Subunit interactions, elongation activity, and phosphorylation by protein kinase CKII. J Biol Chem *272*, 33290-33297.

Shi, J., Feng, Y., Goulet, A.C., Vaillancourt, R.R., Sachs, N.A., Hershey, J.W., and Nelson, M.A. (2003). The p34cdc2-related cyclin-dependent kinase 11 interacts with the p47 subunit of eukaryotic initiation factor 3 during apoptosis. J Biol Chem *278*, 5062-5071.

Shim, E.Y., Walker, A.K., Shi, Y., and Blackwell, T.K. (2002). CDK-9/cyclin T (P-TEFb) is required in two postinitiation pathways for transcription in the C. elegans embryo. Genes Dev *16*, 2135-2146.

Shimono, K., Shimono, Y., Shimokata, K., Ishiguro, N., and Takahashi, M. (2005). Microspherule protein 1, Mi-2beta, and RET finger protein associate in the nucleolus and up-regulate ribosomal gene transcription. J Biol Chem *280*, 39436-39447.

Shimono, Y., Murakami, H., Hasegawa, Y., and Takahashi, M. (2000). RET finger protein is a transcriptional repressor and interacts with enhancer of polycomb that has dual transcriptional functions. J Biol Chem *275*, 39411-39419.

Shimono, Y., Murakami, H., Kawai, K., Wade, P.A., Shimokata, K., and Takahashi, M. (2003). Mi-2 beta associates with BRG1 and RET finger protein at the distinct regions with transcriptional activating and repressing abilities. J Biol Chem *278*, 51638-51645.

Shin, B.S., Maag, D., Roll-Mecak, A., Arefin, M.S., Burley, S.K., Lorsch, J.R., and Dever, T.E. (2002). Uncoupling of initiation factor eIF5B/IF2 GTPase and translational activities by mutations that lower ribosome affinity. Cell *111*, 1015-1025.

Silva, E., Tsatskis, Y., Gardano, L., Tapon, N., and McNeill, H. (2006). The tumor-suppressor gene fat controls tissue growth upstream of expanded in the hippo signaling pathway. Curr Biol *16*, 2081-2089.

Silverman, E., Edwalds-Gilbert, G., and Lin, R.J. (2003). DExD/H-box proteins and their partners: helping RNA helicases unwind. Gene *312*, 1-16.

Sims, R.J., 3rd, Belotserkovskaya, R., and Reinberg, D. (2004). Elongation by RNA polymerase II: the short and long of it. Genes Dev *18*, 2437-2468.

Singh, C.R., Curtis, C., Yamamoto, Y., Hall, N.S., Kruse, D.S., He, H., Hannig, E.M., and Asano, K. (2005). Eukaryotic translation initiation factor 5 is critical for integrity of the scanning preinitiation complex and accurate control of GCN4 translation. Mol Cell Biol *25*, 5480-5491.

Singh, C.R., Lee, B., Udagawa, T., Mohammad-Qureshi, S.S., Yamamoto, Y., Pavitt, G.D., and Asano, K. (2006). An eIF5/eIF2 complex antagonizes guanine nucleotide exchange by eIF2B during translation initiation. EMBO J *25*, 4537-4546.

Singh, C.R., Udagawa, T., Lee, B., Wassink, S., He, H., Yamamoto, Y., Anderson, J.T., Pavitt, G.D., and Asano, K. (2007). Change in nutritional status modulates the abundance of critical pre-initiation intermediate complexes during translation initiation in vivo. J Mol Biol *370*, 315-330.

Singh, C.R., Yamamoto, Y., and Asano, K. (2004). Physical association of eukaryotic initiation factor (eIF) 5 carboxyl-terminal domain with the lysine-rich eIF2beta segment strongly enhances its binding to eIF3. J Biol Chem *279*, 49644-49655.

Singh, R., Banerjee, H., and Green, M.R. (2000). Differential recognition of the polypyrimidine-tract by the general splicing factor U2AF65 and the splicing repressor sex-lethal. RNA *6*, 901-911.

Siridechadilok, B., Fraser, C.S., Hall, R.J., Doudna, J.A., and Nogales, E. (2005). Structural roles for human translation factor eIF3 in initiation of protein synthesis. Science *310*, 1513-1515.

Sjoblom, T., Jones, S., Wood, L.D., Parsons, D.W., Lin, J., Barber, T.D., Mandelker, D., Leary, R.J., Ptak, J., Silliman, N., *et al.* (2006). The consensus coding sequences of human breast and colorectal cancers. Science *314*, 268-274.

Small, E.C., Leggett, S.R., Winans, A.A., and Staley, J.P. (2006). The EF-G-like GTPase Snu114p regulates spliceosome dynamics mediated by Brr2p, a DExD/H box ATPase. Mol Cell *23*, 389-399.

Smith, E.R., Cayrou, C., Huang, R., Lane, W.S., Cote, J., and Lucchesi, J.C. (2005). A human protein complex homologous to the Drosophila MSL complex is responsible for the majority of histone H4 acetylation at lysine 16. Mol Cell Biol *25*, 9175-9188.

Smith, E.R., Pannuti, A., Gu, W., Steurnagel, A., Cook, R.G., Allis, C.D., and Lucchesi, J.C. (2000). The drosophila MSL complex acetylates histone H4 at lysine 16, a chromatin modification linked to dosage compensation. Mol Cell Biol *20*, 312-318.

Sonenberg, N. (1981). ATP/Mg++-dependent cross-linking of cap binding proteins to the 5' end of eukaryotic mRNA. Nucleic Acids Res *9*, 1643-1656.

Song, H., Li, Y., Chen, G., Xing, Z., Zhao, J., Yokoyama, K.K., Li, T., and Zhao, M. (2004). Human MCRS2, a cell-cycle-dependent protein, associates with LPTS/PinX1 and reduces the telomere length. Biochem Biophys Res Commun *316*, 1116-1123.

Song, H., Mugnier, P., Das, A.K., Webb, H.M., Evans, D.R., Tuite, M.F., Hemmings, B.A., and Barford, D. (2000). The crystal structure of human eukaryotic release factor

eRF1--mechanism of stop codon recognition and peptidyl-tRNA hydrolysis. Cell *100*, 311-321.

Spahr, H., Khorosjutina, O., Baraznenok, V., Linder, T., Samuelsen, C.O., Hermand, D., Makela, T.P., Holmberg, S., and Gustafsson, C.M. (2003). Mediator influences Schizosaccharomyces pombe RNA polymerase II-dependent transcription in vitro. J Biol Chem *278*, 51301-51306.

Spangler, L., Wang, X., Conaway, J.W., Conaway, R.C., and Dvir, A. (2001). TFIIH action in transcription initiation and promoter escape requires distinct regions of downstream promoter DNA. Proc Natl Acad Sci U S A *98*, 5544-5549.

Spradling, A.C., and Rubin, G.M. (1982). Transposition of cloned P elements into Drosophila germ line chromosomes. Science *218*, 341-347.

Srebrow, A., and Kornblihtt, A.R. (2006). The connection between splicing and cancer. J Cell Sci *119*, 2635-2641.

Staknis, D., and Reed, R. (1994). SR proteins promote the first specific recognition of Pre-mRNA and are present together with the U1 small nuclear ribonucleoprotein particle in a general splicing enhancer complex. Mol Cell Biol *14*, 7670-7682.

Staley, J.P., and Guthrie, C. (1998). Mechanical devices of the spliceosome: motors, clocks, springs, and things. Cell *92*, 315-326.

Staley, J.P., and Guthrie, C. (1999). An RNA switch at the 5' splice site requires ATP and the DEAD box protein Prp28p. Mol Cell *3*, 55-64.

Stark, H., and Luhrmann, R. (2006). Cryo-electron microscopy of spliceosomal components. Annu Rev Biophys Biomol Struct *35*, 435-457.

Stefani, G., Fraser, C.E., Darnell, J.C., and Darnell, R.B. (2004). Fragile X mental retardation protein is associated with translating polyribosomes in neuronal cells. J Neurosci *24*, 7272-7276.

Stevens, S.W., and Abelson, J. (1999). Purification of the yeast U4/U6.U5 small nuclear ribonucleoprotein particle and identification of its proteins. Proc Natl Acad Sci U S A *96*, 7226-7231.

Stevens, S.W., Barta, I., Ge, H.Y., Moore, R.E., Young, M.K., Lee, T.D., and Abelson, J. (2001). Biochemical and genetic analyses of the U5, U6, and U4/U6 x U5 small nuclear ribonucleoproteins from Saccharomyces cerevisiae. Rna *7*, 1543-1553.

Stevens, S.W., Ryan, D.E., Ge, H.Y., Moore, R.E., Young, M.K., Lee, T.D., and Abelson, J. (2002). Composition and functional characterization of the yeast spliceosomal penta-snRNP. Mol Cell *9*, 31-44.

Stocker, H., Radimerski, T., Schindelholz, B., Wittwer, F., Belawat, P., Daram, P., Breuer, S., Thomas, G., and Hafen, E. (2003). Rheb is an essential regulator of S6K in controlling cell growth in Drosophila. Nat Cell Biol *5*, 559-565.

Sun, X., Zhang, Y., Cho, H., Rickert, P., Lees, E., Lane, W., and Reinberg, D. (1998). NAT, a human complex containing Srb polypeptides that functions as a negative regulator of activated transcription. Mol Cell *2*, 213-222.

Sun, Z.W., and Allis, C.D. (2002). Ubiquitination of histone H2B regulates H3 methylation and gene silencing in yeast. Nature *418*, 104-108.

Sun, Z.W., and Hampsey, M. (1995). Identification of the gene (SSU71/TFG1) encoding the largest subunit of transcription factor TFIIF as a suppressor of a TFIIB mutation in Saccharomyces cerevisiae. Proc Natl Acad Sci U S A *92*, 3127-3131.

Svitkin, Y.V., Pause, A., Haghighat, A., Pyronnet, S., Witherell, G., Belsham, G.J., and Sonenberg, N. (2001). The requirement for eukaryotic initiation factor 4A (elF4A) in translation is in direct proportion to the degree of mRNA 5' secondary structure. RNA *7*, 382-394.

Sykes, S.M., Mellert, H.S., Holbert, M.A., Li, K., Marmorstein, R., Lane, W.S., and McMahon, S.B. (2006). Acetylation of the p53 DNA-binding domain regulates apoptosis induction. Mol Cell *24*, 841-851.

Taatjes, D.J., Naar, A.M., Andel, F., 3rd, Nogales, E., and Tjian, R. (2002). Structure, function, and activator-induced conformations of the CRSP coactivator. Science *295*, 1058-1062.

Tabata, T. (2001). Genetics of morphogen gradients. Nat Rev Genet *2*, 620-630.

Taipale, M., Rea, S., Richter, K., Vilar, A., Lichter, P., Imhof, A., and Akhtar, A. (2005). hMOF histone acetyltransferase is required for histone H4 lysine 16 acetylation in mammalian cells. Mol Cell Biol *25*, 6798-6810.

Takahashi, K., Yamada, H., and Yanagida, M. (1994). Fission yeast minichromosome loss mutants mis cause lethal aneuploidy and replication abnormality. Mol Biol Cell *5*, 1145-1158.

Tamburini, B.A., and Tyler, J.K. (2005). Localized histone acetylation and deacetylation triggered by the homologous recombination pathway of double-strand DNA repair. Mol Cell Biol *25*, 4903-4913.

Tan, S., Aso, T., Conaway, R.C., and Conaway, J.W. (1994a). Roles for both the RAP30 and RAP74 subunits of transcription factor IIF in transcription initiation and elongation by RNA polymerase II. J Biol Chem *269*, 25684-25691.

Tan, S., Garrett, K.P., Conaway, R.C., and Conaway, J.W. (1994b). Cryptic DNA-binding domain in the C terminus of RNA polymerase II general transcription factor RAP30. Proc Natl Acad Sci U S A *91*, 9808-9812.

Tang, D., Gururajan, R., and Kidd, V.J. (1998). Phosphorylation of PITSLRE p110 isoforms accompanies their processing by caspases during Fas-mediated cell death. J Biol Chem *273*, 16601-16607.

Tanner, N.K., Cordin, O., Banroques, J., Doere, M., and Linder, P. (2003). The Q motif: a newly identified motif in DEAD box helicases may regulate ATP binding and hydrolysis. Mol Cell *11*, 127-138.

Tapon, N., Harvey, K.F., Bell, D.W., Wahrer, D.C., Schiripo, T.A., Haber, D.A., and Hariharan, I.K. (2002). salvador Promotes both cell cycle exit and apoptosis in Drosophila and is mutated in human cancer cell lines. Cell *110*, 467-478.

Tardiff, D.F., and Rosbash, M. (2006). Arrested yeast splicing complexes indicate stepwise snRNP recruitment during in vivo spliceosome assembly. RNA *12*, 968-979.

Tarn, W.Y., Hsu, C.H., Huang, K.T., Chen, H.R., Kao, H.Y., Lee, K.R., and Cheng, S.C. (1994). Functional association of essential splicing factor(s) with PRP19 in a protein complex. EMBO J *13*, 2421-2431.

Tarn, W.Y., Lee, K.R., and Cheng, S.C. (1993). Yeast precursor mRNA processing protein PRP19 associates with the spliceosome concomitant with or just after dissociation of U4 small nuclear RNA. Proc Natl Acad Sci U S A *90*, 10821-10825.

Tarun, S.Z., Jr., and Sachs, A.B. (1995). A common function for mRNA 5' and 3' ends in translation initiation in yeast. Genes Dev *9*, 2997-3007.

Tassan, J.P., Jaquenoud, M., Fry, A.M., Frutiger, S., Hughes, G.J., and Nigg, E.A. (1995). In vitro assembly of a functional human CDK7-cyclin H complex requires MAT1, a novel 36 kDa RING finger protein. EMBO J *14*, 5608-5617.

Taylor, S.S., Knighton, D.R., Zheng, J., Sowadski, J.M., Gibbs, C.S., and Zoller, M.J. (1993). A template for the protein kinase family. Trends Biochem Sci *18*, 84-89.

Tee, A.R., Manning, B.D., Roux, P.P., Cantley, L.C., and Blenis, J. (2003). Tuberous sclerosis complex gene products, Tuberin and Hamartin, control mTOR signaling by acting as a GTPase-activating protein complex toward Rheb. Curr Biol *13*, 1259-1268.

Teigelkamp, S., Newman, A.J., and Beggs, J.D. (1995). Extensive interactions of PRP8 protein with the 5' and 3' splice sites during splicing suggest a role in stabilization of exon alignment by U5 snRNA. EMBO J *14*, 2602-2612.

Ter-Avanesyan, M.D., Kushnirov, V.V., Dagkesamanskaya, A.R., Didichenko, S.A., Chernoff, Y.O., Inge-Vechtomov, S.G., and Smirnov, V.N. (1993). Deletion analysis of the SUP35 gene of the yeast Saccharomyces cerevisiae reveals two non-overlapping functional regions in the encoded protein. Mol Microbiol *7*, 683-692.

Thomas, A., Goumans, H., Voorma, H.O., and Benne, R. (1980). The mechanism of action of eukaryotic initiation factor 4C in protein synthesis. Eur J Biochem *107*, 39-45.

Thomas, M.C., and Chiang, C.M. (2006). The general transcription machinery and general cofactors. Crit Rev Biochem Mol Biol *41*, 105-178.

Thomas, T., Dixon, M.P., Kueh, A.J., and Voss, A.K. (2008). Mof (MYST1 or KAT8) is essential for progression of embryonic development past the blastocyst stage and required for normal chromatin architecture. Mol Cell Biol *28*, 5093-5105.

Thomas, T., and Voss, A.K. (2007). The diverse biological roles of MYST histone acetyltransferase family proteins. Cell Cycle *6*, 696-704

Thompson, H.A., Sadnik, I., Scheinbuks, J., and Moldave, K. (1977). Studies on native ribosomal subunits from rat liver. Purification and characterization of a ribosome dissociation factor. Biochemistry *16*, 2221-2230.

Tirode, F., Busso, D., Coin, F., and Egly, J.M. (1999). Reconstitution of the transcription factor TFIIH: assignment of functions for the three enzymatic subunits, XPB, XPD, and cdk7. Mol Cell *3*, 87-95.

Tong, J.K., Hassig, C.A., Schnitzler, G.R., Kingston, R.E., and Schreiber, S.L. (1998). Chromatin deacetylation by an ATP-dependent nucleosome remodelling complex. Nature *395*, 917-921.

Trachsel, H., and Staehelin, T. (1979). Initiation of mammalian protein synthesis. The multiple functions of the initiation factor eIF-3. Biochim Biophys Acta *565*, 305-314.

Tran, H.G., Steger, D.J., Iyer, V.R., and Johnson, A.D. (2000). The chromo domain protein chd1p from budding yeast is an ATP-dependent chromatin-modifying factor. EMBO J *19*, 2323-2331.

Trembley, J.H., Hu, D., Hsu, L.C., Yeung, C.Y., Slaughter, C., Lahti, J.M., and Kidd, V.J. (2002). PITSLRE p110 protein kinases associate with transcription complexes and affect their activity. J Biol Chem *277*, 2589-2596.

Trembley, J.H., Hu, D., Slaughter, C.A., Lahti, J.M., and Kidd, V.J. (2003). Casein kinase 2 interacts with cyclin-dependent kinase 11 (CDK11) in vivo and phosphorylates both the RNA polymerase II carboxyl-terminal domain and CDK11 in vitro. J Biol Chem *278*, 2265-2270.

Trembley, J.H., Tatsumi, S., Sakashita, E., Loyer, P., Slaughter, C.A., Suzuki, H., Endo, H., Kidd, V.J., and Mayeda, A. (2005). Activation of pre-mRNA splicing by human RNPS1 is regulated by CK2 phosphorylation. Mol Cell Biol *25*, 1446-1457.

Tsai, R.T., Fu, R.H., Yeh, F.L., Tseng, C.K., Lin, Y.C., Huang, Y.H., and Cheng, S.C. (2005). Spliceosome disassembly catalyzed by Prp43 and its associated components Ntr1 and Ntr2. Genes Dev *19*, 2991-3003.

Tsai, R.T., Tseng, C.K., Lee, P.J., Chen, H.C., Fu, R.H., Chang, K.J., Yeh, F.L., and Cheng, S.C. (2007). Dynamic interactions of Ntr1-Ntr2 with Prp43 and with U5 govern the recruitment of Prp43 to mediate spliceosome disassembly. Mol Cell Biol *27*, 8027-8037.

Tsai, W., Chow, Y., Chen, H., Huang, K., Hong, R., Jan, S., Kuo, N., Tsao, T., Chen, C., and Cheng, S. (1999). Cef1p is a component of the Prp19p-associated complex and essential for pre-mRNA splicing. J Biol Chem *274*, 9455-9462.

Tsubota, S., and Schedl, P. (1986). Hybrid dysgenesis-induced revertants of insertions at the 5' end of the rudimentary gene in Drosophila melanogaster: transposon-induced control mutations. Genetics *114*, 165-182.

Tyzack, J.K., Wang, X., Belsham, G.J., and Proud, C.G. (2000). ABC50 interacts with eukaryotic initiation factor 2 and associates with the ribosome in an ATP-dependent manner. J Biol Chem *275*, 34131-34139.

Udan, R.S., Kango-Singh, M., Nolo, R., Tao, C., and Halder, G. (2003). Hippo promotes proliferation arrest and apoptosis in the Salvador/Warts pathway. Nat Cell Biol *5*, 914-920.

Umen, J., and Guthrie, C. (1995a). Prp16p, Slu7p, and Prp8p interact with the 3' splice site in two distinct stages during the second catalytic step of pre-mRNA splicing. RNA *1*, 584-597.

Umen, J.G., and Guthrie, C. (1995b). Prp16p, Slu7p, and Prp8p interact with the 3' splice site in two distinct stages during the second catalytic step of pre-mRNA splicing. RNA *1*, 584-597.

Umen, J.G., and Guthrie, C. (1995c). The second catalytic step of pre-mRNA splicing. RNA *1*, 869-885.

Unbehaun, A., Borukhov, S.I., Hellen, C.U., and Pestova, T.V. (2004). Release of initiation factors from 48S complexes during ribosomal subunit joining and the link between establishment of codon-anticodon base-pairing and hydrolysis of eIF2-bound GTP. Genes Dev *18*, 3078-3093.

Urano, J., Comiso, M.J., Guo, L., Aspuria, P.J., Deniskin, R., Tabancay, A.P., Jr., Kato-Stankiewicz, J., and Tamanoi, F. (2005). Identification of novel single amino acid changes that result in hyperactivation of the unique GTPase, Rheb, in fission yeast. Mol Microbiol *58*, 1074-1086.

Urlaub, H., Hartmuth, K., and Luhrmann, R. (2002). A two-tracked approach to analyze RNA-protein crosslinking sites in native, nonlabeled small nuclear ribonucleoprotein particles. Methods *26*, 170-181.

Urushiyama, S., Tani, T., and Ohshima, Y. (1997). The prp1+ gene required for pre-mRNA splicing in Schizosaccharomyces pombe encodes a protein that contains TPR motifs and is similar to Prp6p of budding yeast. Genetics *147*, 101-115.

Utley, R.T., Lacoste, N., Jobin-Robitaille, O., Allard, S., and Cote, J. (2005). Regulation of NuA4 histone acetyltransferase activity in transcription and DNA repair by phosphorylation of histone H4. Mol Cell Biol *25*, 8179-8190.

Vaisman, N., Tsouladze, A., Robzyk, K., Ben-Yehuda, S., Kupiec, M., and Kassir, Y. (1995). The role of Saccharomyces cerevisiae Cdc40p in DNA replication and mitotic spindle formation and/or maintenance. Mol Gen Genet *247*, 123-136.

Valasek, L., Hasek, J., Trachsel, H., Imre, E.M., and Ruis, H. (1999). The Saccharomyces cerevisiae HCR1 gene encoding a homologue of the p35 subunit of human translation initiation factor 3 (eIF3) is a high copy suppressor of a temperature-sensitive mutation in the Rpg1p subunit of yeast eIF3. J Biol Chem *274*, 27567-27572.

Valasek, L., Nielsen, K.H., and Hinnebusch, A.G. (2002). Direct eIF2-eIF3 contact in the multifactor complex is important for translation initiation in vivo. EMBO J *21*, 5886-5898.

Valasek, L., Nielsen, K.H., Zhang, F., Fekete, C.A., and Hinnebusch, A.G. (2004). Interactions of eukaryotic translation initiation factor 3 (eIF3) subunit NIP1/c with eIF1 and eIF5 promote preinitiation complex assembly and regulate start codon selection. Mol Cell Biol *24*, 9437-9455.

Valasek, L., Phan, L., Schoenfeld, L.W., Valaskova, V., and Hinnebusch, A.G. (2001). Related eIF3 subunits TIF32 and HCR1 interact with an RNA recognition motif in PRT1 required for eIF3 integrity and ribosome binding. EMBO J *20*, 891-904.

van de Peppel, J., Kettelarij, N., van Bakel, H., Kockelkorn, T.T., van Leenen, D., and Holstege, F.C. (2005). Mediator expression profiling epistasis reveals a signal transduction pathway with antagonistic submodules and highly specific downstream targets. Mol Cell *19*, 511-522.

van Nues, R., and Beggs, J. (2001a). Functional contacts with a range of splicing proteins suggest a central role for Brr2p in the dynamic control of the order of events in spliceosomes of Saccharomyces cerevisiae. Genetics *157*, 1451-1467.

van Nues, R.W., and Beggs, J.D. (2001b). Functional contacts with a range of splicing proteins suggest a central role for Brr2p in the dynamic control of the order of events in spliceosomes of Saccharomyces cerevisiae. Genetics *157*, 1451-1467.

Vander Haar, E., Lee, S.I., Bandhakavi, S., Griffin, T.J., and Kim, D.H. (2007). Insulin signalling to mTOR mediated by the Akt/PKB substrate PRAS40. Nat Cell Biol *9*, 316-323.

Vattem, K.M., and Wek, R.C. (2004). Reinitiation involving upstream ORFs regulates ATF4 mRNA translation in mammalian cells. Proc Natl Acad Sci U S A *101*, 11269-11274.

Verrijzer, C.P., Chen, J.L., Yokomori, K., and Tjian, R. (1995). Binding of TAFs to core elements directs promoter selectivity by RNA polymerase II. Cell *81*, 1115-1125.

Verrijzer, C.P., Yokomori, K., Chen, J.L., and Tjian, R. (1994). Drosophila TAFII150: similarity to yeast gene TSM-1 and specific binding to core promoter DNA. Science *264*, 933-941.

Vijayraghavan, U., Company, M., and Abelson, J. (1989). Isolation and characterization of pre-mRNA splicing mutants of Saccharomyces cerevisiae. Genes Dev *3*, 1206-1216.

Villa, T., and Guthrie, C. (2005). The Isy1p component of the NineTeen complex interacts with the ATPase Prp16p to regulate the fidelity of pre-mRNA splicing. Genes Dev *19*, 1894-1904.

Vithana, E.N., Abu-Safieh, L., Allen, M.J., Carey, A., Papaioannou, M., Chakarova, C., Al-Maghtheh, M., Ebenezer, N.D., Willis, C., Moore, A.T., *et al.* (2001). A human homolog of yeast pre-mRNA splicing gene, PRP31, underlies autosomal dominant retinitis pigmentosa on chromosome 19q13.4 (RP11). Mol Cell *8*, 375-381.

von der Haar, T., and McCarthy, J.E. (2002). Intracellular translation initiation factor levels in Saccharomyces cerevisiae and their role in cap-complex function. Mol Microbiol *46*, 531-544.

Wade, P.A., Jones, P.L., Vermaak, D., and Wolffe, A.P. (1998). A multiple subunit Mi-2 histone deacetylase from Xenopus laevis cofractionates with an associated Snf2 superfamily ATPase. Curr Biol *8*, 843-846.

Wagner, J.D., Jankowsky, E., Company, M., Pyle, A.M., and Abelson, J.N. (1998). The DEAH-box protein PRP22 is an ATPase that mediates ATP-dependent mRNA release from the spliceosome and unwinds RNA duplexes. EMBO J *17*, 2926-2937.

Wang, H.Y., Lin, W., Dyck, J.A., Yeakley, J.M., Songyang, Z., Cantley, L.C., and Fu, X.D. (1998). SRPK2: a differentially expressed SR protein-specific kinase involved in mediating the interaction and localization of pre-mRNA splicing factors in mammalian cells. J Cell Biol *140*, 737-750.

Wang, W., Carey, M., and Gralla, J.D. (1992). Polymerase II promoter activation: closed complex formation and ATP-driven start site opening. Science *255*, 450-453.

Wang, X., Beugnet, A., Murakami, M., Yamanaka, S., and Proud, C.G. (2005). Distinct signaling events downstream of mTOR cooperate to mediate the effects of amino acids and insulin on initiation factor 4E-binding proteins. Mol Cell Biol *25*, 2558-2572.

Wang, X., Li, W., Williams, M., Terada, N., Alessi, D.R., and Proud, C.G. (2001). Regulation of elongation factor 2 kinase by p90(RSK1) and p70 S6 kinase. EMBO J *20*, 4370-4379.

Wang, Y., and Guthrie, C. (1998). PRP16, a DEAH-box RNA helicase, is recruited to the spliceosome primarily via its nonconserved N-terminal domain. RNA *4*, 1216-1229.

Webb, B.L., and Proud, C.G. (1997). Eukaryotic initiation factor 2B (eIF2B). Int J Biochem Cell Biol *29*, 1127-1131.

Weeks, J.R., Coulter, D.E., and Greenleaf, A.L. (1982). Immunological studies of RNA polymerase II using antibodies to subunits of Drosophila and wheat germ enzyme. J Biol Chem *257*, 5884-5892.

Weeks, J.R., Hardin, S.E., Shen, J., Lee, J.M., and Greenleaf, A.L. (1993). Locus-specific variation in phosphorylation state of RNA polymerase II in vivo: correlations with gene activity and transcript processing. Genes Dev *7*, 2329-2344.

Wek, R.C., Jiang, H.Y., and Anthony, T.G. (2006). Coping with stress: eIF2 kinases and translational control. Biochem Soc Trans *34*, 7-11.

Wells, S.E., Hillner, P.E., Vale, R.D., and Sachs, A.B. (1998). Circularization of mRNA by eukaryotic translation initiation factors. Mol Cell *2*, 135-140.

Welsh, G.I., Miller, C.M., Loughlin, A.J., Price, N.T., and Proud, C.G. (1998). Regulation of eukaryotic initiation factor eIF2B: glycogen synthase kinase-3 phosphorylates a conserved serine which undergoes dephosphorylation in response to insulin. FEBS Lett *421*, 125-130.

Welsh, G.I., and Proud, C.G. (1992). Regulation of protein synthesis in Swiss 3T3 fibroblasts. Rapid activation of the guanine-nucleotide-exchange factor by insulin and growth factors. Biochem J *284 (Pt 1)*, 19-23.

Wen, Y., and Shatkin, A.J. (1999). Transcription elongation factor hSPT5 stimulates mRNA capping. Genes Dev *13*, 1774-1779.

West, S., Gromak, N., and Proudfoot, N.J. (2004). Human 5' --> 3' exonuclease Xrn2 promotes transcription termination at co-transcriptional cleavage sites. Nature *432*, 522-525.

West, S., Proudfoot, N.J., and Dye, M.J. (2008). Molecular dissection of mammalian RNA polymerase II transcriptional termination. Mol Cell *29*, 600-610.

West, S., Zaret, K., and Proudfoot, N.J. (2006). Transcriptional termination sequences in the mouse serum albumin gene. RNA *12*, 655-665.

Westerling, T., Kuuluvainen, E., and Makela, T.P. (2007). Cdk8 is essential for preimplantation mouse development. Mol Cell Biol *27*, 6177-6182.

Willecke, M., Hamaratoglu, F., Kango-Singh, M., Udan, R., Chen, C.L., Tao, C., Zhang, X., and Halder, G. (2006). The fat cadherin acts through the hippo tumor-suppressor pathway to regulate tissue size. Curr Biol *16*, 2090-2100.

Williams, C.J., Naito, T., Arco, P.G., Seavitt, J.R., Cashman, S.M., De Souza, B., Qi, X., Keables, P., Von Andrian, U.H., and Georgopoulos, K. (2004). The chromatin remodeler Mi-2beta is required for CD4 expression and T cell development. Immunity *20*, 719-733.

Williams, D.D., Price, N.T., Loughlin, A.J., and Proud, C.G. (2001). Characterization of the mammalian initiation factor eIF2B complex as a GDP dissociation stimulator protein. J Biol Chem *276*, 24697-24703.

Winkler, C., Eggert, C., Gradl, D., Meister, G., Giegerich, M., Wedlich, D., Laggerbauer, B., and Fischer, U. (2005). Reduced U snRNP assembly causes motor axon degeneration in an animal model for spinal muscular atrophy. Genes Dev *19*, 2320-2330.

Wood, A., Schneider, J., Dover, J., Johnston, M., and Shilatifard, A. (2003). The Paf1 complex is essential for histone monoubiquitination by the Rad6-Bre1 complex, which signals for histone methylation by COMPASS and Dot1p. J Biol Chem *278*, 34739-34742.

Wu, J.Y., and Maniatis, T. (1993). Specific interactions between proteins implicated in splice site selection and regulated alternative splicing. Cell *75*, 1061-1070.

Wu, S., Huang, J., Dong, J., and Pan, D. (2003a). hippo encodes a Ste-20 family protein kinase that restricts cell proliferation and promotes apoptosis in conjunction with salvador and warts. Cell *114*, 445-456.

Wu, S., Liu, Y., Zheng, Y., Dong, J., and Pan, D. (2008). The TEAD/TEF family protein Scalloped mediates transcriptional output of the Hippo growth-regulatory pathway. Dev Cell *14*, 388-398.

Wu, S., Romfo, C.M., Nilsen, T.W., and Green, M.R. (1999). Functional recognition of the 3' splice site AG by the splicing factor U2AF35. Nature *402*, 832-835.

Wu, S.Y., Zhou, T., and Chiang, C.M. (2003b). Human mediator enhances activator-facilitated recruitment of RNA polymerase II and promoter recognition by TATA-binding protein (TBP) independently of TBP-associated factors. Mol Cell Biol *23*, 6229-6242.

Wullschleger, S., Loewith, R., and Hall, M.N. (2006). TOR signaling in growth and metabolism. Cell *124*, 471-484.

Xiao, S.H., and Manley, J.L. (1997). Phosphorylation of the ASF/SF2 RS domain affects both protein-protein and protein-RNA interactions and is necessary for splicing. Genes Dev *11*, 334-344.

Xie, J., Beickman, K., Otte, E., and Rymond, B.C. (1998). Progression through the spliceosome cycle requires Prp38p function for U4/U6 snRNA dissociation. Embo J *17*, 2938-2946.

Xu, T., and Rubin, G.M. (1993). Analysis of genetic mosaics in developing and adult Drosophila tissues. Development *117*, 1223-1237.

Xu, T., Wang, W., Zhang, S., Stewart, R.A., and Yu, W. (1995). Identifying tumor suppressors in genetic mosaics: the Drosophila lats gene encodes a putative protein kinase. Development *121*, 1053-1063.

Xu, Y.Z., Newnham, C.M., Kameoka, S., Huang, T., Konarska, M.M., and Query, C.C. (2004). Prp5 bridges U1 and U2 snRNPs and enables stable U2 snRNP association with intron RNA. EMBO J *23*, 376-385.

Xu, Y.Z., and Query, C.C. (2007). Competition between the ATPase Prp5 and branch region-U2 snRNA pairing modulates the fidelity of spliceosome assembly. Mol Cell *28*, 838-849.

Yamada, T., Yamaguchi, Y., Inukai, N., Okamoto, S., Mura, T., and Handa, H. (2006). P-TEFb-mediated phosphorylation of hSpt5 C-terminal repeats is critical for processive transcription elongation. Mol Cell *21*, 227-237.

Yamamoto, Y., Singh, C.R., Marintchev, A., Hall, N.S., Hannig, E.M., Wagner, G., and Asano, K. (2005). The eukaryotic initiation factor (eIF) 5 HEAT domain mediates multifactor assembly and scanning with distinct interfaces to eIF1, eIF2, eIF3, and eIF4G. Proc Natl Acad Sci U S A *102*, 16164-16169.

Yan, Q., Moreland, R.J., Conaway, J.W., and Conaway, R.C. (1999). Dual roles for transcription factor IIF in promoter escape by RNA polymerase II. J Biol Chem *274*, 35668-35675.

Yang, L., Li, N., Wang, C., Yu, Y., Yuan, L., Zhang, M., and Cao, X. (2004). Cyclin L2, a novel RNA polymerase II-associated cyclin, is involved in pre-mRNA splicing and induces apoptosis of human hepatocellular carcinoma cells. J Biol Chem *279*, 11639-11648.

Yang, X.J. (2004). The diverse superfamily of lysine acetyltransferases and their roles in leukemia and other diseases. Nucleic Acids Res *32*, 959-976.

Yankulov, K.Y., and Bentley, D.L. (1997). Regulation of CDK7 substrate specificity by MAT1 and TFIIH. EMBO J *16*, 1638-1646.

Yarunin, A., Panse, V.G., Petfalski, E., Dez, C., Tollervey, D., and Hurt, E.C. (2005). Functional link between ribosome formation and biogenesis of iron-sulfur proteins. EMBO J *24*, 580-588.

Yokomori, K., Admon, A., Goodrich, J.A., Chen, J.L., and Tjian, R. (1993). Drosophila TFIIA-L is processed into two subunits that are associated with the TBP/TAF complex. Genes Dev *7*, 2235-2245.

Yudkovsky, N., Ranish, J.A., and Hahn, S. (2000). A transcription reinitiation intermediate that is stabilized by activator. Nature *408*, 225-229.

Yuryev, A., Patturajan, M., Litingtung, Y., Joshi, R.V., Gentile, C., Gebara, M., and Corden, J.L. (1996). The C-terminal domain of the largest subunit of RNA polymerase II interacts with a novel set of serine/arginine-rich proteins. Proc Natl Acad Sci U S A *93*, 6975-6980.

Zachariou, A., Tenev, T., Goyal, L., Agapite, J., Steller, H., and Meier, P. (2003). IAP-antagonists exhibit non-redundant modes of action through differential DIAP1 binding. EMBO J *22*, 6642-6652.

Zalfa, F., Giorgi, M., Primerano, B., Moro, A., Di Penta, A., Reis, S., Oostra, B., and Bagni, C. (2003). The fragile X syndrome protein FMRP associates with BC1 RNA and regulates the translation of specific mRNAs at synapses. Cell *112*, 317-327.

Zawel, L., Kumar, K.P., and Reinberg, D. (1995). Recycling of the general transcription factors during RNA polymerase II transcription. Genes Dev *9*, 1479-1490.

Zhang, C., and Burton, Z.F. (2004). Transcription factors IIF and IIS and nucleoside triphosphate substrates as dynamic probes of the human RNA polymerase II mechanism. J Mol Biol *342*, 1085-1099.

Zhang, L., Ren, F., Zhang, Q., Chen, Y., Wang, B., and Jiang, J. (2008). The TEAD/TEF family of transcription factor Scalloped mediates Hippo signaling in organ size control. Dev Cell *14*, 377-387.

Zhang, P., McGrath, B.C., Reinert, J., Olsen, D.S., Lei, L., Gill, S., Wek, S.A., Vattem, K.M., Wek, R.C., Kimball, S.R., *et al.* (2002). The GCN2 eIF2alpha kinase is required for adaptation to amino acid deprivation in mice. Mol Cell Biol *22*, 6681-6688.

Zhang, Y., LeRoy, G., Seelig, H.P., Lane, W.S., and Reinberg, D. (1998). The dermatomyositis-specific autoantigen Mi2 is a component of a complex containing histone deacetylase and nucleosome remodeling activities. Cell *95*, 279-289.

Zhao, X., and Herr, W. (2002). A regulated two-step mechanism of TBP binding to DNA: a solvent-exposed surface of TBP inhibits TATA box recognition. Cell *108*, 615-627.

Zhao, Z., Fang, L.L., Johnsen, R., and Baillie, D.L. (2004). ATP-binding cassette protein E is involved in gene transcription and translation in Caenorhabditis elegans. Biochem Biophys Res Commun *323*, 104-111.

Zhou, Z., and Reed, R. (1998). Human homologs of yeast prp16 and prp17 reveal conservation of the mechanism for catalytic step II of pre-mRNA splicing. EMBO J *17*, 2095-2106.

Zhu, B., Zheng, Y., Pham, A.D., Mandal, S.S., Erdjument-Bromage, H., Tempst, P., and Reinberg, D. (2005). Monoubiquitination of human histone H2B: the factors involved and their roles in HOX gene regulation. Mol Cell *20*, 601-611.

Zhu, J., Mayeda, A., and Krainer, A.R. (2001). Exon identity established through differential antagonism between exonic splicing silencer-bound hnRNP A1 and enhancer-bound SR proteins. Mol Cell *8*, 1351-1361.

Zink, B., and Paro, R. (1989). In vivo binding pattern of a trans-regulator of homoeotic genes in Drosophila melanogaster. Nature *337*, 468-471.

Zorio, D.A., and Blumenthal, T. (1999). Both subunits of U2AF recognize the 3' splice site in Caenorhabditis elegans. Nature *402*, 835-838.

Zuo, P., and Maniatis, T. (1996). The splicing factor U2AF35 mediates critical protein-protein interactions in constitutive and enhancer-dependent splicing. Genes Dev *10*, 1356-1368.